



HAL
open science

Application of vacuum for the intensification of fruits and vegetables freezing

Yuqi Huang

► **To cite this version:**

Yuqi Huang. Application of vacuum for the intensification of fruits and vegetables freezing. Chemical and Process Engineering. Université de Technologie de Compiègne, 2024. English. NNT : 2024COMP2817 . tel-04854931

HAL Id: tel-04854931

<https://theses.hal.science/tel-04854931v1>

Submitted on 24 Dec 2024

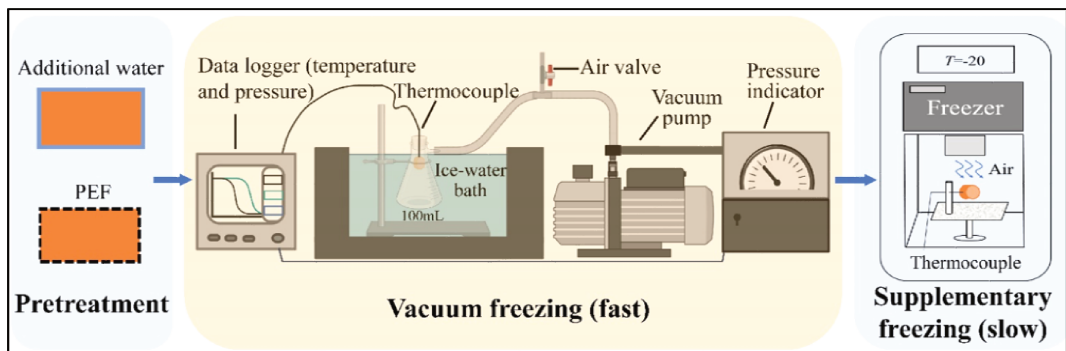
HAL is a multi-disciplinary open access archive for the deposit and dissemination of scientific research documents, whether they are published or not. The documents may come from teaching and research institutions in France or abroad, or from public or private research centers.

L'archive ouverte pluridisciplinaire **HAL**, est destinée au dépôt et à la diffusion de documents scientifiques de niveau recherche, publiés ou non, émanant des établissements d'enseignement et de recherche français ou étrangers, des laboratoires publics ou privés.

Par Yuqi HUANG

*Application du vide pour l'intensification de
la congélation des fruits et légumes*

Thèse présentée
pour l'obtention du grade
de Docteur de l'UTC



Soutenu le 22 juillet 2024

Spécialité : Génie des Procédés : Transformations intégrées
de la matière renouvelable (EA-4297)

D2817



THÈSE DE DOCTORAT DE L'UNIVERSITÉ DE
TECHNOLOGIE DE COMPIÈGNE

Présentée par

Madame Yuqi HUANG

En vue d'obtenir le grade de
DOCTEUR DE L'UNIVERSITÉ DE TECHNOLOGIE DE
COMPIÈGNE

**Application du vide pour l'intensification de
la congélation des fruits et légumes**

Spécialité : Génie des Procédés

École doctorale : Sciences pour l'ingénieur

Unité de recherche : Transformations Intégrées de la Matière Renouvelable

Équipe de recherche : Technologies Agro-Industrielles (TAI)

Thèse soutenue à Compiègne le 22 juillet 2024 devant le jury composé de :

Dr Hayat BENKHELIFA, Université de Paris-Saclay	(Rapporteur)
Pr. Luc MARCHAL, Université de Nantes	(Rapporteur)
Pr. Nabil GRIMI, Université de Technologie de Compiègne	(Examinateur)
Pr. Olivier BALS, Université de Technologie de Compiègne	(Directeur de thèse)

Application of vacuum for the intensification of fruits and vegetables freezing

By Yuqi HUANG

Spécialité : Génie des Procédés

Thesis defended in Compiègne on 22 July 2024

Acknowledgement

My PhD journey has been an unforgettable and enriching experience, thanks to the support and encouragement of many people. I would like to express my deepest gratitude to all those who have contributed. I would like to thank the China Scholarship Council (CSC) for providing the scholarship, and Prof. Zhenzhou ZHU for guiding me to have the valuable opportunity to continue my study at the University of Technology of Compiègne (UTC). This experience has broadened my academic horizons and enriched my personal growth.

For the past nearly four years, first of all I would like to express my sincere gratitude to my supervisor, Prof. Olivier BALS. His dedication to scientific purity, curiosity in research, and never backing down in the face of problems profoundly influenced me. His kindness, patience, and sense of humor made my four-year research life less difficult.

I would also like to thank Professors Eugène VOROBIEV and Nikolai LBOVKA for their insightful advice and support in my research plan, and for their generous sharing of their knowledge and professional experience.

I would like to thank Prof. Nabil GRIMI for his warm welcome to the team and his constant concern for my research status, as well as his agreement to participate in the thesis jury.

I am grateful to M. Luc MARCHAL and Mme. Hayat BENKHELIFA who agreed to be the rapporteurs of this thesis. Thank you for your invaluable time and many constructive suggestions, which will undoubtedly improve the quality of this thesis and help me in my future work.

I would like to acknowledge my colleagues Océane Adriaio, Rachele El Hajj, Adila Gherabli, Georgeo Nemer, Yassine EL Khayat Driaa, Amine Zakhia, Malak Tabib, Sarah Joe Salameh, Nicole Najjoun, Sarah Mahfoud, and Mariam Battikh. The moments shared with all of you have been a meaningful part of my journey, creating many fond memories.

I also want to thank my friends Kaidi Peng, Ye Tao, Zhao Zhang, Xin Zheng, Xiangjun Kong, Shuli Liu, Junting Hong, Xinyu Wang, Jiashuo Qi, Yamei Zhang, Huihui Qiao, Jingqi Zhang, Yanqin Deng, and Wanru Zeng. Your companionship and care have made life in Compiègne beautiful and joyous.

Last but not least, I would like to say a big and loving thanks to my parents, my family, and my boyfriend Qing TANG. Your unconditional love, support, and encouragement have been my driving force.

Thank you all.

Abstract

The main goal of this thesis is to explore an innovative vacuum-based freezing technique for fruits and vegetables. For this purpose, a laboratory vacuum freezing system was constructed first, which has the advantages of fast vacuuming, flexible control, real-time temperature and pressure detection.

Considering that the temperature reduction and even crystallization during vacuum freezing depend on the evaporation of water in the sample, the application of vacuum freezing was limited to a specific small temperature range to minimize unnecessary water loss. The small temperature range includes the freezing critical zone. The fast vacuuming contributes to passing through this freezing critical zone rapidly. The combined freezing protocol was set as vacuum freezing (VF) applied at 2 to -6 °C, followed by air freezing at -20 °C (AF-20) to complete the rest of the freezing process from -6 to -20 °C. From the texture, water loss, and microstructure analysis of carrot discs, the application of vacuum freezing was proven to improve the quality attributes of thawed carrot discs, and it was also applicable to relatively large size samples.

The pulsed electric field (PEF) pretreatment was demonstrated to accelerate the continuous vacuum freezing, conventional air freezing (AF-20), and also the combined freezing (VF+AF-20). However, a significant tissue softening was found with the increase of the cell disintegration index *Z*. Overall, combined freezing (VF+AF-20) was better than AF because of less water loss and relatively less damage to the microstructure.

The degree of the effect of PEF treatment on continuous vacuum freezing varied for different materials due to their componential and structural differences. In the comparison of thawed potatoes, apples, and carrots, we also found that AF-20 and VF+AF-20 were not suitable for apples with or without PEF pretreatment because of their larger porosity and thinner cell walls. The low water loss and high textural and microstructural preservation of potato and carrot discs demonstrated in combined freezing VF+AF-20 all evidenced that this freezing protocol can be applied to fruits and vegetables with low porosity and a rigid initial structure.

Keywords: Vacuum freezing; Conventional air freezing; Fruits and vegetables; Quality attributes; Pulsed electric field; Applicability

Résumé

L'objectif principal de cette thèse est d'explorer une technique innovante de congélation sous vide des fruits et légumes. À cette fin, un système de congélation sous vide de laboratoire a d'abord été construit, qui présente les avantages d'une aspiration rapide, d'un contrôle flexible et d'une détection de la température et de la pression en temps réel.

Considérant que la réduction de température et même la cristallisation pendant la congélation sous vide dépendent de l'évaporation de l'eau dans l'échantillon, l'application de la congélation sous vide a été limitée à une petite plage de température spécifique afin de minimiser les pertes d'eau inutiles. La petite plage de température comprend la zone critique de congélation. L'aspiration rapide contribue à traverser rapidement cette zone critique de congélation. Le protocole de congélation combiné a été défini comme une congélation sous vide (VF) appliquée entre 2 et -6 °C, suivie d'une congélation à l'air à -20 °C (AF-20) pour compléter le processus de congélation restant de -6 à -20 °C. D'après l'analyse de la texture, de la perte d'eau et de la microstructure des disques de carottes, il a été prouvé que l'application de la congélation sous vide améliorerait les attributs de qualité des disques de carotte décongelés, et qu'elle était également applicable à des échantillons de taille relativement grande.

Il a été démontré que le prétraitement par champ électrique pulsé (CEP) accélère la congélation sous vide continue, la congélation à l'air conventionnelle (AF-20) ainsi que la congélation combinée (VF+AF-20). Cependant, un ramollissement significatif des tissus a été constaté avec l'augmentation de l'indice de désintégration cellulaire Z. Dans l'ensemble, la congélation combinée (VF + AF-20) était meilleure que l'AF en raison de moins de perte d'eau et de relativement moins de dommages à la microstructure.

Le degré d'effet du traitement CEP sur la congélation sous vide continue variait selon les matériaux en raison de leurs différences composantes et structurelles. En comparant les pommes de terre, les pommes et les carottes décongelées, nous avons également constaté que les AF-20 et VF+AF-20 ne convenaient pas aux pommes avec ou sans prétraitement CEP en raison de leur plus grande porosité et de leurs parois

cellulaires plus fines. La faible perte d'eau et la préservation élevée de la texture et de la microstructure des disques de pomme de terre et de carotte démontrées dans la congélation combinée VF+AF-20 prouvent que ce protocole de congélation peut être appliqué aux fruits et légumes à faible porosité et à structure initiale rigide.

Mots clés : Congélation sous vide; Congélation conventionnelle à l'air ; Fruits et légumes; Attributs de qualité ; Champ électrique pulsé ; Applicabilité

TABLE OF CONTENTS

General Introduction	1
Chapter I Literature Review	8
I.1 Freezing of fruits and vegetables	8
I.1.1 Composition and structure of plant cells.....	9
I.1.2 Freezing process.....	17
I.1.3 Freezing damage	21
I.1.4 Factors affecting the quality of frozen fruits and vegetables	23
I.2 New trends in freezing technology.....	45
I.2.1 Pressure-related freezing.....	46
I.2.2 Electric field (EF) and magnetic field (MF) assisted freezing	53
I.2.3 Ultrasound-assisted freezing	62
I.3 Conclusion and research objectives	64
Chapter II Materials and methodology	86
II.1 Introduction.....	86
II.2 Construction of vacuum freezing system.....	87
II.3 Freezing protocols.....	89
II.3.1 Vacuum freezing.....	91
II.3.2 Conventional air freezing.....	91
II.3.3 Freezing procedures for verification of the temperature range of the application of vacuum freezing	92
II.4 PEF pretreatment	93
II.5. Characterization techniques	94
II.5.1. Force relaxation tests	94
II.5.2. Moisture loss.....	94
II.5.3. Scanning electron microscopy (SEM)	95
II.6. Statistical analysis.....	95

Chapter III Application of vacuum freezing to improve the quality of thawed carrot discs.....	97
III.1 Chapter introduction	97
III.2 Results	98
III.2.1 Application of vacuum freezing to improve the quality of thawed carrot discs	98
III.2.2 Determination of the equivalent air freezing parameters of vacuum freezing	120
III.3 Chapter conclusion	125
Chapter IV Pulsed electric field assisted combined freezing of carrot tissue: Preliminary vacuum freezing followed by supplementary conventional freezing	127
IV.1 Chapter introduction.....	127
IV.2 Results	127
IV.3 Chapter conclusion	145
Chapter V Effect of pulsed electric field assisted combined vacuum freezing on quality attributes of thawed carrots, potatoes, and apples	146
V.1 Chapter introduction	146
V.2 Results	147
V.3 Chapter conclusion	158
General conclusion and prospects	161
Annexe.....	164

General Introduction

The COVID-19 pandemic further highlights the importance of humans' relationship with nature. Moreover, since the Russia-Ukraine war in 2022, the situation has dramatically escalated into a full-blown global energy crisis. In this context, promoting and accelerating the goal of sustainable development has become our primary concern. To achieve sustainable development with a balance between economic growth and environmental protection, a critical approach to this issue is to reduce food loss and waste (FLW) (Magalhães, Ferreira, & Silva, 2022). In developed countries, FLW is generated at the distribution and consumption stages of the food supply chain. In contrast, a significant portion of FLW is lost in the production and post-harvest steps in developing countries, which is primarily owed to the deterioration of perishable crops in warm and humid. Studies conducted by various international and national organizations led by the FAO indicated that about one-third of global edible food (1.3 metric billion tons (MT)) is lost and not consumed annually (Porat, Lichter, Terry, Harker, & Buzby, 2018; Y. Wang, Yuan, & Tang, 2021). In other words, large amount of cultivated products have already been lost before they reach the consumption stage. Fruits and vegetables are the most wasted products, partly due to their higher production than required, and also due to their short shelf life because of high water content. In addition to classical postharvest management operations, further development and implementation of novel techniques in food preservation is crucial to reduce FLW, which can maintain the quality of the product from the time it leaves the grower until it is consumed.

Historically, people have started to preserve food thousands of years ago. Even today, when people encounter harsh conditions, hoarding durable foods has become a priority, which is called “searching for ways to preserve life by preserving food” (Knorr & Augustin, 2022). Common industrial processes for food preservation, including heating, dehydration, concentration, packaging, cooling, freezing, etc., all have the purpose of slowing down or stopping (killing) endogenous or exogenous bacterial spoilage activity. It is well known that it is the main reason for food deterioration. Among these methods, freezing has been one of the most versatile and convenient techniques for food preservation which can greatly extend preservation duration across time and geography. As early as 1000 BC, people were already using

winter frost, ice cellars, and compressed snow in insulated cellars for natural food freezing. In the 1930s, Clarence Birdseye pioneered the modern frozen food industry (Ojha, Kerry, Tiwari, & O'Donnell, 2016). Subsequently, food freezing has rapidly evolved, with more consideration for improving process efficiency, and productivity, reducing costs, and improving the post-freeze quality of food products. With the changes in consumers' lifestyles, the demand for low-processed, additive-free, natural foods and convenience foods is growing, which provides opportunities and drives positive growth in the frozen food market. It is estimated that the frozen food market will continue to increase, growing from \$291.8 billion in 2019 to \$404.8 billion by 2027 (Wire, 2021).

The freezing process involves the transfer of heat from the food to the surrounding cryogenic medium or environment, accompanied by the reduction in temperature that converts the internal freezable water into ice crystals. Under low temperatures and low water activity, biochemical changes are retarded, growth of microorganisms and enzymatic activity are inhibited. Compared to other thermal processes, chemical preservation, and fermentation processes, food freezing can better preserve its original qualities, such as nutritional value, organoleptic properties, etc. However, improper freezing conditions may also cause some undesirable effects. There are many factors prior to, during, and after the freezing process that impact the final quality of the food products. First of all, the initial quality of the product determines the highest quality that frozen food can achieve. During the freezing process, high-quality products rely on a hygienic equipment environment, appropriate freezing rate, suitable packing and handling conditions. The subsequent transportation and storage conditions also matter.

Conventional freezing methods (air blast freezing, immersion freezing, and plate freezing) are mainly classified according to the material of the freezing medium (air, liquid, and metal plate) (Muthukumarappan, Marella, & Sunkesula, 2019). For the aim of better preservation by freezing, a large number of studies have been investigated on the basis of conventional freezing. One approach is by prior altering the freezable water content of the food itself, which can be achieved by partial dehydration or the introduction of cryoprotectant agents. Fluidized bed freezing, impingement freezing, etc. can directly help intensify the freezing process. However, the core principle of these methods is to improve the surface heat transfer efficiency by increasing the contact or convection between the sample and the freezing medium.

As is known, the process of cooling and freezing has already been energy intensive and a major source of greenhouse gas emissions (Wróbel-Jędrzejewska & Polak, 2022). For new technologies to improve food freezing, they are expected to be more energy efficient and environmentally friendly. Recently, some innovative technologies have also been applied in food freezing, including high-pressure, ultrasound, magnetic fields, electric field, microwave, and radio-frequency, which all present a great potential for improving product quality and freezing process efficiency (Sutariya & Sunkesula, 2021). Moreover, naturally sourced bio-substances also positively affected food freezing by regulating the freezing point. However, all of the above methods require cryogenic medium, and they involve either high energy consumption, introduction of foreign substances, or high costs.

As a rapid freezing technology, vacuum freezing can reduce the temperature according to the principle of water evaporation under low pressure, which is totally different from previous freezing methods with the necessity of a cryogenic medium. It has the characteristics of high efficiency, hygiene, and energy-saving, increasingly attracting interest in the food industry. Vacuum cooling with the same cooling principle has been widely used in post-harvest pre-cooling of porous and high-moisture fruits and vegetables. It has shown significant advantages over conventional cooling methods in studies on the pre-cooling of lettuce, cabbage, cauliflower, broccoli, etc. (Zhu, Geng, & Sun, 2019). However, because the freezing process concerns the more complex mass and heat transfer of water into ice, current research in vacuum freezing has mainly focused on mathematical simulation and visualization of simple matrices such as water, liquid droplets, etc. (Cheng & Lin, 2007; Cogné, Nguyen, Lanoisellé, Van Hecke, & Clause, 2013; Peng, et al., 2023). More practical applications are limited to induced nucleation, especially prior to freeze-drying, to improve inter- and intra-vial product homogeneity in the pharmaceutical industry (Arsiccio, et al., 2020; Oddone, Van Bockstal, De Beer, & Pisano, 2016). A recent study also showed that vacuum freezing with pre-added external water (30%) could achieve better quality apple slices than traditional contact freezing (H. Wang, et al., 2022), which revealed the great prospects of vacuum freezing for improving the freezing process of fruits and vegetables. However, the large temperature decrease induced by vacuum freezing is achieved at the expense of a large loss of moisture, as more and more water evaporates or freezes, the water within the product that can

continue to evaporate to maintain the reduction in temperature is more limited. Therefore, relevant research on the effective application of vacuum freezing within a specific temperature range is necessary and has not yet been studied. Also, the applicability of vacuum freezing for better quality attributes of food samples with different raw materials and sizes has not been proven yet. For food samples with complex compositions, the heat and mass transfer theory of the vacuum freezing process also needs to be further explored. On this basis, approaches to intensify vacuum freezing (pulsed electric field pretreatment or pre-addition of external water) deserve further investigation.

Therefore, the objective of this thesis is to intensify the freezing of fruits and vegetables with the application of vacuum freezing. In addition, this study also focused on the effects of pulsed electric field pretreatment and pre-addition of external water on vacuum freezing and the final quality attributes of the fruits and vegetables. This study will improve the understanding of the complex mechanisms of mass and heat transfer during vacuum freezing of fruits and vegetables. The result will provide insights and theoretical support for the freezing process of fruits and vegetables with VF, also further expanding the industrial application of vacuum freezing in food and other industries. The manuscript of this dissertation consists of the following five chapters:

Chapter I presents an overview on the freezing process of fruits and vegetables, approaches and techniques to improve food freezing, effects of the freezing and thawing process on final quality and characterization of freezing damage, and also concludes on the objective of this work;

Chapter II explains the different experimental equipment, methodology and protocols used in this thesis;

Chapter III is composed of two parts. The first part investigated the effective application temperature range of vacuum freezing and its effect on the quality attributes of thawed carrot disc. The second part involves the prediction of the freezing time for the specific shape of the carrot disc, which can be applied for better comparison of the air freezing and vacuum freezing or even other innovative freezing techniques.

Chapter IV introduces the PEF pretreatment, which can theoretically enhance the heat and mass transfer processes through electroporation. The PEF treatment with different cell disintegration index (0-0.9) is applied before three freezing protocols, including P₁ continuous vacuum freezing, P₂ conventional air freezing at -20 °C, and combined freezing P₃ (vacuum freezing from 2 to -6 °C, followed by conventional air freezing at -20 °C from -6 to -20 °C). The texture, water loss, and microstructure of thawed carrot discs after P₂ and P₃ is also discussed.

Chapter V presents the comparison of different species of fruits and vegetables when they are subjected to the same PEF pretreatment and freezing protocols. The applicability of combined freezing P₃ in fruits and vegetables of different compositions and structures has been studied.

Finally, general conclusions related to this work review the main results obtained from the conducted research and present some suggestions for further work.

- Arsiccio, A., Matejtschuk, P., Ezeajughi, E., Riches-Duit, A., Bullen, A., Malik, K., Raut, S., & Pisano, R. (2020). Impact of controlled vacuum induced surface freezing on the freeze drying of human plasma. *International Journal of Pharmaceutics*, 582, 119290. <https://doi.org/10.1016/j.ijpharm.2020.119290>
- Cheng, H. P., & Lin, C. T. (2007). The morphological visualization of the water in vacuum cooling and freezing process. *Journal of Food Engineering*, 78(2), 569-576. <https://doi.org/10.1016/j.jfoodeng.2005.10.025>
- Cogné, C., Nguyen, P. U., Lanoisellé, J. L., Van Hecke, E., & Clausse, D. (2013). Modeling heat and mass transfer during vacuum freezing of puree droplet. *International Journal of Refrigeration*, 36(4), 1319-1326. <https://doi.org/10.1016/j.ijrefrig.2013.02.003>
- Knorr, D., & Augustin, M. A. (2022). Preserving the food preservation legacy. *Critical Reviews in Food Science and Nutrition*, 1-20. <https://doi.org/10.1080/10408398.2022.2065459>
- Magalhães, V. S. M., Ferreira, L. M. D. F., & Silva, C. (2022). Prioritising food loss and waste mitigation strategies in the fruit and vegetable supply chain: A multi-criteria approach. *Sustainable Production and Consumption*, 31, 569-581. <https://doi.org/10.1016/j.spc.2022.03.022>
- Muthukumarappan, K., Marella, C., & Sunkesula, V. (2019). Chapter 15 - Food Freezing Technology. In M. Kutz (Ed.), *Handbook of Farm, Dairy and Food Machinery Engineering (Third Edition)* (pp. 389-415): Academic Press.
- Oddone, I., Van Bockstal, P.-J., De Beer, T., & Pisano, R. (2016). Impact of vacuum-induced surface freezing on inter- and intra-vial heterogeneity. *European Journal of Pharmaceutics and Biopharmaceutics*, 103, 167-178. <https://doi.org/10.1016/j.ejpb.2016.04.002>
- Ojha, K. S., Kerry, J. P., Tiwari, B. K., & O'Donnell, C. (2016). Freezing for Food Preservation. In *Reference Module in Food Science*: Elsevier.
- Peng, R., Liu, J., Yang, Z., Liu, S., Wang, W., Zhai, H., Sun, J., & Cao, W. (2023). Study on the response law between cooling rate and temperature with process parameters during vacuum freezing of liquid. *Vacuum*, 213, 112040. <https://doi.org/10.1016/j.vacuum.2023.112040>
- Porat, R., Lichter, A., Terry, L. A., Harker, R., & Buzby, J. (2018). Postharvest losses of fruit and vegetables during retail and in consumers' homes: Quantifications, causes, and means of prevention. *Postharvest Biology and Technology*, 139, 135-149. <https://doi.org/10.1016/j.postharvbio.2017.11.019>
- Sutariya, S. G., & Sunkesula, V. (2021). 3.03 - Food Freezing: Emerging Techniques for Improving Quality and Process Efficiency a Comprehensive Review. In K. Knoerzer & K. Muthukumarappan (Eds.), *Innovative Food Processing Technologies* (pp. 36-63). Oxford: Elsevier.
- Wang, H., Xue, Y., Hu, Z., Ba, L., Shamim, S., Xie, H., Xia, T., & Zhao, R. (2022). Addition of external water improves the quality attributes of vacuum-frozen and thawed apple slices. *International Journal of Refrigeration*. <https://doi.org/10.1016/j.ijrefrig.2022.01.027>
- Wang, Y., Yuan, Z., & Tang, Y. (2021). Enhancing food security and environmental sustainability: A critical review of food loss and waste management. *Resources, Environment and Sustainability*, 4, 100023. <https://doi.org/10.1016/j.resenv.2021.100023>
- Wire, B. (2021). Frozen food market by product type and user: global opportunity analysis and industry forecast, 2020–2027. In.

- Wróbel-Jędrzejewska, M., & Polak, E. (2022). Determination of carbon footprint in the processing of frozen vegetables using an online energy measurement system. *Journal of Food Engineering*, 322, 110974.<https://doi.org/10.1016/j.jfoodeng.2022.110974>
- Zhu, Z., Geng, Y., & Sun, D.-W. (2019). Effects of operation processes and conditions on enhancing performances of vacuum cooling of foods: A review. *Trends in Food Science & Technology*, 85, 67-77.<https://doi.org/10.1016/j.tifs.2018.12.011>

Chapter I Literature Review

I.1 Freezing of fruits and vegetables

Fruits and vegetables are excellent sources of essential nutrients such as vitamins, minerals, antioxidants, and many phytonutrients (plant-derived micronutrients), playing a decisive role in a balanced diet with numerous health benefits (Grover & Negi, 2023). In contrast to animal-derived foods, fruits and vegetables are considered living entities even postharvest, as they continue to respire and perform a variety of metabolic processes at the cellular level (Jha, Xanthakis, Chevallier, Jury, & Le-Bail, 2019). Therefore, proper preservation before consumption is crucial to protect the integrity of cell structure as well as the viability of cells for plant cellular foods.

The biological processes, including respiration, ripening, and senescence, are self-consumption of fruits and vegetables, leading to loss of quality and a shorter shelf life. In addition, their high moisture content also makes it difficult for them to maintain their quality for long time in non-interventionist conditions. Water content of most of the fruits and vegetables ranges from 70% to 95%, except for 10% to 20% of the weight in wet crops and dry crops, respectively (Sumonsiri & Barringer, 2014). Wet foods are generally much more unstable than dry foods because the water remaining in wet foods has higher activity. Since fresh produce is not sterile, the high moisture content is quite conducive for microbial activity and enzymatic reactions inside the cells, which, if supplemented with the appropriate temperatures, can very easily lead to the deterioration and spoilage of fruits and vegetables. To minimize food loss and waste caused by improper storage of fruits and vegetables after harvest, as well as to obtain high-quality fruits and vegetables independent of time and geography, it is essential to find efficient, simple and low-cost preservation methods.

Freezing is a widely used unit operation involving the removal of latent heat and ice crystallization under low temperatures, which plays an important role in long-term food preservation. It is regarded as the most suitable method to maintain the nutritional value and sensory attributes of fresh fruits and vegetables. On the one hand, low temperatures decrease metabolic activity and also inhibit microbial activity. Also, due to the solidifying of water in fruits and vegetables, the water necessary for microbial growth, biochemical and physicochemical reactions is under mobility

restrictions and is no longer available, inhibiting the growth of deteriorative and pathogenic microorganisms (Augusto, Soares, & Castanha, 2018). Although various reactions inside the food slow down at low temperatures, the relevant enzymes and microorganisms are still in a latent state, but not completely “frozen to death”. Therefore, stable storage environments and cold chain temperatures are usually required to succeed freezing for better quality assurance until it is consumed.

I.1.1 Composition and structure of plant cells

Plant-based foods, often referred to as fruits and vegetables, are composed of a very diverse food group. Under the “fruits and vegetables” category, humans regularly consume many different plant species and different plant tissues obtained from roots, shoots, leaves, fruits, seeds, and flowers (Berry, Fletcher, McClure, & Wilkinson, 2008). Prior to discussing the freezing process of fruits and vegetables, it is necessary to understand their composition as well as the nature and features of their cellular structure, since it involves the depolymerization of the cell wall, the rupture of the cell membrane, the alteration of osmotic pressure, etc. (D. Li, Zhu, & Sun, 2018), affecting significantly the quality and physiochemical property of foods.

Fruits and vegetables provide a rich array of vitamins, minerals, fiber, antioxidants, and phytochemicals. [Table I. 1](#) lists the composition of several raw fruits and vegetables.

Table I. 1: Composition of several raw fruits and vegetables (per 100 g of raw fruits and vegetables with skin) (Sumonsiri, et al., 2014).

Fruit/ vegetable	Water (g)	Carbohydrate (g)	Protein (g)	Fat (g)	Vitamin C (mg)	Thiamin (mg)	Potassium (mg)
Apple	85.56	13.81	0.26	0.17	4.6	0.017	107
Tomato (ripe)	94.52	3.89	0.88	0.20	13.7	0.037	237
Potato	83.29	12.44	2.57	0.10	11.4	0.021	413
Green beans	90.32	6.97	1.83	0.22	12.2	0.082	211
Apricot	86.35	11.12	1.40	0.39	10.0	0.030	259
Strawberries	90.95	7.68	0.67	0.30	58.8	0.024	153
Carrot	88.29	9.58	0.93	0.24	5.9	0.066	320
Avocado	73.23	8.53	2.00	14.66	10.0	0.067	485

Among these, water is the most abundant component, which is also the main factor involved in the freezing damage, either directly or indirectly. In a broad classification, water in food materials can be classified as free and bound water (Joardder, Kumar, &

Karim, 2017). As the name implies, free water refers to water that is relatively free to diffuse and transport in plant foods, whereas bound water is water that is physically confined in a restricted environment. Furthermore, it is reported that bound water can be frozen only at very low temperatures, or even unable to freeze because bound water is the proportion of water in a system associated with the colloid phase with such strength that it is no longer available to act as a solvent or to be separated from the colloid phase by freezing (Briggs, 1932; Khan & Karim, 2017). Based on the spatial distribution of water, it is defined that water in the intercellular space is free water, water inside the cell is intracellular water, and water occupying the fine space inside the cell wall is called cell wall water (Khan, Nagy, & Karim, 2018). According to the close degree of water and matter bonding, the water in fruit and vegetable is divided into free water, immobile water and bond water. They respectively correspond to water located in the vacuole (as the solvent of some low weight compounds) and extracellular compartment, water in the cytoplasm that is weakly bound to macromolecules (e.g. the cytoskeleton proteins and enzyme or other components in cytoplasm), and water strongly bound to cell-wall polysaccharides in material tissue. In the LF-NMR transverse relaxation measurements of fresh *Hericium erinaceus*, three proton peaks (T_{21} , T_{22} , and T_{23}) were observed (Fig. I. 1), indicating the presence of the three moisture species with different mobility in the mushroom (Zhong, et al., 2024). For example, in carrots, the ratio of free water, immobile water and bound water were measured to be 86.32%, 10.20 and 3.48% respectively (Sun, Zhang, & Yang, 2019). During the freezing process, in addition to the mechanical damage caused by the formation of ice from water, the migration of moisture is also one of the factors affecting the final quality of the product, which concerns the self-diffusion coefficient (D_w) of water in plant-based food systems. Generally, vacuole water shows the biggest D_w , followed by cytoplasm and extracellular water, and then cell wall water (D. Li, et al., 2018). These are in turn closely related to other components in the plant cell.

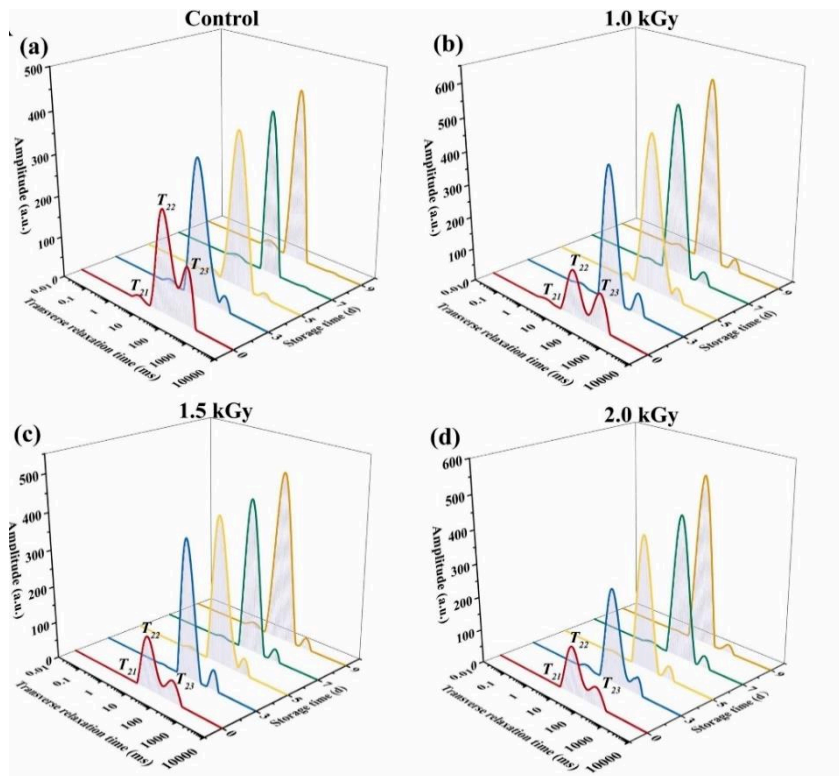


Fig. 1. 1: Changes in Transverse relaxation time (T_2) curves of different water components in postharvest *H. rinaceus* with different irradiation treatments during storage (Zhong, et al., 2024).

The largest proportion of dry basis in fruits and vegetables is carbohydrates, including starches, sugars, dietary fibers (Sumonsiri, et al., 2014). Starch content in fruits and vegetables varies greatly depending on the species (e.g., starch accounts for approximately 60 to 80% of the dry matter in potatoes, but only about 12% in carrots) (Brar, Bhatia, Pandey, & Kumari, 2017; Nagraj, Jaiswal, Harper, & Jaiswal, 2020). Sugars, such as fructose, glucose, and sucrose, contribute to the sweet taste of fruits, while vegetables generally contain lower levels of sugars. According to the solubility in water, dietary fiber can be divided into soluble dietary fiber (pectin, gum, and mucilage) and insoluble dietary fiber (cellulose, hemicellulose, and lignin), which provide structural rigidity to the plant cell wall (Cui, et al., 2019; Hussain, Jōudu, & Bhat, 2020). Although both are composed of many sugar units bonded together, however, unlike most starches, these bonds in dietary fiber cannot be broken down by digestive enzymes and enter the large intestine relatively intact (Slavin & Lloyd, 2012). There, fiber can be fermented by the colonic microflora to gases such as hydrogen and carbon dioxide while producing some SCFA that can be absorbed and used as energy in the body, or it can pass through the large intestine and bind water, increasing stool weight. While animal products have long been recognized as primary

protein sources, proteins from fruits and vegetables have also shown their ability for protein fortification and complementation (M. Kumar, et al., 2022), as well as meeting daily protein requirements in vegetarian and vegan diets, with relatively high levels in beans, nuts, and seeds. Vitamins such as C, A, K, and various B vitamins are essential for metabolism, immune function, vision, and overall health, but they can only be obtained from foods, especially fruits and vegetables, as the body is unable to synthesize these vitamins (Köprüalan Aydın, Baysan, Altay, İlder Baysan, Kaymak Ertekin, & Jafari, 2023). Minerals like potassium, magnesium, calcium, iron, and zinc play pivotal roles in bone health, nerve function, and enzymatic activities. Fruits and vegetables are rich sources of the aforementioned carbohydrates, fiber, some micronutrients (vitamins, minerals), and a wide array of phytochemicals that individually, or in combination, benefit human health. This is why health authorities worldwide, such as the World Health Organization (WHO), promote high consumption of fruits and vegetables, recommending daily intake of more than 400 g per person (Yahia, García-Solís, & Celis, 2019).

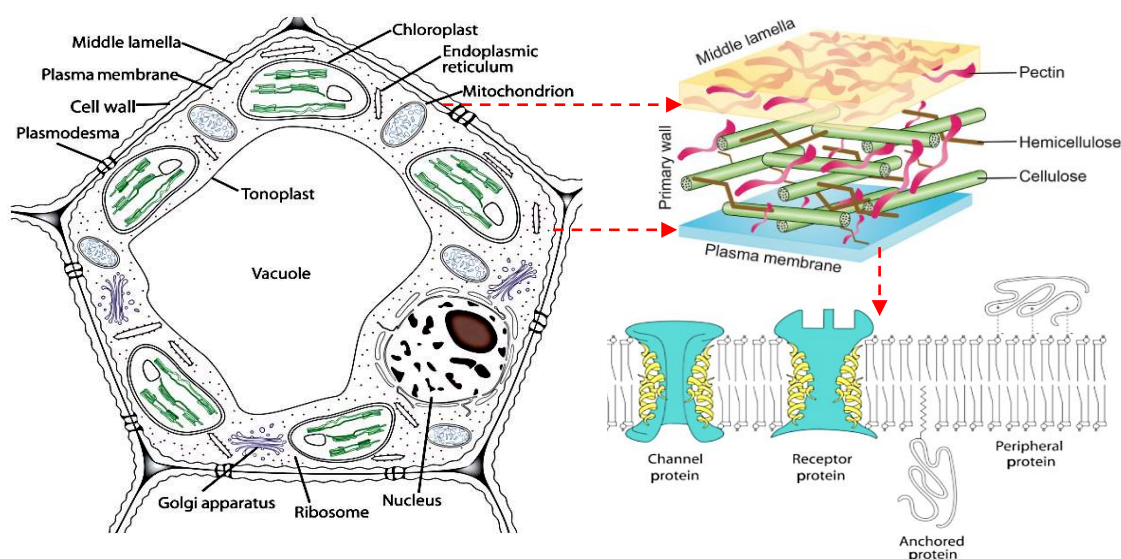


Fig. I. 2: Components of a plant cell, schematic illustration of the plant primary cell wall architecture and its major polysaccharides, and schematic diagram of the structure of the plasma membrane (C. Li, Hu, & Zhang, 2021; Mac Adam, 2009).

Biochemically, the major compositions above-mentioned are distributed in specific locations in plant cellular to play significant roles in structure, stability, and nutritional value of thousands of fruits and vegetables. Although they differ in overall appearance (morphology), plants have the same basic unit of structure at the cellular

level (Mac Adam, 2009). These basic units correspond to different compartments. They are relatively independent and connected, arranged together and well-organized to form the tissue with some small air gaps (1-25%). The majority of the cellular organization of the edible portion of fruits and vegetables is composed of parenchyma cells (Fig. I. 2), which are typically rectangular, spherical, or polyhedral in shape, with equivalent diameters ranging from 30 to 300 μm (D. Li, et al., 2018). Usually, plant cells are composed of two parts: cell wall and protoplast, where protoplast is the part of the cell other than the cell wall, mainly including the nucleus and cytoplasm. The principal structural components of the plant cell and their respective functions are briefly shown in Table I. 2 (Verma & Joshi, 2000).

Table I. 2: Cellular components of a plant cell (Verma, et al., 2000).

Components (size)	Compositions	Functions
1. Cell wall		
A. Middle lamella	Mainly pectin	It acts to bind adjacent cells together. And this pectin layer is important for the mechanical strength and porosity of the wall, as well as the cell wall slippage, extension, and intercellular signaling.
B. Primary cell wall (1-3 μm thick)	Cellulose (9-25%), Hemicelluloses (25-50%), pectic substances, structural proteins and glycoproteins (10%)	It stretches plastically during cell growth and allows the free passage of water and materials dissolved in water.
C. Secondary cell wall (4 μm or > 4 μm thick)	Cellulose (45%), hemicelluloses (30%), and lignin (22-28%)	It provides flexibility for the movement of cell walls and the structural support to the plants.
D. Plasmodesmata (30-100 nm in diameter)		A small opening present in the cell walls that connects the cytoplasm of neighboring plant cells, thus establishing a living bridge/channel between cells.
2. Protoplast (contents of the cell without cell wall)		
A. Cytoplasm		
i). Plasma membrane/ cytoplasmic membrane/ plasmalemma (10 nm thick)	Lipids (phospholipids) and proteins	They are selectively permeable membranes that enclose the living contents of the cell and control the movement of materials (mainly water and solute) into and out of

ii). Vacuolar membrane/tonoplast (7.5 nm thick)		the cell, relating to the cell and organ turgor, and metabolic compartmentation.
iii). Microtubules (24-25 nm thick)	Sub-units of a protein known as <i>tublin</i>	Microtubules are long hollow cylinders, found in cytoplasm near the plasmalemma and display an important role in cell wall formation especially in cell division and movements of or within cells.
iv). Microfilaments (5-7 nm thick)	Different types of protein from that found in microtubules	Microfilaments are small solid structures. These units are responsible for cytoplasmic streaming (a flow of cytoplasm around the inside of plant cells) and ameboid movements in fungi.
v). Endoplasmic reticulum (ER) (7.5 nm thick)	Phospholipid membrane	It is a network of interconnecting membrane surfaces of tubules within the cytoplasm and forms a system of transport for various molecules (e.g., proteins, lipids, hormones) within the cell and even between the cells via plasmodesmata.
vi). Ribosomes (0.025 μ m in diameter)	Ribosomal RNA (rRNA) molecules and ribosomal proteins (RPs or r-proteins)	Thousands of free ribosomes also occur in the cytoplasm form, often as a chain like string of beads, which are called polyribosomes or polysomes, and each is held together by strand of mRNA, the genetic information of which is being translated into a protein. Some identical ribosomes are also attached to the cytosol side of the outer membranes that surrounds the nucleus.
vii). Golgi bodies (Dictyosomes) (0.5-2.0 μ m in diameter)		It has the appearance of series of staked flattened vesicles that bud-off smaller vesicles. Golgi bodies are believed to be involved in the synthesis of cell wall by synthesizing polysaccharides and plasma membrane constituents (phospholipids and glycoproteins).
viii). Mitochondria (1-5 μ m in diameter)	Phospholipid bilayers and proteins	Mitochondria are the sites of much chemical activity in cells perhaps over half of the cell's metabolism. Mitochondria contains the respiratory enzymes of the tricarboxylic acid (<i>TCA</i>) cycle and the <i>respiratory electron system</i> . After a series of biochemical reactions, it generates the energy in the form of adenosine triphosphate (ATP). Thus, it is also called as the power house of the cell.
ix). Plastids	Chloroplast (about 50%)	Plastids are membrane-bound organelles found in the cells of plants, algae, and some

	protein, 50-55% lipid, and small amounts of nucleic acids)	other eukaryotic organisms. They often contain pigments used in photosynthesis, and the types of pigments in a plastid determine the cell's color, including chloroplasts (used for photosynthesis), chromoplasts (used for pigment synthesis and storage), and leucoplasts (non-pigmented plastids that can sometimes differentiate).
x). Microbodies (1-5 μm in diameter)	Phospholipid bilayer membrane and intracellular material including enzymes and other proteins	Microbodies contain enzymes that participate in the preparatory or intermediate stages of biochemical reactions within the cell. Generally, microbodies are involved in detoxification of peroxides and in photorespiration in plants.
xi). Spherosomes (0.1-1 μm in diameter)	Phospholipid monolayer, fat and protein	These are fat bodies derived from ER and are responsible for fat synthesis and storage.
B. Vacuoles	water, inorganic salts, organic acids, oil droplets, sugar, water soluble pigments, amino acids, vitamins, etc.	These are the reservoir of the cell and may occupy as much as 80-90% of the cell volume. The vacuoles enlarge during growth, and this enlargement occurs by water uptake. Defined by a membrane called the tonoplast, vacuoles are filled with water containing a variety of inorganic ions, sugars, amino acids, organic acids, gums, mucilages, tannins, flavonoids, phenolics, pigments and other nitrogenous compounds.
C. Nucleus (5-20 μm in diameter)	Protein, lipid and the nucleic acids RNA and DNA	This is the largest organelle of the cell and considered as the site for having all the genetic information about the cell. The cytoplasmic RNA (mRNA) exported from DNA directs the systems of specific proteins required for chemical reactions.
D. Ergastic substances	calcium oxalate tannins, fats, carbohydrates and proteins	Ergastic substances (crystals like calcium oxalate tannins, fats, carbohydrates and proteins) are stored by the various components of plant cell and known as the products of protoplasmic activity.

Different from animals, plants do not have skeletal systems. The mechanical and structural properties of fresh plant-based foods, such as firmness, hardness, toughness, and stiffness are mainly determined by the strength of cell wall and the adhesion between cells (Cen, Lu, Mendoza, Beaudry, & Technology, 2013). The plant cell wall is located in the outermost layer of the cell, wrapped like a protective shell around the

protoplast. On the one hand, the plant cell wall is supposed to be hard enough to provide protection for cell rigidity; on the other hand, it also needs to be sufficiently flexible to withstand osmotic pressure generated by the difference in solute concentration between the interior and exterior cell, as well as the enormous tensile and compressive forces from the external environment (C. Li, et al., 2021). The specific architecture and chemical compositions assist in these functions. The plant cell wall is consisting of the primary and secondary cell wall, and the middle lamella, with some small openings called plasmodesmata connecting the neighbor cells. Generally, fruits and vegetables lack secondary cell wall, but if present, they are in order from outside to inside, middle cell lamella, primary cell wall, and secondary cell wall (Jackman & Stanley, 1995; Jha, et al., 2019). Chemically, the plant cell wall is a complex assembly of (mostly) polysaccharides, including cellulose, hemicelluloses, and pectins, as well as structural proteins and phenolic compounds (X. Hu, Zhang, Hamaker, & Miao, 2022; C. Li, et al., 2021). Among these, cellulose imparts rigidity and tearing resistance to the cell wall, while pectic substances and hemicelluloses provide plasticity and the ability to stretch, as glue connecting neighboring cells, thus significantly impacting on intercellular adhesion (Jha, et al., 2019; D. Li, et al., 2018). Remarkably, the plant cell wall is a considerable hindrance in food processing such as extraction, drying, and freezing, as it is one of the major factors in slowing down heat and mass transfer.

The plasma membrane lies on the interior of the cell wall. It is mainly composed of lipids (phospholipids) and proteins. The lipid bilayer of the plasma membrane self-assembles from phospholipids, which have hydrophilic, glycerol-containing “heads” oriented outward, and hydrophobic fatty acid “tails” oriented inward (Fig. I. 2). Membrane proteins may extend through the lipid bilayer to act as channels or receptors (green), or they may be bonded to or embedded in the inner or outer surface. Plasma membrane, as well as the vacuolar membrane, separates the cytoplasm from the external environment and the tonoplast surrounding the vacuole. The selective permeability of these membranes also tightly controls the flow of nutrients from the intra- and extracellular environment. Water, as well as oxygen and carbon dioxide gases, however, can cross the lipid bilayer of the plasma membrane relative easily (Mac Adam, 2009). There are multiple compartments that perform different functions within the cell, namely organelles. Because of the periodic contraction and diastole,

vacuole is specialized an osmoregulatory organelle that balances water flow into the cell (containing water, inorganic salts, organic acids, oil droplets, sugar, water soluble pigments, amino acids, vitamins, etc.) (Jha, et al., 2019). The nucleus is the location of the genetic material (DNA, deoxyribonucleic acid) contained in almost all cells. It directs the synthesis of the majority of enzyme production and is therefore considered the control center of the cell, since enzymes perform the work (or metabolism) of cells (Mac Adam, 2009). In addition, plant-based organelles also include microtubules, microfilaments, endoplasmic reticulum, ribosomes, Golgi bodies, mitochondria, plastids, microbodies, spherosomes, etc.

I.1.2 Freezing process

When the fruits and vegetables are exposed to low temperatures, heat is transferred to the cryogenic environment because of the temperature differences. In this kind of heat transfer relationship, the heat release is a function of temperature, in the case of constant pressure. There are two main contributions to the heat exchange as an object is cooled. One is the sensible heat, or specific heat, associated with the reducing temperature and reflects the changes in molecular motion and so on. The second source of heat is associated with phase changes. These changes in heat content are not necessarily related to temperature change. Indeed, for a pure material, e.g. pure water, the phase change may happen at a constant temperature. The change in heat content is associated with changes in the internal bonding and structure of the material. To properly account for the changes associated with the removal of heat and also to quantify the heat release to be expected as accompanying a particular temperature change, both sensible and latent heat changes during freezing process must be understood and estimated (Reid, 1997).

The typical freezing curves of water and food are shown in [Fig. I. 3](#) as a-b-c-d-e (water) and a-b'-c'-d'-e' (food). In broad terms, freezing comprises three stages: i) precooling (removing sensible heat); ii) phase transition (removal of the latent heat of crystallization of water); and iii) tempering (removing sensible heat) (Rondineli & Silva, 2024; Sutariya & Sunkesula, 2021).

This freezing process of pure water usually begins with a decrease in the temperature linearly below the initial freezing point of water (0 °C at atmospheric pressure). During this stage (a-b in [Fig. I. 3](#)), the water always remains in a liquid state. The

duration during which the temperature is below the freezing point is known as supercooling. It is necessary to overcome the free energy that accompanies the formation of a new phase (an ordered solid ice particle) from the melted phase (Chaves & Zaritzky, 2018). Pure water (free of impurities such as dust particles that would act as nucleation sites) can be supercooled to around $-40\text{ }^{\circ}\text{C}$ (Nesvadba, 2008). That means pure water can stay in the liquid phase to very low temperatures until the randomly fluctuating small ice nuclei accidentally reach a critical size and form a critical ice nucleus.

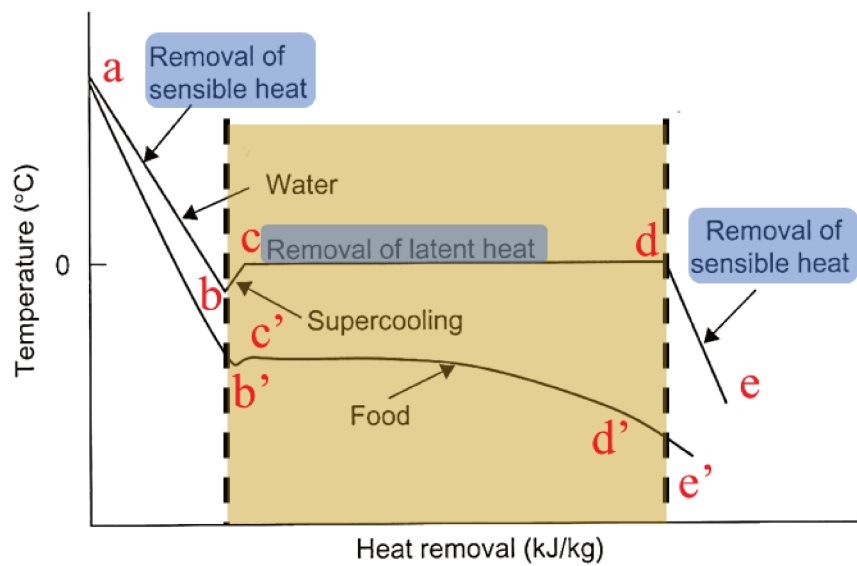


Fig. I. 3: Typical freezing curves of water and food.

The formation of critical ice nuclei is the key to nucleation (b in Fig. I. 3) (Bai, Gao, Liu, Zhou, & Wang, 2019). It acts as a “trigger point” for the instantaneous formation of a large amount of ice nucleation. Once nucleation begins, the water starts to freeze with the exothermic nature of this phase transition process (about 335kJ/kg) inducing an instantaneous rise in temperature to the freezing point (b-c in Fig. I. 3). The temperature of pure water is maintained at $0\text{ }^{\circ}\text{C}$ until all water freezes into ice (c-d in Fig. I. 3). In this phase of the coexistence of water and ice, the heat absorbed by the cryogenic medium and the latent heat of fusion released are equivalent.

When the phase change ends, the water completely turns into ice. While the volume increases by about 9%, the rate of heat diffusion in the ice also accelerates. Sensible heat is further removed until the temperature drops to cryogenic ambient temperature (d-e in Fig. I. 3).

For fruits and vegetables, although they undergo the same three stages as pure water, their freezing curves differ, as other components exist. During precooling, similar decrease in temperature can be found (a-b' in Fig. I. 3). However, unlike pure water, which requires a large degree of supercooling to produce homogenous ice crystals in the primary nucleation step, the supercooling degree can be smaller in food system because of the presence of solutes acting as nucleation promoters (heterogeneous nucleation) (Muthukumarappan, Marella, & Sunkesula, 2019). Moreover, it is important to note that, in food freezing, large thermal gradients are usually established between the outer side and center of the product (Sutariya, et al., 2021). When this occurs, supercooling and nucleation only take place at the product surface in contact with the refrigerant. The temperature rise caused by the crystallization of ice from surface generally impedes any subsequent nucleation at the center of the product.

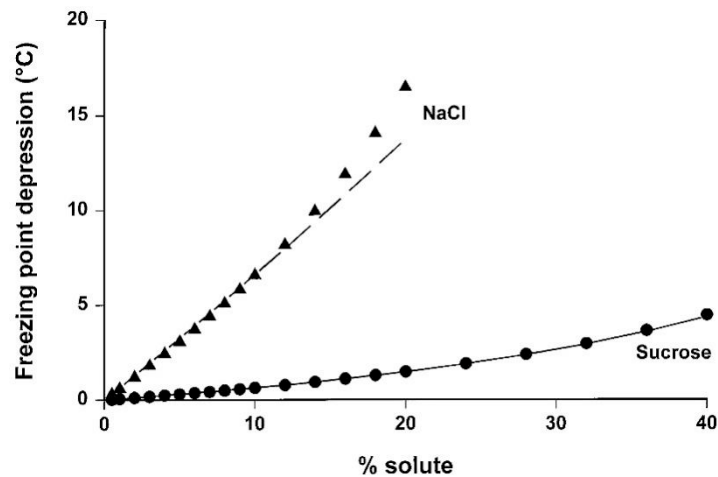


Fig. I. 4: Initial freezing point of sucrose and salt solutions (% solute by mass) (Christopher A. Miles, Mayer, Morley, & HousÆka, 1997).

When phase transition begins, the temperature reaches point c' in Fig. I. 3, the initial freezing point, which is no longer 0 °C as in water, but below 0 °C. The difference, named freezing point depression, can be affected by the solute concentration and hydrogen-bonded environment (Tian, Zhu, & Sun, 2020). Normally, higher molar solute concentration allows greater freezing point depression (Fig. I. 4). Since fruits and vegetables can be thought of as a kind of mixture of water and various solutes, this leads to the different freezing point reductions exhibited in different types of fruits and vegetables due to their different compositions. Due to the barriers of cell walls, cell membranes, plasma membranes, etc., aqueous solutions of different

concentrations are non-uniformly distributed in tissues. Transformation of some of the liquid water to ice results in a higher concentration of the solutes, which in turn lowers the freezing point and shows progressive decline in temperature (c'-d' in Fig. I. 3). There is no sharp phase transition at a constant temperature but rather a gradual "critical of freezing", starting at the temperature of the initial freezing point (Berk, 2009). This stage (shadow area in Fig. I. 3), especially in the freezing of fruits and vegetables, is the focal point of the whole process. Since it is usually the maximum ice crystal formation zone, the size, quantity, and distribution of the ice crystals formed during the freezing process are largely determined at this stage. Thus it dictates the efficiency of the freezing process and the quality of the frozen product, also known as the freezing critical zone (Jia, Chen, Sun, & Orlien, 2022). In the case of carrot tissue, for example, during freezing, crystallization has not started when the temperature of carrots drops to -1 °C, hence, the unfrozen water content is still 100%, while the unfrozen water drops rapidly to 20% at -6 °C (black curve in Fig I. 5). This means that 80% of water in carrots is frozen in such a small temperature range from -1 to -6 °C. Subsequently, the unfrozen water content of carrots stabilizes after -6 °C. This evolution is associated with the change in its enthalpy (red curve in Fig I. 5). Enthalpy is a thermal property of great importance in characterizing food products and processing systems. It is the heat content in a system per unit mass and hence the unit is J/kg in the SI system (Teferra, 2019). Since the freezing process is a process of removing heat, the temperature range (-1 to -6 °C) where large number of ice crystals are formed exhibits a relatively large enthalpy decrease as well. Therefore, when under fixed freezing conditions, the sample passes through this temperature range more slowly because more heat has to be removed. In addition, the latent heat of some other components of food such as carbohydrates, fats are also removed at this stage. But in most fruits and vegetables they are present in smaller amounts compared to water. Hence, the slight temperature rebound to the eutectic temperature is ignored in Fig. I. 3, which is related to the release of latent heat of crystallization of solutes that are supersaturated and crystallize in the food.

Finally, when all the freezable water is frozen, the sensible heat is further removed and the temperature drops further towards the temperature of the cryogenic medium (d'-e' in Fig. I. 3).

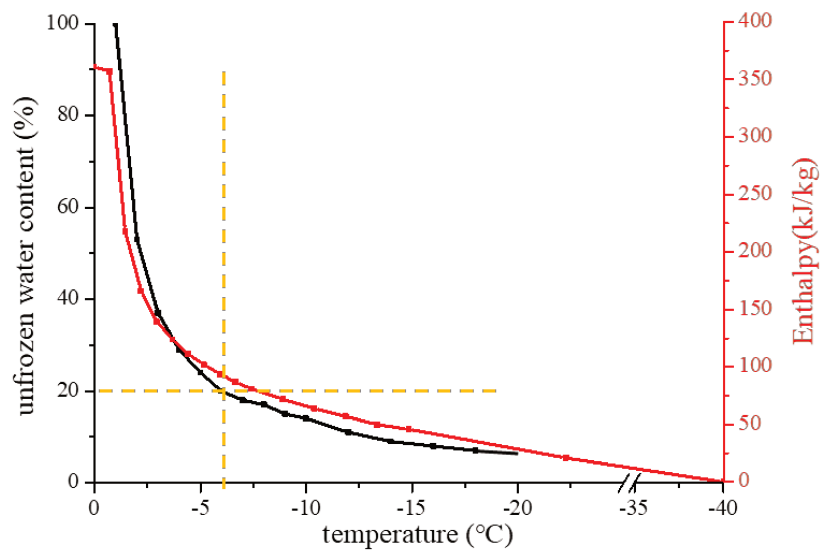


Fig. I. 5: Evolution of unfrozen water content (%) and enthalpy (kJ/kg) of carrot with temperature (Data from Rao et al.) (Rao, Rizvi, Datta, & Ahmed, 2014).

I.1.3 Freezing damage

Improper freezing in fruits and vegetables can cause a variety of harmful effects, including mechanical damage, cryoconcentration, freeze burn and recrystallization, which may subsequently result in the disruption of metabolic systems, dislocation of enzyme systems, cell membrane damage and eventually cell lysis (Mohsen Dalvi-Isfahan, Jha, Tavakoli, Daraei-Garmakhany, Xanthakis, & Le-Bail, 2019). Individually or in combination, these damages greatly affect the functionality and texture property of cellular food tissues, which are reflected in the deterioration of quality and sensory characteristics of the final product, including loss of nutrients, mass, flavor, texture and color. An understanding of the freeze damage and their formation processes can contribute to assist in minimizing unnecessary freezing damage as well as to the frozen product quality.

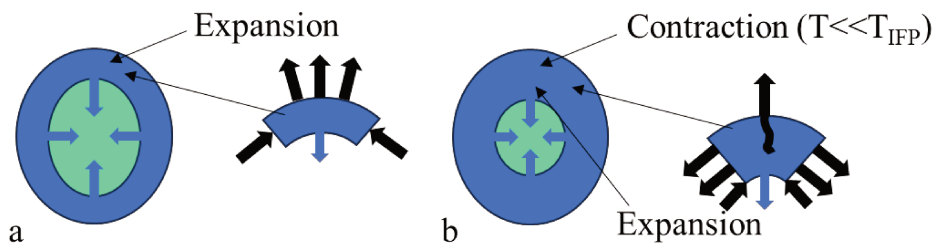


Fig. I. 6: Scheme presenting the expansion and compression (a) at start of freezing followed by tensile stress (b) due to ice contraction. Edited from (Mohsen Dalvi-Isfahan, et al., 2019).

Mechanical damage is one of the most important reasons for textural alterations during freezing of fruits and vegetables, which is greatly controlled by the integrity of the cellular structures and the original adhesion of adjacent cells (D. Li, et al., 2018). It is caused by combined factors including, but not limited to, 1) irreversible breakdown of the cellular structure (disruption of cell membranes and cell wall, releasing the degradative enzymes) caused by volume expansion of ice formation from unevenly distributed water, for example, the growth of adjacent ice crystals towards each other compresses the cell wall material in between, 2) freeze cracks induced by changes in types of stress between the surface and the core of the product during different freezing stages particularly at quite high freezing rates as occur during cryogenic freezing (from compression to tangential tensile stress in the outer surface) (Details are shown in [Fig. I. 6](#)).

Cryoconcentration (freeze concentration) is one of the common phenomena in freezing processes, especially slow freezing. Since freezing is not instantaneous, cellular water separated by cell walls and various cell membranes crystallize successively during the freezing process due to the concentration difference. Usually, the formation of ice crystals starts in the extracellular space and the central vacuole, because of a lower concentration and a relatively high freezing point. Besides, the cell wall surrounding the extracellular space, water can also serve as a site for initiating nucleation. The large volume of the vacuole, which occupies at least 80% of the cell, with a lower surface-to-volume ratio may also be the reason for the faster nucleation. If ice is crystallizing from a solution, water molecules diffuse from the surrounding solution to the surface of the ice crystals and are incorporated into the growing solid phase. At the same time, solute molecules must be rejected from the region occupied by the pure ice crystals and diffuse away from the solid surface (Zaritzky, 2010). Similarly, the formation of ice crystals in fruit and vegetables tissue reduces the amount of water used as the solvent, increasing the concentration of the solute and disrupting the original equilibrium. To return to equilibrium, unfrozen water nearby transfers to the frozen portion due to the difference in osmotic pressure. The concentration of the intracellular space further increases until all the freezable water is frozen. A slow freezing rate thus leads to differentiated crystallization of ice crystals between the intra and extracellular environment and redistribution of water. During this process, the pH value and ionic strength can be changed, and emulsion

breakdown or even protein denaturation may occur (Fellows, 2017). These irreversible damages make it difficult for the water to return to its original position, causing drip loss during the thawing process, and destructively impacting food quality.

Freezer burn mostly appears during frozen storage of unpackaged or poorly packaged fruits and vegetables. The reason for this occurrence is that the water vapor pressure (V_p) of the frozen product is greater than the ambient water vapor pressure inside the freezer (Schmidt & Lee, 2009). For equilibrating the water vapor pressure, ice sublimates from the surface of the fruits and vegetables. Freezer burn inevitably entails degradation of color, texture, and flavor as weight loss and exposure to oxygen increase over time in frozen storage (Mohsen Dalvi-Isfahan, et al., 2019; Kawai & Hagiwara, 2018).

Maturation (recrystallization) happens during frozen storage and transportation, especially temperature fluctuations after initial solidification is complete. Typically, the storage temperature is higher than the glass transition temperature of the food matrix, which means that moisture is still sufficiently mobile to diffuse through the unfrozen phase and cause changes in the morphology of the frozen phase (van der Sman, 2020). It is mainly characterized by an increase in the average size of the ice crystals, a decrease in their number (Chaves, et al., 2018). The driving force of this evolution is to minimize its energy level, obtain a more compact structure, and ultimately reach a state of equilibrium. This is similar to a spontaneous transition of electrons from a high energy state to a low energy state, since remaining in a higher energy state is unstable. Different types of recrystallizations have been observed during food storage but more attention has been paid to the Ostwald ripening, which is an isothermal process, where small size ice crystals with three or four sides show concave surfaces. In that case, the molecules are less surrounded than their neighbors on the other side of the interface and tend to escape because they are energetically more unstable (Mohsen Dalvi-Isfahan, et al., 2019). Recrystallization (coarsening) leads to further growth of the largest ice crystals, at the expense of smaller ice crystals, which reduces the advantages of fast freezing, inducing physio-chemical changes that alter the product quality.

I.1.4 Factors affecting the quality of frozen fruits and vegetables

Frozen fruits and vegetables undergo multiple steps from harvest to consumption, and their own and external processing procedures all have an impact on the final quality. Taking these factors into account, the operations at each stage can be optimized to obtain the best final fruits and vegetables for freezing.

I.1.4.1 Endogenous factors in fruits and vegetables

Factors originating from fruits and vegetables themselves mainly include: 1) raw materials type and variety; 2) condition and integrity of the materials. For instance, when we freeze apples and potatoes separately under the same conditions, the magnitude of changes in various indicators for the final product must be different. Firstly, they have different compositions, which directly determine the physical and thermal properties of the materials, including density, thermal conductivity, latent heat during freezing, etc. In addition, although they have similar plant cell structures, the size and arrangement of the cells are not consistent. The cell dimension of potato tissue is 5500-11,200 μm^2 , which is much lower than that of apple tissue (39,465-59051 μm^2) (Konstankiewicz, Czachor, Gancarz, Król, Pawlak, & Zdunek, 2002; McAtee, Hallett, Johnston, & Schaffer, 2009). Generally, larger cells in plant tissue are found loosely packed when compared with smaller cells which lead to making it more porous (Khan, et al., 2018). Therefore, the initial porosity of potato tissue is close to zero, while apple is considered to be a kind of highly porous food material, with around 25% of gas-filled intercellular spaces (Van Buggenhout, Sila, Duvetter, Van Loey, & Hendrickx, 2009). These intercellular gaps can impact the transfer of heat and mass during freezing and provide the spaces for the formation of extracellular ice crystals. It is also the reason that cellular structures with few or tiny extracellular spaces (e.g. potatoes, carrots) allow minimal water movement and produce a compact texture, whereas large cells with large extracellular spaces (e.g. apples) lead to more water movement and produce a coarse or spongy texture (Jha, et al., 2019; REEVE, 1970). According to their inherent structural characteristics, fruits and vegetables have different susceptibility to freezing injury. Due to the fibrous structures, most vegetables allow to maintain their structure when they are thawed after freezing, while most fruits are physically much more susceptible to firmness loss (C. L. M. Silva, Gonçalves, & Brandão, 2008). [Table I. 3](#) lists several fresh fruits and vegetables categorized by their susceptibility to freezing, including most susceptible, moderately susceptible, and least susceptible. Moreover, the state of fruits and

vegetables before freezing is also crucial, which determines the best state they might achieve after freezing. This is easy to understand, because freezing does not improve the quality of food materials, it can only preserve them as much as possible.

Table I. 3: Several fresh fruits and vegetables categorized by their susceptibility to freezing (Jha, et al., 2019).

Most susceptible	Moderately susceptible	Least susceptible
Apricots	Apples	Beets
Asparagus	Broccoli	Brussels sprouts
Avocados	Carrots	Cabbage, mature and savory
Bananas	Cauliflower	Dates
Beans, snap	Celery	Kale
Berries (except cranberries)	Cranberries	Kohlrabi
Cucumbers	Grapefruit	Parsnips
Eggplants	Grapes	Rutabagas
Lemons	Onion (dry)	Salsify
Lettuce	Oranges	Turnips
Limes	Parsley	
Okra	Pears	
Peaches	Peas	
Peppers, sweet	Radishes	
Plums	Spinach	
Potatoes	Squash, winter	
Squash, summer		
Sweet potatoes		
Tomatoes		

I.1.4.2 Freezing pretreatments

Since fruits and vegetables are still alive after being harvested, they remain self-consumption until and even after being frozen and further processed. Several pretreatments such as grading, sorting, removal of defective produce, cleaning, inspecting and packaging, and in some cases peeling, shelling, trimming, cutting and slicing prior to freezing process are the main common operations for fruits and vegetables (C. L. M. Silva, et al., 2008). As an important method to inactivate some endogenous enzymes such as lipid oxidase and peroxidase to reduce quality deterioration (e.g., unpleasant odor and enzymatic browning) in frozen fruits and vegetables, blanching is also one of the most important steps in freezing pretreatment (van der Sman, 2020). Dehydration can also be applied as a step in freezing pretreatment for the improvement of texture and reduction of freezing time, thereby

significantly reducing energy consumption. These operations all have the consistent objective of exposing the fresh materials to freezing with the best initial state as possible and preventing possible deterioration before freezing. Below, we discuss these steps in detail and understand their impact on subsequent freezing.

- Precooling

To slow down the deteriorative process in the postharvest environment, it is important to cool the product to safe (low, non-freezing) temperatures as quickly and efficiently as possible after harvesting, which is called precooling (Sinha, Sidhu, Barta, Wu, & Cano, 2012). It can also be employed as buffering process prior to freezing, with cold acclimation induced by the slow decline in temperature of raw materials. Studies inducing cold acclimation by storing carrots at 0 °C (Gómez G & Sjöholm, 2004) and cold acclimation of spinach (Demir, Dymek, & Galindo, 2018) by changing the ambient temperature during growth before freezing have shown significant reductions in freezing damage. Many factors affect the precooling process of fruit and vegetables, including the characteristics of fruit and vegetables (e.g., shape, size, surface to volume ratio, porosity, internal structure, density, thermal properties, and respiratory heat generation rate), the temperature and velocity of the cooling medium, as well as the relative humidity of the ambient environment (Pathare, Opara, Vigneault, Delele, & Al-Said, 2012).

- Preparation

Preliminary grading, sorting, and removal of defective produce is sometimes employed to eliminate the foreign materials, thus reducing the possibility of spoilage from the source of fruits and vegetables during the freezing process. Cleaning and washing reduce microbial load and minimize product variation (Jha, et al., 2019). For consumer convenience, or to enhance the heating rate of thermal processing like blanching, cooling or freezing, reducing the size of fruits and vegetables is applied by cutting and slicing (van der Sman, 2020). However, this is also a kind of physical damage to raw materials, inevitably breaking down the protective barrier and exposing the inner constituents to oxygen. At the same time, the enzymes and their substrates are dispersed in the cells, leading to biochemical deteriorations such as enzymatic browning, off-flavors and texture breakdown, as well as increased respiration rate and ethylene synthesis (Chaves, et al., 2018).

- Blanching

Typically, subsequent blanching may reduce the biochemical changes activated during cutting or slicing due to enzyme inactivation. At the same time, the expelling of air between cells also facilitates heat transfer in subsequent freezing, drying and other thermal processes. However, it may cause greater loss of solute leaching, texture, pigment and aroma (Xin, Zhang, Xu, Adhikari, & Sun, 2015). Tansey et al. recorded the level of texture softening and gravity drip loss with the help of scanning electron microscopy during the blanching process (Tansey, Gormley, & Butler, 2010). The result showed tightly packed parenchyma or vascular cells and the xylem cells in the fresh carrot tissue. However, physical changes (such as cell separation and cell damage) were found in the cell structure of blanched carrot tissues compared to untreated raw tissue. These phenomena can be explained since the breakdown in cellular structure has taken place.

For traditional hot water blanching, the processing time and temperature are the key factors. Previous studies have shown that Low-Temperature-Long-Time (LTLT) blanching activated native Pectin Methyl Esterase (PME) in the tissue of those products, which could remove the methyl groups from the pectin molecules and create negatively charged carboxyl groups in the process, thereby resulting in a lower degree of pectin depolymerization, better adhesion of the cell walls and overall stronger mechanical properties of thermally processed plant materials compared to those that have not been pre-treated (Day, Xu, Øiseth, & Mawson, 2012; Z. Lin & Schyvens, 1995). The combination of additional Ca^{2+} and LTLT blanching also showed a synergistic effect in enhancing the strength of the cell wall due to the increased interaction between pectins, as well as Ca crosslinked pectin biopolymer network (Lemmens, et al., 2009; Niranjana, 2022). And the strengthened cell wall may resist better the compression induced by the growing ice crystals during freezing (Neri, Hernando, Pérez-Munuera, Sacchetti, Mastrocola, & Pittia, 2014). Another strategy to reduce the texture loss during blanching is high temperature short time (HTST) blanching, involving a high heating rate which is significantly faster than the kinetics of the β -elimination of pectins to obtain a higher inactivation efficiency of enzymes and better maintained physiochemical properties of products (Richter Reis, 2023). Besides, combination of LTLT and HTST was proposed to prevent excessive softening of frozen product. It was found that two-step blanching (70 °C for 10 min

followed by 97 °C for 2 min) was effective in improving the texture of core potato tissue subjected to freeze-thaw stress (Carbonell, Oliveira, & Kelly, 2006). The combined blanching condition (60 °C 120 min + 100 °C 4 min) performed better than HTST alone (100 °C 4 min) on Japanese radish for better maintain the firmness of the sample and inactivate the enzyme (Nishida & Ando, 2023). Peroxidase (POD) activity assay showed that high-temperature blanching for 4 min in boiling water (100 °C) is necessary for effective blanching with or without low-temperature blanching. However, high-temperature blanching alone led to excessive softening after freezing.

In recent years, techniques that assist in achieving higher heating efficiency can also be applied on the basis of HTST blanching. Radio frequency (RF), microwave (MW) and ohmic blanching provide faster heating rates compared to conventional heating because the thermal energy is generated directly inside the food (C. Chen, Abdelrahim, & Beckerich, 2010; Manzocco, Anese, & Nicoli, 2008; Ruiz-Ojeda & Peñas, 2013). Although these dry blanching techniques are sometimes accompanied by dehydration, this kind of volumetric heating makes the heating rate quite independent of the size of the product, avoiding the surface over-processing of traditional blanching on large or intact food materials. Yao et al. (Yao, Sun, Cui, Fu, Chen, & Wang, 2021) found that the heating uniformity of RF blanching was affected by the electrode gap and sample height. Moreover, compared with RF heating at slower heating rates, RF heating at a faster heating rate can reduce thermal damage to cell walls and membranes, and the loss of cell turgor at the same POD activity level by shortening the processing time, which may be more suitable to maintain original sensory qualities before freezing of fruits and vegetables. Prior to freezing, microwave blanching was compared with blanching in water, blanching in a solution of sodium metabisulphite and citric acid, and combined blanching (first in water, then in a microwave oven) for *Agaricus bisporus*, the result showed that microwave-blanched mushrooms got higher dry matter, ash, vitamin B₁ and B₂ content, lower polyphenol oxidase activity, and superior flavor and aroma (Bernaś & Jaworska, 2014). However, non-uniformity has always been a significant drawback of microwave-assisted processing. Therefore, it has certain difficulties in practical industrial applications. At this point, ohmic heating behaves better. It provides rapid and also uniform heating with a lower capital cost compared to other electro heating methods such as RF and MW blanching (Marra, Zell, Lyng, Morgan, & Cronin, 2009). Priyadarshini et al. (Priyadarshini, Rayaguru,

Biswal, Panda, Lenka, & Misra, 2023) compared the impact of conventional and ohmic blanching on color, phytochemical, structural, and sensory properties of raw Totapuri mango cubes, the result showed that ohmic blanching gave the shortest critical inactivation time of 40-110 s depending on the voltage gradients, whereas conventional blanching at 90 °C in a hot water bath took 130 s. The result also indicated that remained bioactive compounds including ascorbic acid, total carotenoid, and flavonoid content were highest in samples treated by ohmic blanching at 20 V/cm.

High pressure (HP), ultrasound and infrared (IR) have also shown great potential in enzyme inactivation. High-pressure blanched sweet green and red bell peppers (Castro, et al., 2008), carrot tissue (Rastogi, Nguyen, & Balasubramaniam, 2008), beetroot slices (Paciulli, Medina-Meza, Chiavaro, & Barbosa-Cánovas, 2016) all got good enzyme inactivation, while maintaining a firm texture. However, for more sensitive fruits and vegetables such as zucchini and apricot, they can be significantly softened after high pressure treatment (Nguyen, Tay, Balasubramaniam, Legan, Turek, & Gupta, 2010). Guo et al. (Guo, et al., 2021) studied the effects of ultrasonication (US) and thermo-sonication (TS) blanching at varying frequencies on the carrot peroxidase (POD) inactivation and potential mechanisms. The result showed that TS decreased the POD activity to a greater extent, with a dual-frequency of 22/40 kHz showing the most significant effect. Electron paramagnetic resonance (EPR) spectra revealed that the formed free radicals from the ultrasound-induced decomposition of water played important roles in the POD inactivation during TS treatments. Galindo et al. (Galindo, Toledo, & Sjöholm, 2005) compared the blanching of the carrot slices for 7 s with radiant energy in the far infrared region at a radiant surface of 810 K, for 5 to 30 s in boiling water. It was observed that cell damage was superficial and less pronounced in infrared blanching than in boiling water blanching for 5 s. The carrot slices blanched by infrared heating maintained higher quality in terms of tissue strength than those blanched in boiling water. In a study of infrared blanching of apple slices, it was found that thinner slices fit the model better than thicker slices, possibly due to uneven temperature distribution within the thicker slices (Y. L. Lin, Li, Zhu, Bingol, Pan, & McHugh, 2009). Although these studies have shown a positive impact on the quality of some blanched fruits and vegetables to a certain extent, in practice, further research is needed based on the types of fruits and vegetables,

blanching technology and process conditions, as well as the impact on the subsequent freezing process.

- Partial dehydration

Partial dehydration alone or after blanching is also one of the important pretreatments before freezing. Partial dehydration applied individually before freezing can reduce the amount of cellular water and increase solute concentration. On the one hand, this pretreatment theoretically makes the plant cells under less turgor pressure and thus more relaxed, reducing the damage to cell structure induced by volume expansion of ice formed (Schudel, Prawiranto, & Defraeye, 2021). It also has the potential to reduce the freezing time, the initial freezing point, and the amount of extracellular ice formed within the product (C. James, Purnell, & James, 2014). It can also be applied after blanching for some vegetables to remove surface water to avoid clumping during freezing operation in the tunnel or oil splashing during par-frying (van der Sman, 2020). However, the qualitative characteristics of the final food product depend on the dehydration method, applied temperature, quantity of water removed, tissue texture, and degree of cell structure damage before freezing-thawing.

The most commonly used techniques to reduce water content before freezing in fruits and vegetables are partial air-drying and osmotic dehydration. Air dehydration has advantages such as shorter dehydration times and lower loss of nutrients. However, the high temperatures used in air-drying can be disruptive to the cell membrane (Ando, Maeda, Mizutani, Wakatsuki, Hagiwara, & Nabetani, 2016), which is also one of the adverse effects of other thermo-processing such as hot blanching, greatly affecting the texture of frozen-thawed fruits and vegetables. Therefore, milder conditions for partial dehydration before freezing are preferred, e.g., air drying at a set temperature of 40 °C (Ando & Watanabe, 2023), airflow drying at 45 °C air temperature, 2 m/s air velocity and 12% air relative humidity (Ben Haj Said, Bellagha, & Allaf, 2015), vacuum drying at moderate temperatures inside potato samples (below 50 °C) (C. Liu, Grimi, Bals, Lebovka, & Vorobiev, 2021).

Osmotic dehydration (OD) has also been widely used as a milder pretreatment of freezing, involving the partial removal of water without phase change by immersing the food product in hypertonic aqueous solutions, containing carbohydrates and/or salts (Giannakourou, Dermesonlouglou, & Taoukis, 2020). Factors that influence

osmotic dehydration are mainly the rates of water removal and solute impregnation, induced by the properties of the food material, the composition and the concentration of the osmotic solutes in the osmotic solution, the temperature of the osmotic solution, the immersion time, the level of agitation in the solution, the geometry (size and shape) of the food, and the solution-to-food ratio (Giannakourou, et al., 2020). It has the main advantages of low energy consumption, low cost for packaging, distribution and storage, and improved food quality (L. Cheng, Sun, Zhu, & Zhang, 2017). Several studies reported that osmo-dehydration pretreatment can significantly reduce the energy for freezing of red pepper (Topuz & BaŞÜNal GÜLmez, 2022), increase the firmness of frozen apple (Ben Haj Said, Bellagha, & Allaf, 2016), improve color, reduce nutritional quality loss, and texture degradation of tomatoes (J. Li, et al., 2017), improve total polyphenol bioaccessibility and Ferric reduction retention of arazá (Reyes-Alvarez & Lanari, 2023). Despite acknowledging the benefits of osmotic dehydration for quality maintenance, the mass transfer rate caused by the free diffusion of molecules alone is rather low and often takes a long time to reach the target dehydration amount. So, complementary methods are recommended to accelerate and enhance the OD process, such as pulsed electric fields that can increase the cell membrane permeability, or vacuum impregnation that remove the air in the intercellular space.

I.1.4.3 Freezing operation

The final quality of fruits and vegetables can be directly affected by the characteristics of the ice crystals (i.e., location, morphology, size, and number) formed in the tissues which further depends on freezing kinetics, rate of ice nucleation, and crystal growth (Jha, et al., 2019; Kaur & Kumar, 2020; D.-K. Liu, Xu, Guo, & Zhang, 2020).

As is mentioned in I.1.2, nucleation serves as the initial process of freezing that produces the initial seed or nucleus on which the crystal grows. The rate of nucleation depends upon many factors such as temperature, freezing rate, the presence of impurity, volume of sample, the presence of a water/vapor interface, surface tension, diffusivity, molar density, viscosity, particularly, supercooling (Kang, You, & Jun, 2020; Kiani & Sun, 2011). Overall, the greater the number of nuclei, the smaller the ice crystal size, which is beneficial for maintaining the final quality. For this purpose, high degrees of supercooling and rapid freezing rates are usually considered to be favorable.

Classical nucleation theory (CNT) provides a basic platform to predict a temperature-dependent nucleation rate via thermodynamic and kinetic data, which respectively describe the characteristics of the system under equilibrium conditions, and the rates at which equilibrium might be approached as water is converted into ice (Chaves, et al., 2018; Kang, et al., 2020). It is said that the nucleation has to overcome the energy barrier (activation energy) imposed by the surface energy. While supercooling, as the driving force to overcome this energy barrier, is proportional in magnitude to the degree of supercooling, i.e., the difference between freezing point and the actual temperature of the unfrozen phase, which is a critical parameter for nucleation that determines the number of ice crystals formed per unit of time and volume. Due to the presence of foreign material, nucleation in fruits and vegetables is mainly heterogeneous and requires a lower degree of supercooling compared to the homogeneous nucleation of pure water. Especially the extracellular space (if filled with air) can be a preferred nucleation site, while intracellular ice formation often requires homogeneous nucleation. Hence, low degree of supercooling and low rate of heat transfer is generally more likely to result in the formation of large extracellular ice. James et al. (C. James, Hanser, & James, 2011) have studied the supercooling phenomena for several vegetables during freezing at $-30\text{ }^{\circ}\text{C}$, including garlic cloves and bulbs, broccoli, cauliflower, carrots, leeks, parsnips, and shallots, the result revealed the dependence of the degree of supercooling on the type of sample. In particular, garlic showed a surprisingly high average degree of supercooling of $10.3\text{ }^{\circ}\text{C}$, whereas other vegetables ranged from 0.7 to $3.8\text{ }^{\circ}\text{C}$. Martins and Lopes (Martins & Lopes, 2007) evaluated the supercooling capacity of frozen strawberries and obtained that the mean nucleation temperature and freezing point of the surface and center positions of strawberries are $-4.1\text{ }^{\circ}\text{C}$ and $-1.3\text{ }^{\circ}\text{C}$ as well as $-1.3\text{ }^{\circ}\text{C}$ and $-0.6\text{ }^{\circ}\text{C}$, respectively. Thus, the surface supercooling capacity is higher than that of the center position. Since ice nucleation is induced by stochastic processes and the supercooled state is highly probabilistic nature and unstable, it is quite difficult to achieve accurate predictions, technical stability, and reproducibility of results. Sometimes, even slight fluctuations in temperature can initiate nucleation and induce freezing-related damage to foods (D.-K. Liu, et al., 2020). Hence the detected nucleation temperature and the degree of supercooling usually exhibit large deviations for a given type of fruit or vegetable, e.g. broccoli and cauliflower (Table I. 4). Nevertheless, the investigation of controlling nucleation is essential for the homogeneity of the same batch, especially in

the biopharmaceutical industry (Luoma, Ingham, Lema Martinez, & Allmendinger, 2020). For improving the final quality of frozen products, there have been considerable interests in prolonging the supercooling state and/or increasing the degree of supercooling by controlling the nucleation (Mohsen Dalvi-Isfahan, Hamdami, Xanthakis, & Le-Bail, 2017; Jia, et al., 2022; Kim, et al., 2014).

Table I. 4: Freezing and nucleation points (to 1 d.p.) of vegetable samples, frozen at $-30\pm 1^\circ\text{C}$ (n=10, *n=15) (C. James, et al., 2011)

Vegetable	Freezing point ($^\circ\text{C}$) Mean (SD)	Occurrences of supercooling	Nucleation temperature * ($^\circ\text{C}$)			Degrees of supercooling *		
			Min	Max	Mean (SD)	Min	Max	Mean (SD)
Broccoli	-2.1 (0.3)	9/10	-2.3	-9.8	-4.4 (2.4)	0.4	7.7	2.5 (2.3)
Carrot	-1.6 (0.6)	9/10	-1.3	-3.9	-2.7 (0.8)	0.4	2.6	1.1 (0.7)
Cauliflower	-1.5 (0.3)	7/10	-1.9	-8.3	-5.2 (2.6)	0.6	6.9	3.8 (2.6)
Garlic*	-2.7 (0.3)	15/15	-7.7	-14.6	-13.0 (1.7)	4.9	12.0	10.3 (1.6)
Leek	-1.9 (0.3)	9/10	-2.3	-3.9	-3.3 (0.6)	0.6	2.3	1.6 (0.6)
Parsnip	-2.2 (0.2)	4/10	-2.6	-3.1	-2.8 (0.2)	0.4	0.9	0.7 (0.2)
Shallot	-1.6 (0.2)	10/10	-2.7	-7.3	-5.4 (1.4)	1.1	4.7	3.3 (1.3)

*When supercooling occurred

The freezing rate directly affects the nucleation on one hand, and the growth of ice crystals on the other hand. Energetically, water molecules are more likely to migrate to existing nuclei than to form new ones (Fellows, 2017). Higher heat transfer rates promote the formation of more nuclei therefore produce a large number of small ice crystals, whereas slow heat transfer rates get less nuclei and also give the water molecules more time to migrate to the growing nuclei to be large ice crystals (Muthukumarappan, et al., 2019). Consequently, the time it takes for the temperature of the food to pass through the “critical zone”, i.e. the rate of freezing, determines the number and size of ice crystals (He, Feng, Tao, & Zhang, 2024; Tang, Shao, & Tian, 2020). For fast freezing and slow freezing, the most significant difference can be seen in the temperature curves is their duration in the freezing critical zone (Fig. I. 7). Normally, we expect this duration to be as short as possible. The major part of ice in the food materials is also formed during this critical zone, thus it’s also called the maximum ice crystal formation zone, which greatly affects the final quality of fruits and vegetables. From Ramaswamy and Tung (Ramaswamy & Tung, 1984), the duration in this zone appears to be the more acceptable definition of freezing time. In

some study, this zone is defined to be a temperature range of 0 °C to -5 °C (Muthukumarappan, et al., 2019), the temperature ranging from -1 °C to -5 °C (He, et al., 2024; Tian, Li, et al., 2020), the temperature range from -1°C to -8°C (Stebel, Smolka, Palacz, Eikevik, & Tolstorebrov, 2022), the temperature range between TIFP (Initial Freezing Point Temperature) and 7 °C below TIFP (Añón & Calvelo, 1980). The International Institute of refrigeration also proposes to consider that a food is frozen if the temperature has been lowered to -10 °C or to a temperature for which 80% of the freezable water has been frozen (Mohsen Dalvi-Isfahan, et al., 2019; Refrigeration, 1986).

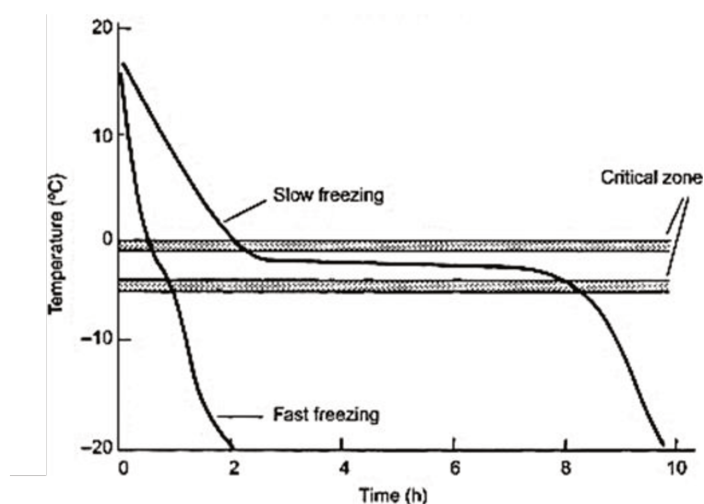


Fig. I. 7: Freezing: temperature changes of food through the critical zone (Fellows, 2017).

The freezing rate can be simply defined as the difference between the initial and final product temperatures divided by the freezing time (°C/s). In this case, a starting criterion and an ending criterion for freezing must be defined. But the temperature change will vary considerably from the surface to the center, thus making this definition quite limited for characterizing certain freezing processes, especially for some large size of samples. Freezing rate is normally expressed, therefore, as the average velocity at which the ice front advances from the surface to the thermal center. When depth is measured in centimeters and freezing time in hours, the freezing rate is expressed in cm/h. And depending on the different freezing rates, they can be categorized as listed in Table I. 5.

Table I. 5: Freezing rate of different freezing methods (C. L. M. Silva, et al., 2008)

Freezing method	Freezing rate (cm/h)
Ultra rapid freezing	Over 10

Rapid freezing	1–10
Normal freezing	0.3–1
Slow freezing	0.1–0.3
Very slow freezing	less than 0.1

The freezing rate can be calculated by the determination of several factors, namely the size of the food, thermal conductivity of the food, area of food available for heat transfer, the heat transfer coefficient of the coolant medium, and the freezer temperature, as indicated by Planck's equation developed in 1941 (Heldman, 2006; Muthukumarappan, et al., 2019).

$$t_f = \frac{\rho L}{T_i - T_m} \left[\frac{Pa}{h} + \frac{Ra^2}{k} \right]$$

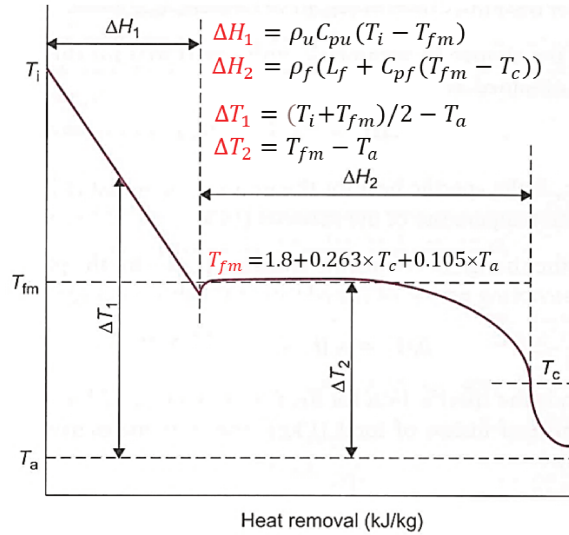
where t_f is freezing time (s), ρ is density of the product (kg/m^3), L is latent heat of fusion (J/kg), T_i is initial freezing temperature of the food (K), T_m is freezing medium temperature (K), a is thickness of the slab or the diameter of the sphere or infinite cylinder (m), h is surface heat transfer coefficient ($\text{Wm}^{-2}\text{K}^{-1}$), k is thermal conductivity of the frozen food ($\text{Wm}^{-1}\text{K}^{-1}$), and P and R are geometric factors. For the infinite slab, $P=1/2$ and $R=1/8$. For a sphere, P and R are $1/6$ and $1/24$, respectively, and for an infinite cylinder, $P=1/4$ and $R=1/16$.

Subsequently, other prediction models have been developed to overcome some of the limitations of the Planck equation, including not taking into account the removal of sensible heat from unfrozen foods or from foods after freezing, and the lack of accurate data on the density and thermal conductivity of many frozen foods (Fellows, 2017). Of these, Pham (Pham, 1986) developed a simplified equation that included the time taken to lose sensible heat.

$$t = \frac{d_c}{E_f h} \left(\frac{\Delta H_1}{\Delta T_1} + \frac{\Delta H_2}{\Delta T_2} \right) \left(1 + \frac{N_{Bi}}{2} \right)$$

where d_c (m) is the characteristic dimension (the smallest distance from the center), E_f is the shape factor (=1 for slab, 2 for a cylinder and 3 for a sphere), ΔH (Jm^{-3}) is the change in enthalpy with subscripts 1 for precooling unfrozen food and 2 for phase change and cooling of frozen food obtained from equations in Fig. I. 8, ΔT ($^{\circ}\text{C}$) represent the temperature gradients shown in Fig. I. 8, and N_{Bi} is the Biot number which can be calculated by hd_c/k . In these equations, ρ (kg/m^3) is the density of the food material, C_p ($\text{Jkg}^{-1}\text{K}^{-1}$) is the heat capacity of the food material, which can be calculated based on the percentage of each components in the food according to the

formula. Their subscripts u and f represent the unfrozen and frozen states, respectively. T_i ($^{\circ}\text{C}$) is the initial temperature and T_{fm} ($^{\circ}\text{C}$) is the mean freezing temperature of the food material. T_c ($^{\circ}\text{C}$) is the final temperature at the center of the food. T_a ($^{\circ}\text{C}$) is the



temperature of the freezing medium.

Fig. I. 8 Freezing diagram of food, divided into sections for Pham's method.

In this model, the factors that affect the freezing time and thus the freezing rate become obvious. Table I. 6 lists these factors and summarizes their correlation with freezing time. For freezing operation, the freezing time can be shortened by increasing convective heat transfer and lowering the temperature of the freezing medium, inducing a rapid freezing rate. However, as mentioned in I.1.3, mechanical damage can be caused by the volume expansion of ice under too rapid freezing rate, where the stress has insufficient time to relax and cracks occur (Yang, Hu, Takaki, Yu, & Yuan, 2021). Thus, studies about the effects of the freezing rate on the final quality of frozen croissant dough (Ban, et al., 2016), frozen mangoes (Charoenrein & Owcharoen, 2016), frozen strawberries (Da Silva, Silveira, Ronzoni, & Hermes, 2022), and apple tissue (Narayana, Jha, Rawson, & Le-Bail, 2023) have been widely investigated for optimal operation parameters.

Table I. 6: Factors related to freezing time

Factors	freezing time
Size of the sample	↑
Density of the sample	↑

Heat capacity of the sample	↑
Convective heat transfer coefficient at the surface	↓
Thermal conductivity of the sample	↓
Initial temperature of the sample	↑
Temperature of the freezing medium	↑

↑ indicates the increase of freezing time with the factor, ↓ indicates the decrease of freezing time with the factor

In addition to promoting nucleation and increasing the freezing rate to form small ice crystals, inhibition of coarsening induced by the mass transfer of water has also been considered as another controlling factor of ice crystal size. In fact, although a large amount of cellular water in fruits and vegetables crystallizes when frozen, little unfrozen water is still available even at the common commercial freezing temperature of -18°C . In this case, moisture still has sufficient mobility to diffuse through the unfrozen phase, increasing the possibility of recrystallization and the replacement of small ice crystals with large ones, which is the main cause of quality deterioration during long-term storage.

The operation that can be performed during the freezing process is to freeze the fruits and vegetables below their glass transition temperature. A glass (vitreous state) is defined as a non-equilibrium, metastable, amorphous, disordered solid of very high viscosity (Meste, Champion, Roudaut, Blond, & Simatos, 2002). Simply put, during the freezing process, the solutes are concentrated due to the crystallization of water, resulting in the formation of “rubbery” textured concentrate with a highly viscous. Further decrease in temperature will cause the supersaturated unfrozen phase to convert into a metastable amorphous solid (glassy matrix) from the rubbery state (Mahato, Zhu, & Sun, 2019). This highly viscous (between 10^{12} and 10^{14} Pa·s) and concentrated state limits the mobility of water molecules and also makes it more difficult to extract water by crystallization. T'_g is defined as the temperature at which the maximum amount of ice is formed, leading to a maximally freeze-concentrated solution (Chaves, et al., 2018). If a product is stored at a temperature below T'_g , it may be expected to be composed of ice and a freeze-concentrated phase in the glassy state, which protects the texture of the food and gives good storage stability (Tian, Li, et al., 2020). However, the glass transition temperature of some fruits and vegetables are quite low as shown in [Table I. 7](#), which means that they must have suffered mechanical damage from ice crystals before reaching that temperature. Besides, it

may not be practically viable to freeze the fruits and vegetables under the glass transition temperature due to the high cost (Narayana, et al., 2023), but it is important for the cryopreservation of biological materials.

Table I. 7: Glass transition temperatures for several fruits and vegetables. Adapted from (Fellows, 2017).

Fruits and vegetables	Glass transition temperature T _g (°C)
Apple	-41 to -42
Banana	-35
Peach	-36
Strawberry	-33 to -41
Tomato	-33 to -41
Broccoli, head	-12
Carrot	-26
Green beans	-27
Maize kernel	-15
Pea	-25
Potato	-12
Spinach	-17

I.1.4.4 Storage

Although freezing has the ability to extend the shelf life of perishable and seasonal plants, this extension does not last indefinitely. For consumers, taste, odor, and appearance are the most obvious shelf-life criteria. In academia and in the industry, shelf-life assessments usually involve sensory evaluation and instrumental measurements based on a given quality index (e.g., vitamin C level) (Chaves, et al., 2018).

Firstly, changes in fruit and vegetables during frozen storage are related to their varieties. Ascorbic acid, riboflavin, α -tocopherol, and β -carotene were evaluated in fresh and frozen corn, carrots, broccoli, spinach, peas, green beans, strawberries, and blueberries. Among these, β -Carotene was not found in significant amounts in blueberries, strawberries, and corn, no significant change in green beans and spinach, while decreasing drastically in peas, carrots, and spinach during the frozen storage (Bouzari, Holstege, & Barrett, 2015). In the study of Jha et al., (Jha, Chapleau, Meyers, Pathier, & Le-Bail, 2024) melon firmness increased, while apple firmness decreased compared to fresh samples post-freezing. Besides, melon exhibited a

substantial increase in firmness compared to the fresh sample, while the firmness value remained relatively stable up to 30 days in frozen apple.

There have been reports that the initial freezing condition has a direct impact on the quality attributes of beef (Qian, Li, Zhang, & Blecker, 2022), tofu (Qian, et al., 2022), apples (Narayana, et al., 2023), etc. during the storage period. In general, frozen plant foods are characterized by lower textural properties than those of the initial raw material, and further deteriorated by recrystallization that may occur during frozen storage. The effects of ice crystals on tissue structure and cellular integrity also affect the chemical properties of plant products during freezing and the frozen storage, including loss or change of natural pigments, degradation or complexation of specific components, and leaching of micronutrients, etc. Theoretically, large numbers of nuclei during initial freezing, with smaller sized ice crystals before storage, less damage to cellular integrity, which attribute to the maintaining of frozen quality in the following storage. However, for antioxidant activity in some products, the great destruction of tissue from large ice crystals had a positive effect, although it would significantly decrease during long-term storage. A study on the application of individual quick freezing (IQF) (-35°C) and conventional freezing (-28°C) on strawberries and raspberries before frozen storage also showed similar phenomenon. The free radical scavenging (AO) activity was found to be higher in frozen samples compared to fresh fruits, which may be attributed to freezing associated cellular disruption leading to easier antioxidant detected after freezing (Stevanović, et al., 2022), and then significant decrease was found after 8 months of frozen storage. Since the antioxidant capacity of a food depends on the presence and concentration of bioactive molecules that can prevent oxidative reactions, greater damage during freezing can allow the elevated release of bioactive compounds such as bound phenolic acids and anthocyanins (Neri, Faieta, Di Mattia, Sacchetti, Mastrocola, & Pittia, 2020). This immediate increase in antioxidant activity does not represent an increase in the original content of the bioactive compounds of the product and may result in greater losses during long-term storage. Therefore, considering all these variations in quality, the less damage produced during the initial freezing, the more favorable to the subsequent frozen storage.

Subsequently, the quality change is controlled by the storage temperature and period of the frozen storage. It is common practice that frozen foods are stored lower or

equal to $-18\text{ }^{\circ}\text{C}$, which is the limit set by legislation (such as the European directive for Quick Frozen Foods) (van der Sman, 2020). This storage temperature, while sufficient for prolonging the stability, is still above the glass transition temperature of many fruits and vegetables (Neri, et al., 2020). Since microorganisms are usually unable to grow at this temperature, they are not a problem in frozen foods. But it inevitably attributes to recrystallization and slow biochemical reactions, which plays the critical role in leading to irreversible quality deterioration (e.g., conversion of chlorophylls to pheophytins, formation of brown compounds, degradation of carotenoids, etc.) in long-term frozen storage (Neri, et al., 2020). Gonçalves et al. (E. M. Gonçalves, Pinheiro, Abreu, Brandão, & Silva, 2011) have studied the effects of different storage temperature ($-7\text{ }^{\circ}\text{C}$, $-15\text{ }^{\circ}\text{C}$, and $-25\text{ }^{\circ}\text{C}$) on the pumpkin quality attributes (such as texture, vitamin C content, and color), the result showed that the quality attributes were lost significantly during a storage period of 140 days under all the conditions, and the highest and fastest change was recorded for the higher storage temperature ($-7\text{ }^{\circ}\text{C}$). Gonçalves et al. (Elsa M. Gonçalves, Abreu, Pinheiro, Brandão, & Silva, 2020) also reported faster vitamin C degradation in carrots stored at higher temperatures at the end of 57 days of storage period (70% of vitamin C degraded at $-7\text{ }^{\circ}\text{C}$ as opposed to 49% at $-25\text{ }^{\circ}\text{C}$). Dawson et al. (Dawson, Al-Jeddawi, & Rieck, 2020) reported that frozen storage temperatures (-7 , -12 , -18 , -29 , and $-77\text{ }^{\circ}\text{C}$) affected the firmness of pre-frozen peach only after a certain storage period. It was found that no difference existed amongst these storage temperatures during the initial 90 days. Further, increase in the storage duration to 180 days and beyond (360 days), the lowest frozen storage temperature ($-77\text{ }^{\circ}\text{C}$) exhibited a higher firmness value compared to higher freezing temperatures (-12 and $-7\text{ }^{\circ}\text{C}$). Only at the end of 360 days, the -18 and $-29\text{ }^{\circ}\text{C}$ samples exhibited significantly higher texture compared to -12 and $-7\text{ }^{\circ}\text{C}$ samples. Different nutrients also have different performances during the storage period. Ratinho et al. (Araújo-Rodrigues, Santos, Campos, Ratinho, M. Rodrigues, & E. Pintado, 2021) reported approximately 32.19% and 65.50% reductions for total phenolic content (TPC) in cherry tomato and baby carrot pulps after 6 months of frozen storage at $-20\text{ }^{\circ}\text{C}$, respectively. However, their antioxidant capacity (2,2-diphenyl-1-picryl-hydrazyl-hydrate Assay) at the end of the storage showed only 7.22% and 1.69% reduction, respectively. Frozen storage increased polyphenols in the first 6 months of frozen storage but then decreased polyphenols at 8th month to levels similar to initial values (King, Noll, Glenn, & Bolling, 2022). In

general, the lower the temperatures and the shorter the freezing times, the more the damage caused by freezing was reduced.

Moreover, fluctuations in temperature, during frozen storage, subsequent transport, and distribution, are detrimental to the preservation of final quality, especially textural properties. When the temperature rises, the small ice crystals melt. Following temperature decrease cannot support the new ice nuclei formation, thus water is converted to ice on the existing crystals leading to an increase in their size (Narayana, et al., 2023). As is known that big size of ice crystals is always harmful for the quality of frozen products. Lower storage temperature, shorter oscillation periods and smaller temperature fluctuations, as well as packaging with good insulating properties can lower the effects of fluctuations (P. K. Kumar, Rasco, Tang, & Sablani, 2020).

I.1.4.5 Thawing

The thawing process is usually considered an essential step before the consumption of frozen foods. In contrast to the freezing process, it involves the melting of ice into water. Generally, thawing is performed more slowly than freezing when temperature differences and other conditions are similar (Fadiji, Ashtiani, Onwude, Li, & Opara, 2021). This is mainly due to the difference in the thermal properties of ice and water. It was reported that the specific heat capacity of a frozen aqueous food at low temperature (-20 °C, say) is dominated by the specific heat capacity of ice, around 2 kJ kg⁻¹ K⁻¹, whereas when thawed, it is dominated by the specific heat capacity of water, around 4 kJ kg⁻¹ K⁻¹ (C. A. Miles, Morley, & Rendell, 1999). Therefore, during the thawing process, the layer that melts first on the surface will become a resistance to internal melting, slowing the heat transfer. Cleland et al. (Cleland, Cleland, & Earle, 1987a, 1987b) developed equations to predict thawing time.

$$t = \frac{d_c}{E_f h} \left(\frac{\Delta H_{10}}{T_a - T_f} \right) (P_1 + P_2 N_{Bi})$$

$$P_1 = 0.7754 + 2.2828 N_{Ste} \times N_{Pk}$$

$$P_2 = 0.5 (0.4271 + 2.122 N_{Ste} - 1.4847 N_{Ste}^2)$$

$$\text{Stephan number } (N_{Ste}) = \rho_u C_u (T_a - T_f) / \Delta H_{10}$$

$$\text{Plank number } (N_{Pk}) = \rho_f C_f (T_f - T_i) / \Delta H_{10}$$

where d_c (m) is the characteristic dimension, E_f is the shape factor (=1 for slab, 2 for a cylinder and 3 for a sphere), h ($W\ m^{-2}\ K^{-1}$) is the convective heat transfer coefficient at the surface of the food, T_f ($^{\circ}C$) is the freezing temperature of the food material and T_a ($^{\circ}C$) is the temperature of the thawing medium. ΔH_{10} is the change in enthalpy of the product from 0 to $-10\ ^{\circ}C$. N_{Bi} is the Biot number, and calculated as hd_c/k_u (Fellows, 2017).

According to the equation above, it is clear that the size as well as the shape of the thawing material, thermal conductivity, initial and final temperature, thermal characteristics and temperature of the thawing medium, humidity (when thawing in the air), as well as the velocity of the thawing medium will all have an effect on the thawing time (J. Wu, Zhang, Bhandari, & Yang, 2021). In fact, the thawing time is supposed to be not too short, to avoid overheating the food and dehydration of the surface. On the other hand, slow thawing gives the food time to relax mechanical stresses induced by freezing and allow melted moisture to be reabsorbed to the original position before freezing. This avoid the loss of water after thawing (drip loss) (van der Sman, 2020). But a long thawing time may cause physical and chemical changes, including changes to the flavor, texture, color, carotenoid degradation, decreased antioxidant activity, ascorbic acid degradation, degeneration, and aggregation of protein (Y. Liu, et al., 2019; B. Wang, Kong, Li, Liu, Zhang, & Xia, 2020). Moreover, the reactivation and growth of psychrotrophic spoilage and pathogenic microorganisms in this period can be fatal to food safety, as the nutrients from drip loss also provides the substrates for enzyme activity and microbial growth (Fellows, 2017). Thus, rapid thawing at low temperatures to prevent a significant temperature rise and excessive dehydration is an ideal way to retain the original food quality as well as higher energy efficiency (B. Li & Sun, 2002).

Traditional thawing methods rely on heat transfer through (moving) air, water or condensed steam, which can be accelerated by mechanical approaches such as forced convection. However, for big volume products, these methods are time-consuming and inefficient due slow conduction within the products (S. J. James, James, & Purnell, 2017). More recently, certain effective thawing methods have been reported, such as far-infrared radiation thawing, high hydrostatic pressure thawing, ohmic thawing, ultra-high-pressure thawing, vacuum thawing, high-voltage pulsed electric field thawing, ultrasonic thawing as well as microwave thawing (J. Wu, et al., 2021).

It is generally considered that high pressure lowers the melting point of ice and allows the increase of the temperature gap between the heat source and the phase change front, thus accelerating the thawing process (LeBail, Chevalier, Mussa, & Ghoul, 2002); ultrasound treatment can convert acoustic energy into heat energy by the collapse of cavitation bubbles, accelerating the phase transition speed from ice to water (B. Wang, et al., 2020); ohmic heating thawing mainly uses Joule thermal effect for the purposes (Chysirichote, Phumchom, Chintapum, Klinthong, Ohtaguchi, & Yoovidhya, 2024); the generation of ionic wind is the main reason for the faster thawing rate of high voltage electric field (Y. Zhang & Ding, 2020); the vibrations of water molecules in the microwave electromagnetic field attributes to the rapid heating (Watanabe & Ando, 2021); magnetic nanoparticles would shift to a paramagnetic state when being heated, which would promote heat conduction caused by the strong movement of polar molecules in samples (Cai, Cao, Regenstein, & Cao, 2019); etc. Although most of them have shown great potential, especially in meat products, research on their effects on the thawing properties of frozen fruits and vegetables is quite limited. For different varieties of fruits and vegetables, selecting appropriate technology and parameters is also crucial to reduce quality loss during thawing. For instance, combined microwave- and infrared-assisted thawing is proposed as novel means to improve thawing efficiency of selected materials, namely, green pepper, carrot and cantaloupe (B. Chen, Zhang, Wang, Devahastin, & Yu, 2022). However, it is important to note that the same thawing method exhibited different effects on different test materials. Thawing loss experienced by cantaloupe was more extensive than those experienced by green pepper and carrot. This led in turn to a significant decrease in hardness and loss of ascorbic acid of cantaloupe (B. Chen, et al., 2022). Xu et al. (B. Xu, Chen, Yuan, Azam, & Zhang, 2021) also studied the effects of different ways of thawing, including air thawing (AT), water thawing (WT), refrigeration thawing (RT), ultrasound-assisted water thawing (UWT), and microwave thawing (MT) on the thawing time and quality of radish samples. In comparison with the AT, WT, and RT, the result showed a significant reduction in thawing time could be achieved for UWT ($P < 0.05$). Ultrasound-assisted water thawing exhibited the highest retention of color and vitamin C, and a lower destructive effect on the microstructure. [Table I. 8](#) lists several examples of new technology-assisted thawing on frozen fruits and vegetables.

Table I. 8: Several examples of new technology-assisted thawing on frozen fruits and vegetables.

Thawing method	Materials	Effects	References
Ohmic thawing	Spinach puree	Thawing times were shortened by about 70–80% with ohmic thawing (OT). OT with 15 V/cm had the highest energetic efficiency (64.2% ± 4.0%) and highest exergy efficiency value (40.5% ± 2.6%)	(Çabas, Azazi, Döner, Bayana, Çokgezme, & İçier, 2022)
Ultrasound-assisted thawing	Edamame [<i>Glycine max</i> (L.) Merrill]	The time of thawing was dramatically lowered by the usage of ultrasound during thawing process. Ultrasound intensity at 1.8 W/g was most effective in preserving original attributes of edamame, ultrasound intensity at 2.4 W/g caused largest loss of ascorbic acid.	(X.-f. Cheng, Zhang, & Adhikari, 2014)
Ultrasound-assisted thawing	Mango pulp	Utilization of ultrasonic irradiation in the process of thawing reduced 16–64% of thawing time and retain more phenolic acids contents of mango pulp.	(Y. Liu, et al., 2019)
Microwave-assisted thawing	Mango	The thawing time was further decreased with the increase in microwave power. Microwave thawing enhanced the quality of mangoes in terms of less color change and drip loss, reduced loss of firmness and vitamin C content.	(Y. Peng, Zhao, Wen, & Ni, 2022)
Microwave-assisted thawing and Vacuum microwave-assisted thawing	Apple cubes	Vacuum microwave inhibited the localized overheating of the sample during thawing compared to microwave thawing. The level of browning was significantly lower in microwave and vacuum microwave thawing	(Watanabe, et al., 2021)

			than in air thawing at 20 °C because they required a relatively short thawing time.	
Ultra-high-pressure thawing	Mango		The thawing time was significantly reduced. Thawed mangoes showed the least color changes, but also the greatest loss of firmness and vitamin C.	(Y. Peng, et al., 2022)
Ultra-high-pressure thawing	Strawberry		The thawing time under 200 MPa was reduced to 11 min compared with normal atmospheric pressure thawing at 20 °C taking 81 min.	(Van Buggenhout, Messagie, Maes, Duvetter, Van Loey, & Hendrickx, 2006)
Thawing with PEF pretreatment	Apple		The total thawing time was reduced by 71.5%	(Wiktor, Schulz, Voigt, Witrowa-Rajchert, & Knorr, 2015)
Infrared-hot air thawing	Carrot		The time of thawing was lowered to 6.23 minutes with treatment 8 (air temperature of 40 °C, airflow velocity of 5 m/s, infrared power of 300 watts) compared to the thawing time of control samples at 25 °C of 47.66 minutes. Besides, thawed carrots under this condition also showed the highest amount of β -carotene of 48.12 mg/100g.	(Shahsavar, Kashaninejad, Ziaifa, & Maghsoudlou, 2024)

I.2 New trends in freezing technology

Conventional freezing primarily relies on conduction and convection for heat transfer, which limits its removal of heat to starting at the surface and gradually penetrating deeper into the interior, resulting in a slow freezing rate and generation of large ice crystals. Air-blast freezing, fluidized bed freezing, and impingement freezing are all enhancements to conventional mechanical freezing, while higher capital costs, high energy consumption, and unnecessary mass transfer are their main limitation. Cryogenic freezing, which uses solid or liquid carbon dioxide, or liquid nitrogen directly in contact with the food (Fellows, 2017), has higher heat transfer coefficients and a rapid freezing rate. However, it is also more expensive because refrigerant is not recirculated and is lost to the atmosphere. It is reported that the operating costs of

cryogenic freezing can be times higher than those of mechanical refrigeration systems. Although convective heat transfer between the freezing medium and the product can be improved at the expense of increased cost and extra energy input, in many cases the low conduction efficiency of the products themselves limits its relative heat transfer advantage, which can be adjusted by controlling the size of the food material. Recently, new techniques have been proposed and developed to improve the freezing process and minimize the injuries attributed to conventional freezing methods by controlling nucleation, accelerating heat transfer, and/or reducing the size of ice crystals. This section describes and explains these technologies, their possible mechanisms, and their effect on improving the quality of frozen fruits and vegetables in practical applications.

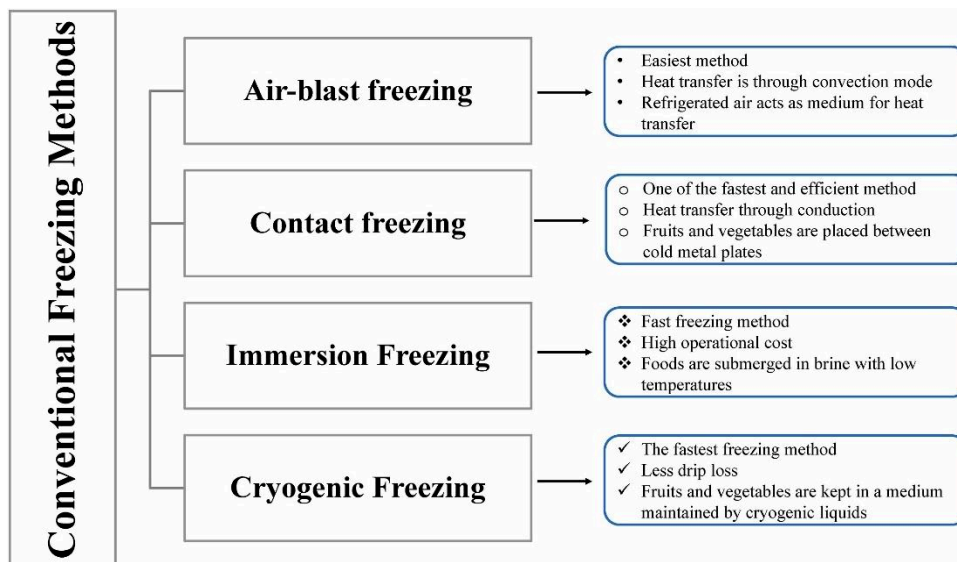


Fig. I. 9: Categorization of traditional freezing methods followed in fruits and vegetables (Navina, Keshav Huthaash, Velmurugan, & Korumilli, 2023).

I.2.1 Pressure-related freezing

Normally, temperature is the main control factor that comes to mind when we consider the freezing. However, there is no doubt that pressure as a thermodynamic variable is theoretically of equal importance to temperature. Only experimental difficulties can explain the relative paucity of pressure-related studies (Smeller, 2002). Fundamental research about extensive data for the phase diagram of pure water has already been carried out by Bridgman (1912) in the past century (Schlüter, Benet, Heinz, & Knorr, 2004). As is shown in Fig. I. 10, at standard atmospheric pressure (1 atm), the freezing point is 273.15K (0 °C), whereas when the pressure rises to

209.9MP, its freezing point drops to 251.165K, which means that for pure water the liquid phase is stabilized even at temperatures below -20 °C by varying the pressure. Since fruits and vegetables can be regarded as complex systems of aqueous solutions, more possibilities for improving freezing are explored by altering the pressure, taking advantage of the phase diagram of water.

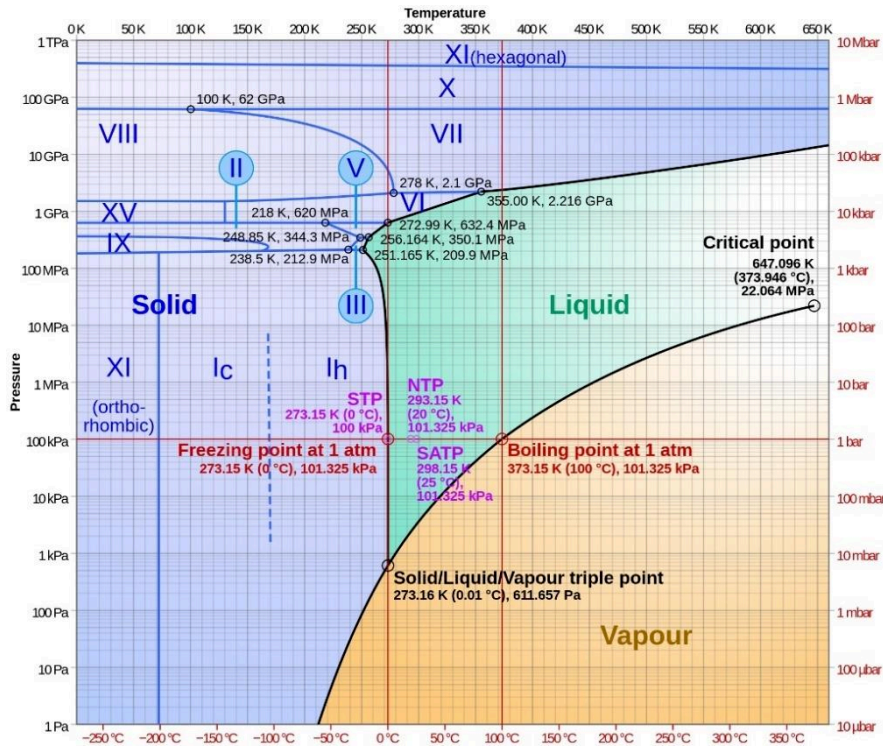


Fig. I. 10: Log–lin pressure–temperature phase diagram of water. The Roman numerals indicate various ice phases.

Several common high-pressure-supported freezing processes are identified in Fig. I. 11. Basically, they utilize the abnormal phase behavior of water under high pressure, thereby controlling the formation of ice crystals within the food with elevated and/not released pressure (Zhu, Li, & Sun, 2021). The high-pressure-assisted freezing (HPAF), ABHI in Fig. I. 11, consists in cooling a sample under pressure up to its phase change temperature at the applied pressure. In this way, the freezing takes place under a constant pressure (LeBail, et al., 2002). High pressure shift freezing (i.e. HPSF, ABCDE in Fig. I. 11) is reported to be superior to HPAF (Fernández, Otero, Guignon, & Sanz, 2006) and more widely investigated in food processing over the past few decades. Since the release of pressure is instantaneous, high degree of supercooling-induced subsequent nucleation is rapid and uniform throughout the volume of the sample. This is particularly advantageous for large samples where conventional

cryopreservation requires a long time for overcoming thermal gradients for cooling and freezing. In this case, shorter phase transition times, smaller ice crystals, and in general, better quality of the frozen food can be achieved, also avoiding the damage of freeze-cracking which might happen when applying cryogenic freezing (B. Li, et al., 2002; Otero, 2023). Meanwhile, if the pressure is elevated high enough (above 210 MPa), in conjunction with certain low temperatures or even above 0 °C, different polymorphs such as ice III (ABCDG), ice V, or ice VI (ABCK) is formed directly, namely high pressure-induced freezing (HPIF). For instance, if the pressure reaches 800 MPa or higher, ice VI with the density of 1.31 g/cm³, may be formed at room temperature, without any form of cooling (L. Cheng, et al., 2017). The formation of ice crystals different from ice I is interesting because ice I is the only kind of ice crystal having a lower density (0.92 g/cm³) than liquid water (Chevalier, Le Bail, & Ghoul, 2000). High-pressure ice (ice II–IX) with higher density does not expand in volume, which may reduce tissue damage (L. Cheng, et al., 2017; B. Li, et al., 2002). Nevertheless these high-pressure ice forms are only stable under high pressure that limits the application of these processes (Xin, et al., 2015). Hence, both HPAF and HPSF perform better than HPIF for food freezing and it is easier to operate HPAF and HPSF for their relatively lower requirement of high pressure (L. Cheng, et al., 2017). Moreover, the synergistic effect of high pressure and subzero temperature on microbial lethality causes some microbial inactivation in the frozen product as an interesting side effect, but higher pressures may also cause unfolding of the proteins structure and the aggregation, denaturation and rearrangement of their structure, as well as other potentially detrimental changes in food quality when compared to the unprocessed product (Dadashi, Fernández-Martín, Mousavi, & Pérez-Mateos, 2024; Norton & Sun, 2008; Otero, 2023). Therefore, the successful application of high-pressure-supported freezing is also largely dependent on the food matrix and the process parameters.

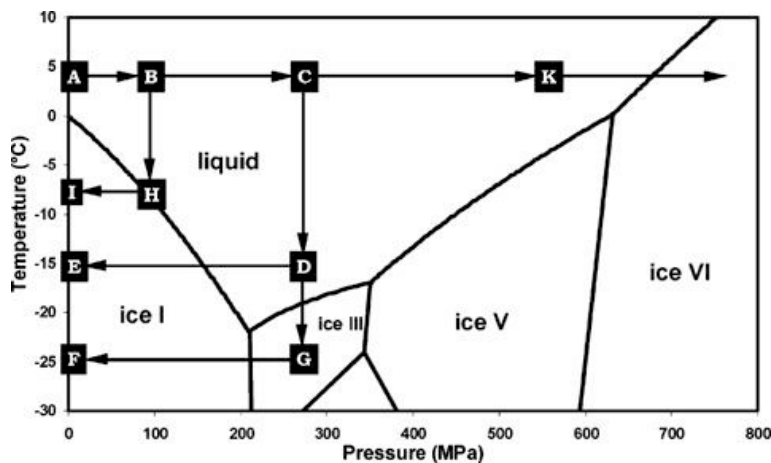


Fig. I. 11: High-pressure-related freezing processes and P – T diagram of water. Pressure-assisted freezing (A, B, H, I), pressure-shift freezing (A, B, C, D, E), freezing to ice III (A, B, C, D, G), freezing to ice III followed by solid—solid transformation to ice I (A, B, C, D, G, F), pressure-induced freezing above 0 °C (A, B, C, K) (Schlüter, et al., 2004).

High-pressure-supported freezing has recently attracted a lot of research activities, especially in food quality parameters, and the advantages of HPSF in fruits and vegetables have been widely reported. Studies of HPSF on potato, carrot, strawberry, mango and peach, aubergines, etc. have been reviewed (Köprüalan Aydın, Yüksel Sarioğlu, Dirim, & Kaymak-Ertekin, 2023; Zhu, Li, et al., 2021). These reviews confirm that HPSF is capable of maintaining the integrity of cell membrane and cell wall and reducing the cellular rupture. Fruits such as strawberries in which texture depends more on the turgor pressure than on the integrity of the cell walls, are strongly affected by HPSF and the softness markedly increases. In this kind of products, pretreatments which enhance demethoxylation of pectin have been tested to improve the firmness of high-pressure shift-frozen strawberries (Chaves, et al., 2018). Xu et al. (Z. Xu, Guo, Ding, An, & Wang, 2014) demonstrated a novel form of HPSF known as high-pressure carbonic immersion (HPCI). This process is based on Joule–Thomson cooling effect, which employs the introduction of carbon dioxide at high pressure inside a pressurized chamber containing the food resulting in even and rapid freezing upon pressure release. HPCI of carrot slices showed that the technique allowed a 33% reduction in drip loss upon thawing in comparison to ultralow temperature freezing at -80°C for 13 min. In spite of the exciting possibilities that high-pressure freezing offers, some obstacles make it difficult to introduce this technology into the food industry, including large size of the pressure equipment, as well as long processing times (Sanz & Otero, 2014).

Isochoric (constant volume) freezing is also a pressure-related freezing approach which has been explored more recently. It is very interesting because, although it is a method of freezing, it minimizes the possibility of the food products being frozen at sub-zero temperatures, which directly avoids the mechanical disruption from the formed ice crystals during freezing, the main source of freezing damage. Isochoric freezing, as the name implies, the volume of the system is held constant (physically constrained by a rigid container without air inside), and the temperature and pressure are left to vary in tandem (Powell-Palm & Rubinsky, 2019). In contrast to an isobaric system where an equal volume of liquid at atmospheric pressure will fully freeze at the phase change temperature, only a fraction of the volume will freeze in an isobaric system (Fig. I. 12A) (Wan, et al., 2018). This is attributed to the fact that when the temperature is below the phase transition temperature, the formation of ice crystals guided by the nucleation site starts, however, the lower-density ice I cannot freely expand within the restriction of a constant volume, and it thus compresses the yet-unfrozen portion of the liquid, elevating the hydrostatic pressure in the system, which further reduces the phase change temperature (Zhao, Powell-Palm, Wang, Bilbao-Sainz, McHugh, & Rubinsky, 2021). Therefore, the freezing process proceeds along the “liquidus line” of the Temperature-Pressure phase diagram (Fig. I. 12B). In this case, pressure and temperature are always interrelated, creating a two-phase system in which a liquid portion exists in equilibrium with the frozen portion at temperatures well below the freezing point under atmospheric conditions (Powell-Palm, et al., 2019).

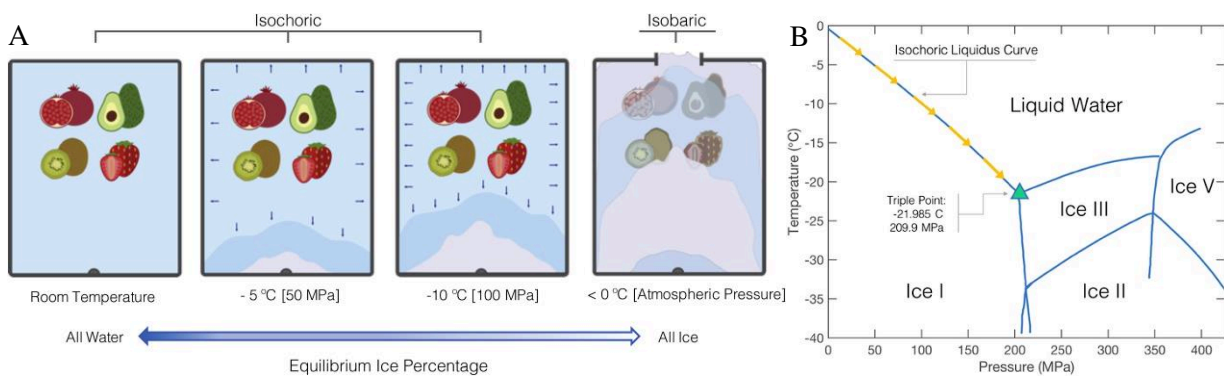


Fig. I. 12: A, Equilibrium states of isochoric systems at various temperatures and comparison to a standard isobaric system frozen at atmospheric pressure. B, Isochoric liquidus curve in the phase diagram of pure water. The liquidus curve between liquid water, ice I, and ice III marks the equilibrium

pressure that an isochoric system will experience at a given subzero temperature higher than the triple point (Powell-Palm, et al., 2019).

The solution in which the food product is immersed in the container is usually an isotonic solution of selected fruits and vegetables, so that the cryoconcentration caused by conventional freezing can also be eliminated (Chaves-Quesada & Acosta-Montoya, 2023). Recently, the potential for greatly enhancing the quality of foods stored at subfreezing temperatures has been demonstrated, with studies of sweet cherries (Bilbao-Sainz, et al., 2019), grape tomato (Bilbao-Sainz, et al., 2021), potato (Zhao, Bilbao-Sainz, et al., 2021), pomegranate (Bilbao-Sainz, et al., 2022), spinach (Bilbao-Sainz, et al., 2020) all demonstrating significant improvements in the mass, appearance, color, microstructure, texture properties, and phytochemical components of foods stored in isochoric systems compared to conventional freezing systems due to no ice crystals formed inside foods. Moreover, the pressure generated during isochoric freezing can cause the infusion of the liquid solution into the pores of a food product, thus the introduction of some active components during this process can also serve as a complement to intensify its cryopreservation benefits (Bilbao-Sainz, Millé, Chiou, Takeoka, Rubinsky, & McHugh, 2024). In addition to the above advantages, the method is quite simple to implement, a transition from an unconstrained volume to a constrained volume, with no electricity or moving parts required, reducing up to 70% energy consumption, especially for long-term storage (Kumari, Chauhan, & Tyagi, 2022; Zhao, Powell-Palm, et al., 2021). However, for soft or highly porous fruits and vegetables, such as strawberry, pepper or eggplant, the disruption in peels, the decrease in firmness and juiciness, and even the destruction of pectin structure during high pressure-related freezing can have negative effects on further industrialization of the technology, also, there is still a need to design and manufacture industrial-scale isochoric freezing chambers to cost-effectively meet industrial needs (Zhao, Bilbao-Sainz, et al., 2021; Zhu, Li, et al., 2021).

In addition to pressurization, depressurization is as effective in the cooling and freezing of fruits and vegetables. The principle of vacuum cooling and vacuum freezing is based on the evaporative heat transfer mechanism (Zhu, Geng, & Sun, 2019). The product is set in a confined space and the pressure of the surrounding is reduced. This promotes evaporation of surface and internal moisture, which usually accompanies the absorption of heat. Therefore, with the evaporation of water from the

product, a large amount of heat is also taken away. While the only heat source in the system is the sensible and latent heat of the product itself, the temperature of the product decreases. It was reported that the heat transfer rate of evaporation is up to 16 times higher than that of conduction (A. C. C. Silva & Schmidt, 2022). This is why vacuum cooling and vacuum freezing are so fast compared to traditional methods. Certainly, since the temperature-reducing function of the technique mainly derives from the evaporation of water, all factors limiting the evaporation of water will be a hindrance to the effective operation. Among these factors, we can mention the pressure variation, the low water content of the food material, a low ratio between the surface area and the mass, an effective barrier to water loss from the produce surface (Huang, Kan, Lu, Li, & Wang, 2021; L. Wang & Sun, 2001).

Vacuum cooling technique has been widely used in processing of fruit, vegetables, meat, fish, sauces, soups, bakery, and ready meals attributed to its superior performance in cooling rate and temperature distribution (N. Wang, Kan, Mao, Huang, & Li, 2021). Many scholars simulated the heat and mass transfer process of fruit and vegetables under vacuum pre-cooling from different research perspectives and tested their quality after pre-cooling (Huang, et al., 2021; N. Wang, Kan, Huang, & Lu, 2020; Zhu, et al., 2019; Zhu, Geng, & Sun, 2021). The vacuum cooling turns into vacuum freezing if the vapor pressure in the vacuum chamber is dropped below 0.6 kPa, the saturation pressure of water at 0 °C (Cengel, Boles, & Kanoğlu, 2011). Vacuum freezing was originally proposed by Kramer et al. in 2002, but it was used just as a pretreatment for freeze-drying for the reduction in drying time and lower residual moisture (Kramer, Sennhenn, & Lee, 2002). High drying rates without compromising its aromatic profile have been proven in freeze-dried soluble coffee using the vacuum freezing method (A. C. C. Silva, et al., 2022). Especially in pharmaceutical formulations, it is of great significance to control nucleation by vacuum freezing to achieve uniformity of the same batch or inter- and intra-vial of products in subsequent freeze-drying processes (Allmendinger, Butt, Mietzner, Schmidt, Luemkemann, & Lema Martinez, 2020; Arsiccio, Barresi, De Beer, Oddone, Van Bockstal, & Pisano, 2018). Besides, the vacuum flash ice-making system has also attracted the attention of relevant domestic and foreign experts in recent years, which has been reported to have a cooling rate that is at least 50 times higher than the traditional method (R. Peng, et al., 2023). Since the latent heat of evaporation (2501.4 kJ/kg at 273.16 K) is much

greater than the latent heat of water crystallization (333.4 kJ/kg), the amount of evaporated water is relatively much smaller than the amount of water frozen into ice crystals (Zou, Zhang, & Zheng, 2021). The morphological visualization and mathematical simulation of water, liquid droplets, as well as puree droplets during vacuum freezing, were investigated for governing the main parameters in this freezing process (H. P. Cheng & Lin, 2007; Cogné, Nguyen, Lanoisellé, Van Hecke, & Clause, 2013; Kazemi, Zandavi, Zargartalebi, Sinton, & Elliott, 2023). However, research on its application to the intensification of freezing of fruits and vegetables is still quite rare. In comparison, the vacuum freezing process of fruit and vegetable tissues with biological structures is more complicated, especially since the barrier of biological membranes may affect the evaporation of moisture. In addition, water loss (WL) due to evaporation of moisture during the freezing process is also a great challenge for frozen products, which alters the microstructure of the tissues, affects product quality, and reduces the commercial interest of the producer. For this point, Wang et al. (H. Wang, et al., 2022) investigated the effects of different amounts of pre-added external water on the quality attributes of vacuum-frozen and thawed apple slices. And good-quality frozen products could be achieved by VF treatment with a higher amount of pre-added external water (30%) because of smaller evaporation activity from the original water in the apple samples during VF.

I.2.2 Electric field (EF) and magnetic field (MF) assisted freezing

In recent years, the possible influences of EF and MF on freezing processes have been extensively investigated with much interest (Jiang, Zhang, & Mujumdar, 2023). It has been indicated that both electrostatic and magnetic fields can speed the freezing process and enhance the quality of the thawed product (R. Hu, Zhang, & Mujumdar, 2022). Manufacturers of electromagnetic freezers on the market also claimed that the combination of electric and magnetic fields can synergistically prohibit water molecule clusters during freezing process so that cells can be well preserved without intracellular ice formation (Mohsen Dalvi-Isfahan, et al., 2017).

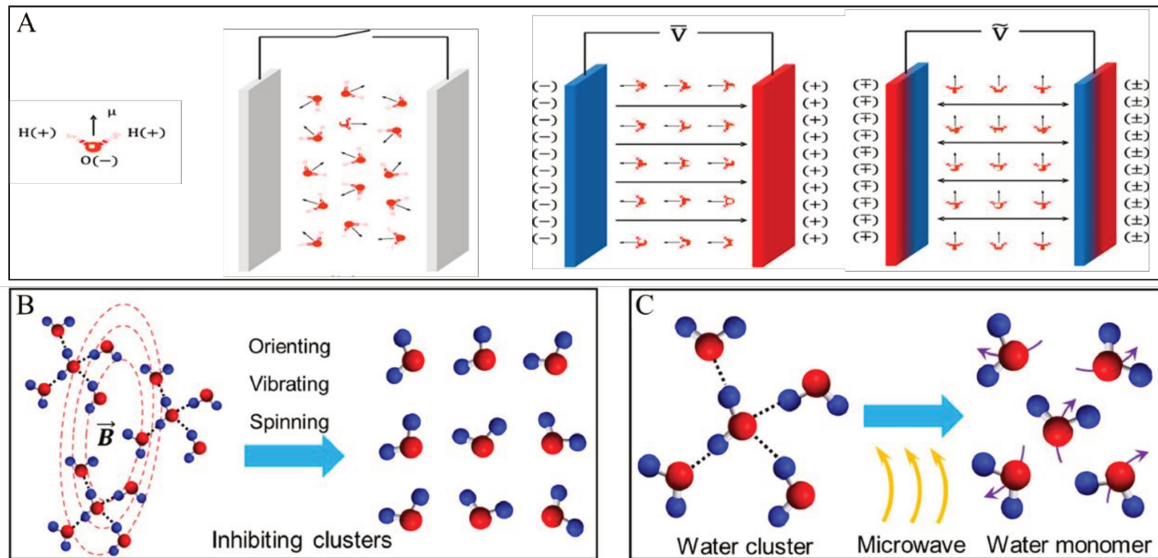


Fig. I. 13: A. From left to right: dipole moment of water molecules, typical random orientation in the absence of any applied field, dipole alignment characteristics of water molecules under external electrostatic and oscillating electric fields, respectively (H. Wu, Ghaani, Nandi, & English, 2022). B. Disturbing effect of oscillating magnetic fields on water clusters by orienting, vibrating, and spinning (M. Lin, Cao, & Li, 2023). C. Disturbing effect of microwave irradiation on water clusters (M. Lin, et al., 2023).

- Electric field assisted-freezing

Electric field can be divided into two categories, namely static electric field (SEF) and oscillating electric field (OEF), depending on whether the strength and direction of the electric field vary with time.

- Electric field assisted-freezing—static electric field (SEF)

SEF is a constant field, which does not change in intensity or direction over time. Two mainstream explanations based on molecular dynamic simulation and thermodynamic laws have been proposed to describe the potential mechanism of crystallization process under a static electric field. Molecular dynamics simulation studies showed that polar materials such as bulk and clusters of water (under the influence of sufficiently high electric fields of $1.0\text{--}1.5 \times 10^7$ V/cm, respectively) will undergo an abrupt structural change that all molecular dipoles tend to be aligned in ordered clusters direction of the electric field. Additionally, hydrogen bonds in random directions are destroyed and stronger hydrogen bonds are created in the direction along the field (Fallah-Joshaqani, Hamdami, & Keramat, 2021). These

findings are in accord with the results of Matsutomo et al. (Matsumoto, Saito, & Ohmine, 2002) which indicate that ice nucleation occurs when a sufficient number of relatively long-lived hydrogen bonds develop spontaneously at the same location to form a fairly compact nucleus. From a thermodynamic perspective, when water is exposed to an external electric field, the dipoles have the tendency to turn into the field. This behavior results in a weakening or destruction of some hydrogen bonds which in turn reduces the entropy of the system and the energy barrier for a phase transition, accordingly, the critical radius which corresponds to the size of a stable ice crystal is also shifted to lower values (M. Dalvi-Isfahan, Hamdami, & Le-Bail, 2016; Mohsen Dalvi-Isfahan, et al., 2017). These all contribute to easier nucleation and promote a higher nucleation rate. However, the magnitude of this behavior depends upon the applied electric field and dielectric constant of the materials (Fallah-Joshaqani, Hamdami, Keshavarzi, Keramat, & Dalvi-Isfahan, 2019). In the review of Kang et al. (Kang, et al., 2020), there are some discrepancies of effective intensity of SEF between simulation and experimental studies. It was also observed that there was an optimal point for increasing the intensity of electric field for different food systems (Fallah-Joshaqani, et al., 2019), therefore more experiments are needed to determine the exact effect of electric field intensity on different food materials. Existing research can only confirm that as the SEF intensity increases during the freezing of animal (lamb and pork) tissues, the supercooling degree and the ice crystal size decrease, as well as reduced drip loss and enhanced texture quality (M. Dalvi-Isfahan, et al., 2016; E. Xanthakis, Havet, Chevallier, Abadie, & Le-Bail, 2013). However, the air ionization or air breakdown occurred on the electrodes can lead to an unstable electric field or a breakdown of the experimental set-up and therefore limit the increase of applied voltage (Q. Wang, Li, Sun, & Zhu, 2019). Thus, in the study of Xie et al. (Xie, et al., 2021), they investigated the effect of low voltage electric field (LVEF) on the freezing of beef muscle. The results showed that LVEF (with lower energy input than high voltage electric field) could also accelerate the freezing rate and thawing rate of the beef muscle, resulting in smaller ice crystals in the muscle tissue. The water holding capacity and the textural property were also proved to be enhanced by LVEF assisted freezing. For plant tissues, which have a higher moisture content than animal tissues, there are relatively few studies on the impact of SEF on the freezing process. The first published report on the electro-freezing of plant tissues (button mushroom) has shown that application of an electric field during freezing improved the

microstructure and texture of mushroom samples without any significant effects on their color parameters and electrolyte leakages. There was an electric field intensity (3.2×10^5 V/m in this case) at which the qualitative characteristics of the product reached their best values (Fallah-Joshaqani, et al., 2021).

Pulsed electric field (PEF) can also be considered an SEF with a pulsed power supply. During PEF treatment, pulses of high-voltage electric fields for a short time (from nanoseconds to milliseconds) were applied to the material between two electrodes, inducing reversible or irreversible perforation of the cell membrane, namely electroporation (electropermeabilization), as well as occurrence of electrochemical and electrolytic reactions, polarization and realignment of molecules, and reduction of activation energy of chemical reactions (Niu, et al., 2020; Wiktor, et al., 2015). These operating characteristics of PEF treatment make it widely used in food processing applications such as microorganism/enzyme inactivation, recovery of bioactive compounds, dehydration, and also freezing (Arshad, et al., 2020). Although the literature about impact of PEF on freezing is limited, existing publications prove that PEF exhibits high potential regarding the improvement of freezing progress and the quality of final products. Different to the static electric field, which is easily integrated with commercially available freezing equipment, PEF treatment is usually difficult to use during the freezing process, but rather as a pre-treatment. The main reason why PEF can be beneficial for freezing and/or thawing kinetics can be attributed to the potential mechanism of pore formation. On one hand, these pores make the heat transfer in the cellular matrix much easier and faster. Besides, small fragments of ruptured cell membranes or cell walls can act as additional centers of crystallization (Dadan, Nowacka, Czyzewski, & Witrowa-Rajchert, 2020). Review on the application of PEF treatment prior to freezing indicated that the freezing and thawing kinetics of potatoes, apples, and carrots were improved in comparison to untreated samples, the total freezing time and phase transition time were also shortened (Dadan, et al., 2020). But for the quality attributes such as drip loss during thawing and textural properties, the results are context-dependent. Although it is generally accepted that certain PEF treatments (high field intensity, long treatment times) can have tissue softening and ohmic heating effects that we do not expect in the freezing of fruits and vegetables. Thus, in addition to adjusting the operating parameters of the treatment for raw materials with different biological properties,

cryoprotectants are usually used in combination with PEF prior to freezing, in order to preserve quality (especially texture) after thawing (Alabi, Olalusi, Olaniyan, Fadeyibi, & Gabriel, 2022). It should be pointed out that the combined technique PEF + VI (vacuum infusion) has been commercialized by OptiFreeze (<http://optifreeze.se>) on plant products (Dadan, et al., 2020).

- Electric field assisted-freezing—oscillating electric field (OEF)/alternated electric field (AEF)

Electric field produced by alternating currents is called an oscillating electric field (OEF), or an alternated electric field (AEF). In contrast to SEF, which orients water molecules, as the direction of the electric field in the AEF changes, the alternating electric frequency causes the water dipole to continuously spin, rotate, and translate, hydrogen bonds break, and the water molecules rearrange (G. Wu, Yang, Bruce, Roy, Li, & Zhang, 2023). These behaviors increase the allowable degree of supercooling (enhance supercooling), suppress or retard spontaneous ice nucleation, and represent a kinetic constrain to ice formation by interfering with both ice nucleation and kinetics of crystal growth (Mohsen Dalvi-Isfahan, et al., 2017). Compared to SEF assisted freezing, there are fewer studies on freezing assisted by AEF, and the majority of the studies focused on freezing of aqueous solutions and a few on water freezing (Jha, Xanthakis, Jury, Havet, & Le-Bail, 2018). Recently, the first application of AEF-assisted freezing in a real food system (*longissimus dorsi* muscle) was explored (G. Wu, Yang, Bruce, Roy, Li, & Zhang, 2022; G. Wu, et al., 2023). Although the meat quality was not as good as that of the only postmortem aging (OA) group, the group assisted by AEF was significantly enhanced in color, water-holding capacity, and tenderness. Moreover, the effects of AEF on microstructural damage and protein structural changes during aging of beef after freezing-thawing were relatively small compared to only aging (OA) group and freezing-thawing-aging sequence (FA) group. This is due to AEF treatment reduced the degree of protein fragmentation as well as aggregation, decreased the degree of protein oxidation and exposure of amino acid residues, and obtained better stability (G. Wu, et al., 2022). However, these results are based on observations from a combined freezing and aging protocol, and the results of AEF-assisted freezing alone, as well as the effects on fruits and vegetables completely different structural and compositional compositions, remain to be further explored.

- Magnetic fields assisted-freezing

Although involving a different potential mechanism to electric fields, the application of magnetic fields (MF) can also impact the ice nucleation and crystallization processes during freezing. All matters exhibit magnetic effects since the electrons in atoms spin and create tiny magnetic fields. As a typical diamagnetic material, water has no net magnetic moment in the absence of an external MF since the orbital magnetic moment and the electron spin magnetic moment cancel each other. However, once under MF, the orbital motion of electrons is changed and a small magnetic moment is induced in the opposite direction of the applied MF (Kang, et al., 2020). When the MF is strong, the influential force can even be macroscopically visualized. Similar to EF, magnetic fields commonly employed in freezing operations can be divided into two types, including static magnetic field (SMF) and oscillating magnetic field (OMF). SMF is most likely to be generated by permanent magnets, and OMF is mainly achieved with different types of electromagnets (Kang, et al., 2020). SMF does not vary with time in terms of direction or intensity, while OMF shows variation with time and turns azimuthally around the magnetic field line's center (Kaur, et al., 2020). Tang et al. (Tang, Zhang, Tian, & Shao, 2020) investigated the magnetic field-assisted freezing of cherry and found that both static and alternating magnetic fields reduced the size of ice crystals by microscopy observation. Although the variations of the phase change time with the intensity for two kinds of MF are different.

For SMF, there are some conflicting experimental conclusions, examples as 20 kHz square wave electric field and the static 0.2 T magnetic field on saline solution and meat samples, static magnetic field of 40–50 mT or 150–200 mT on potatoes both showed no improvement on the freezing dynamics, degree of supercooling, and also the quality of the samples (Abie, Münch, Egeland, Bjerke, Wergeland, & Martinsen, 2021; Otero & Pozo, 2022). In the study of Leng et al. (Leng, Zhang, Tian, Li, Kong, & Zhan, 2023), they investigated the effects of 0 to 45 mT SMF intensities on the freezing of apple, peach, cucumber and Indian jujube. From this comparison, Indian jujube is the only one showed positive effects of SMF on macro-scale parameters, and stronger intensity brought better quality. This also indicated that in addition to being affected by the applied intensity and frequency, the effect of MF varies on the species of tested samples. The majority of studies with positive results suggest that the potential mechanism of SMF might be due to hydrogen bonds

between water molecules becoming strengthened under SMF, and the molecules and/or water clusters are more ordered and stably distributed, therefore, ice nucleation is promoted.

OMF is more widely used than SMF in food freezing research. It is accepted that OMF makes the thermal vibration caused by the electron spin appear and prevents the normal crystallization of water below freezing temperature. The water will enter a longer period of supercooling, which will gradually exceed the amount of cooling required for water solidification. At this stage, the lower temperature or the sudden decrease of thermal vibration will cause the water molecules to rearrange according to the hydrogen bond and complete the instantaneous crystallization, so that numerous fine ice crystals will be generated at the same time (Jiang, Zhang, Mujumdar, & Gan, 2023). A commercial system utilizing OMF is the Cells Alive System (CAS) patented and marketed by the ABI Corporation Ltd. (Chiba, Japan), which claims to provide a process where a product can be frozen in such a manner as to “approximate the quality of a fresh product” once thawed (Purnell, James, & James, 2017). Several authors in the scientific literature have performed experimental measurements for different “CAS energy” conditions on the food product in ABI freezers. However, these results showed that oscillating weak magnetic fields had no effect on the freezing curves and cellular microstructures of potato, apple, and crab sticks (Otero, Pérez-Mateos, Rodríguez, & Sanz, 2017; Antonio Carlos Rodríguez, et al., 2020). Such a situation is the same as for pure water and 0.9% NaCl solutions at frozen in a 0.8-mT magnetic field at different frequencies (20, 50, 200, and 2000 Hz) (Otero, Rodríguez, & Sanz, 2020). Although excessively small intensities have no significant effect, this does not mean that the stronger the better. The ice crystal area variation of blueberry with different alternating magnetic field (AMF) intensities ranging from 0 mT (b) 1.74 mT showed that the ice crystal size reduced first and then increased with the AMF intensity increasing (Tang, Shao, et al., 2020). Zhou et al. evaluated the effects of magnetic field-assisted immersion freezing (MIF) with different magnetic field intensities (0, 20, 40, 60, and 80 mT) on the freezing curves, ice crystal area, microstructure, and physicochemical properties of golden pompano (*Trachinotus ovatus*) muscle. The result showed that, compared with refrigerator freezing and immersion freezing (MIF-0), magnetic fields prolonged the freezing time. But an appropriate magnetic field intensity (20 mT) inhibited the formation of large ice

crystals, promoted a uniform distribution of ice crystals, and weakened the mechanical damage of muscle tissue by ice crystals. The centrifugal loss and cooking loss of MIF-20 were 23.55 % and 29.18 % lower than those of MIF-0 group, respectively. Moreover, Rodríguez et al. (A. C. Rodríguez, Otero, Cobos, & Sanz, 2019) stated that any variable magnetic fields will induce variable non-conservative electric fields according to Faraday's law. This may also be one of the principles to explain the potential effects of oscillating magnetic fields on freezing.

- Electromagnetic field assisted-freezing

In fact, the EF and MF are interdependent when dealing with time-varying fields, implying that time-varying EF produces time-varying MF and vice versa according to Ampere-Maxwell law and Faraday's law (Ida, 2015). Electromagnetic field is a combination of EF and MF that change with space and time. It has a broad definition, which includes energy fields in different frequency bands such as microwave, visible light and X-rays. For freezing food products, researches mainly focus on microwave (MW) and radiofrequency (RF), and results proved that these electromagnetic fields also had great potential to control ice formation and growth in cells or tissues during freezing and to reduce freezing damages in frozen food products (Zhan, Zhu, & Sun, 2019).

RF waves are a form of electromagnetic radiation with wavelengths ranging from 300 kHz to 300 GHz and MW is a subset of RF and ranges from 300 MHz to 300 GHz. These waves create an alternating field between two electrodes which causes polarization in bipolar molecules like water and charged ions in food materials and thus molecules continuously reorient to poles, without inducing thermal effects but producing more nucleation sites (Hafezparast-Moadab, Hamdami, Dalvi-Isfahan, & Farahnaky, 2018; Manzocco, Alongi, Cortella, & Anese, 2022). Although little information is available on RF-assisted freezing and its effects on food quality, the preliminary results have indicated that this process (RF of 27.12 MHz) could reduce the size of ice crystals during freezing and increase the textural quality of rainbow trout (Hafezparast-Moadab, et al., 2018), as well as pork when combined with cryogenic freezing (Anese, Manzocco, Panozzo, Beraldo, Foschia, & Nicoli, 2012; Manzocco, et al., 2022). It should be pointed out that the liquid nitrogen used as a

cooling media during RF freezing is expensive, and other freezing media and more exploration on fruits and vegetables could be studied in future.

Generally, the total freezing time is not affected by the RF treatment since no thermal effect is induced, while MW can induce a thermal effect due to the friction of water molecules which occurred through their torque, increasing the total freezing time (Hafezparast-Moadab, et al., 2018; E. Xanthakis, Le-Bail, & Ramaswamy, 2014). Although longer freezing times are usually considered negative, several researches have shown that microwave-assisted freezing can reduce the size of ice crystals, and thus improving frozen product quality (Sadot, Curet, Le-Bail, Rouaud, & Havet, 2020; Epameinondas Xanthakis, Huen, Eliasson, Jha, Le-Bail, & Shrestha, 2018; E. Xanthakis, et al., 2014).

However, the potential mechanism to explain the observed ice crystal size reduction in MAF samples varies. Jha et al. (Jha, Chevallier, Xanthakis, Jury, & Le-Bail, 2020) compared the effect of conventional freezing and MAF on the freezing parameters and quality properties of apples and potatoes. They reported that microwave irradiation during freezing of potato and apple had no significant effect on the freezing time and freezing rate, but the quality properties of apple and potato consist of drip loss and firmness improved by using microwave irradiation. Also, microstructure analysis of apple and potato showed that microwave-assisted freezing leads to an increase in the population of small pores with more homogenous size distributions. In addition, two concepts were proposed to explain the observed ice crystal size reduction in MAF frozen systems (Jha, et al., 2020). The “NITOM” concept (Nucleation Induced by Temperature Oscillation caused by MWs) which is based on the fact that under specific duty ratio, the temperature of the sample undergoing freezing will oscillate. The fluctuating temperature is expected to favor secondary nucleation which in turn suppresses the crystal growth. The second concept is called “NIMIW” (Nucleation Induced by constant or pulsed Microwave power) and it is based on constant or pulsed (short time) emission. NIMIW can be explained by the impact of MW radiation on the hydrogen bonds between water molecules, which may affect the water cluster structures during freezing. It is expected that MWs would exert a torque and displace the water molecules from their equilibrium relationships in the ice cluster resulting in fragmentation of existing ice crystals when ice crystals are in the form of nuclei. The fragmented ice crystals nuclei may act as new nucleation

sites and promote the secondary nucleation, thus, causing ice crystal size reduction. However, Mathieu et al. (Sadot, Curet, Chevallier, Le-Bail, Rouaud, & Havet, 2020) disconfirmed the hypothesis that the ice crystal size reduction may be due to temperature oscillations, but instead be due to the perturbation of the H-bond network in water, which could be a precursor to crystalline structure. Limited oscillation of temperature during the freezing process leads to alternative melting and growth of ice crystals which prevent the crystal growth and lead to the formation of numerous small ice crystals. From the study of the effect of microwave-assisted freezing (MAF) on some quality attributes of lamb meat, microwave irradiation during the freezing process improved the microstructure of frozen meat by reducing the size of ice crystals and consequently reducing the amount of drip loss and color change (Atani, Hamdami, Dalvi-Isfahan, Soltanizadeh, & Fallah-Joshaqani, 2022). The author also indicated limited oscillation of temperature during the freezing process leads to alternative melting and regeneration of ice crystals which prevent the crystal growth and lead to the formation of numerous small ice crystals.

I.2.3 Ultrasound-assisted freezing

Ultrasound is defined as a sound wave having frequencies higher than the hearing threshold of humans (>16 kHz). It has been considered a kind of vibrational energy produced by ultrasound transducers, which have the ability to convert electrical energy to ultrasonic energy (Islam, Zhang, & Adhikari, 2017; Qiu, Zhang, Chitrakar, & Bhandari, 2020). The US process is classified based on frequency and power into high-frequency low power (>100 kHz, MHz range) and low-frequency high power (20–100 kHz). The latter type of ultrasound, namely power ultrasound (20-100 kHz, generally above 1 W cm^{-2}) is widely used in food processing and has proven to be useful in facilitating the nucleation process, increasing heat transfer efficiency, and controlling the crystallization process during freezing (Basse, Cheng, & Sun, 2021; Mohsen Dalvi-Isfahan, et al., 2017; Qiu, et al., 2020). Cavitation is generally considered to be the basic principle of ultrasound action. A number of compression and rarefaction cycles occur when ultrasound passes through a medium (such as solid, liquid, or gases other than air). Cavitation bubbles are created when rarefaction exceeds the attractive forces among molecules in a liquid phase at high power condition (Islam, et al., 2017). The gradual growth and final collapse of the cavitation bubbles led to acoustic cavitation, which caused mechanical effects (turbulence, shear

forces, shock waves, and pressure), chemical effects (free radicals), and thermal effects (temperature) (H. Zhang, Chen, Liu, Mei, Yu, & Kan, 2020).

The positive role of ultrasound-generated cavitation in nucleation can be explained from three aspects. Firstly, acoustic cavitation forms microstreaming, which leads to intensive collision between micro-particles in the medium, thus generating thinner solid–liquid interface. Secondly, the generation of cavitation bubbles in the transport media as well as the collapse of the bubbles contribute to the production of ultrahigh pressure (100 MPa). The high supercooling degree produced by the instantaneous high pressure promotes the instantaneous nucleation. Thirdly, primary nucleation is induced by cavitation bubbles with certain size and secondary nucleation is realized by the small pieces from large dendritic ice crystals (Qiu, et al., 2020; C. Zhang, Li, Xia, Sun, Sun, & Kong, 2023). Islam et al. (Islam, Zhang, Adhikari, Xinfeng, & Xu, 2014) reported that ultrasound at 0.39 W/cm^2 (20 kHz) advanced the time of nucleation of *Lentinula edodes*, *Agaricus bisporus*, and *Pleurotus eryngii* by 24 %, 53 % and 34 %, respectively. The acceleration in nucleation which depended on duration of US was also observed during the freezing of solid model food (agar gel) (Kiani, Zhang, Delgado, & Sun, 2011).

Microflow effect is closely related to the cavitation effect, depending on whether the cavitation bubbles collapse into steady-state cavitation or transient cavitation (Yu, Mei, & Xie, 2022). In the steady-state cavitation effect, the internal air is continuously exchanged with the loaded cooling medium under the action of ultrasonic cavitation bubbles, and the exchange can generate eddy currents around the cavitation bubbles, resulting in a microfluidic effect (Z. Zhang, Sun, Zhu, & Cheng, 2015); In transient cavitation, the generated cavitation bubble bursts and generates energy when its volume increases and reaches the critical size, resulting in turbulence and micro-flow effect. As a consequence, a formation of microchannels is noted, which enhances the heat and mass transfer processes due to released cells' contents (Dadan, Matys, Kaminska-Dworznicka, Lammerskitten, Toepfl, & Parniakov, 2021). Moreover, extreme pressure, microturbulence, as well as the enhancement of transfer of solid molecules from bulk to the surface of growing crystals, contribute significantly to the control of the ice crystal size (Dadan, et al., 2021). Previous studies have been reported on ultrasound assisted freezing of fruit and vegetables, like strawberries, apples, mushrooms, lotus root, radishes, and potatoes, and increases in freezing rate,

freezing efficiencies, and reduction in the size of ice crystals were obtained (Tian, Chen, Zhu, & Sun, 2020; Zhu, Zhang, & Sun, 2020).

Selection of the appropriate ultrasound parameters on the suitable materials also affects the action of the ultrasound and the freezing characteristics. Ultrasound significantly reduced the freezing time of broccoli only when strictly defined intensity was applied (Xin, Zhang, & Adhikari, 2014). Temperature of nucleation was also reported to increase with the growth of intensity of ultrasound (B. Xu, Azam, Wang, Zhang, & Bhandari, 2019). However, higher thermal effect might be observed at higher ultrasound power, which is negative for the freezing rate and final quality. Compared to conventional ultrasonic cleaners and single-frequency UAF devices, multi-frequency UAF devices could increase the cavitation yield, due to the increased number of mechanical interference and cavitation nuclei in multi-frequency UAF. The study on the effects of single-, dual- and multi-frequency UAF on muscle quality and myofibrillar protein structure in large yellow croaker also proved that multi-frequency UAF significantly improved the freezing rate, reduced lipid oxidation, and maintained the myofibrillar structure (Bian, Yu, Yang, Mei, & Xie, 2022). Similar results were also found in the freezing rate and the quality attributes of the frozen potato samples with multi-frequency ultrasonic treatment (Zhu, et al., 2020). However, more hydroxyl radicals it should generated by multi-frequency ultrasonic treatment could not be ignored, which might decrease the nutritional value of the potato. Due to the great ultrasonic attenuation coefficient of porous materials, the ultrasonic efficiency and the strength of ultrasonic cavitation could thus be much influenced as well (Villamiel, García-Pérez, Montilla, Carcel, & Benedito, 2017). The effect of voids on ultrasound-assisted immersion freezing (UF) in selected plant tissues, apple, radish, and potato was investigated. The results indicated that UF was more effective in freezing fruit or vegetables with a highly dense structure (Zhu, et al., 2018).

I.3 Conclusion and research objectives

From the literature review we have learned that the freezing of fruits and vegetables involves a series of physical and biochemical changes that are influenced by their original species and structure, condition and integrity, as well as by the subsequent processing, including pretreatment (precooling, peeling, dicing, blanching, and partial dehydration, etc.), freezing process, storage and transportation, and finally thawing

process. The negative impacts of these operations are usually cumulative and irreversible. Therefore, every step from harvest to final consumption of fruits and vegetables is essential and needs to be considered comprehensively in order to obtain a suitable operating parameter.

In this study we focused our exploration on the freezing operation. Conventional freezing methods, due to slow freezing rates, can lead to the formation of large ice crystals and the migration of large amounts of water, which can damage the cellular structure of the product at the microscopic level, while at the macroscopic level, textural deterioration can occur, as well as significant drip losses during thawing. Thus, the foundations including principles, mechanisms, and related research findings of several innovative freezing technologies such as pressure-related freezing, electric field (EF) and magnetic field (MF) assist freezing, ultrasound assist freezing are described. They improve freezing kinetics, freezing efficiency, and quality attributes (microstructure, drip loss, texture, color and nutrition) by accelerating or inhibiting nucleation (raising or lowering the nucleation temperature), increasing heat and mass transfer rates, and controlling ice crystal size. Although some of the results are positive, they are always highly dependent on raw material characteristics and operation parameters. Besides, cost and energy consumption are also factors to consider. Among them, vacuum freezing, as a fast freezing technology, has great potential in the fruits and vegetables freezing industry. This process can even be achieved without the involvement of any freezing medium, which is one of the interesting points about it. In addition, the pulsed electric field can be a possibility as a pretreatment for intensive vacuum freezing by making the diffusion of moisture easier through electro-permeabilization. On the basis of the literature review, the aims of this thesis are:

- (1) Understand the impact of vacuum freezing on the quality characteristics of thawed carrot discs
 - Construction of the vacuum freezing system and determination of the application range of vacuum freezing (including the freezing critical zone).
 - Comparison of the quality attributes of thawed carrot discs after conventional freezing and vacuum freezing.

- Discussing the impact of the size of carrot discs on the effectiveness of vacuum freezing.
 - Determination of the equivalent air freezing parameters of vacuum freezing by using the Pham model.
- (2) Investigate of the effect of PEF pretreatment on the intensification of vacuum freezing.
- Effect of different PEF parameters on the kinetics of vacuum freezing.
 - Comparison of the quality of thawed carrot discs after PEF-pretreated vacuum freezing and conventional freezing.
- (3) In order to understand the applicability of the PEF pretreated vacuum freezing to different fruits and vegetables, the same freezing operation was performed on selected materials (carrots, apples, and potatoes), and their freezing processes and quality attributes were compared.

- Abie, S. M., Münch, D., Egelanddal, B., Bjerke, F., Wergeland, I., & Martinsen, Ø. G. (2021). Combined 0.2 T static magnetic field and 20 kHz, 2 V/cm square wave electric field do not affect supercooling and freezing time of saline solution and meat samples. *Journal of Food Engineering*, 311, 110710. <https://doi.org/10.1016/j.jfoodeng.2021.110710>
- Alabi, K. P., Olalusi, A. P., Olaniyan, A. M., Fadeyibi, A., & Gabriel, L. O. (2022). Effects of osmotic dehydration pretreatment on freezing characteristics and quality of frozen fruits and vegetables. *Journal of Food Process Engineering*, 45(8), e14037. <https://doi.org/10.1111/jfpe.14037>
- Allmendinger, A., Butt, Y. L., Mietzner, R., Schmidt, F., Luemkemann, J., & Lema Martinez, C. (2020). Controlling Ice Nucleation during Lyophilization: Process Optimization of Vacuum-Induced Surface Freezing. In *Processes* (Vol. 8).
- Ando, Y., Maeda, Y., Mizutani, K., Wakatsuki, N., Hagiwara, S., & Nabetani, H. (2016). Effect of air-dehydration pretreatment before freezing on the electrical impedance characteristics and texture of carrots. *Journal of Food Engineering*, 169, 114-121. <https://doi.org/10.1016/j.jfoodeng.2015.08.026>
- Ando, Y., & Watanabe, T. (2023). Mechanical properties of dehydrofrozen carrots as a function of cell membrane damage, ice crystal development, and rehydration. *Journal of Food Engineering*, 357, 111643. <https://doi.org/10.1016/j.jfoodeng.2023.111643>
- Anese, M., Manzocco, L., Panozzo, A., Beraldo, P., Foschia, M., & Nicoli, M. C. (2012). Effect of radiofrequency assisted freezing on meat microstructure and quality. *Food Research International*, 46(1), 50-54. <https://doi.org/10.1016/j.foodres.2011.11.025>
- Añón, M. C., & Calvelo, A. (1980). Freezing rate effects on the drip loss of frozen beef. *Meat Science*, 4(1), 1-14. [https://doi.org/10.1016/0309-1740\(80\)90018-2](https://doi.org/10.1016/0309-1740(80)90018-2)
- Araújo-Rodrigues, H., Santos, D., Campos, D. A., Ratinho, M., M. Rodrigues, I., & E. Pintado, M. (2021). Development of Frozen Pulps and Powders from Carrot and Tomato by-Products: Impact of Processing and Storage Time on Bioactive and Biological Properties. In *Horticulturae* (Vol. 7).
- Arshad, R. N., Abdul-Malek, Z., Munir, A., Buntat, Z., Ahmad, M. H., Jusoh, Y. M. M., Bekhit, A. E.-D., Roobab, U., Manzoor, M. F., & Aadil, R. M. (2020). Electrical systems for pulsed electric field applications in the food industry: An engineering perspective. *Trends in Food Science & Technology*, 104, 1-13. <https://doi.org/10.1016/j.tifs.2020.07.008>
- Arsiccio, A., Barresi, A., De Beer, T., Oddone, I., Van Bockstal, P.-J., & Pisano, R. (2018). Vacuum Induced Surface Freezing as an effective method for improved inter- and intra-vial product homogeneity. *European Journal of Pharmaceutics and Biopharmaceutics*, 128, 210-219. <https://doi.org/10.1016/j.ejpb.2018.04.002>
- Atani, S. H., Hamdami, N., Dalvi-Isfahan, M., Soltanizadeh, N., & Fallah-Joshaqani, S. (2022). Effects of microwave-assisted freezing on the quality attributes of lamb meat. *International Journal of Refrigeration*, 143, 192-198. <https://doi.org/10.1016/j.ijrefrig.2022.03.019>
- Augusto, P. E. D., Soares, B. M. C., & Castanha, N. (2018). Chapter 1 - Conventional Technologies of Food Preservation. In F. J. Barba, A. S. Sant'Ana, V. Orlie & M. Koubaa (Eds.), *Innovative Technologies for Food Preservation* (pp. 3-23): Academic Press.
- Bai, G., Gao, D., Liu, Z., Zhou, X., & Wang, J. J. N. (2019). Probing the critical nucleus size for ice formation with graphene oxide nanosheets. *576(7787)*, 437-441

- Ban, C., Yoon, S., Han, J., Kim, S. O., Han, J. S., Lim, S., & Choi, Y. J. (2016). Effects of freezing rate and terminal freezing temperature on frozen croissant dough quality. *LWT*, 73, 219-225. <https://doi.org/10.1016/j.lwt.2016.05.045>
- Bassey, E. J., Cheng, J.-H., & Sun, D.-W. (2021). Novel nonthermal and thermal pretreatments for enhancing drying performance and improving quality of fruits and vegetables. *Trends in Food Science & Technology*, 112, 137-148. <https://doi.org/10.1016/j.tifs.2021.03.045>
- Ben Haj Said, L., Bellagha, S., & Allaf, K. (2015). Measurements of texture, sorption isotherms and drying/rehydration kinetics of dehydrofrozen-textured apple. *Journal of Food Engineering*, 165, 22-33. <https://doi.org/10.1016/j.jfoodeng.2015.04.029>
- Ben Haj Said, L., Bellagha, S., & Allaf, K. (2016). Dehydrofreezing of Apple Fruits: Freezing Profiles, Freezing Characteristics, and Texture Variation. *Food and Bioprocess Technology*, 9(2), 252-261. <https://doi.org/10.1007/s11947-015-1619-4>
- Berk, Z. (2009). Chapter 19 - Refrigeration, chilling and freezing. In Z. Berk (Ed.), *Food Process Engineering and Technology* (pp. 391-411). San Diego: Academic Press.
- Bernaś, E., & Jaworska, G. (2014). Effect of microwave blanching on the quality of frozen *Agaricus bisporus*. *Food Science and Technology International*, 21(4), 245-255. <https://doi.org/10.1177/1082013214529956>
- Berry, M., Fletcher, J., McClure, P., & Wilkinson, J. (2008). Effects of freezing on nutritional and microbiological properties of foods. In J. A. Evans (Ed.), *Frozen Food Science and Technology* (pp. 26-50).
- Bian, C., Yu, H., Yang, K., Mei, J., & Xie, J. (2022). Effects of single-, dual-, and multi-frequency ultrasound-assisted freezing on the muscle quality and myofibrillar protein structure in large yellow croaker (*Larimichthys crocea*). *Food Chemistry: X*, 15, 100362. <https://doi.org/10.1016/j.fochx.2022.100362>
- Bilbao-Sainz, C., Chiou, B.-S., Takeoka, G., Williams, T., Wood, D., Powell-Palm, M. J., Rubinsky, B., Wu, V. C. H., & McHugh, T. (2022). Isochoric freezing and isochoric supercooling as innovative postharvest technologies for pomegranate preservation. *Postharvest Biology and Technology*, 194, 112072. <https://doi.org/10.1016/j.postharvbio.2022.112072>
- Bilbao-Sainz, C., Millé, A., Chiou, B.-S., Takeoka, G., Rubinsky, B., & McHugh, T. (2024). Calcium impregnation during isochoric cold storage to improve postharvest preservation of fresh blueberries. *Postharvest Biology and Technology*, 211, 112841. <https://doi.org/10.1016/j.postharvbio.2024.112841>
- Bilbao-Sainz, C., Sinrod, A., Powell-Palm, M. J., Dao, L., Takeoka, G., Williams, T., Wood, D., Ukpai, G., Aruda, J., Bridges, D. F., Wu, V. C. H., Rubinsky, B., & McHugh, T. (2019). Preservation of sweet cherry by isochoric (constant volume) freezing. *Innovative Food Science & Emerging Technologies*, 52, 108-115. <https://doi.org/10.1016/j.ifset.2018.10.016>
- Bilbao-Sainz, C., Sinrod, A. G. J., Dao, L., Takeoka, G., Williams, T., Wood, D., Bridges, D. F., Powell-Palm, M. J., Ukpai, G., Chiou, B.-S., Wu, V. C. H., Rubinsky, B., & McHugh, T. (2020). Preservation of spinach by isochoric (constant volume) freezing. *International Journal of Food Science & Technology*, 55(5), 2141-2151. <https://doi.org/10.1111/ijfs.14463>
- Bilbao-Sainz, C., Sinrod, A. J. G., Dao, L., Takeoka, G., Williams, T., Wood, D., Chiou, B.-S., Bridges, D. F., Wu, V. C. H., Lyu, C., Powell-Palm, M. J., Rubinsky, B., & McHugh, T. (2021).

- Preservation of grape tomato by isochoric freezing. *Food Research International*, 143, 110228. <https://doi.org/10.1016/j.foodres.2021.110228>
- Bouzari, A., Holstege, D., & Barrett, D. M. (2015). Vitamin Retention in Eight Fruits and Vegetables: A Comparison of Refrigerated and Frozen Storage. *Journal of Agricultural and Food Chemistry*, 63(3), 957-962. <https://doi.org/10.1021/jf5058793>
- Brar, A., Bhatia, A., Pandey, V., & Kumari, P. (2017). Biochemical and phytochemical properties of potato: A Review. *Chemical Science Review and Letters*, 6, 117-129
- Briggs, D. B. (1932). Water relationships in colloids II. . *Journal of Physical Chemistry*, 36(1), 367-386
- Çabas, B. M., Azazi, I., Döner, D., Bayana, D., Çokgezme, Ö. F., & İçier, F. (2022). Comparative performance analysis of ohmic thawing and conventional thawing of spinach puree. *Journal of Food Process Engineering*, 45(7), e14015. <https://doi.org/10.1111/jfpe.14015>
- Cai, L., Cao, M., Regenstein, J., & Cao, A. (2019). Recent Advances in Food Thawing Technologies. *COMPREHENSIVE REVIEWS IN FOOD SCIENCE AND FOOD SAFETY*, 18(4), 953-970. <https://doi.org/10.1111/1541-4337.12458>
- Carbonell, S., Oliveira, J. C., & Kelly, A. L. (2006). Effect of pretreatments and freezing rate on the firmness of potato tissue after a freeze–thaw cycle. *International Journal of Food Science & Technology*, 41(7), 757-767. <https://doi.org/10.1111/j.1365-2621.2005.01054.x>
- Castro, S. M., Saraiva, J. A., Lopes-da-Silva, J. A., Delgadillo, I., Loey, A. V., Smout, C., & Hendrickx, M. (2008). Effect of thermal blanching and of high pressure treatments on sweet green and red bell pepper fruits (*Capsicum annuum* L.). *Food Chemistry*, 107(4), 1436-1449. <https://doi.org/10.1016/j.foodchem.2007.09.074>
- Cen, H., Lu, R., Mendoza, F., Beaudry, R. M. J. P. B., & Technology. (2013). Relationship of the optical absorption and scattering properties with mechanical and structural properties of apple tissue. 85, 30-38
- Cengel, Y. A., Boles, M. A., & Kanoğlu, M. (2011). *Thermodynamics: an engineering approach* (Vol. 5): McGraw-hill New York.
- Charoenrein, S., & Owcharoen, K. (2016). Effect of freezing rates and freeze-thaw cycles on the texture, microstructure and pectic substances of mango. *International Food Research Journal*, 23(2), 613
- Chaves-Quesada, J., & Acosta-Montoya, O. (2023). Congelación isocórica: ventajas y oportunidades de investigación en la industria de alimentos. *Agronomía Mesoamericana*, 34(3). <https://doi.org/10.15517/am.2023.52879>
- Chaves, A., & Zaritzky, N. (2018). Cooling and Freezing of Fruits and Fruit Products. In A. Rosenthal, R. Deliza, J. Welti-Chanes & G. V. Barbosa-Cánovas (Eds.), *Fruit Preservation: Novel and Conventional Technologies* (pp. 127-180). New York, NY: Springer New York.
- Chen, B., Zhang, M., Wang, Y., Devahastin, S., & Yu, D. (2022). Comparative study of conventional and novel combined modes of microwave- and infrared-assisted thawing on quality of frozen green pepper, carrot and cantaloupe. *LWT*, 154, 112842. <https://doi.org/10.1016/j.lwt.2021.112842>
- Chen, C., Abdelrahim, K., & Beckerich, I. (2010). Sensitivity analysis of continuous ohmic heating process for multiphase foods. *Journal of Food Engineering*, 98(2), 257-265. <https://doi.org/10.1016/j.jfoodeng.2010.01.005>

- Cheng, H. P., & Lin, C. T. (2007). The morphological visualization of the water in vacuum cooling and freezing process. *Journal of Food Engineering*, 78(2), 569-576.<https://doi.org/10.1016/j.jfoodeng.2005.10.025>
- Cheng, L., Sun, D.-W., Zhu, Z., & Zhang, Z. (2017). Emerging techniques for assisting and accelerating food freezing processes: A review of recent research progresses. *Critical Reviews in Food Science and Nutrition*, 57(4), 769-781.<https://doi.org/10.1080/10408398.2015.1004569>
- Cheng, X.-f., Zhang, M., & Adhikari, B. (2014). Effects of ultrasound-assisted thawing on the quality of edamames [Glycine max (L.) Merrill] frozen using different freezing methods. *Food Science and Biotechnology*, 23(4), 1095-1102.<https://doi.org/10.1007/s10068-014-0150-0>
- Chevalier, D., Le Bail, A., & Ghoul, M. (2000). Freezing and ice crystals formed in a cylindrical food model: part II. Comparison between freezing at atmospheric pressure and pressure-shift freezing. *Journal of Food Engineering*, 46(4), 287-293.[https://doi.org/10.1016/S0260-8774\(00\)00090-X](https://doi.org/10.1016/S0260-8774(00)00090-X)
- Chysirichote, T., Phumchom, N., Chintapum, S., Klinthong, W., Ohtaguchi, K., & Yoovidhya, T. (2024). Using ohmic heating to shorten the tempering time for frozen fish. *International Journal of Food Science & Technology*, 59(3), 1375-1383.<https://doi.org/10.1111/ijfs.16881>
- Cleland, D. J., Cleland, A. C., & Earle, R. L. (1987a). Prediction of freezing and thawing times for multi-dimensional shapes by simple formulae Part 1: regular shapes. *International Journal of Refrigeration*, 10(3), 156-164.[https://doi.org/10.1016/0140-7007\(87\)90006-5](https://doi.org/10.1016/0140-7007(87)90006-5)
- Cleland, D. J., Cleland, A. C., & Earle, R. L. (1987b). Prediction of freezing and thawing times for multi-dimensional shapes by simple formulae part 2: irregular shapes. *International Journal of Refrigeration*, 10(4), 234-240.[https://doi.org/10.1016/0140-7007\(87\)90058-2](https://doi.org/10.1016/0140-7007(87)90058-2)
- Cogné, C., Nguyen, P. U., Lanoisellé, J. L., Van Hecke, E., & Clause, D. (2013). Modeling heat and mass transfer during vacuum freezing of pure droplet. *International Journal of Refrigeration*, 36(4), 1319-1326.<https://doi.org/10.1016/j.ijrefrig.2013.02.003>
- Cui, J., Lian, Y., Zhao, C., Du, H., Han, Y., Gao, W., Xiao, H., & Zheng, J. (2019). Dietary fibers from fruits and vegetables and their health benefits via modulation of gut microbiota. *COMPREHENSIVE REVIEWS IN FOOD SCIENCE AND FOOD SAFETY*, 18(5), 1514-1532.<https://doi.org/10.1111/1541-4337.12489>
- Da Silva, D. L., Silveira, A. S., Ronzoni, A. F., & Hermes, C. J. L. (2022). Effect of freezing rate on the quality of frozen strawberries (*Fragaria x ananassa*). *International Journal of Refrigeration*, 144, 46-54.<https://doi.org/10.1016/j.ijrefrig.2022.07.006>
- Dadan, M., Matys, A., Kaminska-Dworznicka, A., Lammerskitten, A., Toepfl, S., & Parniakov, O. (2021). 9 - Improvement of freezing processes assisted by ultrasound. In F. J. Barba, G. Cravotto, F. Chemat, J. M. L. Rodriguez & P. E. S. Munekata (Eds.), *Design and Optimization of Innovative Food Processing Techniques Assisted by Ultrasound* (pp. 217-273): Academic Press.
- Dadan, M., Nowacka, M., Czyzewski, J., & Witrowa-Rajchert, D. (2020). 9 - Modification of food structure and improvement of freezing processes by pulsed electric field treatment. In F. J. Barba, O. Parniakov & A. Wiktor (Eds.), *Pulsed Electric Fields to Obtain Healthier and Sustainable Food for Tomorrow* (pp. 203-226): Academic Press.

- Dadashi, S., Fernández-Martín, F., Mousavi, M., & Pérez-Mateos, M. (2024). Impact of high-pressure shift freezing on physicochemical and functional properties of egg edible parts. *Journal of Food Engineering*, 361, 111753. <https://doi.org/10.1016/j.jfoodeng.2023.111753>
- Dalvi-Isfahan, M., Hamdami, N., & Le-Bail, A. (2016). Effect of freezing under electrostatic field on the quality of lamb meat. *Innovative Food Science & Emerging Technologies*, 37, 68-73. <https://doi.org/10.1016/j.ifset.2016.07.028>
- Dalvi-Isfahan, M., Hamdami, N., Xanthakis, E., & Le-Bail, A. (2017). Review on the control of ice nucleation by ultrasound waves, electric and magnetic fields. *Journal of Food Engineering*, 195, 222-234. <https://doi.org/10.1016/j.jfoodeng.2016.10.001>
- Dalvi-Isfahan, M., Jha, P. K., Tavakoli, J., Daraei-Garmakhany, A., Xanthakis, E., & Le-Bail, A. (2019). Review on identification, underlying mechanisms and evaluation of freezing damage. *Journal of Food Engineering*, 255, 50-60. <https://doi.org/10.1016/j.jfoodeng.2019.03.011>
- Dawson, P., Al-Jeddawi, W., & Rieck, J. (2020). The effect of different freezing rates and long-term storage temperatures on the stability of sliced peaches. *International Journal of Food Science*, 2020. <https://doi.org/10.1155/2020/9178583>
- Day, L., Xu, M., Øiseth, S. K., & Mawson, R. (2012). Improved mechanical properties of retorted carrots by ultrasonic pre-treatments. *Ultrasonics Sonochemistry*, 19(3), 427-434. <https://doi.org/10.1016/j.ultsonch.2011.10.019>
- Demir, E., Dymek, K., & Galindo, F. G. (2018). Technology Allowing Baby Spinach Leaves to Acquire Freezing Tolerance. *Food and Bioprocess Technology*, 11(4), 809-817. <https://doi.org/10.1007/s11947-017-2044-7>
- Fadji, T., Ashtiani, S.-H. M., Onwude, D. I., Li, Z., & Opara, U. L. (2021). Finite Element Method for Freezing and Thawing Industrial Food Processes. In *Foods* (Vol. 10).
- Fallah-Joshaqani, S., Hamdami, N., & Keramat, J. (2021). Qualitative attributes of button mushroom (*Agaricus bisporus*) frozen under high voltage electrostatic field. *Journal of Food Engineering*, 293, 110384. <https://doi.org/10.1016/j.jfoodeng.2020.110384>
- Fallah-Joshaqani, S., Hamdami, N., Keshavarzi, E., Keramat, J., & Dalvi-Isfahan, M. (2019). Evaluation of the static electric field effects on freezing parameters of some food systems. *International Journal of Refrigeration*, 99, 30-36. <https://doi.org/10.1016/j.jrefrig.2018.12.011>
- Fellows, P. J. (2017). 22 - Freezing. In P. J. Fellows (Ed.), *Food Processing Technology (Fourth Edition)* (pp. 885-928): Woodhead Publishing.
- Fernández, P. P., Otero, L., Guignon, B., & Sanz, P. D. (2006). High-pressure shift freezing versus high-pressure assisted freezing: Effects on the microstructure of a food model. *Food Hydrocolloids*, 20(4), 510-522. <https://doi.org/10.1016/j.foodhyd.2005.04.004>
- Galindo, F. G., Toledo, R. T., & Sjöholm, I. (2005). Tissue damage in heated carrot slices. Comparing mild hot water blanching and infrared heating. *Journal of Food Engineering*, 67(4), 381-385. <https://doi.org/10.1016/j.jfoodeng.2004.05.004>
- Giannakourou, M. C., Dermesonlouoglou, E. K., & Taoukis, P. S. (2020). Osmodehydrofreezing: An Integrated Process for Food Preservation during Frozen Storage. In *Foods* (Vol. 9).
- Gómez G, F., & Sjöholm, I. (2004). Applying biochemical and physiological principles in the industrial freezing of vegetables: a case study on carrots. *Trends in Food Science & Technology*, 15(1), 39-43. <https://doi.org/10.1016/j.tifs.2003.07.006>

- Gonçalves, E. M., Abreu, M., Pinheiro, J., Brandão, T. R. S., & Silva, C. L. M. (2020). Quality changes of carrots under different frozen storage conditions: A kinetic study. *Journal of Food Processing and Preservation*, 44(12), e14953. <https://doi.org/10.1111/jfpp.14953>
- Gonçalves, E. M., Pinheiro, J., Abreu, M., Brandão, T. R. S., & Silva, C. L. M. (2011). Kinetics of quality changes of pumpkin (*Curcubita maxima* L.) stored under isothermal and non-isothermal frozen conditions. *Journal of Food Engineering*, 106(1), 40-47. <https://doi.org/10.1016/j.jfoodeng.2011.04.004>
- Grover, Y., & Negi, P. S. (2023). Recent developments in freezing of fruits and vegetables: Striving for controlled ice nucleation and crystallization with enhanced freezing rates. *Journal of Food Science*. <https://doi.org/10.1111/1750-3841.16810>
- Guo, Y., Wu, B., Guo, X., Liu, D., Wu, P., Ma, H., & Pan, Z. (2021). Ultrasonication and thermosonication blanching treatments of carrot at varying frequencies: Effects on peroxidase inactivation mechanisms and quality characterization evaluation. *Food Chemistry*, 343, 128524. <https://doi.org/10.1016/j.foodchem.2020.128524>
- Hafezparast-Moadab, N., Hamdami, N., Dalvi-Isfahan, M., & Farahnaky, A. (2018). Effects of radiofrequency-assisted freezing on microstructure and quality of rainbow trout (*Oncorhynchus mykiss*) fillet. *Innovative Food Science & Emerging Technologies*, 47, 81-87. <https://doi.org/10.1016/j.ifset.2017.12.012>
- He, T., Feng, R., Tao, H., & Zhang, B. (2024). A comparative study of magnetic field on the maximum ice crystal formation zone and whole freezing process for improving the frozen dough quality. *Food Chemistry*, 435, 137642. <https://doi.org/10.1016/j.foodchem.2023.137642>
- Heldman, D. R. (2006). Food freezing. In Dennis R. Heldman, Daryl B. Lund & C. Sabliov (Eds.), *Handbook of food engineering* (pp. 439-482): CRC Press.
- Hu, R., Zhang, M., & Mujumdar, A. S. (2022). Novel assistive technologies for efficient freezing of pork based on high voltage electric field and static magnetic field: A comparative study. *Innovative Food Science & Emerging Technologies*, 80, 103087. <https://doi.org/10.1016/j.ifset.2022.103087>
- Hu, X., Zhang, G., Hamaker, B. R., & Miao, M. (2022). The contribution of intact structure and food processing to functionality of plant cell wall-derived dietary fiber. *Food Hydrocolloids*, 127, 107511. <https://doi.org/10.1016/j.foodhyd.2022.107511>
- Huang, Z., Kan, A., Lu, J., Li, F., & Wang, T. (2021). Numerical simulation and experimental study of heat and mass transfer in cylinder-like vegetables during vacuum cooling. *Innovative Food Science & Emerging Technologies*, 68, 102607. <https://doi.org/10.1016/j.ifset.2021.102607>
- Hussain, S., Jōudu, I., & Bhat, R. (2020). Dietary Fiber from Underutilized Plant Resources—A Positive Approach for Valorization of Fruit and Vegetable Wastes. In *Sustainability* (Vol. 12).
- Ida, N. (2015). *Engineering electromagnetics* (3 ed.): Springer.
- Islam, M. N., Zhang, M., & Adhikari, B. (2017). Ultrasound-Assisted Freezing of Fruits and Vegetables: Design, Development, and Applications. In G. V. Barbosa-Cánovas, G. María Pastore, K. Candoğan, I. G. Medina Meza, S. Caetano da Silva Lannes, K. Buckle, R. Y. Yada & A. Rosenthal (Eds.), *Global Food Security and Wellness* (pp. 457-487). New York, NY: Springer New York.
- Islam, M. N., Zhang, M., Adhikari, B., Xinfeng, C., & Xu, B.-g. (2014). The effect of ultrasound-assisted immersion freezing on selected physicochemical properties of mushrooms.

- International Journal of Refrigeration*, 42, 121-133.<https://doi.org/10.1016/j.ijrefrig.2014.02.012>
- Jackman, R. L., & Stanley, D. W. (1995). Perspectives in the textural evaluation of plant foods. *Trends in Food Science & Technology*, 6(6), 187-194.[https://doi.org/10.1016/S0924-2244\(00\)89053-6](https://doi.org/10.1016/S0924-2244(00)89053-6)
- James, C., Hanser, P., & James, S. J. (2011). Super-cooling phenomena in fruits, vegetables and seafoods. In *11th International Congress on Engineering and Food (ICEF 2011), Athens, Greece* (pp. 22-26).
- James, C., Purnell, G., & James, S. J. (2014). A Critical Review of Dehydrofreezing of Fruits and Vegetables. *Food and Bioprocess Technology*, 7(5), 1219-1234.<https://doi.org/10.1007/s11947-014-1293-y>
- James, S. J., James, C., & Purnell, G. (2017). 12 - Microwave-assisted thawing and tempering. In M. Regier, K. Knoerzer & H. Schubert (Eds.), *The Microwave Processing of Foods (Second Edition)* (pp. 252-272): Woodhead Publishing.
- Jha, P. K., Chapleau, N., Meyers, P.-E., Pathier, D., & Le-Bail, A. (2024). Can cryogenic freezing preserve the quality of fruit matrices during long-term storage compared to the mechanical method? *Applied Food Research*, 4(1), 100374.<https://doi.org/10.1016/j.afres.2023.100374>
- Jha, P. K., Chevallier, S., Xanthakis, E., Jury, V., & Le-Bail, A. (2020). Effect of innovative microwave assisted freezing (MAF) on the quality attributes of apples and potatoes. *Food Chemistry*, 309, 125594.<https://doi.org/10.1016/j.foodchem.2019.125594>
- Jha, P. K., Xanthakis, E., Chevallier, S., Jury, V., & Le-Bail, A. (2019). Assessment of freeze damage in fruits and vegetables. *Food Research International*, 121, 479-496.<https://doi.org/10.1016/j.foodres.2018.12.002>
- Jha, P. K., Xanthakis, E., Jury, V., Havet, M., & Le-Bail, A. (2018). Advances of electro-freezing in food processing. *Current Opinion in Food Science*, 23, 85-89.<https://doi.org/10.1016/j.cofs.2018.06.007>
- Jia, G., Chen, Y., Sun, A., & Orlien, V. (2022). Control of ice crystal nucleation and growth during the food freezing process. *COMPREHENSIVE REVIEWS IN FOOD SCIENCE AND FOOD SAFETY*, 21(3), 2433-2454.<https://doi.org/10.1111/1541-4337.12950>
- Jiang, Q., Zhang, M., & Mujumdar, A. S. (2023). Application of physical field-assisted freezing and thawing to mitigate damage to frozen food. *Journal of the Science of Food and Agriculture*, 103(5), 2223-2238.<https://doi.org/10.1002/jsfa.12260>
- Jiang, Q., Zhang, M., Mujumdar, A. S., & Gan, S. (2023). Effects of magnetic field-assisted liquid carbon dioxide spray freezing on the quality of honeydew melon. *Food Chemistry*, 417, 135850.<https://doi.org/10.1016/j.foodchem.2023.135850>
- Joardder, M. U., Kumar, C., & Karim, M. (2017). Food structure: Its formation and relationships with other properties. *Critical reviews in food science nutrition Research*, 57(6), 1190-1205.<https://doi.org/10.1080/10408398.2014.971354>
- Kang, T., You, Y., & Jun, S. (2020). Supercooling preservation technology in food and biological samples: a review focused on electric and magnetic field applications. *Food Science and Biotechnology*, 29(3), 303-321.<https://doi.org/10.1007/s10068-020-00750-6>

- Kaur, M., & Kumar, M. (2020). An Innovation in Magnetic Field Assisted Freezing of Perishable Fruits and Vegetables: A Review. *Food Reviews International*, 36(8), 761-780.<https://doi.org/10.1080/87559129.2019.1683746>
- Kawai, K., & Hagiwara, T. (2018). Control of Physical Changes in Food Products. In M. Iwaya-Inoue, M. Sakurai & M. Uemura (Eds.), *Survival Strategies in Extreme Cold and Desiccation: Adaptation Mechanisms and Their Applications* (Vol. 1081, pp. 385-399). Singapore: Springer Singapore.
- Kazemi, M. A., Zandavi, S. H., Zargartalebi, M., Sinton, D., & Elliott, Janet A. W. (2023). Analysis of the evaporation coefficients of water, heavy water, and methanol in a high vacuum environment. *International Journal of Heat and Mass Transfer*, 204, 123833.<https://doi.org/10.1016/j.ijheatmasstransfer.2022.123833>
- Khan, M. I. H., & Karim, M. A. (2017). Cellular water distribution, transport, and its investigation methods for plant-based food material. *Food Research International*, 99, 1-14.<https://doi.org/10.1016/j.foodres.2017.06.037>
- Khan, M. I. H., Nagy, S. A., & Karim, M. A. (2018). Transport of cellular water during drying: An understanding of cell rupturing mechanism in apple tissue. *Food Research International*, 105, 772-781.<https://doi.org/10.1016/j.foodres.2017.12.010>
- Kiani, H., & Sun, D.-W. (2011). Water crystallization and its importance to freezing of foods: A review. *Trends in Food Science & Technology*, 22(8), 407-426.<https://doi.org/10.1016/j.tifs.2011.04.011>
- Kiani, H., Zhang, Z., Delgado, A., & Sun, D.-W. (2011). Ultrasound assisted nucleation of some liquid and solid model foods during freezing. *Food Research International*, 44(9), 2915-2921.<https://doi.org/10.1016/j.foodres.2011.06.051>
- Kim, J., Chun, H. H., Park, S., Choi, D., Choi, S. R., Oh, S., & Yoo, S. M. J. J. o. B. E. (2014). System design and performance analysis of a quick freezer using supercooling. 39(4), 330-335.<https://doi.org/10.5307/JBE.2014.39.4.330>
- King, E. S., Noll, A., Glenn, S., & Bolling, B. W. (2022). Refrigerated and frozen storage impact aronia berry quality. *Food Production, Processing and Nutrition*, 4(1), 3.<https://doi.org/10.1186/s43014-021-00080-y>
- Konstankiewicz, K., Czachor, H., Gancarz, M., Król, A., Pawlak, K., & Zdunek, A. (2002). Cell structural parameter of potato tuber tissue. *International agrophysics*, 16(2)
- Köprüalan Aydın, Ö., Baysan, U., Altay, Ö., İter Baysan, I., Kaymak Ertekin, F., & Jafari, S. M. (2023). Vitamin delivery systems by spray-drying encapsulation within plant protein-based carriers: A review. *Food Bioscience*, 56, 103341.<https://doi.org/10.1016/j.fbio.2023.103341>
- Köprüalan Aydın, Ö., Yüksel Sarioğlu, H., Dirim, S. N., & Kaymak-Ertekin, F. (2023). Recent Advances for Rapid Freezing and Thawing Methods of Foods. *Food Engineering Reviews*, 15(4), 667-690.<https://doi.org/10.1007/s12393-023-09356-0>
- Kramer, M., Sennhenn, B., & Lee, G. (2002). Freeze-drying using vacuum-induced surface freezing. *Journal of Pharmaceutical Sciences*, 91(2), 433-443.<https://doi.org/10.1002/jps.10035>
- Kumar, M., Tomar, M., Punia, S., Dhakane-Lad, J., Dhumal, S., Changan, S., Senapathy, M., Berwal, M. K., Sampathrajan, V., Sayed, A. A. S., Chandran, D., Pandiselvam, R., Rais, N., Mahato, D. K., Udikeri, S. S., Satankar, V., Anitha, T., Reetu, Radha, Singh, S., Amarowicz, R., &

- Kennedy, J. F. (2022). Plant-based proteins and their multifaceted industrial applications. *LWT*, 154, 112620. <https://doi.org/10.1016/j.lwt.2021.112620>
- Kumar, P. K., Rasco, B. A., Tang, J., & Sablani, S. S. (2020). State/Phase Transitions, Ice Recrystallization, and Quality Changes in Frozen Foods Subjected to Temperature Fluctuations. *Food Engineering Reviews*, 12(4), 421-451. <https://doi.org/10.1007/s12393-020-09255-8>
- Kumari, A., Chauhan, A. K., & Tyagi, P. (2022). Isochoric freezing: An innovative and emerging technology for retention of food quality characteristics. *Journal of Food Processing and Preservation*, 46(8), e16704. <https://doi.org/10.1111/jfpp.16704>
- LeBail, A., Chevalier, D., Mussa, D. M., & Ghoul, M. (2002). High pressure freezing and thawing of foods: a review. *International Journal of Refrigeration*, 25(5), 504-513. [https://doi.org/10.1016/S0140-7007\(01\)00030-5](https://doi.org/10.1016/S0140-7007(01)00030-5)
- Lemmens, L., Tibäck, E., Svelander, C., Smout, C., Ahrné, L., Langton, M., Alminger, M., Van Loey, A., & Hendrickx, M. (2009). Thermal pretreatments of carrot pieces using different heating techniques: Effect on quality related aspects. *Innovative Food Science & Emerging Technologies*, 10(4), 522-529. <https://doi.org/10.1016/j.ifset.2009.05.004>
- Leng, D., Zhang, H., Tian, C., Li, P., Kong, F., & Zhan, B. (2023). Static magnetic field assisted freezing of four kinds of fruits and vegetables: Micro and macro effects. *International Journal of Refrigeration*, 146, 118-125. <https://doi.org/10.1016/j.ijrefrig.2022.10.018>
- Li, B., & Sun, D.-W. (2002). Novel methods for rapid freezing and thawing of foods – a review. *Journal of Food Engineering*, 54(3), 175-182. [https://doi.org/10.1016/S0260-8774\(01\)00209-6](https://doi.org/10.1016/S0260-8774(01)00209-6)
- Li, C., Hu, Y., & Zhang, B. (2021). Plant cellular architecture and chemical composition as important regulator of starch functionality in whole foods. *Food Hydrocolloids*, 117, 106744. <https://doi.org/10.1016/j.foodhyd.2021.106744>
- Li, D., Zhu, Z., & Sun, D.-W. (2018). Effects of freezing on cell structure of fresh cellular food materials: A review. *Trends in Food Science & Technology*, 75, 46-55. <https://doi.org/10.1016/j.tifs.2018.02.019>
- Li, J., Chotiko, A., Kyereh, E., Zhang, J., Liu, C., Ortega, V. V. R., Bankston, D., & Sathivel, S. (2017). Development of a Combined Osmotic Dehydration and Cryogenic Freezing Process for Minimizing Quality Changes During Freezing with Application to Fruits and Vegetables. *Journal of Food Processing and Preservation*, 41(1), e12926. <https://doi.org/10.1111/jfpp.12926>
- Lin, M., Cao, H., & Li, J. (2023). Control strategies of ice nucleation, growth, and recrystallization for cryopreservation. *Acta Biomaterialia*, 155, 35-56. <https://doi.org/10.1016/j.actbio.2022.10.056>
- Lin, Y. L., Li, S. J., Zhu, Y., Bingol, G., Pan, Z., & McHugh, T. H. (2009). Heat and Mass Transfer Modeling of Apple Slices Under Simultaneous Infrared Dry Blanching and Dehydration Process. *Drying Technology*, 27(10), 1051-1059. <https://doi.org/10.1080/07373930903218446>
- Lin, Z., & Schyvens, E. (1995). INFLUENCE of BLANCHING TREATMENTS ON the TEXTURE and COLOR of SOME PROCESSED VEGETABLES and FRUITS. *Journal of Food Processing and Preservation*, 19(6), 451-465. <https://doi.org/10.1111/j.1745-4549.1995.tb00306.x>

- Liu, C., Grimi, N., Bals, O., Lebovka, N., & Vorobiev, E. (2021). Effects of pulsed electric fields and preliminary vacuum drying on freezing assisted processes in potato tissue. *Food and Bioprocess Processing*, 125, 126-133. <https://doi.org/10.1016/j.fbp.2020.11.002>
- Liu, D.-K., Xu, C.-C., Guo, C.-X., & Zhang, X.-X. (2020). Sub-zero temperature preservation of fruits and vegetables: A review. *Journal of Food Engineering*, 275, 109881. <https://doi.org/10.1016/j.jfoodeng.2019.109881>
- Liu, Y., Chen, S., Pu, Y., Muhammad, A. I., Hang, M., Liu, D., & Ye, T. (2019). Ultrasound-assisted thawing of mango pulp: Effect on thawing rate, sensory, and nutritional properties. *Food Chemistry*, 286, 576-583. <https://doi.org/10.1016/j.foodchem.2019.02.059>
- Luoma, J., Ingham, E., Lema Martinez, C., & Allmendinger, A. (2020). Comparison of Techniques to Control Ice Nucleation during Lyophilization. In *Processes* (Vol. 8).
- Mac Adam, J. W. (2009). *Structure and function of plants*: John Wiley & Sons.
- Mahato, S., Zhu, Z., & Sun, D.-W. (2019). Glass transitions as affected by food compositions and by conventional and novel freezing technologies: A review. *Trends in Food Science & Technology*, 94, 1-11. <https://doi.org/10.1016/j.tifs.2019.09.010>
- Manzocco, L., Alongi, M., Cortella, G., & Anese, M. (2022). Optimizing radiofrequency assisted cryogenic freezing to improve meat microstructure and quality. *Journal of Food Engineering*, 335, 111184. <https://doi.org/10.1016/j.jfoodeng.2022.111184>
- Manzocco, L., Anese, M., & Nicoli, M. C. (2008). Radiofrequency inactivation of oxidative food enzymes in model systems and apple derivatives. *Food Research International*, 41(10), 1044-1049. <https://doi.org/10.1016/j.foodres.2008.07.020>
- Marra, F., Zell, M., Lyng, J. G., Morgan, D. J., & Cronin, D. A. (2009). Analysis of heat transfer during ohmic processing of a solid food. *Journal of Food Engineering*, 91(1), 56-63. <https://doi.org/10.1016/j.jfoodeng.2008.08.015>
- Martins, R. C., & Lopes, V. V. (2007). Modelling supercooling in frozen strawberries: Experimental analysis, cellular automation and inverse problem methodology. *Journal of Food Engineering*, 80(1), 126-141. <https://doi.org/10.1016/j.jfoodeng.2006.05.009>
- Matsumoto, M., Saito, S., & Ohmine, I. (2002). Molecular dynamics simulation of the ice nucleation and growth process leading to water freezing. *Nature*, 416(6879), 409-413. <https://doi.org/10.1038/416409a>
- McAtee, P. A., Hallett, I. C., Johnston, J. W., & Schaffer, R. J. (2009). A rapid method of fruit cell isolation for cell size and shape measurements. *Plant Methods*, 5(1), 5. <https://doi.org/10.1186/1746-4811-5-5>
- Meste, M. L., Champion, D., Roudaut, G., Blond, G., & Simatos, D. (2002). Glass Transition and Food Technology: A Critical Appraisal. *Journal of Food Science*, 67(7), 2444-2458. <https://doi.org/10.1111/j.1365-2621.2002.tb08758.x>
- Miles, C. A., Mayer, Z., Morley, M. J., & HousÆka, M. (1997). Estimating the initial freezing point of foods from composition data. *International Journal of Food Science & Technology*, 32(5), 389-400. <https://doi.org/10.1046/j.1365-2621.1997.00125.x>
- Miles, C. A., Morley, M. J., & Rendell, M. (1999). High power ultrasonic thawing of frozen foods. *Journal of Food Engineering*, 39(2), 151-159. [https://doi.org/10.1016/S0260-8774\(98\)00155-1](https://doi.org/10.1016/S0260-8774(98)00155-1)

- Muthukumarappan, K., Marella, C., & Sunkesula, V. (2019). Chapter 15 - Food Freezing Technology. In M. Kutz (Ed.), *Handbook of Farm, Dairy and Food Machinery Engineering (Third Edition)* (pp. 389-415): Academic Press.
- Nagraj, G. S., Jaiswal, S., Harper, N., & Jaiswal, A. K. (2020). Chapter 20 - Carrot. In A. K. Jaiswal (Ed.), *Nutritional Composition and Antioxidant Properties of Fruits and Vegetables* (pp. 323-337): Academic Press.
- Narayana, G. P., Jha, P. K., Rawson, A., & Le-Bail, A. (2023). Changes in the quality of apple tissue subjected to different freezing rates during long-term frozen storage at different temperatures. *International Journal of Refrigeration*, *151*, 397-405. <https://doi.org/10.1016/j.ijrefrig.2023.03.022>
- Navina, B., Keshav Huthaash, K., Velmurugan, N. K., & Korumilli, T. (2023). Insights into recent innovations in anti browning strategies for fruit and vegetable preservation. *Trends in Food Science & Technology*, *139*, 104128. <https://doi.org/10.1016/j.tifs.2023.104128>
- Neri, L., Faieta, M., Di Mattia, C., Sacchetti, G., Mastrocola, D., & Pittia, P. (2020). Antioxidant Activity in Frozen Plant Foods: Effect of Cryoprotectants, Freezing Process and Frozen Storage. In *Foods* (Vol. 9).
- Neri, L., Hernando, I., Pérez-Munuera, I., Sacchetti, G., Mastrocola, D., & Pittia, P. (2014). Mechanical properties and microstructure of frozen carrots during storage as affected by blanching in water and sugar solutions. *Food Chemistry*, *144*, 65-73. <https://doi.org/10.1016/j.foodchem.2013.07.123>
- Nesvadba, P. (2008). Thermal properties and ice crystal development in frozen foods. In J. A. Evans (Ed.), *Frozen food science technology* (pp. 1-25).
- Nguyen, L. T., Tay, A., Balasubramaniam, V. M., Legan, J. D., Turek, E. J., & Gupta, R. (2010). Evaluating the impact of thermal and pressure treatment in preserving textural quality of selected foods. *LWT - Food Science and Technology*, *43*(3), 525-534. <https://doi.org/10.1016/j.lwt.2009.09.022>
- Niranjan, K. (2022). Thermal Processing of Foods. In K. Niranjan (Ed.), *Engineering Principles for Food Process and Product Realization* (pp. 145-159). Cham: Springer International Publishing.
- Nishida, N., & Ando, Y. (2023). Improvement of Mechanical Properties of Frozen Japanese Radish by Combination of Low- and High-temperature Blanching Pretreatment. *Food and Bioprocess Technology*, *16*(12), 2789-2799. <https://doi.org/10.1007/s11947-023-03098-x>
- Niu, D., Zeng, X.-A., Ren, E.-F., Xu, F.-Y., Li, J., Wang, M.-S., & Wang, R. (2020). Review of the application of pulsed electric fields (PEF) technology for food processing in China. *Food Research International*, *137*, 109715. <https://doi.org/10.1016/j.foodres.2020.109715>
- Norton, T., & Sun, D.-W. (2008). Recent Advances in the Use of High Pressure as an Effective Processing Technique in the Food Industry. *Food and Bioprocess Technology*, *1*(1), 2-34. <https://doi.org/10.1007/s11947-007-0007-0>
- Otero, L. (2023). Chapter Eleven - Application of high pressure processing in freezing and thawing processes. In S. M. Jafari & N. Therdthai (Eds.), *Non-thermal Food Processing Operations* (pp. 359-405): Woodhead Publishing.

- Otero, L., Pérez-Mateos, M., Rodríguez, A. C., & Sanz, P. D. (2017). Electromagnetic freezing: Effects of weak oscillating magnetic fields on crab sticks. *Journal of Food Engineering*, 200, 87-94. <https://doi.org/10.1016/j.jfoodeng.2016.12.018>
- Otero, L., & Pozo, A. (2022). Effects of the application of static magnetic fields during potato freezing. *Journal of Food Engineering*, 316, 110838. <https://doi.org/10.1016/j.jfoodeng.2021.110838>
- Otero, L., Rodríguez, A. C., & Sanz, P. D. (2020). Effect of the frequency of weak oscillating magnetic fields on supercooling and freezing kinetics of pure water and 0.9% NaCl solutions. *Journal of Food Engineering*, 273, 109822. <https://doi.org/10.1016/j.jfoodeng.2019.109822>
- Paciulli, M., Medina-Meza, I. G., Chiavaro, E., & Barbosa-Cánovas, G. V. (2016). Impact of thermal and high pressure processing on quality parameters of beetroot (*Beta vulgaris* L.). *LWT - Food Science and Technology*, 68, 98-104. <https://doi.org/10.1016/j.lwt.2015.12.029>
- Pathare, P. B., Opara, U. L., Vigneault, C., Delele, M. A., & Al-Said, F. A.-J. (2012). Design of Packaging Vents for Cooling Fresh Horticultural Produce. *Food and Bioprocess Technology*, 5(6), 2031-2045. <https://doi.org/10.1007/s11947-012-0883-9>
- Peng, R., Liu, J., Yang, Z., Liu, S., Wang, W., Zhai, H., Sun, J., & Cao, W. (2023). Study on the response law between cooling rate and temperature with process parameters during vacuum freezing of liquid. *Vacuum*, 213, 112040. <https://doi.org/10.1016/j.vacuum.2023.112040>
- Peng, Y., Zhao, J., Wen, X., & Ni, Y. (2022). The Comparison of Microwave Thawing and Ultra-High-Pressure Thawing on the Quality Characteristics of Frozen Mango. In *Foods* (Vol. 11).
- Pham, Q. T. (1986). Simplified equation for predicting the freezing time of foodstuffs. *International Journal of Food Science & Technology*, 21(2), 209-219. <https://doi.org/10.1111/j.1365-2621.1986.tb00442.x>
- Powell-Palm, M. J., & Rubinsky, B. (2019). A shift from the isobaric to the isochoric thermodynamic state can reduce energy consumption and augment temperature stability in frozen food storage. *Journal of Food Engineering*, 251, 1-10. <https://doi.org/10.1016/j.jfoodeng.2019.02.001>
- Priyadarshini, A., Rayaguru, K., Biswal, A. K., Panda, P. K., Lenka, C., & Misra, P. K. (2023). Impact of conventional and ohmic blanching on color, phytochemical, structural, and sensory properties of mango (*Mangifera indica* L.) cubes: A comparative analysis. *Food Chemistry Advances*, 2, 100308. <https://doi.org/10.1016/j.focha.2023.100308>
- Purnell, G., James, C., & James, S. J. (2017). The Effects of Applying Oscillating Magnetic Fields During the Freezing of Apple and Potato. *Food and Bioprocess Technology*, 10(12), 2113-2122. <https://doi.org/10.1007/s11947-017-1983-3>
- Qian, S., Li, X., Zhang, C., & Blecker, C. (2022). Effects of initial freezing rate on the changes in quality, myofibrillar protein characteristics and myowater status of beef steak during subsequent frozen storage. *International Journal of Refrigeration*, 143, 148-156. <https://doi.org/10.1016/j.ijrefrig.2022.06.028>
- Qiu, L., Zhang, M., Chitrakar, B., & Bhandari, B. (2020). Application of power ultrasound in freezing and thawing Processes: Effect on process efficiency and product quality. *Ultrasonics Sonochemistry*, 68, 105230. <https://doi.org/10.1016/j.ultsonch.2020.105230>
- Ramaswamy, H. S., & Tung, M. A. (1984). A REVIEW ON PREDICTING FREEZING TIMES OF FOODS. *Journal of Food Process Engineering*, 7(3), 169-203. <https://doi.org/10.1111/j.1745-4530.1984.tb00302.x>

- Rao, M. A., Rizvi, S. S. H., Datta, A. K., & Ahmed, J. (2014). *Engineering Properties of Foods*: CRC Press.
- Rastogi, N. K., Nguyen, L. T., & Balasubramaniam, V. M. (2008). Effect of pretreatments on carrot texture after thermal and pressure-assisted thermal processing. *Journal of Food Engineering*, 88(4), 541-547. <https://doi.org/10.1016/j.jfoodeng.2008.03.016>
- REEVE, R. M. (1970). RELATIONSHIPS OF HISTOLOGICAL STRUCTURE TO TEXTURE OF FRESH AND PROCESSED FRUITS AND VEGETABLES. *Journal of Texture Studies*, 1(3), 247-284. <https://doi.org/10.1111/j.1745-4603.1970.tb00730.x>
- Refrigeration, I. I. o. (1986). *Recommendations for the Processing and Handling of Frozen Foods* (3rd ed.): International Institute of Refrigeration.
- Reid, D. S. (1997). Overview of Physical/Chemical Aspects of Freezing. In M. C. Erickson & Y.-C. Hung (Eds.), *Quality in Frozen Food* (pp. 10-28). Boston, MA: Springer US.
- Reyes-Alvarez, C. A., & Lanari, M. C. (2023). Effect of freezing, osmodehydro-freezing, freeze-drying and osmodehydro-freeze-drying on the physicochemical and nutritional properties of arazá (*Eugenia stipitata* McVaugh). *Food Chemistry Advances*, 3, 100496. <https://doi.org/10.1016/j.focha.2023.100496>
- Richter Reis, F. (2023). 8 - Blanching in the food industry. In S. M. Jafari (Ed.), *Thermal Processing of Food Products by Steam and Hot Water* (pp. 211-246): Woodhead Publishing.
- Rodríguez, A. C., Otero, L., Cobos, J. A., & Sanz, P. D. (2019). Electromagnetic Freezing in a Widespread Frequency Range of Alternating Magnetic Fields. *Food Engineering Reviews*, 11(2), 93-103. <https://doi.org/10.1007/s12393-019-09190-3>
- Rodríguez, A. C., Pérez-Mateos, M., Careche, M., Sánchez-Alonso, I., Escribano, M. I., Sanz, P. D., & Otero, L. (2020). Evaluation of the effects of weak oscillating magnetic fields applied during freezing on systems of different complexity. *International journal of food engineering*, 16(4). <https://doi.org/doi:10.1515/ijfe-2019-0178>
- Rondineli, A., & Silva, E. K. (2024). Pulsed electric field as a pre-treatment in food freezing processes: Fundamentals, mechanisms, applications and impacts on frozen food quality. *Food Bioscience*, 104275. <https://doi.org/10.1016/j.fbio.2024.104275>
- Ruiz-Ojeda, L. M., & Peñas, F. J. (2013). Comparison study of conventional hot-water and microwave blanching on quality of green beans. *Innovative Food Science & Emerging Technologies*, 20, 191-197. <https://doi.org/10.1016/j.ifset.2013.09.009>
- Sadot, M., Curet, S., Chevallier, S., Le-Bail, A., Rouaud, O., & Havet, M. (2020). Microwave assisted freezing part 2: Impact of microwave energy and duty cycle on ice crystal size distribution. *Innovative Food Science & Emerging Technologies*, 62, 102359. <https://doi.org/10.1016/j.ifset.2020.102359>
- Sadot, M., Curet, S., Le-Bail, A., Rouaud, O., & Havet, M. (2020). Microwave assisted freezing part 1: Experimental investigation and numerical modeling. *Innovative Food Science & Emerging Technologies*, 62, 102360. <https://doi.org/10.1016/j.ifset.2020.102360>
- Sanz, P. D., & Otero, L. (2014). Chapter 28 - High-Pressure Freezing. In D.-W. Sun (Ed.), *Emerging Technologies for Food Processing (Second Edition)* (pp. 515-538). San Diego: Academic Press.

- Schlüter, O., Benet, G. U., Heinz, V., & Knorr, D. (2004). Metastable States of Water and Ice during Pressure-Supported Freezing of Potato Tissue. *Biotechnology Progress*, 20(3), 799-810.<https://doi.org/10.1021/bp0340279>
- Schmidt, S. J., & Lee, J. W. (2009). How Does the Freezer Burn Our Food? , 8(2), 45-52.<https://doi.org/10.1111/j.1541-4329.2009.00072.x>
- Schudel, S., Prawiranto, K., & Defraeye, T. (2021). Comparison of freezing and convective dehydrofreezing of vegetables for reducing cell damage. *Journal of Food Engineering*, 293, 110376.<https://doi.org/10.1016/j.jfoodeng.2020.110376>
- Shahsavari, R., Kashaninejad, M., Ziaifia, A. M., & Maghsoudlou, Y. (2024). The Impact of a Combined Infrared-Hot Air System on the Thawing Process and Quality Attributes of Carrots. *Journal of Food Science and Technology*, 20(144).<https://doi.org/10.22034/FSCT.20.144.213>
- Silva, A. C. C., & Schmidt, F. C. (2022). Intensification of freeze-drying rate of coffee extract by vacuum freezing. *Innovative Food Science & Emerging Technologies*, 78, 103022.<https://doi.org/10.1016/j.ifset.2022.103022>
- Silva, C. L. M., Gonçalves, E. M., & Brandão, T. R. S. (2008). Freezing of Fruits and Vegetables. In J. A. Evans (Ed.), *Frozen Food Science and Technology* (pp. 165-183).
- Sinha, N. K., Sidhu, J., Barta, J., Wu, J., & Cano, M. P. (2012). *Handbook of Fruits and Fruit Processing*: Wiley.
- Slavin, J. L., & Lloyd, B. (2012). Health Benefits of Fruits and Vegetables. *Advances in Nutrition*, 3(4), 506-516.<https://doi.org/10.3945/an.112.002154>
- Smeller, L. (2002). Pressure–temperature phase diagrams of biomolecules. *Biochimica et Biophysica Acta (BBA) - Protein Structure and Molecular Enzymology*, 1595(1), 11-29.[https://doi.org/10.1016/S0167-4838\(01\)00332-6](https://doi.org/10.1016/S0167-4838(01)00332-6)
- Stebel, M., Smolka, J., Palacz, M., Eikevik, T. M., & Tolstorebrov, I. (2022). Numerical modelling of conjugate heat and mass transfer during hydrofluidisation food freezing in different water solutions. *Innovative Food Science & Emerging Technologies*, 75, 102898.<https://doi.org/10.1016/j.ifset.2021.102898>
- Stevanović, S. M., Petrović, T. S., Marković, D. D., Milovančević, U. M., Stevanović, S. V., Urošević, T. M., & Kozarski, M. S. (2022). Changes of quality and free radical scavenging activity of strawberry and raspberry frozen under different conditions. *Journal of Food Processing and Preservation*, 46(10), e15981.<https://doi.org/10.1111/jfpp.15981>
- Sumonsiri, N., & Barringer, S. A. (2014). Fruits and vegetables—processing technologies and applications. In Stephanie Clark, Stephanie Jung & B. Lamsal (Eds.), *Food Processing: Principles and Applications, Second Edition* (pp. 363-381).
- Sun, Q., Zhang, M., & Yang, P. (2019). Combination of LF-NMR and BP-ANN to monitor water states of typical fruits and vegetables during microwave vacuum drying. *LWT*, 116, 108548.<https://doi.org/10.1016/j.lwt.2019.108548>
- Sutariya, S. G., & Sunkesula, V. (2021). 3.03 - Food Freezing: Emerging Techniques for Improving Quality and Process Efficiency a Comprehensive Review. In K. Knoerzer & K. Muthukumarappan (Eds.), *Innovative Food Processing Technologies* (pp. 36-63). Oxford: Elsevier.

- Tang, J., Shao, S., & Tian, C. (2020). Effects of the magnetic field on the freezing process of blueberry. *International Journal of Refrigeration*, 113, 288-295. <https://doi.org/10.1016/j.ijrefrig.2019.12.022>
- Tang, J., Zhang, H., Tian, C., & Shao, S. (2020). Effects of different magnetic fields on the freezing parameters of cherry. *Journal of Food Engineering*, 278, 109949. <https://doi.org/10.1016/j.jfoodeng.2020.109949>
- Tansey, F., Gormley, R., & Butler, F. (2010). The effect of freezing compared with chilling on selected physico-chemical and sensory properties of sous vide cooked carrots. *Innovative Food Science & Emerging Technologies*, 11(1), 137-145. <https://doi.org/10.1016/j.ifset.2009.11.001>
- Teferra, T. F. (2019). Chapter 3 - Engineering Properties of Food Materials. In M. Kutz (Ed.), *Handbook of Farm, Dairy and Food Machinery Engineering (Third Edition)* (pp. 45-89): Academic Press.
- Tian, Y., Chen, Z., Zhu, Z., & Sun, D.-W. (2020). Effects of tissue pre-degassing followed by ultrasound-assisted freezing on freezing efficiency and quality attributes of radishes. *Ultrasonics Sonochemistry*, 67, 105162. <https://doi.org/10.1016/j.ultsonch.2020.105162>
- Tian, Y., Li, D., Luo, W., Zhu, Z., Li, W., Qian, Z., Li, G., & Sun, D.-W. (2020). Rapid freezing using atomized liquid nitrogen spray followed by frozen storage below glass transition temperature for Cordyceps sinensis preservation: Quality attributes and storage stability. *LWT*, 123, 109066. <https://doi.org/10.1016/j.lwt.2020.109066>
- Tian, Y., Zhu, Z., & Sun, D.-W. (2020). Naturally sourced biosubstances for regulating freezing points in food researches: Fundamentals, current applications and future trends. *Trends in Food Science & Technology*, 95, 131-140. <https://doi.org/10.1016/j.tifs.2019.11.009>
- Topuz, A., & BaŞÜNAL GÜLmez, H. (2022). Effect of Osmo- and Convective Dehydrofreezing on Energy Efficiency and Some Physicochemical Properties of Frozen Red Pepper. *Akademik Gıda*, 20(2), 103-113. <https://doi.org/10.24323/akademik-gida.1149718>
- Van Buggenhout, S., Messagie, I., Maes, V., Duvetter, T., Van Loey, A., & Hendrickx, M. (2006). Minimizing texture loss of frozen strawberries: effect of infusion with pectinmethylesterase and calcium combined with different freezing conditions and effect of subsequent storage/thawing conditions. *European Food Research and Technology*, 223(3), 395-404. <https://doi.org/10.1007/s00217-005-0218-4>
- Van Buggenhout, S., Sila, D. N., Duvetter, T., Van Loey, A., & Hendrickx, M. (2009). Pectins in Processed Fruits and Vegetables: Part III—Texture Engineering. *COMPREHENSIVE REVIEWS IN FOOD SCIENCE AND FOOD SAFETY*, 8(2), 105-117. <https://doi.org/10.1111/j.1541-4337.2009.00072.x>
- van der Sman, R. G. M. (2020). Impact of Processing Factors on Quality of Frozen Vegetables and Fruits. *Food Engineering Reviews*, 12(4), 399-420. <https://doi.org/10.1007/s12393-020-09216-1>
- Verma, L. R., & Joshi, V. K. (2000). *Postharvest Technology of Fruits and Vegetables: General concepts and principles*: Indus Publishing Company.
- Villamiel, M., García-Pérez, J. V., Montilla, A., Carcel, J. A., & Benedito, J. (2017). *Ultrasound in Food Processing: Recent Advances*: Wiley.
- Wan, L., Powell-Palm, M. J., Lee, C., Gupta, A., Weegman, B. P., Clemens, M. G., & Rubinsky, B. (2018). Preservation of rat hearts in subfreezing temperature isochoric conditions to – 8 °C

- and 78 MPa. *Biochemical and Biophysical Research Communications*, 496(3), 852-857. <https://doi.org/10.1016/j.bbrc.2018.01.140>
- Wang, B., Kong, B., Li, F., Liu, Q., Zhang, H., & Xia, X. (2020). Changes in the thermal stability and structure of protein from porcine longissimus dorsi induced by different thawing methods. *Food Chemistry*, 316, 126375. <https://doi.org/10.1016/j.foodchem.2020.126375>
- Wang, H., Xue, Y., Hu, Z., Ba, L., Shamim, S., Xie, H., Xia, T., & Zhao, R. (2022). Addition of external water improves the quality attributes of vacuum-frozen and thawed apple slices. *International Journal of Refrigeration*. <https://doi.org/10.1016/j.ijrefrig.2022.01.027>
- Wang, L., & Sun, D.-W. (2001). Rapid cooling of porous and moisture foods by using vacuum cooling technology. *Trends in Food Science & Technology*, 12(5), 174-184. [https://doi.org/10.1016/S0924-2244\(01\)00077-2](https://doi.org/10.1016/S0924-2244(01)00077-2)
- Wang, N., Kan, A., Huang, Z., & Lu, J. (2020). CFD simulation of heat and mass transfer through cylindrical *Zizania latifolia* during vacuum cooling. *Heat and Mass Transfer*, 56(2), 627-637. <https://doi.org/10.1007/s00231-019-02736-5>
- Wang, N., Kan, A., Mao, S., Huang, Z., & Li, F. (2021). Study on heat and mass transfer of sugarcane stem during vacuum pre-cooling. *Journal of Food Engineering*, 292, 110288. <https://doi.org/10.1016/j.jfoodeng.2020.110288>
- Wang, Q., Li, Y., Sun, D.-W., & Zhu, Z. (2019). Effects of high-voltage electric field produced by an improved electrode system on freezing behaviors and selected properties of agarose gel. *Journal of Food Engineering*, 254, 25-33. <https://doi.org/10.1016/j.jfoodeng.2019.02.024>
- Watanabe, T., & Ando, Y. (2021). Evaluation of heating uniformity and quality attributes during vacuum microwave thawing of frozen apples. *LWT*, 150, 111997. <https://doi.org/10.1016/j.lwt.2021.111997>
- Wiktor, A., Schulz, M., Voigt, E., Witrowa-Rajchert, D., & Knorr, D. (2015). The effect of pulsed electric field treatment on immersion freezing, thawing and selected properties of apple tissue. *Journal of Food Engineering*, 146, 8-16. <https://doi.org/10.1016/j.jfoodeng.2014.08.013>
- Wu, G., Yang, C., Bruce, H. L., Roy, B. C., Li, X., & Zhang, C. (2022). Effects of Alternating Electric Field Assisted Freezing–Thawing–Aging Sequence on Data-Independent Acquisition Quantitative Proteomics of Longissimus dorsi Muscle. *Journal of Agricultural and Food Chemistry*, 70(40), 12990-13001. <https://doi.org/10.1021/acs.jafc.2c04207>
- Wu, G., Yang, C., Bruce, H. L., Roy, B. C., Li, X., & Zhang, C. (2023). Effects of alternating electric field assisted freezing-thawing-aging sequence on longissimus dorsi muscle microstructure and protein characteristics. *Food Chemistry*, 409, 135266. <https://doi.org/10.1016/j.foodchem.2022.135266>
- Wu, H., Ghaani, M. R., Nandi, P. K., & English, N. J. (2022). Investigation of Dipolar Response of the Hydrated Hen-Egg White Lysozyme Complex under Externally Applied Electric Fields: Insights from Non-equilibrium Molecular Dynamics. *The Journal of Physical Chemistry B*, 126(4), 858-868. <https://doi.org/10.1021/acs.jpcc.1c07096>
- Wu, J., Zhang, M., Bhandari, B., & Yang, C.-h. (2021). Drip loss control technology of frozen fruits and vegetables during thawing: a review. 35(3), 235-250. <https://doi.org/10.31545/intagr/142289>

- Xanthakis, E., Havet, M., Chevallier, S., Abadie, J., & Le-Bail, A. (2013). Effect of static electric field on ice crystal size reduction during freezing of pork meat. *Innovative Food Science & Emerging Technologies*, 20, 115-120. <https://doi.org/10.1016/j.ifset.2013.06.011>
- Xanthakis, E., Huen, J., Eliasson, L., Jha, P. K., Le-Bail, A., & Shrestha, M. (2018). Evaluation of microwave assisted freezing (MAF) impact on meat and fish matrices. In *5th IIR Conference on Sustainability and the Cold Chain, ICC 2018, 6 April 2018 through 8 April 2018* (pp. 176-181).
- Xanthakis, E., Le-Bail, A., & Ramaswamy, H. (2014). Development of an innovative microwave assisted food freezing process. *Innovative Food Science & Emerging Technologies*, 26, 176-181. <https://doi.org/10.1016/j.ifset.2014.04.003>
- Xie, Y., Zhou, K., Chen, B., Wang, Y., Nie, W., Wu, S., Wang, W., Li, P., & Xu, B. (2021). Applying low voltage electrostatic field in the freezing process of beef steak reduced the loss of juiciness and textural properties. *Innovative Food Science & Emerging Technologies*, 68, 102600. <https://doi.org/10.1016/j.ifset.2021.102600>
- Xin, Y., Zhang, M., & Adhikari, B. (2014). Ultrasound assisted immersion freezing of broccoli (*Brassica oleracea* L. var. botrytis L.). *Ultrasonics Sonochemistry*, 21(5), 1728-1735. <https://doi.org/10.1016/j.ultsonch.2014.03.017>
- Xin, Y., Zhang, M., Xu, B., Adhikari, B., & Sun, J. (2015). Research trends in selected blanching pretreatments and quick freezing technologies as applied in fruits and vegetables: A review. *International Journal of Refrigeration*, 57, 11-25. <https://doi.org/10.1016/j.ijrefrig.2015.04.015>
- Xu, B., Azam, R. S. M., Wang, B., Zhang, M., & Bhandari, B. (2019). Effect of infused CO₂ in a model solid food on the ice nucleation during ultrasound-assisted immersion freezing. *International Journal of Refrigeration*, 108, 53-59. <https://doi.org/10.1016/j.ijrefrig.2019.09.005>
- Xu, B., Chen, J., Yuan, J., Azam, S. M. R., & Zhang, M. (2021). Effect of different thawing methods on the efficiency and quality attributes of frozen red radish. *Journal of the Science of Food and Agriculture*, 101(8), 3237-3245. <https://doi.org/10.1002/jsfa.10953>
- Xu, Z., Guo, Y., Ding, S., An, K., & Wang, Z. (2014). Freezing by immersion in liquid CO₂ at variable pressure: Response surface analysis of the application to carrot slices freezing. *Innovative Food Science & Emerging Technologies*, 22, 167-174. <https://doi.org/10.1016/j.ifset.2013.06.005>
- Yahia, E. M., García-Solís, P., & Celis, M. E. M. (2019). Chapter 2 - Contribution of Fruits and Vegetables to Human Nutrition and Health. In E. M. Yahia (Ed.), *Postharvest Physiology and Biochemistry of Fruits and Vegetables* (pp. 19-45): Woodhead Publishing.
- Yang, S., Hu, Y., Takaki, K., Yu, H., & Yuan, C. (2021). Effect of water ice-glazing on the quality of frozen swimming crab (*Portunus trituberculatus*) by liquid nitrogen spray freezing during frozen storage. *International Journal of Refrigeration*, 131, 1010-1015. <https://doi.org/10.1016/j.ijrefrig.2021.06.035>
- Yao, Y., Sun, Y., Cui, B., Fu, H., Chen, X., & Wang, Y. (2021). Radio frequency energy inactivates peroxidase in stem lettuce at different heating rates and associate changes in physiochemical properties and cell morphology. *Food Chemistry*, 342, 128360. <https://doi.org/10.1016/j.foodchem.2020.128360>

- Yu, H., Mei, J., & Xie, J. (2022). New ultrasonic assisted technology of freezing, cooling and thawing in solid food processing: A review. *Ultrasonics Sonochemistry*, *90*, 106185. <https://doi.org/10.1016/j.ultsonch.2022.106185>
- Zaritzky, N. E. (2010). 20 - Chemical and physical deterioration of frozen foods. In L. H. Skibsted, J. Risbo & M. L. Andersen (Eds.), *Chemical Deterioration and Physical Instability of Food and Beverages* (pp. 561-607): Woodhead Publishing.
- Zhan, X., Zhu, Z., & Sun, D.-W. (2019). Effects of extremely low frequency electromagnetic field on the freezing processes of two liquid systems. *LWT*, *103*, 212-221. <https://doi.org/10.1016/j.lwt.2018.12.079>
- Zhang, C., Li, Y., Xia, X., Sun, Q., Sun, F., & Kong, B. (2023). Changes in protein oxidation, structure, and thermal stability of chicken breast subjected to ultrasound-assisted immersion freezing during frozen storage. *Food Chemistry*, *398*, 133874. <https://doi.org/10.1016/j.foodchem.2022.133874>
- Zhang, H., Chen, G., Liu, M., Mei, X., Yu, Q., & Kan, J. (2020). Effects of multi-frequency ultrasound on physicochemical properties, structural characteristics of gluten protein and the quality of noodle. *Ultrasonics Sonochemistry*, *67*, 105135. <https://doi.org/10.1016/j.ultsonch.2020.105135>
- Zhang, Y., & Ding, C. (2020). The Study of Thawing Characteristics and Mechanism of Frozen Beef in High Voltage Electric Field. *IEEE Access*, *8*, 134630-134639. <https://doi.org/10.1109/ACCESS.2020.3010948>
- Zhang, Z., Sun, D.-W., Zhu, Z., & Cheng, L. (2015). Enhancement of Crystallization Processes by Power Ultrasound: Current State-of-the-Art and Research Advances. *COMPREHENSIVE REVIEWS IN FOOD SCIENCE AND FOOD SAFETY*, *14*(4), 303-316. <https://doi.org/10.1111/1541-4337.12132>
- Zhao, Y., Bilbao-Sainz, C., Wood, D., Chiou, B.-S., Powell-Palm, M. J., Chen, L., McHugh, T., & Rubinsky, B. (2021). Effects of Isochoric Freezing Conditions on Cut Potato Quality. In *Foods* (Vol. 10).
- Zhao, Y., Powell-Palm, M. J., Wang, J., Bilbao-Sainz, C., McHugh, T., & Rubinsky, B. (2021). Analysis of global energy savings in the frozen food industry made possible by transitioning from conventional isobaric freezing to isochoric freezing. *Renewable and Sustainable Energy Reviews*, *151*, 111621. <https://doi.org/10.1016/j.rser.2021.111621>
- Zhong, Y., Cui, Y., Yu, J., Yan, S., Bai, J., Xu, H., & Li, M. (2024). Effect of electron-beam generated X-ray irradiation on water status and microstructure of fresh *Hericium erinaceus* by LF NMR, MRI, SEM and TEM. *Postharvest Biology and Technology*, *209*, 112693. <https://doi.org/10.1016/j.postharvbio.2023.112693>
- Zhu, Z., Chen, Z., Zhou, Q., Sun, D.-W., Chen, H., Zhao, Y., Zhou, W., Li, X., & Pan, H. (2018). Freezing Efficiency and Quality Attributes as Affected by Voids in Plant Tissues During Ultrasound-Assisted Immersion Freezing. *Food and Bioprocess Technology*, *11*(9), 1615-1626. <https://doi.org/10.1007/s11947-018-2103-8>
- Zhu, Z., Geng, Y., & Sun, D.-W. (2019). Effects of operation processes and conditions on enhancing performances of vacuum cooling of foods: A review. *Trends in Food Science & Technology*, *85*, 67-77. <https://doi.org/10.1016/j.tifs.2018.12.011>

- Zhu, Z., Geng, Y., & Sun, D.-W. (2021). Effects of Pressure Reduction Modes on Vacuum Cooling Efficiency and Quality Related Attributes of Different Parts of Pakchoi (*Brassica Chinensis* L.). *Postharvest Biology and Technology*, *173*, 111409. <https://doi.org/10.1016/j.postharvbio.2020.111409>
- Zhu, Z., Li, T., & Sun, D.-W. (2021). Pressure-related cooling and freezing techniques for the food industry: fundamentals and applications. *Critical Reviews in Food Science and Nutrition*, *61*(17), 2793-2808. <https://doi.org/10.1080/10408398.2020.1841729>
- Zhu, Z., Zhang, P., & Sun, D.-W. (2020). Effects of multi-frequency ultrasound on freezing rates and quality attributes of potatoes. *Ultrasonics Sonochemistry*, *60*, 104733. <https://doi.org/10.1016/j.ultsonch.2019.104733>
- Zou, L., Zhang, X., & Zheng, Q. (2021). Research progress on preparation of binary ice by vacuum flash evaporation: A review. *International Journal of Refrigeration*, *121*, 72-85. <https://doi.org/10.1016/j.ijrefrig.2020.10.005>

Chapter II Materials and methodology

II.1 Introduction

The schematic diagram of the research involved in this thesis is shown in Fig. II. 1. It began with the construction of a vacuum freezing system. Then we verified this vacuum freezing system, including the detection of pressure values, the theoretical and experimental water loss, as well as the freezing time during the process. As we prefer the samples to lose ignorable water during freezing, vacuum freezing is not applied to the entire freezing process but is applied selectively to a certain temperature range. The remaining part is finished by conventional freezing (air freezing at -20 °C). In comparison to conventional freezing, air freezing at temperatures of -20, -45, and -80 °C was used, which indicated three different freezing rates of the samples. PEF pretreatment with different parameters was also applied prior to freezing to explore potential intensification approach of vacuum freezing. Theoretically, its utilization can accelerate heat and mass transfer and intensify the freezing process, which is verified in this study. Comparison of the different freezing protocols and the quality attributes of the thawed samples is accomplished through the recording of freezing curves and the characterizations including texture, drip loss, and microstructure. In addition, the effect of the size of the sample and the applicability of the method to different varieties of fruits and vegetables have also been covered.

In this chapter, we describe in detail the research methodology in the following points: construction of vacuum freezing system, freezing protocols (vacuum freezing, conventional freezing), PEF pretreatment, and characterizations.

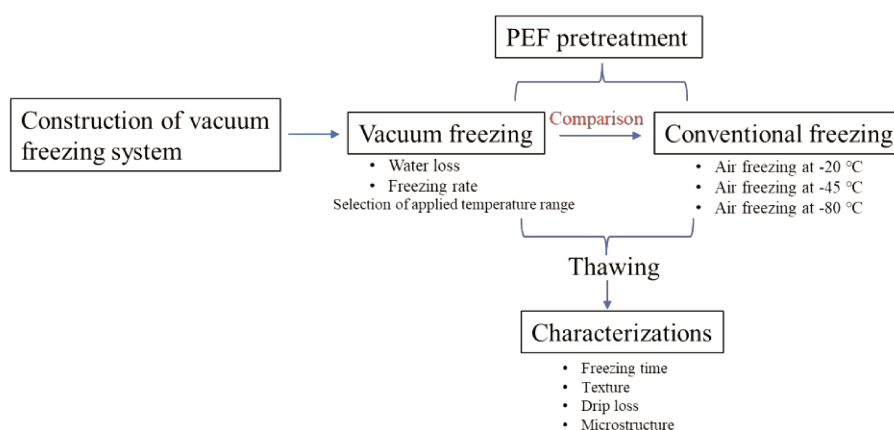


Fig. II. 1: The schematic diagram of the research involved in this thesis.

II.2 Construction of vacuum freezing system

Previously, a vacuum freeze-dryer (Fig. II. 2A) was applied in the research of pulsed electric field assisted vacuum freeze-drying of apple tissue in our team. The temperature curves (Fig. II. 3) of apple tissues with different PEF pretreatments during the process have shown the ability to reduce temperature to sub-zero by low-pressure $P = 10$ mbar. However, the aim of this study was freeze-drying, rather than freezing. Although the initial temperature of the sample was $25\text{ }^{\circ}\text{C}$ and was set in the vacuum chamber with a temperature fixed at $40\text{ }^{\circ}\text{C}$, the starting temperature varied for different samples (temperatures when $t=0s$ in Fig. II. 3). This is due to the large volume (64575 mL) of the cubic vacuum chamber, with a width of 375 mm, a height of 410 mm and a depth of 420 mm, which takes a certain amount of time for the pressure to drop to the specified value. The long waiting time in the vacuum chamber inevitably causes changes in sample temperature. And this makes the end of the process, that is, the return of the pressure to atmospheric pressure, also a long process. This delay limits the flexibility of the freezing process, including the controlling of the beginning and the end, as well as the instant mass measurement and subsequent thawing process. Besides, in our initial test with the vacuum freeze-dryer, it was difficult to connect the thermocouple in the chamber to the external data logger while ensuring the hermeticity of the vacuum chamber.

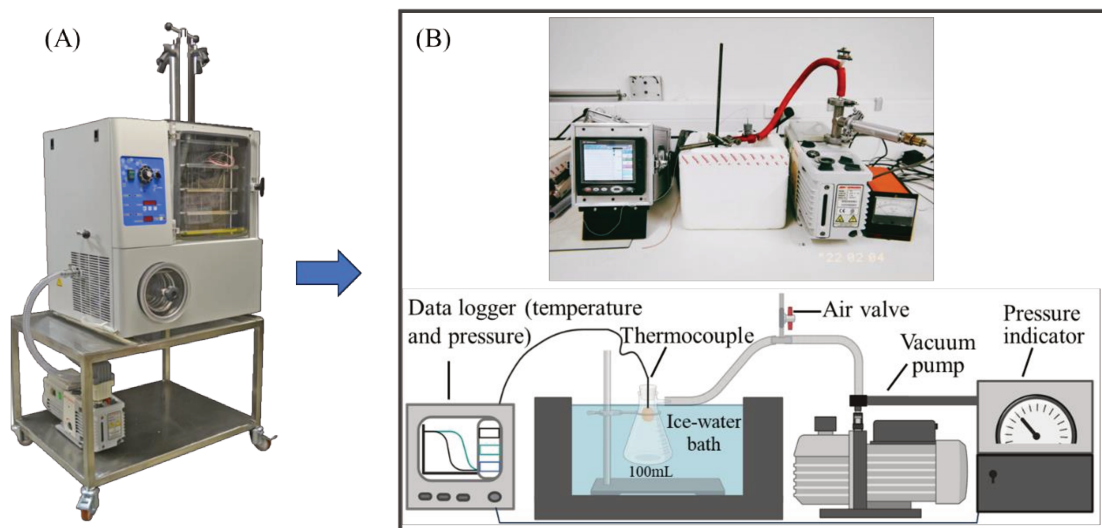


Fig. II. 2: A. The schematic diagram of a vacuum freeze-dryer. B. The schematic diagram of the constructed vacuum freezing system.

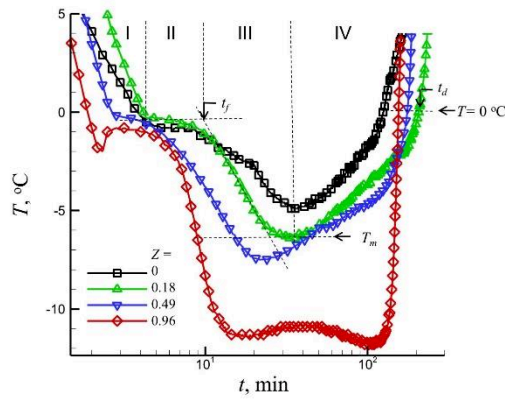


Fig. II. 3: Evolution of the temperature, T , during vacuum freeze-drying at different values of disintegration index, Z . Here T_m is a minimum temperature; t_f and t_d are the effective freezing and drying times, respectively (Parniakov, Bals, Lebovka, & Vorobiev, 2016b).

To solve these problems, a vacuum freezing system was constructed as shown in Fig. II. 2B. It is consisted of a vacuum pump RV8 (Edwards, Sweden), a PB 101 vacuum manometer (Alcatel, France), a switching valve, and a vacuum chamber that was performed by a Buchner flask with a capacity of 100 mL, whose stoper hermetically connected with a T-type thermocouple of 0.5 mm of diameter (TC, Ltd., Dardilly, France) with an accuracy of ± 0.1 °C. The vacuum chamber was placed in the ice-water bath (0 ± 0.1 °C) to maintain a stable environmental temperature. The air valve allows more flexibility in adjusting the beginning and end of the vacuum state. And the pressure during vacuum freezing and temperature of sample was recorded by the data acquisition module during the process.

Fig. II. 4A shows the pressure values of the system as a function of time. The black curve represents the situation for an empty system. As the vacuum pump continues to operate, the pressure value in the vacuum chamber can drop from atmospheric pressure to less than 10 Pa in few seconds and eventually approach approximately 5.6 Pa (Fig. II. 4A), which is theoretically enough to support the evaporation of water at room temperature or even below zero. The variation of the pressure value was also tested with a small amount of pure water in the vacuum chamber (blue curve in Fig. II. 4A). The small volume of the vacuum chamber also allowed a fast drop in the pressure, which could reach the triple point of water (0 °C, 611 Pa) in less than 10 seconds (Fig. II. 4B). Due to the continuous evaporation of water at low pressure, the generated water vapor leads to slower decrease in pressure and a higher ultimate pressure compared to the empty system. The experimental results of pure water also

showed visible ice formation in the vacuum chamber, which also implied the availability of the constructed vacuum freezing system. Additionally, the amount of vapor evaporated from the pure water is theoretically greater than the amount of water vapor from the food samples because of the structural restriction. The evaporated vapor significantly affects the pressure inside the vacuum system. Therefore, the variation of the pressure in the vacuum system with food samples would be between the pressure in the empty system and the system containing little pure water, which is positive for the freezing of food samples. Certainly, if the running time is long enough and no water can be evaporated, the pressure value will then drop again, to the ultimate value for the empty system.

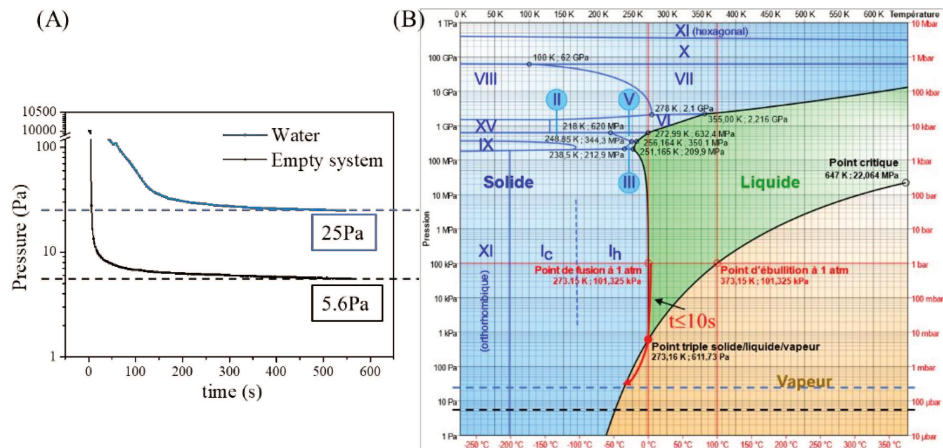


Fig. II. 4: A. The variation of pressure values with time for the empty system and little pure water inside. B. The schematic diagram of the vacuum freezing process of water shown in the phase diagram of water. The black dotted line and the blue dotted line represent the ultimate pressure in the empty system and little water in the system, respectively.

II.3 Freezing protocols

Since the reduction in temperature during vacuum freezing only comes from the evaporation of water originated from the samples, for the same final temperature, the lower the starting temperature, the less moisture is lost. According to the principle of conservation of energy (Brandão, et al., 2020; Wang, et al., 2022), if we assume that the sample mass is constant and the evaporated water is negligible, the amount of water that may be lost during the vacuum freezing process can be calculated by

$$m_{sample} \times \left[C_{pu}(T_i - T_{fm}) + (L_f + C_{pf}(T_{fm} - T_c)) \right] = m_{evap} \times L_{evap} \quad (1)$$

equation (1)

Where L_{evap} is the latent heat of water evaporation, $2.52 \times 10^6 \text{ J/kg}$. L_f is the latent heat of solidification of water, $3.34 \times 10^5 \text{ J/kg}$. C_{pu} is the specific heat capacity of the unfrozen sample, $\text{J/kg} \cdot ^\circ\text{C}$. C_{pf} is the specific heat capacity of the frozen sample, $\text{J/kg} \cdot ^\circ\text{C}$. T_i is the start temperature, $^\circ\text{C}$. T_{fm} is the mean freezing temperature ($T_{\text{fm}} = 1.8 + 0.263 \times T_c + 0.105 \times T_a$). T_c is the final temperature of the sample, e.g. we assume it to be $-6 \text{ }^\circ\text{C}$. If different initial temperatures are applied, the variation of ratios of water loss to the mass of the sample can be obtained. As is shown in Fig. II. 5, the theoretical ratio of the amount of evaporated water to the mass of the sample is approximately 13.3% when the start temperature is $20 \text{ }^\circ\text{C}$. But as the start temperature decreases, the amount of water lost decreases linearly. Start temperature of $2 \text{ }^\circ\text{C}$ was carried out to verify the theoretical results. For a carrot disc with the mass of 2.60 g , the theoretical water loss is $10.5\% \times 2.60 = 0.27 \text{ g}$, while the experimental water loss from 2 to $-6 \text{ }^\circ\text{C}$ was found to be $0.24 \pm 0.02 \text{ g}$, which is quite similar to the theoretical value. Also, a moisture loss of about 10% is very small for the whole sample and is considered acceptable.

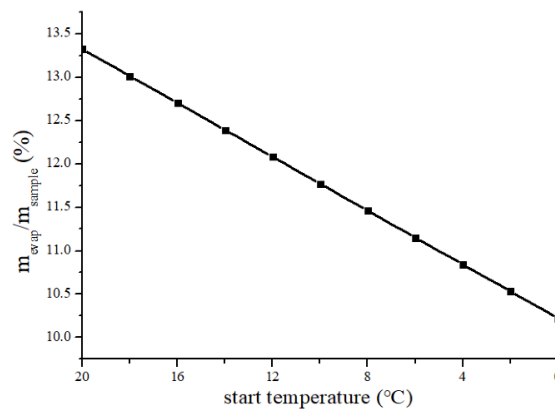


Fig. II. 5: Evolution of the percentage of evaporated water to the total mass of the sample function of the initial temperature of vacuum freezing.

The pre-cooling of the sample is completed in a water-isolated ice-water bath. Although less water will be lost starting from $0 \text{ }^\circ\text{C}$, considering that cooling the sample from room temperature to $0 \text{ }^\circ\text{C}$ in an ice-water bath at $0 \pm 0.1 \text{ }^\circ\text{C}$ is a long process, $2 \text{ }^\circ\text{C}$ was chosen as the freezing start temperature. In order to maintain consistent conditions with vacuum freezing, the starting temperature of other freezing protocols is unified to $2 \text{ }^\circ\text{C}$.

According to EU Directive 89/108 (Quick Frozen Food Directive, QFF), the product should be maintained at -18 °C or colder after thermal stabilization (Chaves & Zaritzky, 2018). In this study, the end of the freezing process was set at -20 °C. The thawing experiments were followed immediately after freezing by placement of the sample in the room maintained at 20 °C.

II.3.1 Vacuum freezing

Vacuum freezing includes continuous vacuum freezing and combined vacuum freezing. For continuous vacuum freezing, the freezing started at 2 °C. When the temperature in the center of the sample dropped to a minimum or even started to rise, it was considered to be finished. For continuous vacuum freezing, no supplementary freezing was applied whether the temperature of samples reached -20 °C or not.

Combined vacuum freezing was a combination of vacuum freezing and conventional air freezing. Vacuum freezing was just applied in a small temperature range to control moisture loss and achieve a fast freezing rate in the freezing critical zone, and the remaining portion was completed by conventional freezing. The initial determination of the freezing critical zone of carrots was based on the freezable water content of carrots. From the evolution of the unfrozen water content of carrots with temperature (Table II.1) (Heldman, Lund, & Sabliov, 2018), most of the water (80%) turns into ice when the temperature drops to -6 °C, and with little change subsequently. Based on the proposal of the International Institute of Refrigeration, food can be considered frozen if the temperature is reduced to -10°C or to a temperature for which 80% of the freezable water has been frozen (Dalvi-Isfahan, Jha, Tavakoli, Daraei-Garmakhany, Xanthakis, & Le-Bail, 2019). Therefore, in the combined vacuum freezing protocol, vacuum freezing was applied from 2 to -6 °C, and then the carrot sample was transferred to conventional air freezing until the temperature of the geometric center of the sample reached -20 °C.

Table II.1: Evolution of unfrozen water content of carrot with temperature.

T	0	-1	-2	-3	-4	-5	-6	-7	-8	-9	-10	-12	-14	-16	-18	-20
%	-	100	53	37	29	24	20	18	17	15	14	11	9	8	7	-

II.3.2 Conventional air freezing

Conventional freezing with three different freezing rates were performed in a ventilated ultra-low-temperature freezer MDF-U2086S (Sanyo, Gunma, Japan) from 2

to $-20\text{ }^{\circ}\text{C}$ (Fig. II. 6). With a modular-type temperature controller SR Mini System (TC Ltd., Dardilly, France) and the software Spec-View Plus (SpecView Corporation, Gig Harbor, USA) supplied. The samples were placed inside the freezer with an air velocity of 1 m/s controlled by an electronic device VEAT 2.5 A (Air-technic, Firminy, France), at temperatures of $-20\text{ }^{\circ}\text{C}$ (AF-20), $-45\text{ }^{\circ}\text{C}$ (AF-45), and $-80\text{ }^{\circ}\text{C}$ (AF-80), respectively. T-type thermocouple mentioned in II.2 was inserted in the geometrical center of the sample to measure and record the temperature evolution during the whole freezing process, and the freezing ended when the temperature of the geometrical center of the sample reached $-20\text{ }^{\circ}\text{C}$.

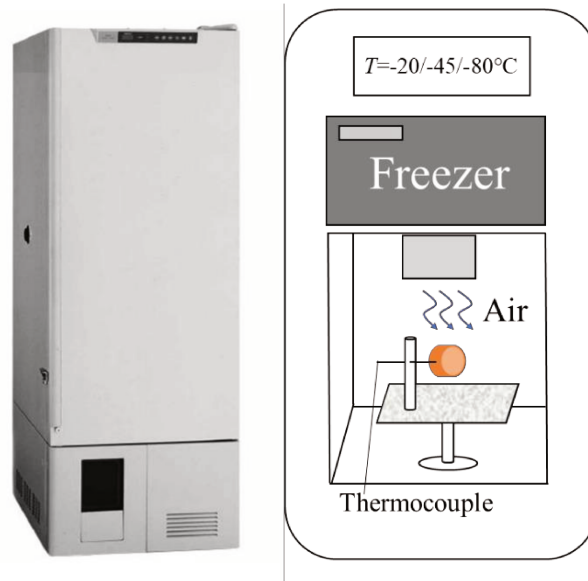


Fig. II. 6: The schematic diagram of conventional air freezing.

II.3.3 Freezing procedures for verification of the temperature range of the application of vacuum freezing

Verification of the temperature range of the application of vacuum freezing was accomplished by the combinations of different freezing rates at temperature ranges of 2 to $-6\text{ }^{\circ}\text{C}$ and -6 to $-20\text{ }^{\circ}\text{C}$. Two freezing rates in the two temperature ranges can be combined to create four freezing procedures, including ①fast freezing + fast freezing, ②fast freezing + slow freezing, ③slow freezing + fast freezing, and ④slow freezing +slow freezing. For the first temperature range of 2 to $-6\text{ }^{\circ}\text{C}$, fast freezing can be carried out by vacuum freezing. It could achieve a faster freezing rate than air freezing at $-45\text{ }^{\circ}\text{C}$, and air freezing at $-45\text{ }^{\circ}\text{C}$ was recognized as fast freezing, while at $-20\text{ }^{\circ}\text{C}$ was slow freezing in preliminary tests for a carrot disc with a thickness of 10 mm and a diameter of 18 mm . However, vacuum freezing cannot achieve the same

fast freezing rate when applied in the temperature range of -6 to -20 °C because its cooling effect depends on the evaporation of water. Most of the water in the carrot sample has already frozen at -6 °C, and the amount of water that can be evaporated to achieve a fast cooling effect is not sufficient. Therefore, vacuum freezing as a fast freezing in the combinations was only applied in the temperature range of 2 and -6 °C. Air freezing can be applied in both temperature ranges as fast freezing or slow freezing when the temperature was set to -45 °C or -20 °C respectively. Since there is only one experimental freezer, when the temperature reaches -6 °C, it is impossible to quickly change the temperature in the freezer to switch freezing conditions. A self-made box containing the sample was placed at -45 °C to achieve similar slow freezing condition as air freezing at -20 °C. When it's time to switch (the temperature of the geometric center of the sample reaches -6 °C), the sample was taken out from the box and directly exposed to -45 °C to complete the slow-to-fast transition under the constant air temperature of -45°C in the same freezer. Thus, four sets of freezing procedures were carried out in two parts (2 to -6 °C and -6 to -20 °C) as follows ① VF + AF-45 (vacuum freezing + air freezing at -45 °C), ②VF + AF-20 (vacuum freezing + air freezing at -20 °C), ③AF-45B + AF-45 (air freezing at -45 °C in the self-made box + air freezing at -45 °C), and ④AF-20 + AF-20 (air freezing at -20 °C + air freezing at -20 °C).

II.4 PEF pretreatment

PEF treatment was done using the PEF generator (5 kV–1 kA, Hazemeyer, Saint-Quentin, France). The applied treatment protocol included application of pulses with the duration of $t_i = 100 \mu\text{s}$, and the time interval between two pulses $\Delta t = 10^{-3} \text{ s}$. The pulses were grouped into N trains, and each train consisted of $n = 10$ pulses. The relatively long pause was applied between the trains ($\Delta t_i = 5 \text{ s}$) in order to maintain the temperature inside of sample nearly constant, $T = 25 \text{ °C}$. The total duration of PEF treatment was evaluated as $t_{\text{PEF}} = n \times N \times t_i$, and it was varied within 0-1s. The electric field strength was varied in the range of 0-400 V/cm. All treatment data were controlled using the Agilent VEE-PRO version 8.5 software (Agilent, Santa Clara, United States). The PEF induced cell disintegration index Z was estimated as (Vorobiev & Lebovka, 2020):

$$Z = (\sigma - \sigma_i) / (\sigma_d - \sigma_i) \quad (2)$$

where σ is the electrical conductivity of a sample, and the subscripts i and d represent the conductivity value of initial (fresh sample) $Z=0$ and completely damaged tissue $Z=1$, respectively. The maximal tissue damage degree ($Z = 1$) was obtained at the strong PEF treatment of sample tissue (at $E = 2000$ V/cm) during time (until the electrical conductivity of a sample σ became constant).

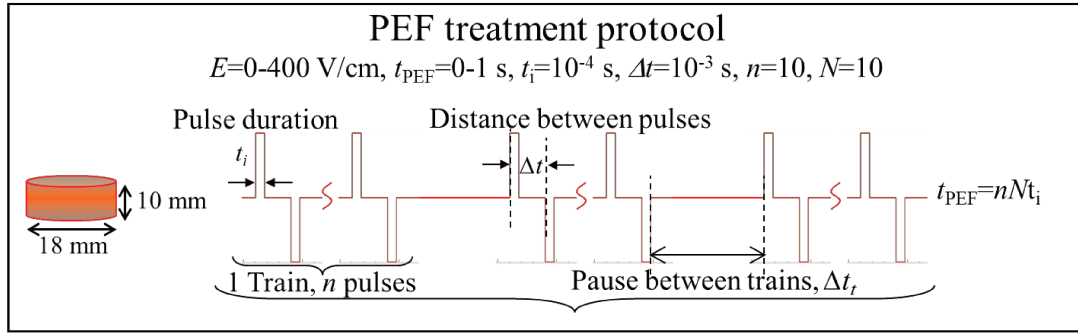


Fig. II. 7: PEF pretreatment applied in this study.

II.5. Characterization techniques

After thawing, samples from different freezing protocols were examined by force relaxation tests, mass loss measurements (from fresh to thawed samples), and microstructure changes in tissue using the scanning electron microscopy (SEM) techniques.

II.5.1. Force relaxation tests

A texture analyzer TA-XT plus (Rhéo, Champlan, France) with 36 mm diameter compression platen was used to perform the non-destructive force relaxation tests. In these tests the preliminary compressing with the constant speed 1.0 mm/s was applied. The compression was stopped at the force level of $F=5$ N and then the force temporary decaying curve $F(t)$ was measured. The previously obtained data for different food tissues (apple, potato, carrot, etc.) evidenced that both PEF-treatment and freeze-thawing can accelerate the force relaxation (Parniakov, Bals, Lebovka, & Vorobiev, 2016a; Vorobiev, et al., 2020). The relative texture index was defined as F^*

$$F^* = F/F_f \quad (3)$$

where F is the force measured at $t=50$ s, and F_f refers the value for fresh tissue.

II.5.2. Moisture loss

After freezing experiments, the samples were stored for one hour at 20°C, then moisture at their surface was removed using the filter paper. The water loss was calculated as (Ajani, Zhu, & Sun, 2023):

$$WL(\%) = (1 - m/m_o) \times 100 \quad (4)$$

where m_o and m are the initial and final masses of the carrot disc.

II.5.3. Scanning electron microscopy (SEM)

The sample discs (fresh samples, samples after PEF treatments, and thawed samples after different freezing protocols) were analysed using the Quanta 250 FEG SEM equipment (FEI, Oregon, USA).

II.6. Statistical analysis

All experiments and measurements of sample characteristics were repeated at least, three times. Significant differences at 95% confidence were evaluated by one-way analysis of variance (ANOVA), using SPSS 25.0. The figures were drawn with Origin Pro 8.5, and the error bars inside correspond to the standard deviations (SD).

- Ajani, C. K., Zhu, Z., & Sun, D. W. (2023). Shrinkage during vacuum cooling of porous foods: Conjugate mechanistic modelling and experimental validation. *Journal of Food Engineering*, 337, 111220. <https://doi.org/10.1016/j.jfoodeng.2022.111220>
- Brandão, V. A., Araújo de Queiroz, R., Lima Dantas, R., Santos de Lima, G., Lima Tresena, N., de Queiroga, A. M., & Barbosa de Lima, A. (2020). Cooling and freezing of cashew apple using computational fluid dynamics. *Diffusion foundations*, 25, 114-132. <https://doi.org/10.4028/www.scientific.net/DF.25.114>
- Chaves, A., & Zaritzky, N. (2018). Cooling and Freezing of Fruits and Fruit Products. In A. Rosenthal, R. Deliza, J. Welti-Chanes & G. V. Barbosa-Cánovas (Eds.), *Fruit Preservation: Novel and Conventional Technologies* (pp. 127-180). New York, NY: Springer New York.
- Dalvi-Isfahan, M., Jha, P. K., Tavakoli, J., Daraei-Garmakhany, A., Xanthakis, E., & Le-Bail, A. (2019). Review on identification, underlying mechanisms and evaluation of freezing damage. *Journal of Food Engineering*, 255, 50-60. <https://doi.org/10.1016/j.jfoodeng.2019.03.011>
- Heldman, D. R., Lund, D. B., & Sabliov, C. (2018). *Handbook of food engineering*: CRC press.
- Parniakov, O., Bals, O., Lebovka, N., & Vorobiev, E. (2016a). Effects of pulsed electric fields assisted osmotic dehydration on freezing-thawing and texture of apple tissue. *Journal of Food Engineering*, 183, 32-38. <https://doi.org/10.1016/j.jfoodeng.2016.03.013>
- Parniakov, O., Bals, O., Lebovka, N., & Vorobiev, E. (2016b). Pulsed electric field assisted vacuum freeze-drying of apple tissue. *Innovative Food Science & Emerging Technologies*, 35, 52-57. <https://doi.org/10.1016/j.ifset.2016.04.002>
- Vorobiev, E., & Lebovka, N. (2020). *Processing of Foods and Biomass Feedstocks by Pulsed Electric Energy*: Springer International Publishing.
- Wang, H., Xue, Y., Hu, Z., Ba, L., Shamim, S., Xie, H., Xia, T., & Zhao, R. (2022). Addition of external water improves the quality attributes of vacuum-frozen and thawed apple slices. *International Journal of Refrigeration*. <https://doi.org/10.1016/j.ijrefrig.2022.01.027>

Chapter III Application of vacuum freezing to improve the quality of thawed carrot discs

III.1 Chapter introduction

The benefits of eating fruits and vegetables are well-recognized by the general consumers. However, keeping the freshness of harvested fruits and vegetables becomes a major issue because of the respiration of plants, resulting in quality deterioration and loss of nutritional value. Freezing is a widely used process for long-term preservation of foods, and it is usually expected to be as fast as possible. In general, rapid freezing produces small ice crystals distributed throughout the tissue, which minimizes the damage to the cell structure or texture of the food.

The behavior of water under sub-atmospheric pressure (negative pressure or vacuum) is of potential research interest as there are important applications such as vacuum cooling, vacuum freezing, spray crystallization, vacuum-induced surface freezing, etc. These processes are typically faster than the conventional approaches, due to the endothermic evaporation of water induced by low pressure. The heat transfer rate of evaporation (occurring in vacuum freezing) is up to 16 times higher than that of conduction (limiting mechanism of conventional freezing methods) (Silva & Schmidt, 2022). The reduction in the food temperature during vacuum freezing relies on the water evaporation starting from the surface and in the tissue of the product. Therefore, during vacuum freezing, the products inevitably lose water, which is undesirable if too much water is lost. To effectively apply the vacuum freezing to obtain a good final result, it is essential to define the conditions in which vacuum freezing is applicable (applied temperature range, sample size, sample species, etc.).

The freezing critical zone, where the most ice crystals are formed, is especially important in the freezing process, and the time to pass through this zone is usually shorter the better. Therefore, our aim is to identify the range of this freezing critical zone and define the operating conditions under which the vacuum freezing can be applied to cross this zone rapidly as well as negligible water loss during this process. The water loss, texture, and the microstructure of the thawed carrot discs after different freezing procedures were compared. This combined freezing mode was also tested in relatively large carrot dishes to test the applicability of vacuum freezing.

Besides, the Pham model was applied to predict the time for conventional air freezing of the particular shape of carrot discs (diameter of 18mm, thickness of 10mm) depending on air temperature and air velocity for better comparison to other freezing approaches. This solves the problem of requiring multiple adjustments of the temperature and air velocity of the conventional air freezer which take a lot of time and experimentation to obtain the freezing time of different freezing parameters. Thus, the research results in this chapter consist of two parts, including the application of vacuum freezing in carrot discs, and the exploration of equivalent parameters of vacuum freezing in conventional air freezing.

III.2 Results

III.2.1 Application of vacuum freezing to improve the quality of thawed carrot discs

The article is presented on the following page.

Application of vacuum freezing to improve the quality of thawed carrot discs

Yuqi Huang*, Olivier Bals

Université de Technologie de Compiègne, ESCOM, TIMR (Integrated Transformations of Renewable Matter), Centre de Recherche Royallieu, CEDEX CS 60319, 60203 Compiègne, France

Abstract

Freezing is a good way for food preservation. In addition to the process effectiveness, modern food freezing techniques should guarantee the high quality of the products after freezing. This study concerns the application of low pressure for food freezing covering a specific temperature range named *freezing critical zone*. Vacuum freezing (VF) allows a fast freezing rate without the use of a cryogenic medium. The application of VF allowed a comparable freezing rate as air freezing at -80 °C in the temperature range of about 2 to -6 °C, which constitutes an advanced technology. Carrot discs with VF (from 2 to -6 °C) were still of good quality by controlling the duration of the freezing critical zone, even with subsequent slow freezing (SF) (from -6 to -20 °C). Carrot samples frozen under different conditions were extensively compared by the results in mass loss, textural property, and microstructural changes of SEM, quantifying the freezing damage. The results showed that carrot discs subjected to the freezing procedure of VF+SF contributed to a comparable texture to that of fast freezing, minimal mass loss, as well as reduced microstructure destruction. Even in the case of increased sample size, which requires more intense freezing conditions, the carrot discs maintained their good quality attributes after VF+SF. In conclusion, the application of VF in the temperature range covering the freezing critical zone can be a promising approach for improving the quality of frozen food products.

Keywords: Vacuum freezing; Temperature critical zone; Quality characteristics; Applicability

1. Introduction

Carrot (*Daucus carota* L.) is one of the most consumed root vegetables and major food crops worldwide. Importantly, it is highly sought-after by consumers due to the

rich content of nutrients and functional components, especially carotenoids which impart distinctive orange colors, with ample health-promoting properties (Vicent, Ndoye, Verboven, Nicolaï, & Alvarez, 2019). High water content makes carrots as perishable as most vegetables and fruits thus leading to a short shelf life. As the most common post-harvest processing method in food industry, freezing plays an invaluable role in the preservation and waste limitation of carrots which inhibits microbial activity and reduces biochemical reactions through the lowered temperature, thereby expanding the selection of carrots, independent of seasonal conditions or geography (Behsnilian & Mayer-Miebach, 2017; Stebel, et al., 2021). However, the conventional freezing methods can cause undesired frozen damages due to possible low freezing rates and unevenly distributed big ice crystals, leading to quality loss, especially texture loss, of frozen fruit and vegetables (Schudel, Prawiranto, & Defraeye, 2021; Tian, Chen, Zhu, & Sun, 2020). Thus, it is critical to search for optimal freezing techniques, which help reduce the harmful damages caused by freezing, to satisfy the consumers' demand of fresh-like in organoleptic properties while well preserved.

Apart from internal factors such as sample size, composition and cellular structure, the quality preservation by freezing mainly depends on controlling the size, number, and location of ice crystals during the freezing process. Thus, the *freezing critical zone*, the temperature range in which the majority of ice crystals formed since the initial freezing point temperature is recognized to be an important period in the freezing process (Dalvi-Isfahan, Jha, Tavakoli, Daraei-Garmakhany, Xanthakis, & Le-Bail, 2019). Generally, the faster the freezing rate, the less time it takes to pass through the critical zone. In this condition, rapid and homogeneous nucleation with very little water migration leads to a greater number of ice crystals, smaller sizes and a more even distribution (Li, Zhu, & Sun, 2018). Numerous approaches have been adopted to accelerate the freezing rate. Based on conventional freezing methods, lowering the temperature of the cryogenic medium and increasing the velocity of the cryogenic medium can increase the freezing rate by accelerating the removal of latent and sensible heat (Muthukumarappan, Marella, & Sunkesula, 2019). But the energy consumption during the process is the main limitation. Some emerging techniques are investigated to affect the freezing process including ultrasound, high pressure, magnetic field, and pulsed electric field (Ben Ammar, Lanoisellé, Lebovka, Van

Hecke, & Vorobiev, 2010; Chen, Liu, Li, Wei, & Li, 2022; Muthukumarappan, et al., 2019). However, these approaches are attractive, but can be challenging. Their utilization is usually coupled with high energy consumption, potential environmental impact and additional infrastructure investment.

Vacuum freezing is a rapid freezing technology that involves the water evaporation under low pressure, removing latent heat so that the temperature of the food product can be quickly reduced. Indeed, the heat transfer rate associated to evaporation (in vacuum freezing) is much higher than that of conduction (in conventional freezing methods) (L. Wang & Sun, 2001). Also, as water is evaporated, with the effect of prior dehydration, the amount of ice crystals formed during the freezing process can be reduced, which has been reported to decrease the initial moisture and accelerate the freeze-drying process of fruits and vegetables (Silva, et al., 2022; H. Wang, Fu, Chen, Hu, & Xie, 2018). Vacuum freezing also has the advantage of low energy consumption compared to conventional freezing because it does not require movement of the cooling medium in the system and vacuum can minimize heat loss from the environment. For the principle of water evaporation, the available studies in food industry have mainly focused on its application in the pre-cooling process of fruits and vegetables with high moisture content, porous structure and adequate specific surface area (Zhu, Geng, & Sun, 2021). Pure water, simulated puree droplets, and nanodroplets were used in the initial exploration of the vacuum freezing process, including the mathematical simulation and visualization (K. Ando, Arakawa, & Terasaki, 2018; Cheng & Lin, 2007; Cogné, Nguyen, Lanoisellé, Van Hecke, & Clause, 2013; Zhang, Zhang, & Zhang, 2016; Zhu, et al., 2021). Recently, studies have shown that process conditions of vacuum freezing including pressure reduction modes, addition of external water, and different pretreatment (freeze-thaw, blanching and ultrasound) can affect the vacuum-freezing characterizes in various extent (H. Wang, et al., 2016; H. Wang, et al., 2022). However, few studies have focused on the quality of the final product (fruits and vegetables) after vacuum freezing and thawing.

In the current study, a laboratory vacuum freezing system was designed for the freezing process of carrot discs in the temperature range covering the freezing critical zone. Preliminary calculations were applied to predict the variation of the potential loss of moisture with temperature range during vacuum freezing. Due to the high enthalpy of evaporation of water, vacuum freezing can achieve a very fast freezing

rate. The application temperature range of vacuum freezing was determined under comprehensive consideration of a small water loss (reducing the application temperature range) and fast passing through the freezing critical zone (covering the freezing critical zone). The texture, mass loss and microstructure of thawed samples after conventional freezing with different freezing rate and freezing procedure with application of vacuum freezing were detected respectively to evaluate of the quality promotion of vacuum freezing. Besides, the applicability of vacuum freezing from the variation of size was also investigated. This study would provide theoretical support for the application of vacuum freezing in the freezing storage of carrots, which is hoped to serve as guidance for industrial applications.

2. Materials and methods

2.1 Sample preparation

Carrot roots (*Daucus carota* L.) were obtained from a local market (Compiègne, France) and stored in a darkness at 6 °C until analysis maximally for one week. The wet-base moisture content of carrot samples was 88-91% that was detected by MA160 Infrared Moisture Analyzer (Sartorius, Germany). The carrot disc-shaped samples (d = 18 mm in diameter and h = 10 mm/20 mm in thickness) were manually prepared by using the special cylindrical knife. Samples were taken from the medium part of the carrots with 3 cm removed from the head and tail. And the carrot discs of 10 mm in thickness were with an approximate mass of 2.60 ± 0.10 g.

2.2 Setup and temperature range for the application of vacuum freezing

Tests were performed by using a self-constructed vacuum freezing system (Fig. II. 2B), which consisted of a vacuum pump RV8 (Edwards, Sweden), a PB 101 vacuum manometer (Alcatel, France), a switching valve, and a vacuum chamber that was performed by a buchner flask with a capacity of 100 mL, whose stopper hermetically connected with a T-type thermocouple of 0.5 mm of diameter (TC, Ltd., Dardilly, France) with an accuracy of ± 0.1 °C. The vacuum chamber was placed in the ice-water bath (0 ± 0.1 °C) to maintain a stable environmental temperature. A data acquisition module recorded the pressure and temperature of sample during vacuum freezing.

According to the conversion of energy, the decrease in sample temperature and formation of internal ice crystals during vacuum freezing is achieved by the evaporation of water within the sample induced by low pressure. If it is assumed that the loss of mass is quite small and the heat transfer between the system and the external environment is negligible, the sample mass can be considered constant. Thus, the mass of evaporated water during vacuum freezing can be calculated by equation (1).

$$\frac{dm_{vap}}{dt} L_{vap} = m C_p \frac{dT}{dt} + \frac{dm_f}{dt} L_f \quad (1)$$

Where m_{vap} is the mass of vaporized water during vacuum freezing (kg); L_{vap} is the latent heat of vaporization of water at 273.16 K, 611.73 Pa, about 2500 kJ/kg; m is the mass of the sample (kg); C_p is the specific heat capacity of the sample, $\text{kJ}\cdot\text{kg}^{-1}\cdot\text{K}^{-1}$; T is the sample temperature (K); m_f is the mass of frozen water in the sample (kg); L_f is the latent heat of fusion of water, 334 kJ/kg.

For the aim of freezing rather than drying, the start temperature of vacuum freezing was set at 2 °C in consideration of reducing the loss of moisture and covering the critical zone. Besides, from the evolution of unfrozen water content of carrot with temperature (Table II.1) (Heldman, Lund, & Sabliov, 2018), most of water (80%) turns into ice when temperature drops to -6 °C, and with little change subsequently. Based on the proposal of the International Institute of refrigeration, food can be considered frozen if the temperature is reduced to -10 °C or to a temperature for which 80% of the freezable water has been frozen (Dalvi-Isfahan, et al., 2019). Therefore, vacuum freezing can be applied in a small temperature range from 2 to -6 °C.

Verification of the temperature range of the application of vacuum freezing was accomplished by the combinations of different freezing rates at temperature range of 2 to -6 °C and -6 to -20 °C. For a carrot disc with a thickness of 10 mm and a diameter of 18 mm, freezing at -20 °C was recognized as slow freezing, while at -45 °C was fast in preliminary tests. Besides, vacuum freezing could achieve a faster freezing rate than freezing at -45 °C through the temperature range from 2 to -6 °C. However, it is difficult to rapidly change freezing conditions from slow to fast within one freezer. A self-made box containing the sample was placed at -45 °C to achieve similar slow

freezing condition as freezing at -20 °C. When it's time to switch, the sample was taken out from the box and directly exposed to -45 °C to complete the slow-to-fast transition. Thus, four sets of freezing procedures were carried out in two parts (2 to -6 °C and -6 to -20 °C) as follows ① fast + fast (vacuum freezing + freezing at -45 °C), ②fast + slow (vacuum freezing + freezing at -20 °C), ③slow + fast (freezing at -45 °C in the self-made box + freezing at -45 °C), and ④slow + slow (freezing at -20 °C + freezing at -20 °C).

2.3 Freezing experiments (Table III.1)

On one hand, to maintain the same freezing condition as vacuum freezing, the starting temperature of conventional freezing for comparison was also set at 2 °C. On the other hand, Schudel et al. showed that pre-cooling prior to conventional freezing significantly reduced drop loss of carrots by 13% and doubled the firmness, which implied that pre-cooling also reduced damage to cell walls and cell membranes by ice crystals in conventional freezing (Schudel, et al., 2021). Therefore, carrot discs were pre-cooled to 2 °C in an ice-water bath mentioned in 2.2 across a plastic bag. Freezing process were all carried out from 2 to -20 °C. The thawing experiments were started immediately after freezing by placement of the sample in the room maintained at 20 °C (Parniakov, Bals, Lebovka, & Vorobiev, 2016). All freezing experiments were performed in 3 replicates.

Table III.1: Experiment procedures for AF-20, AF-45, AF-80, and VF+AF-20.

Experiments	Precooling	Freezing conditions	Thawing
AF-20		Air freezing at -20 °C from 2 to -20 °C	
AF-45	Ice-water bath at 0 ± 0.1 °C from room temperature to 2 °C	Air freezing at -45 °C from 2 to -20 °C	Room temperature (20 ± 1 °C) in the air (free convection).
AF-80		Air freezing at -80 °C from 2 to -20 °C	
VF+AF-20		Vacuum freezing from 2 to -6 °C, and then immediately transferred to air freezing at -20 °C until -20 °C	

2.3.1 Conventional air freezing

Conventional air freezing with three different freezing rates were performed in a ventilated ultra-low-temperature freezer MDF-U2086S (Sanyo, Gunma, Japan) from 2 to -20 °C (Fig. II. 6). With a modular-type temperature controller SR Mini System (TC Ltd., Dardilly, France) and the software Spec-View Plus (SpecView Corporation,

Gig Harbor, USA) supplied. The samples were placed inside the freezer with an air flow rate of 0.5 m/s controlled by an electronic device VEAT 2.5 A (Air-technic, Firminy, France), at temperatures of -20 °C (AF-20), -45 °C (AF-45), and -80 °C (AF-80), respectively. T-type thermocouple mentioned in II.2 was inserted in the geometrical center of the sample to measure and record the temperature evolution during the whole freezing process, and the freezing ended when the temperature of the geometrical center of the carrot discs reached -20 °C.

2.3.2 Vacuum freezing

Vacuum freezing was performed in the setup of Fig. II. 2B in the temperature range of 2 to -6 °C. Then the samples were quickly transferred to the freezer mentioned in 2.3.1 to complete the freezing process of -6 to -20 °C by conventional freezing at temperature of -20 °C (AF-20).

2.4 Analysis of the samples

2.4.1 Force relaxation test

Texture properties were measured using a texture analyzer TA-XT plus (Rhéo, Champlan, France), to perform force relaxation test. The force was set at the level of 5 N, with the speed of piston displacement of 1.0 mm/s. The deformation curves (plot of force vs. time) were recorded with 0.1 s resolution during 60 s (Parniakov, et al., 2016). The F (t=50 s) for untreated and thawed samples after different freezing procedures were selected for subsequent comparison.

2.4.2 Mass loss (ML) measurement by gravimetric method

The ML of the samples, which represents the amount of water loss, was calculated using the mass of carrot discs before freezing (m_0) and after thawing (m_1) as (Ajani, Zhu, & Sun, 2023):

$$ML(\%) = (m_0 - m_1)/m_0 \times 100 \quad (2)$$

2.4.3 Scanning electron microscopy (SEM) observation

The surface and cross-section of carrot discs were observed with Quanta 250 FEG SEM equipment (FEI, Oregon, USA). 15 images from three different samples were analyzed. Distribution of the cell size was obtained from the images by Nano

Measurer 1.2, with statistical measurements of the mean isometric diameter of 120 randomly selected cells.

2.5 Applicability analysis of vacuum freezing on carrots

Two sizes of carrot discs were prepared (d=18 mm in diameter, h=10 mm and h= 20 mm in thickness), and then frozen by the same procedures, followed by texture and mass loss analysis.

2.6 Statistical analysis

All experiments and measurements of characteristics were repeated at least, three times. Significant differences at 95% confidence were evaluated by one-way analysis of variance (ANOVA), using SPSS 25.0. The figures were drawn with Origin Pro 8.5, and the error bars inside correspond to the standard deviations (SD).

3. Results and discussion

3.1 Identification and verification of the freezing critical zone of carrots

The final freezing temperature-force plots recorded from 2 to -20 °C during AF-20, AF-45 and AF-80 are depicted in [Fig. III. 1](#), with the data in [Table II.1](#) shown on the right ordinate. It is shown that at the three different temperatures, the compression stress values become lower as the final temperature of freezing decreases, which means a worse texture for the carrot discs. Meanwhile, this same trend is displayed consistent with the unfrozen water content in carrots. This result is due to the destruction of the cellular structure of food cells during the freezing process, mainly due to mechanical damage caused by ice crystal formation and osmotic dehydration caused by intracellular water migration. (Li, et al., 2018). In other words, the evolution of the texture of the food is related to its unfrozen water content.

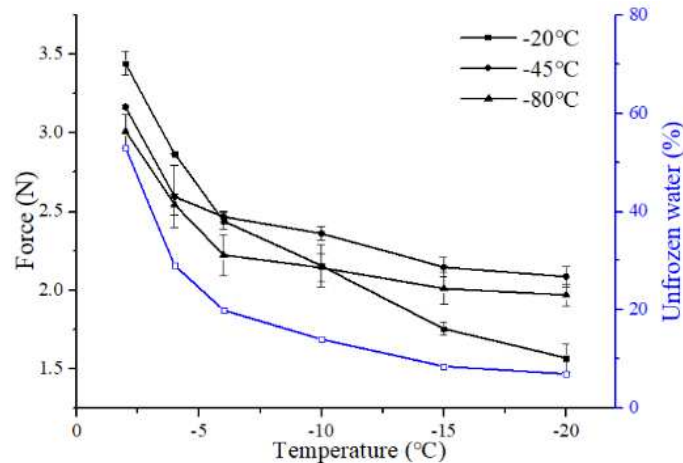


Fig. III. 1: Evolution of texture of carrot discs with temperature during freezing (AF-20, AF-45, and AF-80). Evolution of unfrozen water content of carrot discs (thickness of 10 mm) with temperature (data from Table II.1).

However, in this study, the situation is observed to be not exactly the same for the different freezing rates provided by changing the freezing temperatures, especially in the temperature range of -6 to -20 °C. In Fig. III. 1, the decrease in texture tends to plateau for freezing at lower air temperatures (freezing at -45, -80 °C), while AF-20 continues to decrease substantially in the temperature range of -6 to -20 °C. This may be due to the fact that slow freezing starts with the crystallization of extracellular water (Schudel, et al., 2021). The formation of extracellular ice crystals immediately alters the balance of intracellular and extracellular osmotic pressure. During slow freezing, the long duration in freezing critical zone provides more time for water movement to transfer across the cell membrane, leading to dehydration of the cells and further mechanical injury from the growth of ice crystals (Dalvi-Isfahan, et al., 2019). On the contrary, for fast freezing conditions, the time required to pass through the freezing critical zone is smaller. Ice crystals are then more evenly distributed inside and outside the cells (Schudel, et al., 2021). Simply defined, it's as if the internal water was instantly immobilized (-1 to -6 °C), causing little further deterioration during the subsequent freezing process (-6 to -20 °C). At the end of the freezing critical zone (-6 °C), a similar degree of damage occurs to them, while because of their different durations from -1 to -6 °C (as shown in Fig. III. 3C), the migration of water and ice crystals distribution inside of carrot tissue at this point are already very different, as well as the differences in ice crystals size and numbers (Muthukumarappan, et al., 2019), thus affecting the results of subsequent freezing.

Comparisons of the freezing curves and their texture after thawing among combinations of different freezing rates in temperature ranges from 2 to -6 °C and -6 to -20 °C are shown in Fig. III. 2. For procedure ① and ②, their freezing time in temperature range covering freezing critical zone is much shorter than ③ and ④, which corresponds to their better textural results. And from the comparison between procedure ① and ②, it is found that if frozen rapidly in the temperature range covering the freezing critical zone, the subsequent freezing speed has no obvious effect on the final texture. That's also the reason why the texture of carrot disc plateaued after -6 °C when freezing at -45 °C and -80 °C (Fig. III. 1). But if frozen slowly first, as in procedure ③ and ④, degradation of the texture is inevitable, regardless of whether the following freezing is fast or slow. Moreover, comparisons of ① and ③, as well as ② and ④ further demonstrate that although they have the same freezing process from -6 to -20 °C, respectively, the textural results are significantly altered by the different freezing rates from 2 to -6 °C. All these results confirmed that the final texture of carrot discs can be changed by controlling the freezing time staying in the temperature range covering the freezing critical zone.

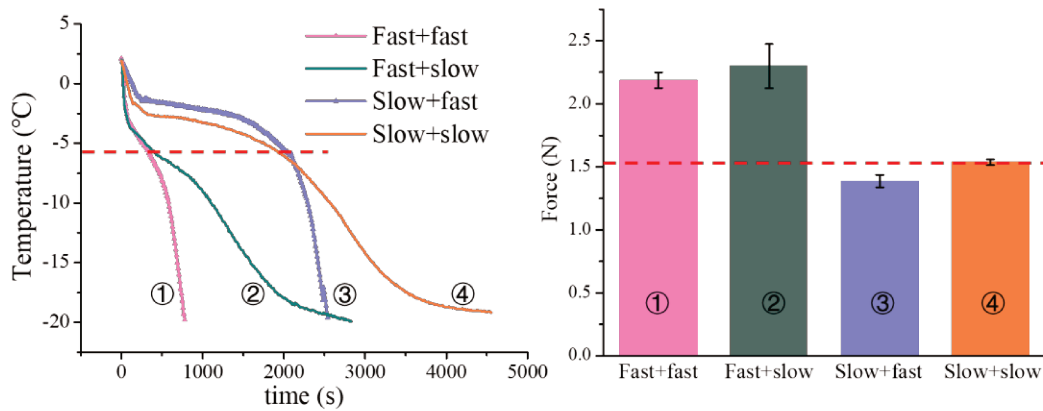


Fig. III. 2: Evolution of the temperature of the carrot discs (thickness of 10 mm) (A), during ① fast + fast (vacuum freezing + freezing at -45 °C), ② fast + slow (vacuum freezing + freezing at -20 °C), ③ slow + fast (freezing at -45 °C in the self-made box + freezing at -45 °C), and ④ slow + slow (freezing at -20 °C + freezing at -20 °C), as well as their texture (B) after thawing, respectively. The red dotted line in the temperature curves represents the temperature of -6 °C, which is also the transition point of the freezing procedures.

3.2 Pressure and temperature monitoring of the freezing process

Temperature-time and pressure-time curves as well as the temperature-pressure curve presented in the phase diagram of water during vacuum freezing are shown in Fig. III.

3A. Due to the small volume (100 mL) of the vacuum chamber, it is possible to reduce the pressure rapidly from atmospheric pressure (101325 Pa) to 240 Pa in about 8 s. Since the pressure fall sharply and reached the flash point of water evaporation, the evaporation of the inner water of the carrot disc start, removing most of the sensible heat from the sample, which resulted in a rapid reduction of the temperature. Similar phenomena were found in the initial stage of vacuum freezing (0-2 min) of apple slices (H. Wang, et al., 2022). Subsequently, with the formation of ice crystals in the carrot disc, a large amount of latent heat was released and the sample temperature would stay briefly near the freezing point (around -1.6 °C). The solute concentration inside the sample also continuously increased, which can be attributed to the formation of ice crystals and to the water loss from the evaporation. Due to this concentration increase, the freezing point is lowered. Besides, due to the presence of the solute components of carrot, the temperature-pressure curve shifted to lower pressure and lower temperature compared to pure water. The triple point of carrot occurred around 80 Pa, -1.6 °C (Fig. III. 3B).

Typical time-temperature plots recorded during AF-20, AF-45, AF-80 and VF+AF-20 experiments are shown in Fig. III. 3C, and detailed freezing time during 2 to -6 °C, -6 to -20 °C, and 2 to -20 °C can be seen in Table III. 2. For the temperature range from 2 to -6 °C, there was no significant difference in the freezing time of VF+AF-20 (427 s) and AF-80 (423 s), but they were significantly smaller than AF-45 (797 s) and AF-20 (1977 s) ($p < 0.05$). This result showed that VF achieve the same fast freezing speed as conventional freezing at -80 °C. Because of the higher efficiency of heat transfer compared with AF-20 and AF-45, the freezing critical zone is rapidly covered without the use of a cryogenic medium. As for the temperature range from -6 to -20 °C, VF+AF-20 (2483 s) and AF-20 (2557 s) show similar variation because of the same freezing process. Compared to AF-45 and AF-80, the temperature difference between the freezer and sample is much smaller for AF-20. This would directly lead to a smaller driving force of heat transfer, thus resulting in a longer freezing time to reach the same final temperature.

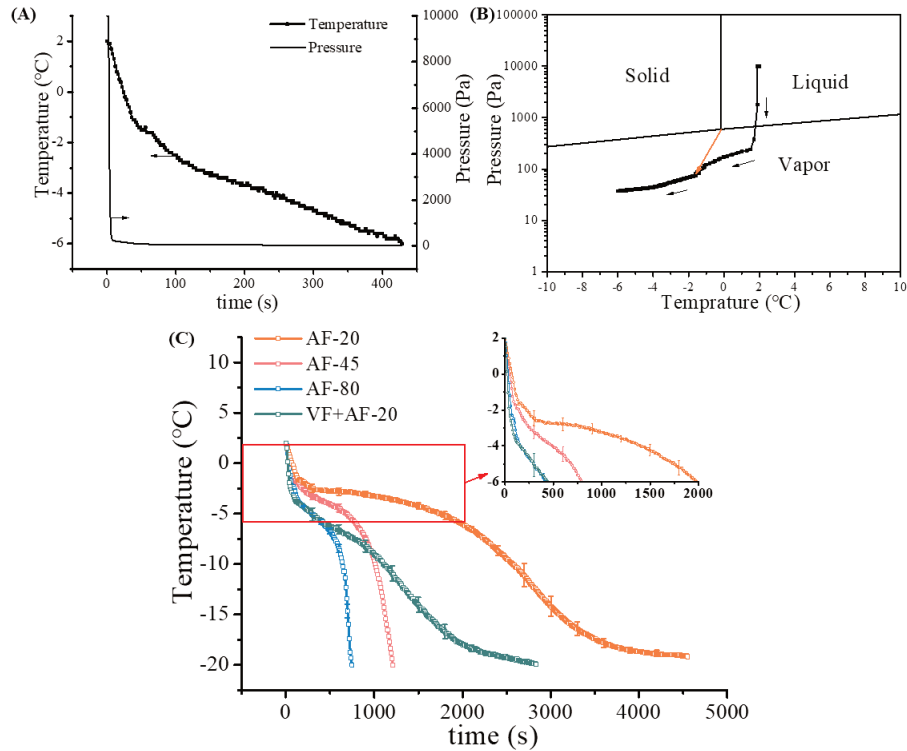


Fig. III. 3: Temperature-time and pressure-time curves (A) of carrot discs (thickness of 10 mm) during VF. Temperature-pressure curve (B) of carrot discs (thickness of 10 mm) presented in the phase diagram of water during VF. (C) Evolution of the temperature of carrot discs (thickness of 10 mm), during AF-20, AF-45, AF-80, and VF+AF-20, respectively.

3.3 Main quality characteristics of thawed carrot discs

Carrot discs quality frozen under AF-20, AF-45, AF-80, and VF+AF-20 was assessed by mass loss, texture, and SEM. Mass loss for conventional freezing was mainly associated to the drip loss during thawing, while for VF+AF-20 it was due to the drip loss and also water evaporated during vacuum freezing. As shown in Table III. 2, the mass loss in the AF-20 was significantly higher than that in other freezing processes ($p < 0.05$). Usually, the number and the size of the formed ice crystals can be affected by the freezing rate, equivalent to the velocity of operation to pass through the freezing critical zone (Dalvi-Isfahan, et al., 2019). The freezing time during 2 to -6 °C of AF-45 (797 s), AF-80 (423 s), and VF+AF-20 (427 s) were all significantly shorter than that of AF-20 (1977 s), resulting in fewer internal changes, including tissue rupture from big ice crystals and volumetric changes from expansion stress in the cellular structure (Panayampadan, Shafiq Alam, Aslam, Kumar Gupta, & Kaur Sidhu, 2022), reducing the drip loss during thawing. Intriguingly, the moisture loss during

VF did not result in an increase in overall mass loss, a small mass loss (11.57%) was observed after VF+AF-20 in contrast. Moreover, as we calculated and experimentally verified that the amount of evaporated water of carrot disc with a thickness of 10 mm during vacuum freezing from 2 to -6 °C was around 10%, this means that the drip loss during thawing after VF+AF-20 was about 1.57%, which is quite smaller compared to conventional freezing. In addition to the rapid freezing rate, this may also be contributed to moisture loss at the beginning of the freezing process limiting the damage to the cell wall structure. Previous studies on dehydrofreezing indicated that pre-drying increased the protecting potential of tissue during freezing, with lower drip loss observed in carrots and strawberries (Hajji, Gliguem, Bellagha, & Allaf, 2022; Schudel, et al., 2021).

Table III. 2: Freezing time of temperature range of 2 to -6 °C, -6 to -20 °C, and 2 to -20 °C for carrot discs (thickness of 10 mm) during AF-20, AF-45, AF-80, and VF+AF-20, respectively. Mass loss (%), and texture (N) for thawed carrot discs (thickness of 10 mm) after AF-20, AF-45, AF-80, and VF+AF-20, respectively. Values with different superscripts among the data in the same column indicate that the means are significantly different at $p < 0.05$.

Freezing conditions	Freezing time (s)			Mass loss (%)	Texture (N)
	2 to -6°C	-6 to -20°C	2 to -20°C		
AF-20	1977±81 ^c	2557±105 ^a	4533±29 ^a	17.46±0.49 ^c	1.54±0.02 ^c
AF-45	797±12 ^b	413±32 ^b	1210±30 ^c	10.97±0.02 ^a	2.37±0.02 ^a
AF-80	423±29 ^a	320±36 ^c	743±12 ^d	13.78±0.44 ^b	2.10±0.10 ^b
VF+AF-20	427±75 ^a	2483±56 ^a	2910±69 ^b	11.57±0.27 ^a	2.30±0.18 ^a

The textural property is also an important quality indicator for potential damage in the collection, handling, processing, and storage of fruits and vegetables, which can be evaluated by force relaxation test (Wu, Wang, & Guo, 2020). Compared with AF-20 (1.54 N), the stress values of the carrot disc after AF-45 (2.37 N) and AF-80 (2.10 N) were significantly higher by a rapid freezing rate induced by a lower temperature of the air in conventional freezing ($p < 0.05$). The same results were reported by Van Buggenhout et al. (Van Buggenhout, Lille, Messagie, Loey, Autio, & Hendrickx, 2006), where applying rapid conventional and cryogenic freezing conditions minimized the texture loss of frozen carrots, revealing that reduced texture loss of carrots was associated with the reduction in cell wall damage in carrot tissue. It can be noted that the compression stress value of the carrot disc after VF+AF-20 was as good

as that of fast freezing, although the freezing time in the temperature range of -6 to -20 °C was much longer. This also proved that the quality of the final product could be modified by controlling the freezing process in the critical zone, VF applied in this study. In this way, the loss of cell turgidity and breakdown of cell wall structure was reduced, leading to less cell rupture and tissue collapse (Tian, et al., 2020). The decrease in water during vacuum freezing may also perform a role. Although the removal of water varied, a previous study has shown that reducing the water content in carrot tissue induced a protective effect by the alleviation of fracture stress relating to cell wall strength after freeze-thawing (H. Ando, Kajiwara, Oshita, & Suzuki, 2012).

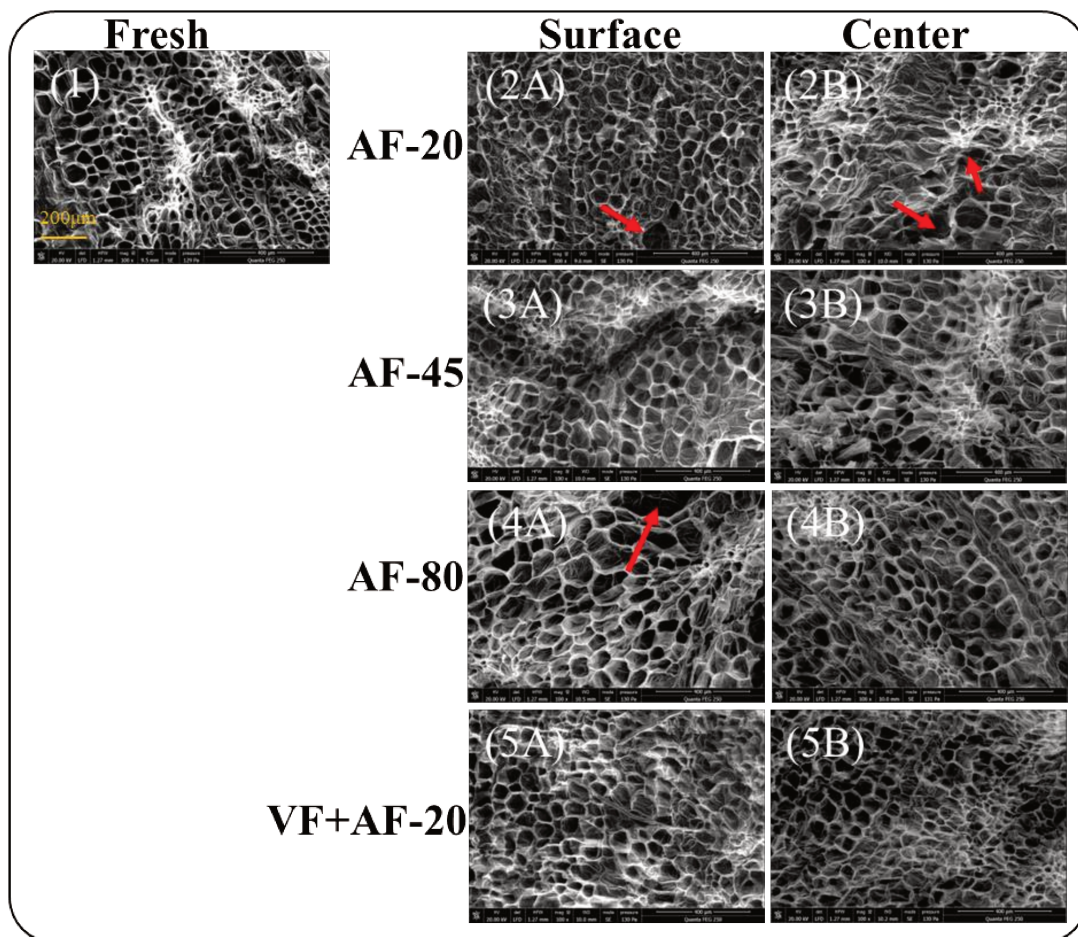


Fig. III. 4: SEM images of carrot discs (thickness of 10 mm) after different freezing treatments. (1) fresh carrot, (2A) the surface of carrot disc after AF-20, (2B) the center of carrot disc after AF-20, (3A) the surface of carrot disc after AF-45, (3B) the center of carrot disc after AF-45, (4A) the surface of carrot disc after AF-80, (4B) the center of carrot disc after AF-80, (5A) the surface of carrot disc after VF+AF-20, (5B) the center of carrot disc after VF+AF-20.

As both texture and drip loss are expected to rely on tissue integrity (Sun, 2011), micrographs were acquired to shed light on the effect of the different freezing processes on carrot discs, further verifying the improvement of quality attributes by VF. Microstructural changes of the surface and central section of carrot discs from SEM produced by the different treatments are shown in [Fig. III. 4](#).

Fresh carrot tissue displayed a regular and complete cell structure with an isodiametric diameter of about 47 μm , which was in accordance with the findings of Van Buggenhout et al. (Van Buggenhout, et al., 2006) who described carrot parenchyma cells as small cells with an isodiametric diameter of about 50 μm . Upon AF-20, large ice crystals were formed especially in the center of the carrot disc ([Fig. III. 4](#)), contributing to more cell disruption and morphological changes, which gave reason for the considerable mass loss and decrease in texture observed after thawing ([Table III. 2](#)). Generally, faster freezing rate results in a greater number of ice crystals with a smaller median size and more uniform size distribution, with fewer adverse effects on the thawed cell structure. However, it can be seen that the surface of the AF-80 sample also exhibited ruptures and contortions in the microstructure. These freeze cracking were possibly caused by the rapid water expansion induced by very fast freezing at ultra-low temperatures on the surface of the carrot disc at the beginning, leading to uniform tensile stresses in the unfrozen core and tensile radial stresses and compressive tangential stresses in the outer surface of frozen food (shell) (Schudel, et al., 2021). After solidification and expansion, solid ice contracts, and the shell frozen body is then exposed to tangential tensile stress instead of compression at the beginning of freezing (Dalvi-Isfahan, et al., 2019). A relatively large isometric diameter was also obtained by about 76 μm on the surface of the carrot disc after AF-80. VF was carried out with a much faster freezing rate than AF-20 during the critical zone, resulting in smaller and more uniform ice crystals in the extracellular and intracellular regions, which is consistent with the favorable results in mass loss and texture. The same result was found in the photomicrograph of apple tissues after VF (H. Wang, et al., 2022). Although they considered that the intensive flash evaporation of the inner original free water inside the apple tissue during VF could destroy the integrity of the cell structure. This phenomenon was not observed for carrots in our study. One possibility is that the large vacuum chamber resulted in a slower pressure drop (2 minutes to flash point of water evaporation), instead of 8 s in our device. Also,

it may be due to the differences in the species of food. It was found by Nikolai I Lebovka et al. that carrots were stronger than apples based on the stress-deformation curves for their tissues after freeze-thawed (Lebovka, Praporscic, & Vorobiev, 2004). Furthermore, vacuum-induced nucleation of VF+AF-20 may also be one of the factors for its uniform microstructure. Applied before freeze-drying, samples produced using the controlled freezing (VF) were more homogeneous than those produced by the uncontrolled freezing (Oddone, Barresi, & Pisano, 2017; Silva & Schmidt, 2019; Silva, et al., 2022).

As shown in Fig. III. 4, the difference in microstructure corresponds to the results of mass loss and texture (Table III. 2), confirming the interpretation of their relationship as previously inferred in the analysis of Table III. 2. For freezing preservation, the least microstructure disruption after VF+AF-20 was desirable to achieve good-quality frozen products.

3. 4 Verification of the applicability of vacuum freezing

As it was discussed in Section 3.3, the application of VF during the critical zone could be a promising approach to improve the quality of frozen carrots, which was based on the results from small carrot discs with a diameter of 18 mm and thickness of 10 mm. Carrot discs with double thickness (18 mm diameter and 20 mm thickness) were tested in the same four freezing procedures. Their freezing times in the temperature range of 2 to -6 °C, covering the critical zone, are shown in Table III. 3, as expected to be relatively longer than those of the smaller size. Fig. III. 5 presents the comparison of the mass loss and texture between the two sizes of carrot discs after thawing.

Table III. 3: Freezing time for carrot discs with thicknesses of 10 mm and 20 mm in the temperature range of 2 to -6 °C during AF-20, AF-45, AF-80, and VF+AF-20, respectively. Values with different superscripts for each data indicate that the means are significantly different at $p < 0.05$.

Thickness/mm	AF-20 (s)	AF-45 (s)	AF-80 (s)	VF+AF-20 (s)
10	1977±81 ^f	797±12 ^e	423±29 ^a	427±75 ^a
20	3193±99 ^g	1603±47 ^e	1073±21 ^d	653±21 ^b

For conventional air freezing, the freezing time increased as the sample size increased (Table III. 3). Similar results were obtained in a study on spherical potatoes freezing, which mentioned that the freezing time should be proportional to the square of the

sample diameter based on numerical prediction models for the freezing time (Stebel, et al., 2021). This is because the heat transfer inside the sample is due to conduction. The conduction resistance depends on the sample size. The larger the sample size, the greater the conductive resistance and the greater the amount of heat to be removed. Thus by increasing the size of the sample, the freezing time is increased. (Muthukumarappan, et al., 2019). In this case, conventional freezing that only relies on heat conduction may not be able to achieve a fast freezing rate even with a large temperature difference as the driving force. It is worth mentioning that both sizes of carrot discs have the shortest freezing time across the temperature range of 2 to -6 °C for vacuum freezing, which can be explained by the faster rate and increased evaporation of internal water according to the principle of energy conservation (H. Wang, et al., 2022), as the latent heat of evaporation (2500 kJ/kg) removed is much greater than the latent heat of crystallization of water (334 kJ/kg). The fast rate of vacuum freezing of carrot discs may be also attributed to their special vascular system, which has a conductive effect through xylem and phloem (Perrin, et al., 2017). The xylem is a water-filled structure with lignified cell walls, mainly responsible for the transport of water and minerals, while the phloem consists mainly of densely packed, thin-walled cells and is responsible for the transport of nutrients (Genovese, et al., 2023). In this way, deeper water can be evaporated more easily, thereby removing the latent heat and achieving rapid freezing.

Closely related to the freezing rate, carrot discs consistently performed worst in texture and mass loss under AF-20, either in small or large sizes. However, for AF-45, the change in size had a different result. Although the small carrot discs had good texture and low mass loss after AF-45, these quality characteristics deteriorated with size. When the latent and sensible heat to be transferred is increased (product in larger size), the time for the carrot discs under AF-45 to pass through the freezing critical zone is prolonged from 797 s to 1603 s on the basis of the same thermal conductivity. Freezing at -45 °C can't provide enough driving force for large size of carrot discs to achieve a high freezing efficiency. For this case, more intense freezing conditions are required to ensure a fast freezing rate and good final quality of food product, as performed under AF-80 (the greater temperature difference between the cooling medium and the product, the greater the driving force). With the fastest freezing rate during the temperature range of 2 to -6 °C, two sizes of carrot discs after VF+AF-20 both obtained relatively optimal values in texture and mass loss, which implied that

VF could be applied to the relatively large size of carrot discs to improve the final quality.

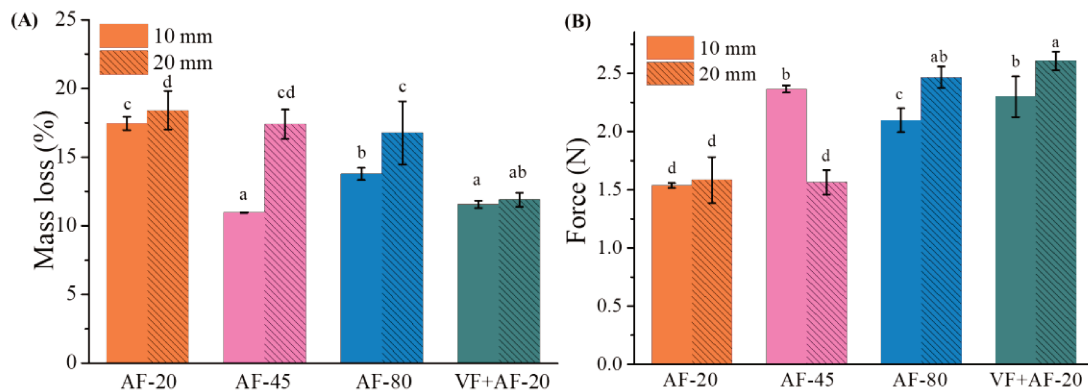


Fig. III. 5: (A) Mass loss (%), and (B) texture (N) for thawed carrot discs with thicknesses of 10 mm and 20 mm after AF-20, AF-45, AF-80, and VF+AF-20, respectively. Columns with different letters above indicate that the means are significantly different at $p < 0.05$.

4. Conclusion

The results presented in this study show that the application of VF in the temperature range covering the freezing critical zone can improve the quality attributes of thawed carrot discs, due to the reduced freezing damage during VF. The present study suggests that VF can achieve the same fast freezing speed as conventional freezing at $-80\text{ }^{\circ}\text{C}$ in the temperature range of 2 to $-6\text{ }^{\circ}\text{C}$. Although followed by AF-20 from -6 to $-20\text{ }^{\circ}\text{C}$, the texture of thawed carrot disc can be as good as fast freezing. The minimal mass loss and the homogenous microstructure verified that VF helped the formation of small and uniform ice crystals. More intense freezing conditions were proven to be required to maintain quality characteristics with increased sample size. Vacuum freezing has broad applicability, and its application can also obtain good texture and small mass loss in relatively large carrot discs, although this may also benefit from the special vascular system of carrot root. These results will provide evidence for the application of VF in reducing freezing damage and maintaining the quality of vegetable products in the food industry. Future research could include optimization of vacuum freezing conditions, such as the addition of external water, pressure reduction rate, and the application of pretreatment to enhance water evaporation.

- Ajani, C. K., Zhu, Z., & Sun, D. W. (2023). Shrinkage during vacuum cooling of porous foods: Conjugate mechanistic modelling and experimental validation. *Journal of Food Engineering*, 337, 111220.<https://doi.org/10.1016/j.jfoodeng.2022.111220>
- Ando, H., Kajiwara, K., Oshita, S., & Suzuki, T. (2012). The effect of osmotic dehydrofreezing on the role of the cell membrane in carrot texture softening after freeze-thawing. *Journal of Food Engineering*, 108(3), 473-479.<https://doi.org/10.1016/j.jfoodeng.2011.08.013>
- Ando, K., Arakawa, M., & Terasaki, A. (2018). Freezing of micrometer-sized liquid droplets of pure water evaporatively cooled in a vacuum. *Physical Chemistry Chemical Physics*, 20(45), 28435-28444.<https://doi.org/10.1039/C8CP05955A>
- Behnsilian, D., & Mayer-Miebach, E. (2017). Impact of blanching, freezing and frozen storage on the carotenoid profile of carrot slices (*Daucus carota* L. cv. Nutri Red). *Food Control*, 73, 761-767.<https://doi.org/10.1016/j.foodcont.2016.09.045>
- Ben Ammar, J., Lanoisellé, J.-L., Lebovka, N. I., Van Hecke, E., & Vorobiev, E. (2010). Effect of a pulsed electric field and osmotic treatment on freezing of potato tissue. *Food Biophysics*, 5, 247-254.<https://doi.org/10.1007/s11483-010-9167-y>
- Chen, X., Liu, H., Li, X., Wei, Y., & Li, J. (2022). Effect of ultrasonic-assisted immersion freezing and quick-freezing on quality of sea bass during frozen storage. *LWT*, 154, 112737.<https://doi.org/10.1016/j.lwt.2021.112737>
- Cheng, H. P., & Lin, C. T. (2007). The morphological visualization of the water in vacuum cooling and freezing process. *Journal of Food Engineering*, 78(2), 569-576.<https://doi.org/10.1016/j.jfoodeng.2005.10.025>
- Cogné, C., Nguyen, P. U., Lanoisellé, J. L., Van Hecke, E., & Clausse, D. (2013). Modeling heat and mass transfer during vacuum freezing of puree droplet. *International Journal of Refrigeration*, 36(4), 1319-1326.<https://doi.org/10.1016/j.ijrefrig.2013.02.003>
- Dalvi-Isfahan, M., Jha, P. K., Tavakoli, J., Daraei-Garmakhany, A., Xanthakis, E., & Le-Bail, A. (2019). Review on identification, underlying mechanisms and evaluation of freezing damage. *Journal of Food Engineering*, 255, 50-60.<https://doi.org/10.1016/j.jfoodeng.2019.03.011>
- Genovese, J., Stručić, M., Serša, I., Novickij, V., Rocculi, P., Miklavčič, D., Mahnič-Kalamiza, S., & Kranjc, M. (2023). PEF treatment effect on plant tissues of heterogeneous structure no longer an enigma: MRI insights beyond the naked eye. *Food Chemistry*, 405, 134892.<https://doi.org/10.1016/j.foodchem.2022.134892>
- Hajji, W., Gliguem, H., Bellagha, S., & Allaf, K. (2022). Structural and textural improvements of strawberry fruits by partial water removal prior to conventional freezing process. *Journal of Food Measurement and Characterization*, 16(5), 3344-3353.<https://doi.org/10.1007/s11694-022-01443-w>
- Heldman, D. R., Lund, D. B., & Sabliov, C. (2018). *Handbook of food engineering*: CRC press.
- Lebovka, N. I., Praporscic, I., & Vorobiev, E. (2004). Effect of moderate thermal and pulsed electric field treatments on textural properties of carrots, potatoes and apples. *Innovative Food Science & Emerging Technologies*, 5(1), 9-16.<https://doi.org/10.1016/j.ifset.2003.12.001>
- Li, D., Zhu, Z., & Sun, D.-W. (2018). Effects of freezing on cell structure of fresh cellular food materials: A review. *Trends in Food Science & Technology*, 75, 46-55.<https://doi.org/10.1016/j.tifs.2018.02.019>

- Muthukumarappan, K., Marella, C., & Sunkesula, V. (2019). Chapter 15 - Food Freezing Technology. In M. Kutz (Ed.), *Handbook of Farm, Dairy and Food Machinery Engineering (Third Edition)* (pp. 389-415): Academic Press.
- Oddone, I., Barresi, A. A., & Pisano, R. (2017). Influence of controlled ice nucleation on the freeze-drying of pharmaceutical products: the secondary drying step. *International Journal of Pharmaceutics*, 524(1), 134-140. <https://doi.org/10.1016/j.ijpharm.2017.03.077>
- Panayampadan, A. S., Shafiq Alam, M., Aslam, R., Kumar Gupta, S., & Kaur Sidhu, G. (2022). Effects of alternating magnetic field on freezing of minimally processed guava. *LWT*, 163, 113544. <https://doi.org/10.1016/j.lwt.2022.113544>
- Parniakov, O., Bals, O., Lebovka, N., & Vorobiev, E. (2016). Effects of pulsed electric fields assisted osmotic dehydration on freezing-thawing and texture of apple tissue. *Journal of Food Engineering*, 183, 32-38. <https://doi.org/10.1016/j.jfoodeng.2016.03.013>
- Perrin, F., Hartmann, L., Dubois-Laurent, C., Welsch, R., Huet, S., Hamama, L., Briard, M., Peltier, D., Gagné, S., & Geoffriau, E. (2017). Carotenoid gene expression explains the difference of carotenoid accumulation in carrot root tissues. *Planta*, 245(4), 737-747. <https://doi.org/10.1007/s00425-016-2637-9>
- Schudel, S., Prawiranto, K., & Defraeye, T. (2021). Comparison of freezing and convective dehydrofreezing of vegetables for reducing cell damage. *Journal of Food Engineering*, 293, 110376. <https://doi.org/10.1016/j.jfoodeng.2020.110376>
- Silva, A. C. C., & Schmidt, F. C. (2019). Vacuum Freezing of Coffee Extract Under Different Process Conditions. *Food and Bioprocess Technology*, 12(10), 1683-1695. <https://doi.org/10.1007/s11947-019-02314-x>
- Silva, A. C. C., & Schmidt, F. C. (2022). Intensification of freeze-drying rate of coffee extract by vacuum freezing. *Innovative Food Science & Emerging Technologies*, 78, 103022. <https://doi.org/10.1016/j.ifset.2022.103022>
- Stebel, M., Smolka, J., Palacz, M., Piechnik, E., Halski, M., Knap, M., Felis, E., Eikevik, T. M., Tolstorebrov, I., Peralta, J. M., & Zorrilla, S. E. (2021). Numerical modelling of the food freezing process in a quasi-hydrofluidisation system. *Innovative Food Science & Emerging Technologies*, 74, 102834. <https://doi.org/10.1016/j.ifset.2021.102834>
- Sun, D. (2011). Quality and safety of frozen foods. In *Handbook of Frozen Food Processing and Packaging (second ed.)*, CRC Press (pp. 303-456): Taylor & Francis.
- Tian, Y., Chen, Z., Zhu, Z., & Sun, D.-W. (2020). Effects of tissue pre-degassing followed by ultrasound-assisted freezing on freezing efficiency and quality attributes of radishes. *Ultrasonics Sonochemistry*, 67, 105162. <https://doi.org/10.1016/j.ultsonch.2020.105162>
- Van Buggenhout, S., Lille, M., Messagie, I., Loey, A. V., Autio, K., & Hendrickx, M. (2006). Impact of pretreatment and freezing conditions on the microstructure of frozen carrots: Quantification and relation to texture loss. *European Food Research and Technology*, 222(5), 543-553. <https://doi.org/10.1007/s00217-005-0135-6>
- Vicent, V., Ndoye, F.-T., Verboven, P., Nicolăi, B., & Alvarez, G. (2019). Effect of dynamic storage temperatures on the microstructure of frozen carrot imaged using X-ray micro-CT. *Journal of Food Engineering*, 246, 232-241. <https://doi.org/10.1016/j.jfoodeng.2018.11.015>

- Wang, H., Chen, S., Fu, Q., Wang, R., Zhang, W., Chen, L., & Wu, J. (2016). Effect of different pretreatments on the vacuum-freezing characteristics. *Modern food science and technology*, 32(11), 241-247. <https://doi.org/10.13982/j.mfst.1673-9078.2016.11.037>
- Wang, H., Fu, Q., Chen, S., Hu, Z., & Xie, H. (2018). Effect of hot-water blanching pretreatment on drying characteristics and product qualities for the novel integrated freeze-drying of apple slices. *J Journal of Food Quality*, 2018, 1-12. <https://doi.org/10.1155/2018/1347513>
- Wang, H., Xue, Y., Hu, Z., Ba, L., Shamim, S., Xie, H., Xia, T., & Zhao, R. (2022). Addition of external water improves the quality attributes of vacuum-frozen and thawed apple slices. *International Journal of Refrigeration*. <https://doi.org/10.1016/j.ijrefrig.2022.01.027>
- Wang, L., & Sun, D.-W. (2001). Rapid cooling of porous and moisture foods by using vacuum cooling technology. *Trends in Food Science & Technology*, 12(5), 174-184. [https://doi.org/10.1016/S0924-2244\(01\)00077-2](https://doi.org/10.1016/S0924-2244(01)00077-2)
- Wu, X., Wang, C., & Guo, Y. (2020). Effects of the high-pulsed electric field pretreatment on the mechanical properties of fruits and vegetables. *Journal of Food Engineering*, 274, 109837. <https://doi.org/10.1016/j.jfoodeng.2019.109837>
- Zhang, Z., Zhang, S., & Zhang, Y. (2016). Vacuum spray evaporate-freezing of nano-droplet. *Nanomedicine: Nanotechnology, Biology and Medicine*, 12(2), 572. <https://doi.org/10.1016/j.nano.2015.12.349>
- Zhu, Z., Geng, Y., & Sun, D.-W. (2021). Effects of Pressure Reduction Modes on Vacuum Cooling Efficiency and Quality Related Attributes of Different Parts of Pakchoi (*Brassica Chinensis* L.). *Postharvest Biology and Technology*, 173, 111409. <https://doi.org/10.1016/j.postharvbio.2020.111409>

III.2.2 Determination of the equivalent air freezing parameters of vacuum freezing

Currently, the common sample shapes used in heat and mass transfer models mainly include plate, cylinder, and sphere. But the prediction of the freezing time of the special shape of disc (diameter of 18 mm and thickness of 10 mm) under different air temperatures and air velocities in conventional air freezing are not available. In fact, most of the parameters in the Pham model can be obtained through known formulas and measurable data. However, the required convective transfer coefficient, h , which can be calculated based on thermal fluid dynamics, is usually easier to obtain for plates, cylinders, and spheres since they already have the relevant formulas for the $\overline{N_u}$ values in function of the Re . E.g., for the cylinder,

$$\overline{N_u} = 0.97 * R_e^{0.42} \quad (200 < Re < 2000) \quad (1)$$

$$\overline{N_u} = 0.21 * R_e^{0.62} \quad (2000 < Re < 20000) \quad (2)$$

Where the Nusselt number (Nu) is a dimensionless number, which is related to convective and conductive transfer. Reynolds number (Re) is a dimensionless number that can be used to characterize fluid flow.

III.2.2.1 Verification of the models in freezing experiments on samples of apple cylinders

Previously, as the relationship between Nu and Re values for cylinder was known, freezing time estimation experiments were conducted using apple cylinders (thickness 4.2cm, diameter 1.8cm) in the freezer. The air temperature was $-39\text{ }^\circ\text{C}$, and the air velocity was adjusted from 1m/s to 17.7m/s. The experimental freezing time for different conditions is recorded in [Table III. 4](#).

[Table III. 4](#): The experimental freezing time of apple cylinders with different air velocity. The calculated convective transfer coefficient with different air velocity.

Air velocity	Experimental freezing time t (17 to $-20\text{ }^\circ\text{C}$), s	Calculated convective transfer coefficient h , $\text{W}/\text{m}^2 \cdot ^\circ\text{C}$
V_0	2213	28.56
V_1	1245	44.31
V_2	673	90.80
V_3	530	122.00

With the experimental freezing time and some related parameters shown in [Table III. 5](#), h can be calculated by the Pham model mentioned in [I.1.4.3](#) as equation (3) and

shown in Table III. 4.

$$t = \frac{d_c}{E_f h} \left(\frac{\Delta H_1}{\Delta T_1} + \frac{\Delta H_2}{\Delta T_2} \right) \left(1 + \frac{N_{Bi}}{2} \right) \rightarrow h = \frac{d_c}{E_f \times \left(\frac{\Delta H_1 + \Delta H_2}{\Delta T_1 + \Delta T_2} - \frac{d_c^2}{2 \times k \times E_f} \right)} \quad (3)$$

Table III. 5: Summary of experimental parameters.

Definition	Notation	Calculation formula	Measured or calculated value
Characteristic dimension (in meters)	d_c		0.009 m (Here the radius of the cylinder with a diameter of 1.8cm)
Shape factor	E_f		2 for a cylinder
Sample diameter	D_{obstacle}		0.018 m
Final temperature at the center of the cylinder (°C)	T_c		-20 °C
Initial temperature at the center of the cylinder (°C)	T_i		17 °C
Temperature in the freezer (°C)	T_a		-39 °C
Average freezing temperature (according to model equation) (°C)	T_{fm}	$T_{fm} = 1.8 + 0.263 \times T_c + 0.105 \times T_a$	-7.55 °C
Temperature difference for the pre-cooling period (°C)	ΔT_1	$\Delta T_1 = (T_i + T_{fm})/2 - T_a$	43.73 °C
Temperature difference for phase change and post-cooling period (°C)	ΔT_2	$\Delta T_2 = T_{fm} - T_a$	31.45 °C
Average Biot Number	N_{Bi}	$N_{Bi} = h \times d_c / k$	0.575
Thermal conductivity of frozen product (W/(m·°C))	k	$1.7869 - 4.5215 \times 10^{-3} \times T_c + 7.7381 \times 10^{-5} \times T_c^2$	1.91 W/(m·°C)
Enthalpy difference for the precooling period (J/m ³)	ΔH_1	$\Delta H_1 = \rho_u \times C_{pu} \times (T_i - T_{fm})$	9.8×10^7 J/m ³
Enthalpy difference for phase change and post-cooling period (J/m ³)	ΔH_2	$\Delta H_2 = \rho_f [L_f + C_{pf} \times (T_{fm} - T_i)]$	2.8×10^8 J/m ³
The characteristic constants of the fluid (in this case air) were taken at film temperature: $T_f = (T_a + T_i)/2$ (K)			
Heat capacity of the fluid (air) (J/(K·kg))	C_p	$1.9324 \times 10^{-10} \times T^4 - 7.9999 \times 10^7 \times T^3 + 1.1407 \times 10^3 \times T^2 - 4.489 \times 10^{-1} \times T + 1.0575 \times 10^{-3}$	1004.7 J/(K·kg)
Thermal conductivity of the fluid (W/(m·°C))	k_{air}	$1.5207 \times 10^{-11} \times T^3 - 4.857 \times 10^{-8} \times T^2 + 1.0184 \times 10^{-4} \times T - 3.933 \times 10^{-4}$	0.023 (W/(m·°C))
Density of the fluid (kg/m ³)	ρ	Calculated from an online tool	1.318 kg/m ³
Fluid flow velocity (m/s)	U		Variable depending on the ventilation power chosen (from 1m/s to 17.7 m/s)
Dynamic viscosity of the fluid (Pa·s)	μ	$8.8848 \times 10^{-15} \times T^3 - 3.2398 \times 10^{-11} \times T^2 + 6.2657 \times 10^{-8} \times T + 2.3543 \times 10^{-6}$	1.67×10^{-5} Pa·s

According to the experimental convective transfer coefficient h under different air velocities, \overline{Nu} can be calculated as follows,

$$\overline{Nu} = \frac{\overline{h} \times D_{obstacle}}{k} \quad (4)$$

Where k is the thermal conductivity of the fluid, air in this case. $D_{obstacle}$ is the characteristic dimension. While Re can be calculated as follows,

$$Re = \frac{\rho_{fluid} \times U_{fluid} \times D_{obstacle}}{\mu_{fluid}} \quad (5)$$

Where ρ_{fluid} , U_{fluid} and μ_{fluid} is the density (kg/m^3), the velocity (m/s), and the dynamic viscosity of the air ($\text{Pa}\cdot\text{s}$ or $\text{N}\cdot\text{s/m}^2$ or $\text{kg}/(\text{m}\cdot\text{s})$) of the air, respectively.

Table III. 6: Calculation of Reynolds and Nusselt numbers: Establishment of a correlation.

Experimental values					Calculated values			
					Re (200-2000)		Re (2000-20000)	
	Nu (Eq.4)	ln(Nu)	Re (Eq.5)	ln(Re)	Nu (Eq. 1)	ln(Nu)	Nu (Eq. 2)	ln(Nu)
V₀	22.03	3.09	1420.2	7.26	20.45	3.02		
V₁	34.37	3.54	3138.76	8.05			30.92	3.43
V₂	70.28	4.25	10640.2	9.27			61.96	4.13
V₃	94.49	4.55	17743.7	9.78			85.04	4.44

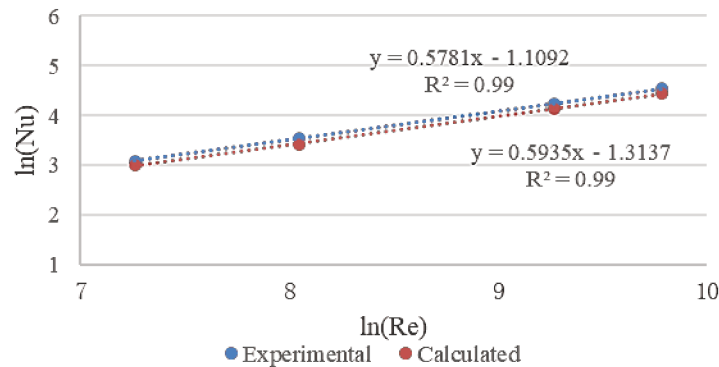


Fig. III. 6: Correlation plot between Reynolds number and Nusselt number

The experimental correlation deduced from the different freezing times is: $\ln(Nu) = 0.5781\ln(Re) - 1.1092 \rightarrow Nu = 0.33 \times Re^{0.58}$, which is very close to the value calculated by the existing combination of equations 1 and 2 (calculated dotted line in Fig. III. 6). Through the experimental validation of the apple cylinder, we considered that it might be possible to speculate on the correlation between Nu and Re for samples of other shapes in this way: $t \rightarrow h \rightarrow Nu \sim Re$.

III.2.2.2 Establishment of correlation of Nu and Re values for special disc-shaped carrots

In order to obtain the corresponding formula for the discs to be applied in the prediction of the freezing time of carrots, several air freezing experiments were carried out under a fixed temperature range (2 to -20 °C) and a specific air temperature (for example -45 °C). By changing the air velocity (0.5, 2.2, 7.5, 12.5 m/s), the experimental freezing times can be recorded and thus calculate the corresponding convective transfer coefficient h by the above-mentioned equation (3),

In our case of the carrot disc, d_c (m) is the characteristic dimension (the smallest distance from the center, 0.005 m), E_f is the shape factor (1.8 in this case), t (s) is the experimental freezing time, ΔH (Jm^{-3}) is the change in enthalpy with subscripts 1 for precooling unfrozen food and 2 for phase change and cooling of frozen food obtained from equations in Fig. I. 8, ΔT (°C) represent the temperature gradients shown in Fig. I. 8. In these equations, ρ (kg/m^3) is the density of the carrot disc, C_p ($\text{Jkg}^{-1}\text{K}^{-1}$) is the heat capacity of the carrot disc. Their subscripts u and f represent the unfrozen and frozen states, respectively. T_i (°C) is the initial temperature (2 °C) and T_{fm} is the mean freezing temperature of the carrot disc. T_c (°C) is the final temperature at the center of the carrot disc (-6 °C). T_a (°C) is the temperature of the freezing medium (-45 °C). Through the existing calculation formulas and the composition of carrots in Table III. 7, we can get some calculation parameters of carrots at 2 °C and -6 °C shown in Table III. 8.

Table III. 7: Carrot composition and content.

Water	Protein	Carbohydrates (starch)	Lipid	Ash(K)
88.29%	0.93%	9.58%	0.24%	0.97%

Table III. 8: Process parameters for the calculation.

2 (°C)	C_{pu} ($\text{J/kg}\cdot\text{°C}$)	3869.9
	ρ_u (kg/m^3)	1042.8
	k_u ($\text{W}/(\text{m}\cdot\text{°C})$)	0.53
-6 (°C)	C_{pf} ($\text{J/kg}\cdot\text{°C}$)	2344.7
	ρ_f (kg/m^3)	980.2
	k_f ($\text{W}/(\text{m}\cdot\text{°C})$)	1.72

According to the experimental convective transfer coefficient h under different air velocities, \overline{N}_u can be calculated by equation (4), and Re can be calculated by equation

(5).

Finally, \overline{N}_u and Re values corresponding to four different air velocities as well as $\ln(\overline{N}_u)$ and $\ln(\text{Re})$ were obtained (Table III. 9) and the fitted relationship between $\ln(\overline{N}_u)$ and $\ln(\text{Re})$ can also be obtained and shown in Fig. III. 7.

Table III. 9: The experimental freezing time from 2 to -6 °C, and the corresponding convective transfer coefficient h, \overline{N}_u , $\ln(\overline{N}_u)$, Re, and $\ln(\text{Re})$ with the air velocity.

U_{air} (m/s)	t_f (experimental) from 2 to -6 °C, min	h, W/m ² .°C	\overline{N}_u	$\ln(\overline{N}_u)$	Re	$\ln(\text{Re})$
0.5	14.42	22.63	10.05	2.31	468.87	6.15
2.2	12.83	25.53	11.34	2.43	2063.03	7.63
7.5	2.83	133.06	59.08	4.08	7033.05	8.86
12.5	2.17	185.02	82.15	4.41	11721.75	9.37

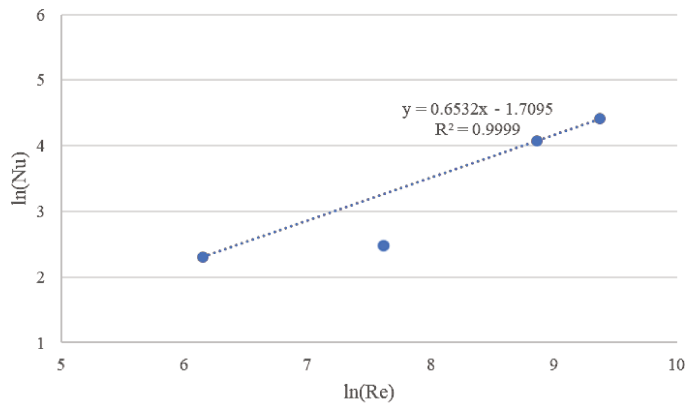


Fig. III. 7: The calculated $\ln(\overline{N}_u)$ values with $\ln(\text{Re})$ under different air velocities. The blue dotted line in the figure represents the fitted curve.

With this fitted equation $\ln(\overline{N}_u)=0.6532\ln(\text{Re})-1.7095 \rightarrow \overline{N}_u = 0.181 R_e^{0.6532}$, when the air temperature and air velocity are known, after the calculation of Re, \overline{N}_u , h, as well as the predicted t_f can also be calculated step by step. The predicted freezing time from 2 to -6 °C with the air temperature and air velocity are shown in Fig. III. 8. Several experiments were carried out to verify this calculation under different conditions, i.e. orange circles in Fig. III. 8. These experimental freezing times showed very close agreement with the predicted results. For the experimental freezing time of vacuum freezing of about 427 s, i.e., 7.12 min, the equivalent parameters in conventional air freezing can be for example $T_{\text{air}}=-35$ °C and $V_{\text{air}}=2.2\text{m/s}$ or $T_{\text{air}}=-80$ °C $V_{\text{air}}=0.5\text{m/s}$, and that parameter at -80°C (423 s, 7.05 min) has been verified in

previous experiments. This means that with a low air velocity of 0.5 m/s, the air temperature has to drop to as low as -80 °C to achieve the same freezing time as in vacuum freezing. For higher air temperatures such as -20 °C, considerably higher air velocities are required to achieve the short freezing time in vacuum freezing. For example, at -20 °C, an air velocity of 2.2 m/s is not sufficient.

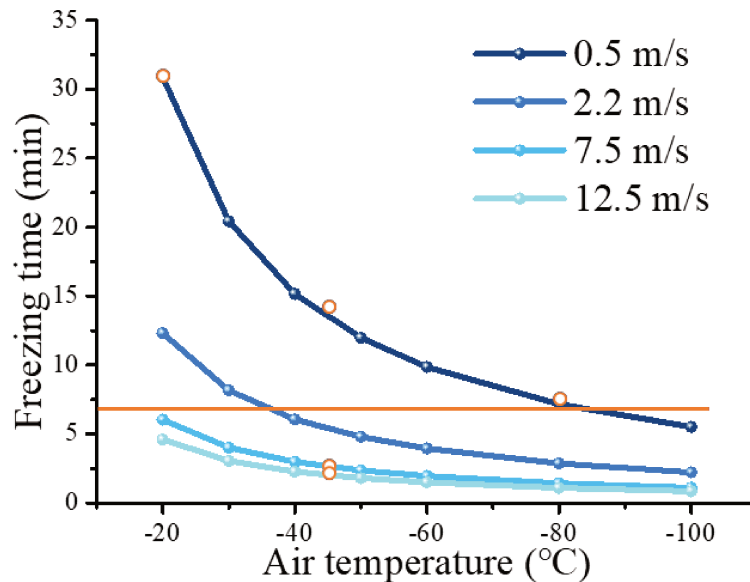


Fig. III. 8: The effects of air temperature and air velocity on the predicted freezing time of carrot disc from 2 to -6 °C. The small orange circles represent the freezing times for several experiments under different conditions, including air freezing at -20, -45, and -80 °C with constant air velocities of 0.5m/s, and air velocities of 0.5, 7.5, and 12.5m/s with constant air temperature of -45 °C, respectively. The orange straight line represents the freezing time of 7.12 minutes for the carrot disc from 2 to -6 °C in vacuum freezing.

III.3 Chapter conclusion

The results presented in this chapter indicate that the textural property is more affected by the freezing rate in the freezing critical zone. Therefore, the application of VF in the temperature range covering the freezing critical zone can effectively improve the quality attributes of thawed carrot discs, due to the same fast freezing rate as conventional air freezing at -80 °C in the temperature range of 2 to -6 °C. This means we don't have to use strong freezing conditions for the entire freezing process. Even followed by slow freezing as AF-20 from -6 to -20 °C, the texture of thawed carrot disc can be as good as fast freezing. The minimal mass loss and the

homogenous microstructure verified that VF helped the formation of small and uniform ice crystals. More intense freezing conditions were proven to be required to maintain quality characteristics with increased sample size. Vacuum freezing has broad applicability, and its application can also obtain good texture and small mass loss in relatively large carrot discs. These results will provide evidence for the application of VF in reducing freezing damage and maintaining the quality of vegetable products in the food industry.

In the comparison between VF and AF, the relationship between the \overline{N}_u value and Re was developed for the specific carrot disc shape. When the air temperature and air velocity are known, the freezing time of the carrot discs in conventional air freezing can be easily predicted to quickly find equivalent parameters compared to VF and also other freezing methods.

Chapter IV Pulsed electric field assisted combined freezing of carrot tissue: Preliminary vacuum freezing followed by supplementary conventional freezing

IV.1 Chapter introduction

Chapter III has studied the effect of vacuum freezing on the quality attributes of thawed carrot discs. The result showed that the application of vacuum freezing in the temperature range covering the freezing critical zone achieved fast freezing rate as for air freezing at -80 °C. Interestingly, this process was completed at temperature above zero with negligible moisture loss. Even for relatively large size of samples, this method can still effectively improve the quality of thawed carrot discs compared to conventional air freezing. All these proved that vacuum freezing is a very promising method of rapid freezing.

Pulsed electric field (PEF), as a pretreatment of conventional freezing, has been demonstrated to be able to intensify the freezing kinetics, which has a positive effect on the formation of small ice crystals and the reduction of freezing damage in fruits and vegetables. Theoretically, PEF pretreatment can also increase the evaporation of water during the vacuum freezing through the electroporation on the cellular membrane, thus accelerating the freezing process. However, there are currently no relevant studies. The aim of this chapter is to investigate the effect of PEF pretreatment on vacuum freezing and the final quality of the thawed carrot discs.

IV.2 Results

The article is presented on the following page.

Pulsed electric field assisted combined freezing of carrot tissue: Preliminary vacuum freezing followed by supplementary conventional freezing

Yuqi Huang^{1*}, Olivier Bals¹, Nikolai Lebovka², Eugène Vorobiev¹

¹*Université de Technologie de Compiègne, ESCOM, TIMR (Integrated Transformations of Renewable Matter), Centre de Recherche Royallieu, CEDEX CS 60319, 60203 Compiègne, France*

²*Institute of Biocolloidal Chemistry named after F. D. Ovcharenko, NAS of Ukraine, 42, blvr. Vernadskogo, Kyiv 03142, Ukraine*

Abstract

Pulsed electric field (PEF) assisted combined mode of freezing with the preliminary vacuum freezing (VF) down to -6 °C followed by conventional air freezing (AF) in the freezer at -20 °C has been studied. The fresh carrot tissue was electroporated to different levels of cell disintegration index $Z=0-0.9$ ($E=0-400$ V/cm, $t_{PEF}=0-1$ s). It was demonstrated that PEF significantly accelerated the kinetics of AF and impacted the texture, moisture losses, and microstructure of thawed carrots. For example, at high disintegration index ($Z=0.9$) the total freezing time was shortened by ≈ 1.21 times for the AF procedure and by ≈ 1.57 times for the combined VF+AF procedure. The softening of textures of carrots was observed, however, for both AF and VF+AF procedures, they were comparable. Application of both AF and VF+AF procedures resulted in the increase of the size of pores inside the carrot tissues. However, the water losses for the combined VF+AF protocol were significantly smaller than those for the AF protocol.

Keywords: Conventional air freezing; Vacuum freezing; Pulsed electric fields; Combined freezing protocol; Textural property; Carrot

1. Introduction

Carrot (*Daucus carota* L.) is one of the most consumed root vegetables and major food crops worldwide. It includes many useful phytochemicals (carotenoids, lycopene, lutein, and vitamins). Carrots have a relatively complex structure (with cortex, core regions and xylem, phloem vascular tissue systems). It has a rich chemical

composition including 86–89% water, ≈10% carbohydrates, 3% of crude fibers, 1.1% total ash, and numerous minerals (Sharma, Karki, Thakur, & Attri, 2012). Crude fiber includes 50–92% cellulose and hemicellulose, ≈4% lignin, ≈0.9% proteins, and ≈0.2% fat. Also, carrot is an important source of phytonutrients including carotenoids (0.6-5.48 %). Note that for the preservation and waste limitation of carrots, freeze-processing is widely used (Behsnilian & Mayer-Miebach, 2017). However, improper freezing methods can result in structural damage to vegetable tissues and undesirable quality deterioration of the final product after thawing (Schudel, Prawiranto, & Defraeye, 2021). Thus, it is of great significance to investigate the impacts of innovative pretreatment and freezing conditions on the quality of thawed products to meet consumers' requirements for frozen foods in terms of sensory, nutritional, and other aspects.

Typically, application of the rapid or cryogenic freezing mode allowed reducing the texture losses of frozen samples, compared to the slowly frozen samples. As a rapid freezing approach, vacuum freezing (VF) has shown great potential in the frozen food industry. Significant intensification of freeze-drying rate by VF has been recently reported (Silva & Schmidt, 2022). The VF allowed reducing the initial moisture in the freezing stage and the amount of water to be removed in the subsequent sublimation and desorption stages. Although this process is quite fast, the cooling and crystallization effects during this process are dependent on the removal of water from the sample. Hence, a large temperature reduction by VF comes at the expense of a large amount of water loss, which is not desirable for frozen products. Recently, our study has shown that using VF in a specific temperature range, supplemented by conventional air freezing, can improve the quality of thawed carrot slices (Huang & Bals, 2024). Compared to conventional air freezing at -20 °C, carrot discs subjected to the freezing procedure of VF + AF contributed to a comparable texture to that of fast freezing (air freezing at -80 °C), minimal mass loss, as well as reduced microstructure destruction.

The minimization of carrot tissue damage could also be achieved by the application of certain pretreatments (e.g., the combined use of blanching and vacuum impregnation) (Santarelli et al. 2021). For VF, except for process conditions (pressure reduction, addition of external water), pretreatment (ultrasound) was proved to affect the product characteristics (H. Wang et al. 2016, 2022).

Nowadays electro-based technologies and particularly, pulsed electric fields (PEF) are widely used for the modification of microstructure, textural properties, quality attributes of different tissues, and for the assistance in the intensification of various processes (e.g., drying, freezing, frying, extraction, etc.) (Shams, et al., 2024; Vorobiev & Lebovka, 2020). In general, such pretreatment leads to reduced time and energy demands. It was approved that the PEF technologies are economical, environmentally friendly, and can be up-scaled for different industrial applications. In freezing processing (conventional air freezing (AF), vacuum freeze-drying (VFD), osmotic dehydro-freezing (ODF)), the application of PEF pretreatment can positively affect the super-cooling of water without negative impacts on color, taste, and texture of food samples (Ben Ammar, Lanoisellé, Lebovka, Van Hecke, & Vorobiev, 2011; Muthukumarappan, Marella, & Sunkesula, 2019). It was found that the impact of the PEF treatment prior to immersion freezing caused the total freezing time to decrease by 31.7 % maximally compared to the PEF-untreated tissue (Wiktor, Schulz, Voigt, Knorr, & Witrowa-Rajchert, 2015). Besides, there were variants of PEF pretreatment that reduced drip loss by 14%–28% in comparison to untreated frozen-thawed samples. PEF pretreatment noticeably improved the rate of freeze-drying for different vegetable products (potatoes, green beans, spinaches, onions) (Ben Ammar, et al., 2011). For potatoes, the impacts of PEF and vacuum drying (VD) on freeze-thawing (FT) and freeze-drying (FD) processes were tested (Liu, Grimi, Bals, Lebovka, & Vorobiev, 2021; Liu, Grimi, Lebovka, & Vorobiev, 2018). PEF treatment accelerated the FD and affected the final level of dehydration after prolonged FD for 24 h. The application of VD combined with FD facilitated the rehydration of deeply dried potato tissue. The combined procedure with VF followed by AF (VF+AF procedure) assisted by PEF pretreatment was never discussed previously. The application of this procedure could give a new possibility of fine regulation of quality attributes of thawed food products (e.g., appearance, texture, flavor and nutritional content).

The goals of this study were to investigate the effects of PEF pretreatment on the different freezing modes (continuous VF, AF, and combined freezing) and the quality characteristics of thawed carrots. The combined mode of freezing includes the preliminary VF followed by AF. Before freezing, the fresh carrot tissue was electroporated to different levels of cell disintegration. The impacts of the combined

mode of freezing and PEF application on the texture, moisture losses, and microstructure of thawed carrots were also discussed.

2. Materials and methods

2.1. Sample preparation

Carrot roots (*Daucus carota* L.) were obtained from a local market (Compiègne, France) and stored in darkness at 6 °C until analysis. The wet-base moisture content of carrot samples ($\approx 88\text{-}91\%$) was detected by MA160 infrared moisture analyzer (Sartorius, Germany). The carrot disc-shaped samples (18 mm in diameter and 10 mm in thickness) were prepared by using the special cylindrical knife. Samples were taken from the medium part of the carrots with 3 cm removed from the head and tail. The initial mass of carrot discs was $m \approx 2.60 \pm 0.10$ g.

2.2. Experimental procedures

Fig. IV. 1 shows the applied experimental procedures. They include the initial treatment of carrot discs by the PEF followed by different protocols (P₀-P₃) and sample characterization.

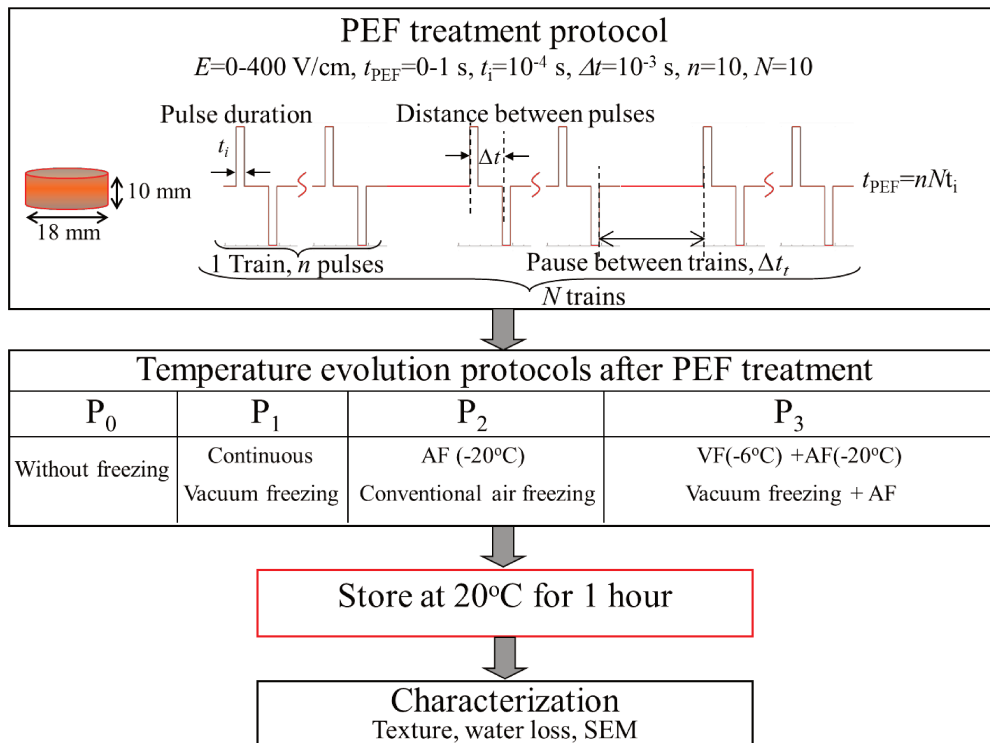


Fig. IV. 1: Description of the applied experimental procedures. They include the PEF treatment, application of different protocols (P₀-P₃), and sample characterization.

2.2. 1. PEF treatment

PEF treatment was done using the PEF generator (5 kV–1 kA, Hazemeyer, Saint-Quentin, France). The applied treatment protocol included application of pulses with the duration of $t_i = 100 \mu\text{s}$, and the time interval between two pulses $\Delta t = 10^{-3} \text{ s}$. The pulses were grouped into N trains, and each train consisted of $n = 10$ pulses. The relatively long pause was applied between the trains ($\Delta t_t = 5 \text{ s}$) in order to maintain the temperature inside of sample nearly constant, $T = 25^\circ\text{C}$. The total duration of PEF treatment was evaluated as $t_{\text{PEF}} = n \times N \times t_i$, and it was varied within 0-1s. The electric field strength was varied in the range of 0-400 V/cm. All treatment data were controlled using the Agilent VEE-PRO version 8.5 software (Agilent, Santa Clara, United States).

The PEF induced cell disintegration index Z was estimated as (Vorobiev, et al., 2020):

$$Z = \frac{\sigma - \sigma_i}{\sigma_d - \sigma_i} \quad (1)$$

where σ is the electrical conductivity of a sample, and the subscripts i and d represent the conductivity value of initial (fresh sample) $Z=0$ and completely damaged tissue $Z=1$, respectively.

The maximal tissue damage degree ($Z = 1$) was obtained at the strong PEF treatment of sample tissue (at $E = 2000 \text{ V/cm}$) during time (until the electrical conductivity of a sample σ became constant).

2.2.2. Freezing protocols (P₁-P₃)

Applied freezing protocols include continuous vacuum freezing (protocol P₁), conventional air freezing (AF) in ventilated ultra-low-temperature freezer MDF-U2086S (Sanyo, Gunma, Japan) operated at $-20 \text{ }^\circ\text{C}$ (protocol P₂), and combined freezing using preliminary vacuum freezing (VF) up to T_v followed by supplementary conventional air freezing (AF) in the freezer at $-20 \text{ }^\circ\text{C}$ (protocol P₃). The starting temperature for all freezing protocols was always set at the same temperature ($2 \text{ }^\circ\text{C}$) to minimize the moisture losses before starting of freezing. The value $T_v = -6 \text{ }^\circ\text{C}$ was selected on the base of preliminary VF experiments. Obtained data were compared with those for samples without freezing (protocol P₀) (Fig. IV. 1).

Protocol P₁ (continuous vacuum freezing) was realized at the pressure $P=5.6$ Pa corresponding to the value measured at in an empty chamber. The T-type thermocouple (with a diameter of 0.5 mm, an accuracy of ± 0.1 °C, TC, Ltd., Dardilly, France) was inserted in the geometrical centre of a sample. The thermocouple was hermetically connected in the middle of the stopper of the vacuum chamber (a Buchner flask with a capacity of 100 mL). The vacuum chamber was placed in the ice-water bath (0 ± 0.1 °C) to maintain a stable environmental temperature.

The laboratory vacuum freezing system (Fig. II. 2B) includes a vacuum pump RV8 (Edwards, Sweden), a PB 101 vacuum manometer (Alcatel, France), and a switching valve. The test was carried out as long as possible until the minimum temperature. The pressure evolution during vacuum freezing process was recorded in continuous mode.

Protocol P₂ (conventional air freezing, AF (-20 °C)) was performed in the freezer at -20 °C for the whole procedure (Fig. II. 6). Protocol P₃ (VF(-6°C)+AF(-20°C)) was realized in the combined mode of freezing. The preliminary vacuum freezing (VF) was performed in the same laboratory vacuum freezing system mentioned in P₁. When the temperature of the sample reached some predefined level $T_v(=-6^\circ\text{C})$ the sample was rapidly transferred to the freezer at -20 °C to complete the supplementary freezing procedure (AF). The temperature was registered in continuous mode.

2.3. Characterization techniques

After application of the experimental treatment procedures (Fig. IV. 1) the samples were stored at 20 °C for 1 hour. Then force relaxation test, measurements of mass losses, and microstructure changes in carrot tissue using the scanning electron microscopy (SEM) techniques were realized.

2.3.1. Force relaxation tests

A texture analyzer TA-XT plus (Rhéo, Champlan, France) with 36 mm diameter compression platen was used to perform the non-destructive force relaxation tests. In these tests the preliminary compressing with the constant speed 1.0 mm/s was applied. The compression was stopped at the force level of $F=5$ N and then the force temporary decaying curve $F(t)$ was measured. The previously obtained data for different food tissues (apple, potato, carrot, etc.) evidenced that both PEF-treatment

and freeze-thawing can accelerate the force relaxation (De Vito, Ferrari, I. Lebovka, V. Shynkaryk, & Vorobiev, 2008; Parniakov, Bals, Lebovka, & Vorobiev, 2016a). The relative texture index was defined as F^*

$$F^* = F/F_f \quad (2)$$

where F is the force measured at $t=50$ s, and F_f refers the value for fresh tissue.

2.3.2. Moisture loss

After freezing experiments, the samples were stored for one hour at 20°C, then moisture at their surface was removed using the filter paper. The water loss was calculated as (Ajani, Zhu, & Sun, 2023):

$$W_L(\%) = (1-m/m_o) \times 100 \quad (3)$$

where m_o and m are the initial and final masses of the carrot disc.

2.3.3. Scanning electron microscopy (SEM)

Cross sectional slices of carrot disc samples (fresh samples, samples after PEF treatments, and thawed samples after different freezing protocols) were analysed using the Quanta 250 FEG SEM equipment (FEI, Oregon, USA) in the mode of Low Vac (≈ 133.32 Pa) and an accelerating voltage of 20 kV.

2.4. Statistical analysis

All experiments and measurements of sample characteristics were repeated at least, three times. Significant differences at 95% confidence were evaluated by one-way analysis of variance (ANOVA), using SPSS 25.0. The figures were drawn with Origin Pro 8.5, and the error bars inside correspond to the standard deviations (SD).

3. Results and discussion

Figure IV. 2 presents the typical dependences of cell disintegration index Z versus PEF treatment time t_{PEF} (a) and versus electric strength E , at the fixed values of $t_{PEF}=0.01$ s or $t_{PEF}=0.1$ s(b). For the relatively low electric field strength of $E=100$ V/cm the value of Z increased slowly with increasing of t_{PEF} , and the PEF induced cell disintegration was not significant even for the prolonged PEF treatment, e.g. $Z \approx 0.37$ at $t_{PEF}=1$ s.

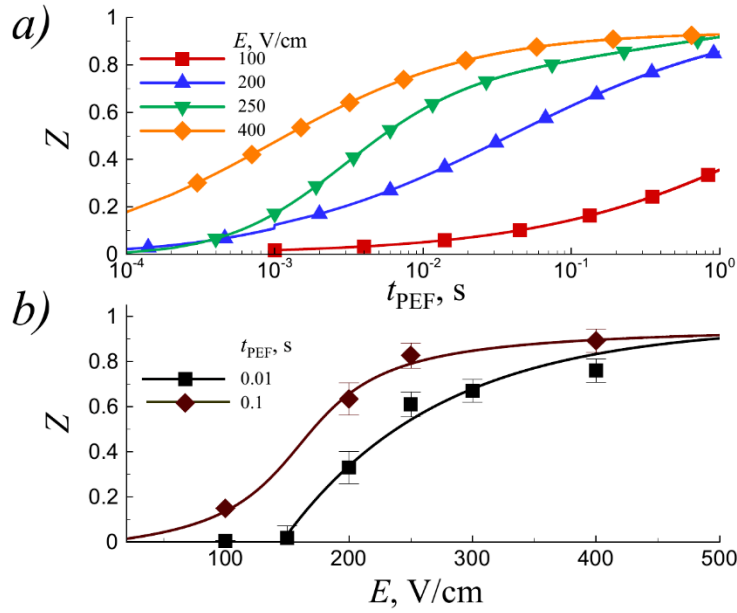


Fig. IV. 2: Examples of cell disintegration index Z versus PEF treatment time t_{PEF} (a, $E=100-400$ V/cm) and versus electric field strength E (b, $t_{PEF}=0.01$ s and $t_{PEF}=0.1$ s) dependencies. The lines are drawn for the convenience of the eye.

However, for the higher electric field strength more significant PEF induced cell disintegration was observed. For example, at $t_{PEF}=0.1$ s the values of cell disintegration index were $Z \approx 0.15$ at $E=100$ V/cm (low level of cell disintegration) and $Z \approx 0.90$ at $E=400$ V/cm (high level of cell disintegration). For comparison of temperature evolution protocols (Fig. IV. 1) the samples with cell disintegration indexes $Z=0$, $Z=0.15$, and $Z=0.9$ were used. Note that in previous work the PEF treatment of ‘Jereda’ variety of carrots (Czech University of Life Sciences, Prague) by one pulse with a duration of 0.01 s and $E=483$ V/cm resulted in a significantly smaller value of $Z \approx 0.2$ (Blahovec, Kouřim, & Lebovka, 2021) as compared with $Z \approx 0.7$ (at 0.01 s and $E=400$ V/cm, Fig. IV. 2). It can be explained by the significant differences in structure of carrot tissues for different varieties and protocols applied for the PEF treatment.

Figure IV. 3 presents typical freezing curves $T(t)$ obtained for the continuous vacuum freezing (Protocol P₁) at different values of cell disintegration index Z . Such curves are typical for the processing of PEF treated tissues (Parniakov, Bals, Lebovka, & Vorobiev, 2016b). In general, the different stages have been observed during continuous vacuum freezing. At the initial period of vacuum cooling (several minutes) the pressure drop causes the fast decrease of the temperature below ≈ 0 °C and initiates

the freezing. Initially, the period of “thermal arrest” characterized by slowing down of the temperature decrease was typically observed. During this period the differences in freezing curves $T(t)$ for the untreated and PEF treated samples were insignificant. Then, after the freezing of some quantity of water at $t > 120$ s the temperature began to fall rapidly. During this process, it can be observed that as Z increased, the temperature curve decreased faster. This may imply that the evaporation of water in the sample, on which the temperature reduction depends, is accelerated.

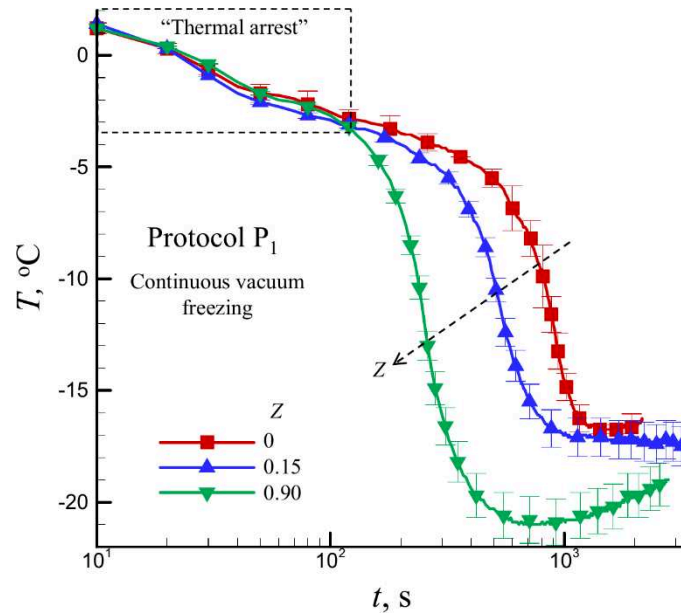


Fig. IV. 3: Freezing curves $T(t)$ for the continuous vacuum freezing (Protocol P₁) at the different values of cell disintegration index Z . The lines are drawn for the convenience of the eye.

In fact, the temperature we recorded was the temperature at the geometric center of the sample. In theory, the temperature distribution in the sample is not uniform during the freezing process (Deck, Košir, & Mazzotti, 2024). Normally, the decrease in temperature during the vacuum cooling or vacuum freezing was more relevant close to the surface of the sample where evaporation occurred (Pisano & Capozzi, 2017; Wang, Kan, Mao, Huang, & Li, 2021). That greatly influences the evolution of the temperature of the sample. In our additional tests, we also found that compared to the temperature at the center of the carrot disc, the temperature at a distance of 1mm from the longitudinal surface of the carrot disc decreased faster.

The temperature reached some minimal value T_m at $t > 700$ s and then it began to increase. This corresponds to the reduction of the remaining unfrozen water and the formation of surface ice layer, which both decreased the subsequent water evaporation.

In addition, although the chamber was set in an ice water bath, it is undoubtedly a kind of heating compared to the sample temperature of lower than $-15\text{ }^{\circ}\text{C}$. The most significant effects (faster freezing and lower minimal temperature) were observed for the strongly PEF disintegrated tissue ($Z=0.9$, Fig. 4).

Figure IV. 4 presents more details on changes of pressure P inside the vacuum chamber and temperature T inside the geometrical centre of sample at the initial stage of vacuum freezing. The data are presented as $P(T)$ and $t(T)$ dependencies (here t is the time) at different values of Z . From such presentation it can be clearly seen that the values of P abruptly decreased during the initial several seconds from the atmospheric level ($P_a \approx 1.013 \times 10^5\text{ Pa}$) up to 200-250 Pa (see inset to Fig. IV. 4) and finally they became nearly constant at $T \geq -6\text{ }^{\circ}\text{C}$.

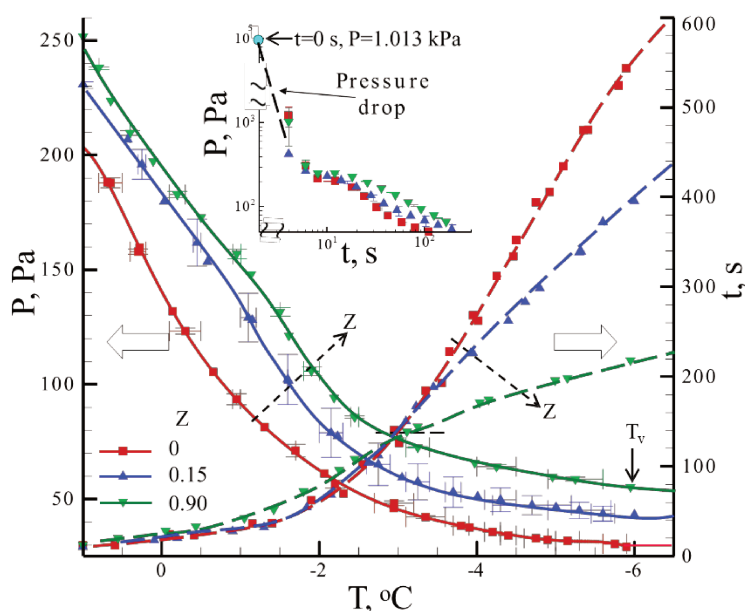


Fig. IV. 4: Pressure P inside the vacuum chamber and time of the vacuum-freezing t versus the temperature T inside the geometrical centre of the carrot disk for different values of cell disintegration index Z . Here $T_v = -6\text{ }^{\circ}\text{C}$ is the predefined level for preliminary vacuum freezing (VF). At the initial stage ($t \rightarrow 0$), the pressure dropped very rapidly from the atmospheric pressure (101.325 kPa) (inset).

The lines are drawn for the convenience of the eye.

The value of P at $T \approx -6\text{ }^{\circ}\text{C}$ increased with increasing of Z (for example, at $T \approx -6\text{ }^{\circ}\text{C}$ we have $P \approx 29\text{ Pa}$ at $Z=0$, $P \approx 44\text{ Pa}$ at $Z=0.15$, and $P \approx 54\text{ Pa}$ at $Z=0.9$). The leveling of pressure at $T_v \approx -6\text{ }^{\circ}\text{C}$ indicates that further vacuum-freezing under the low pressure is inefficient and energy consuming. This leveling reflects formation of the equilibrium

state for water evacuation from the sample. Therefore, in the combined protocol P_3 , the predefined level $T_v = -6\text{ }^\circ\text{C}$ was always applied. It is interesting that the time required to reach the temperature $T = -4\text{ }^\circ\text{C}$ was $t \approx 130\text{ s}$ and nearly independent on the value of Z . However, for the temperature $T_v = -6\text{ }^\circ\text{C}$ this time decreased significantly with increasing Z .

Figure IV. 5 shows the examples of the freezing curves $T(t)$ for the combined protocol with preliminary vacuum freezing up to $T_v = -6\text{ }^\circ\text{C}$ followed by the conventional air freezing in the freezing chamber (Protocol P_3 , VF(-6°C)+AF(-20°C)) at the different values of cell disintegration index Z . For the combined protocol the total freezing time t_f was greatly affected by the value of Z (see inset to Fig. IV. 5). The similar the freezing curves $T(t)$ were also observed for conventional freezing protocol P_2 (AF). These data were used to compare the effect of PEF treatment on freezing at different protocols.

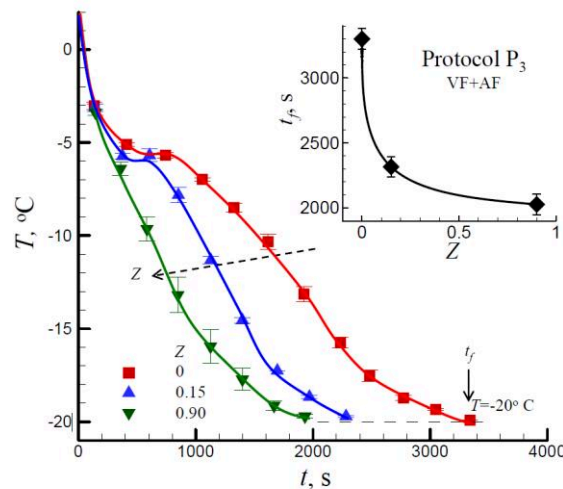


Fig. IV. 5: Examples of the freezing curves $T(t)$ for the combined protocol with preliminary vacuum freezing up to $T_v = -6\text{ }^\circ\text{C}$ followed by the conventional air freezing in the freezing chamber (Protocol P_3 , VF(-6°C)+AF(-20°C)) at the different values of cell disintegration index Z . Here, t_f is the total freezing time required to reach the temperature $-20\text{ }^\circ\text{C}$. Inset shows t_f versus Z dependence. The lines are drawn for the convenience of the eye.

Figure IV. 6 compares the total freezing time t_f for the protocols P_2 (conventional air freezing, AF(-20°C)) and combined protocol P_3 (with the preliminary vacuum freezing followed by the conventional air freezing, VF(-6 °C)+AF(-20 °C)). The increasing in Z values resulted in decreasing of t_f for both the P_2 and P_3 protocols.

Moreover, for the same Z the values of t_f significantly decreased with application of the combined protocol P_3 (Fig. IV. 6). The similar effect of noticeable decrease of the freezing time t_f was previously reported for the impact of PEF pre-treatment on the air-blast freezing of potato tissue (Jalté, Lanoisellé, Lebovka, & Vorobiev, 2009). The promotion of crystallization and reduction of freezing time by application of PEF treatment was also reported for different vegetable tissues, e.g. for leafy vegetables (spinach), tuber (potato), and vegetable-stem (green beans) (J Ben Ammar, Van Hecke, Lebovka, Vorobiev, & Lanoisellé, 2011; Jihène Ben Ammar, Van Hecke, Vorobiev, Lanoisellé, & Lebovka, 2009). Also, it can be observed that the decrease on the total freezing time t_f caused by PEF pretreatment of P_3 was more than that of P_2 , which mainly comes from the temperature range of 2 to -6 °C. This may be due to the greater enhancement of PEF pretreatment on the mass transfer of water evaporation during vacuum freezing. For conventional freezing that relies solely on heat conduction, the acceleration of heat transfer caused by PEF pretreatment was limited.

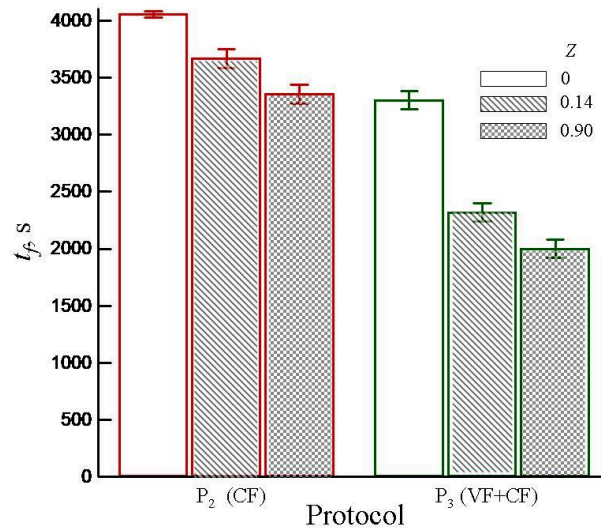


Fig. IV. 6: Comparison of the total freezing time required to reach the temperature -20°C t_f for the protocol P_2 (conventional air freezing, AF) and for the combined protocol P_3 with the preliminary vacuum freezing up to $T_v=-6^{\circ}\text{C}$ followed by conventional air freezing in the freezing chamber (VF(-6°C) +AF(-20°C)) at the different values of cell disintegration index Z .

Figure IV. 7 shows the relative texture index F^* (a) (Eq. (2)) and water loss M_L (b) (Eq. (3)) versus the cell disintegration index Z for the protocol P_2 (conventional air freezing, AF (-20°C)) and for the combined protocol P_3 with preliminary vacuum freezing up to $T_v=-6^{\circ}\text{C}$ followed by conventional air freezing in the freezing chamber

(VF(-6°C)+AF(-20°C)). Application of both protocols P₂ and P₃ resulted in a significant decrease of F^* values, moreover the tissue softening increased with increase of Z . At given Z the values of F^* were approximately the same for P₂ and P₃ protocols. However, the water loss for the protocol P₂ (conventional air freezing) was significantly higher than one for the protocol P₃. It can reflect the different distributions of water inside carrot tissue with application of freezing protocols P₂ and P₃. Applied freezing protocol can greatly affect the homogeneity of distribution of water, formation of ice crystals, and quality attributes of plant tissues. The effects of different freezing protocols assisted with application of ultrasound, high pressure, electric and magnetic fields on the distribution of water and cellular damage was recently comprehensively reviewed (Li, Zhu, & Sun, 2018). Particularly, assistance of freezing of carrot with PEF allowed significant maintaining the quality parameters (color and firmness) after thawing (Shayanfar, Chauhan, Toepfl, & Heinz, 2014).

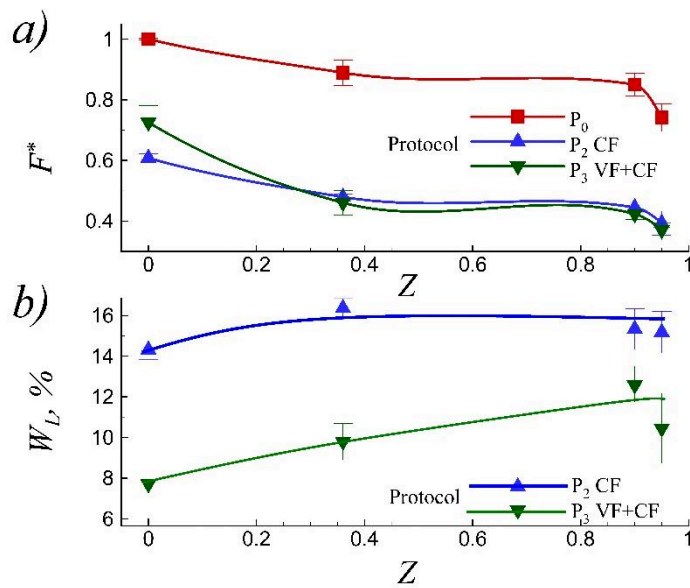


Fig. IV. 7: Relative texture index F^* (a) and water loss M_L (b) versus the cell disintegration index Z for the protocol P₂ (conventional air freezing, AF(-20°C)) and for the combined protocol P₃ with the preliminary vacuum freezing down to $T_v = -6^\circ\text{C}$ followed by the conventional air freezing in the freezing chamber (VF(-6°C)+AF(-20°C)). The lines are drawn for the convenience of the eye.

Finally, Figure IV. 8 compares the SEM images inside geometrical centre's at different PEF disintegration indexes Z for different protocols (Fig. IV. 1): protocol P₀ (fresh tissue without freezing), protocol P₂ (conventional air freezing, AF(-20°C)) and for the combined protocol P₃ with preliminary vacuum freezing up to $T_v = -6^\circ\text{C}$ followed by conventional air freezing in the freezing chamber at -20°C (VF(-6°C)

+AF (-20°C)). For the protocol P₀ the PEF treatment practically unaffected the structure of tissue and arrangement of cell walls. This effect was also observed for different tissues treated by PEF and it was demonstrated that PEF treatment at moderate electric field strength mainly induced electroporation of cell membranes without significant changes in structure of cell walls (Vorobiev, et al., 2020).

However, for the protocol P₂ (conventional air freezing, AF(-20°C)) more significant changes in structure of tissues were observed. Moreover, the effects became even more noticeable for PEF-untreated systems. The effects were similar to that observed for the air-blast freezing of potato tissue (Jalté, et al., 2009). Applied freezing–thawing protocols resulted in significant deformation of cells, perturbation of their polyhedral shape and formation of the intercellular voids. The similar conclusions were done in discussion of SEM data on the microstructure of PEF treated and freeze-thawed carrot tissues (Shayanfar, et al., 2014).

For the combined protocol P₃ with preliminary vacuum freezing up to $T_v=-6^\circ\text{C}$ followed by conventional air freezing in the freezing chamber (VF(-6°C)+AF(-20°C)) the PEF treatment also introduced changes in structure and arrangements of cell walls. These effects reflected impact of PEF treatment on processes of formation of ice crystals inside the carrot tissue.

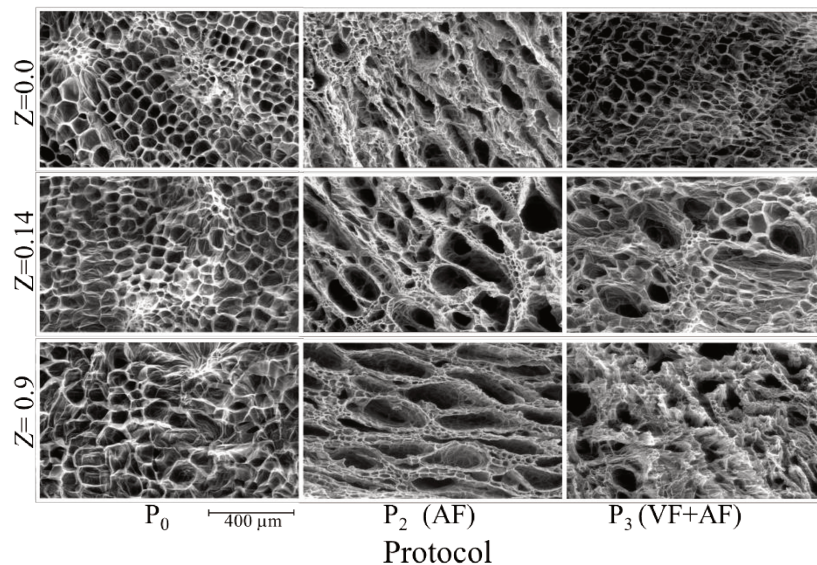


Fig. IV. 8: SEM images of carrot samples inside the geometrical centres at the different cell disintegration indexes Z for different protocols (Fig. IV. 2): P₀ (fresh tissue without freezing), P₂ (conventional air freezing, AF(-20°C)) and for the combined protocol P₃ (VF(-6°C)+AF(-20°C)).

4. Conclusions

PEF treatment was applied to induce electroporation of the carrot tissue to different levels of cell disintegration index ($Z=0-0.9$) before its freezing. The time evolution of sample temperature was compared for the continuous vacuum freezing (VF), conventional air freezing (AF) in freezer at -20°C , and combined mode of freezing with the preliminary VF down to -6°C followed by AF at -20°C . The applied modes of treatment greatly affected the texture, moisture losses, and microstructure of thawed carrots. For the continuous VF, the different stages that include pressure drop, period of “thermal arrest” with slowing down of the temperature decrease, acceleration of the temperature decrease, and development of the secondary drying process with removal of the unfrozen water were observed. In the combined mode of freezing, the initial VF was stopped after the leveling of pressure changes at $T_v=-6^{\circ}\text{C}$. Application of both the PEF pre-treatment and the preliminary VF resulted in a noticeable acceleration of the AF. Application of the both AF and VF+AF protocols resulted in significant tissue softening. Moreover, this softening decreased with the increase of Z . However, the water losses for the AF protocol were significantly higher than those for the combined VF+AF protocol. It can reflect the different distributions of water inside the carrot tissue with application of these freezing protocols. Analysis of SEM images from the geometrical center of samples evidenced significant changes in the structure and arrangement of cell walls at high values of Z for the AF and VF+AF protocols. Evidently, these effects reflected the impact of PEF treatment on the processes of formation of ice crystals inside the carrot tissue. In future studies it is desirable to determine the optimal combined VF+AF protocols for other tissues (like potato, apple, etc.).

- Ajani, C. K., Zhu, Z., & Sun, D. W. (2023). Shrinkage during vacuum cooling of porous foods: Conjugate mechanistic modelling and experimental validation. *Journal of Food Engineering*, 337, 111220. <https://doi.org/10.1016/j.jfoodeng.2022.111220>
- Ammar, J. B., Van Hecke, E., Lebovka, N., Vorobiev, E., & Lanoisellé, J.-L. (2011). Freezing and freeze-drying of vegetables: benefits of a pulsed electric fields pre-treatment. In *6th International CIGR Technical Symposium "Towards a sustainable food chain"* (pp. Abstract N° 467, On-CD 008_Session. 461-462, P. 411-416).
- Ammar, J. B., Van Hecke, E., Vorobiev, E., Lanoisellé, J.-L., & Lebovka, N. (2009). Pulsed electric fields improves freezing process. In *Proceedings of the International Conference on Bio and Food Electrotechnologies, BFE 2009* (pp. 1-6).
- Behnsilian, D., & Mayer-Miebach, E. (2017). Impact of blanching, freezing and frozen storage on the carotenoid profile of carrot slices (*Daucus carota* L. cv. Nutri Red). *Food Control*, 73, 761-767. <https://doi.org/10.1016/j.foodcont.2016.09.045>
- Ben Ammar, J., Lanoisellé, J. L., Lebovka, N. I., Van Hecke, E., & Vorobiev, E. (2011). Impact of a Pulsed Electric Field on Damage of Plant Tissues: Effects of Cell Size and Tissue Electrical Conductivity. *Journal of Food Science*, 76(1), E90-E97. <https://doi.org/10.1111/j.1750-3841.2010.01893.x>
- Blahovec, J., Kouřim, P., & Lebovka, N. (2021). Volumetric Shrinkage and Poisson 's Ratio of Carrot Treated by Pulse Electric Fields. *Food and Bioprocess Technology*, 14(11), 2134-2145. <https://doi.org/10.1007/s11947-021-02711-1>
- De Vito, F., Ferrari, G., I. Lebovka, N., V. Shynkaryk, N., & Vorobiev, E. (2008). Pulse Duration and Efficiency of Soft Cellular Tissue Disintegration by Pulsed Electric Fields. *Food and Bioprocess Technology*, 1(4), 307-313. <https://doi.org/10.1007/s11947-007-0017-y>
- Deck, L.-T., Košir, A., & Mazzotti, M. (2024). Modeling the freezing process of aqueous solutions considering thermal gradients and stochastic ice nucleation. *Chemical Engineering Journal*, 483, 148660. <https://doi.org/https://doi.org/10.1016/j.cej.2024.148660>
- Huang, Y., & Bals, O. (2024). Application of Vacuum Freezing to Improve the Quality of Thawed Carrot Discs. *Food and Bioprocess Technology*. <https://doi.org/10.1007/s11947-024-03462-5>
- Jalté, M., Lanoisellé, J.-L., Lebovka, N. I., & Vorobiev, E. (2009). Freezing of potato tissue pre-treated by pulsed electric fields. *LWT - Food Science and Technology*, 42(2), 576-580. <https://doi.org/10.1016/j.lwt.2008.09.007>
- Li, D., Zhu, Z., & Sun, D.-W. (2018). Effects of freezing on cell structure of fresh cellular food materials: A review. *Trends in Food Science & Technology*, 75, 46-55. <https://doi.org/10.1016/j.tifs.2018.02.019>
- Liu, C., Grimi, N., Bals, O., Lebovka, N., & Vorobiev, E. (2021). Effects of pulsed electric fields and preliminary vacuum drying on freezing assisted processes in potato tissue. *Food and Bioprocess Technology*, 125, 126-133. <https://doi.org/10.1016/j.fbp.2020.11.002>
- Liu, C., Grimi, N., Lebovka, N., & Vorobiev, E. (2018). Effects of pulsed electric fields treatment on vacuum drying of potato tissue. *LWT*, 95, 289-294. <https://doi.org/10.1016/j.lwt.2018.04.090>
- Muthukumarappan, K., Marella, C., & Sunkesula, V. (2019). Chapter 15 - Food Freezing Technology. In M. Kutz (Ed.), *Handbook of Farm, Dairy and Food Machinery Engineering (Third Edition)* (pp. 389-415): Academic Press.

- Parniakov, O., Bals, O., Lebovka, N., & Vorobiev, E. (2016a). Effects of pulsed electric fields assisted osmotic dehydration on freezing-thawing and texture of apple tissue. *Journal of Food Engineering*, 183, 32-38.<https://doi.org/10.1016/j.jfoodeng.2016.03.013>
- Parniakov, O., Bals, O., Lebovka, N., & Vorobiev, E. (2016b). Pulsed electric field assisted vacuum freeze-drying of apple tissue. *Innovative Food Science & Emerging Technologies*, 35, 52-57.<https://doi.org/10.1016/j.ifset.2016.04.002>
- Pisano, R., & Capozzi, L. C. (2017). Prediction of product morphology of lyophilized drugs in the case of Vacuum Induced Surface Freezing. *Chemical Engineering Research and Design*, 125, 119-129.<https://doi.org/https://doi.org/10.1016/j.cherd.2017.07.004>
- Schudel, S., Prawiranto, K., & Defraeye, T. (2021). Comparison of freezing and convective dehydrofreezing of vegetables for reducing cell damage. *Journal of Food Engineering*, 293, 110376.<https://doi.org/10.1016/j.jfoodeng.2020.110376>
- Shams, R., Manzoor, S., Shabir, I., Dar, A. H., Dash, K. K., Srivastava, S., Pandey, V. K., Bashir, I., & Khan, S. A. (2024). Pulsed Electric Field-Induced Modification of Proteins: A Comprehensive Review. *Food and Bioprocess Technology*, 17(2), 351-383.<https://doi.org/10.1007/s11947-023-03117-x>
- Sharma, K. D., Karki, S., Thakur, N. S., & Attri, S. (2012). Chemical composition, functional properties and processing of carrot—a review. *Journal of Food Science and Technology*, 49(1), 22-32.<https://doi.org/10.1007/s13197-011-0310-7>
- Shayanfar, S., Chauhan, O. P., Toepfl, S., & Heinz, V. (2014). Pulsed electric field treatment prior to freezing carrot discs significantly maintains their initial quality parameters after thawing. *International Journal of Food Science & Technology*, 49(4), 1224-1230.<https://doi.org/10.1111/ijfs.12421>
- Silva, A. C. C., & Schmidt, F. C. (2022). Intensification of freeze-drying rate of coffee extract by vacuum freezing. *Innovative Food Science & Emerging Technologies*, 78, 103022.<https://doi.org/10.1016/j.ifset.2022.103022>
- Vorobiev, E., & Lebovka, N. (2020). *Processing of Foods and Biomass Feedstocks by Pulsed Electric Energy*: Springer International Publishing.
- Wang, N., Kan, A., Mao, S., Huang, Z., & Li, F. (2021). Study on heat and mass transfer of sugarcane stem during vacuum pre-cooling. *Journal of Food Engineering*, 292, 110288.<https://doi.org/https://doi.org/10.1016/j.jfoodeng.2020.110288>
- Wiktor, A., Schulz, M., Voigt, E., Knorr, D., & Witrowa-Rajchert, D. (2015). Impact of pulsed electric field on kinetics of immersion freezing, thawing, and on mechanical properties of carrot. *J Food. Science. Technology. Quality*, 22(2), 124-137

IV.3 Chapter conclusion

This chapter studied the effect of PEF pretreatment at different levels of cell disintegration index on vacuum freezing on the basis that the application of vacuum freezing improved the quality of thawed carrot discs. As expected, PEF pretreatment greatly affected the freezing time of continuous VF, AF-20, and combined vacuum freezing (VF+AF-20) due to the electroporation. For the continuous VF the different stages that include pressure drop, period of “thermal arrest” with slowing down of the temperature decrease, acceleration of the temperature decrease, and development of the secondary drying process with removal of the unfrozen water were observed. Although the application of PEF pretreatment on both AF-20 and VF+AF-20 protocols resulted in significant tissue softening with the increase of Z. The water losses for AF-20 protocol were significantly higher than those for the combined VF+AF-20 protocol, which is consistent with the results in Chapter 3 (without PEF pretreatment). It can reflect the different distributions of water inside the carrot tissue with application of these freezing protocols. Analysis of SEM images from the geometrical center of samples evidenced significant changes in the structure and arrangement of cell walls at high values of Z for the AF-20 and VF+AF-20 protocols. Evidently, these effects reflected the impact of PEF treatment on the processes of formation of ice crystals inside the carrot tissue.

Chapter V Effect of pulsed electric field assisted combined vacuum freezing on quality attributes of thawed carrots, potatoes, and apples

V.1 Chapter introduction

Freezing is an efficient approach for the preservation of fruits and vegetables. When it is conducted properly, the food material can be stored even for 12–18 months, maintaining its organoleptic and nutritional quality (Alinovi, Paciulli, Rinaldi, Falsafi, & Chiavaro, 2024). During the freezing process, not only the freezing operations but types of the food to be frozen have a direct impact on mass and heat transfer, as well as the freezing efficiency. In the previous chapters, we have concluded that combined vacuum freezing with conventional freezing protocol gives good results in the quality preservation of carrot discs. To extend the application, we have also tested this process for different kinds of food materials with different compositions and most importantly structural organization at different levels. On one hand, their susceptibility to freezing is different based on their physical property. On the other hand, the combined effect of shortened freezing time and pressure reduction under vacuum freezing system varies in different materials. In general, the shorter the freezing time, especially the shorter the effective freezing time during the freezing critical zone, the smaller the influence on the quality of the product after freezing. While vacuum freezing allows for short freezing times compared to conventional air freezing, the generated low pressure induces the release of native gases, water, and liquids in the tissues (Boonsupthip, Heldman, & Choachamnan, 2015). As the native gases in the pores expand and move away, the pores in the tissues expand (Trusinska, Drudi, Rybak, Tylewicz, & Nowacka, 2023). The expansion pressure may cause mechanical deformation and damage to cells as suffered in other vacuum processing, but different food matrix structures withstand the pressures to different degrees, which is also one of the issues that must be taken into account. Thus, comparing materials with different cell characteristics is very advantageous for enhancing the efficiency of food freezing and final quality of the frozen products.

Moreover, as one of the approaches to improve food processing efficiency, PEF pretreatment has shown great potential in the conventional freezing, drying, extraction of fruits and vegetables at minimum power consumption. It has been proven to cause

cell membrane electroporation, enhancing mass transfer and moisture evacuation (Shynkaryk, Lebovka, & Vorobiev, 2008). Thus implying the potential for improving subsequent vacuum freezing that relies on moisture evaporation. Previous studies by our team have implied that the susceptibility of different samples to PEF treatment varies greatly (N. I. Lebovka, Bazhal, & Vorobiev, 2002), which also strongly influences their conditions during subsequent freezing, including freezing kinetics and quality retention after thawing, a critical aspect for frozen products. Based on the different compositions and cellular structures of different food species, the effect of PEF-assisted combined vacuum freezing on the quality attributes of three kinds of plant-based foods (carrots, apples and potatoes) was studied in this chapter. This is of great significance for the applicability of such freezing method for different fruit and vegetable species and the selection of suitable operating parameters.

Without PEF pretreatment and PEF pretreatment with disintegration index $Z=0.9$ applied prior to continuous vacuum freezing were firstly investigated to understand the effect of the pretreatment on the freezing kinetics of different samples. The effects of PEF-assisted combined vacuum freezing and conventional air freezing on the quality characteristics of thawed carrots, potatoes, and apples were further compared.

V.2 Results

V.2.1 Materials and methods

V.2.1.1 Materials

Fresh, ripe and unblemished carrot (*Daucus carota* L.), apple (Gala Delicious), and potato (Colomba) were obtained from a local market (Compiègne, France) and stored in darkness at 6 °C until the preparation of plant discs. A moisture content W measuring by MA160 Infrared Moisture Analyzer (Sartorius, Germany) was within 82–85% for potatoes, 80–85% for apples, and 87–92% for carrots. For the convenience of the study, all three materials were similarly treated. After cleaning, a special cylindrical knife was used to cut each raw material into disc-shape samples of the same dimensions (18 mm in diameter and 10 mm in thickness).

Table V. 1: Characteristics of applied tissues, including the measured water content, and approximate porosity, density, and mean cell equivalent diameter adapted from (Bazhal, Lebovka, & Vorobiev, 2003; Jaeger, Schulz, Lu, & Knorr, 2012; N. I. Lebovka, et al., 2002).

Sample	Water content, %	Porosity (ϵ), %	Density (ρ), kg m ⁻¹	Cell equivalent diameter, μm
Potato	82–85	2	1050	150
Apple	80–85	14–25	800	200
Carrot	87–92	4	952	80

V.2.1.2 Experimental procedures

Fig. V. 1 shows the applied experimental procedures. They include the initial treatment of carrot, potato and apple discs by PEF followed by different protocols (P₀-P₃) and sample characterization.

Raw material	Pretreatment	Freezing and thawing	Characterizations
Potatoes	PEF treatment $E=400\text{V/cm}$ $t_i = 100 \mu\text{s}$ $n=10$ $\Delta t = 10 \text{ s}$ $Z=0.9$	P ₀ :without FT	<ul style="list-style-type: none"> • Texture, F* • water loss, WL • SEM
Apples		Freezing P ₁ : continuous VF P ₂ : AF at -20 °C	
Carrots		P ₃ : VF(-6°C)+AF(-20°C) Thawing Store at 20°C for 1 hour	

Fig. V. 1: Description of the applied experimental procedures. They include the PEF treatment, application of different protocols (P₀-P₃), and sample characterization.

The procedures, including PEF treatment, freezing, thawing, and characterizations are as explained in [chapter IV.2](#). Only the force relaxation tests for different materials vary a little. In the calculation of F^* , F is the force measured at $t=50 \text{ s}$ for apple and carrot discs (Parniakov, Bals, Lebovka, & Vorobiev, 2016), while it is measured at $t=100 \text{ s}$ for potato discs. This is due to the force relaxation (stress relaxation) is the observed decrease in stress in response to strain generated in the structure. The time required for the relaxation to a constant value varies for different materials. The applied relaxation time for potato discs is according to the method from Liu et al. (Liu, Grimi, Bals, Lebovka, & Vorobiev, 2021).

V.2.2 Results and discussion

Fig. V. 2 presents the typical dependences of cell disintegration index Z versus PEF treatment time t_{PEF} . In these experiments, the PEF treatment was done at the same electric field strength, $E = 400 \text{ V/cm}$. Although the Z values of them all increase with the treatment times and eventually to a specific constant value, the different evolution curves for different materials can be attributed to their different properties, including

cell size and composition, conductivity, pH and ions strength and other factors (Toepfl, Siemer, Saldaña-Navarro, & Heinz, 2014).

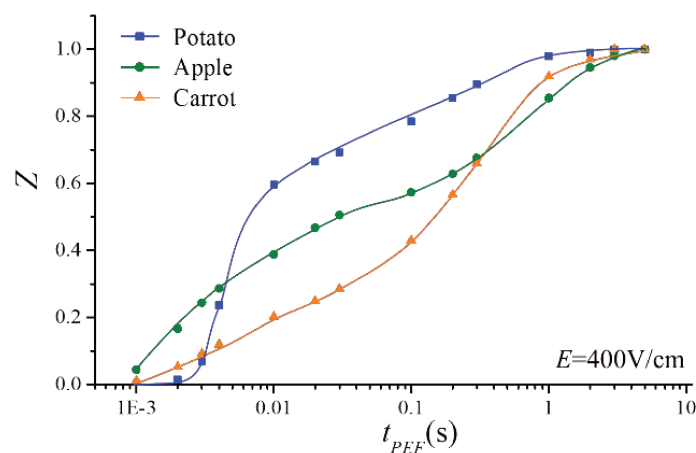


Fig. V. 2: Conductivity disintegration index Z versus total time of PEF treatment t_{PEF} at the electric field strength $E = 400$ V/cm for potato, apple, and carrot discs. Here, symbols correspond to the experimental data and solid lines are drawn for the guidance of an eye.

The characteristic damage time (τ) (time required for Z to attain one-half of its maximal value, i.e., $Z = 0.5$) was observed to rank as potato < apple < carrot. The same result was observed in the investigation of the effects of PEF induced damage in selected fruit and vegetable plant tissues (apple, potato, carrot, courgette, orange, and banana) (Ben Ammar, Lanoisellé, Lebovka, Van Hecke, & Vorobiev, 2011). They attributed this to the larger cell radius of the potato tissue ($47\mu\text{m}$), which is proportional to the transmembrane potential (u_m) and determines the effectiveness of electroporation. However, the largest cell size in orange ($\approx 60\mu\text{m}$) demonstrated kinetics with the longest characteristic damage time τ , which was not consistent with their previous assumption. Besides, Lebovka et al. have shown that the time of PEF treatment needed for membrane disintegration in potato tissue is shorter than that of apple and carrot tissue so it is considered less resistible to PEF treatment (N. I. Lebovka, et al., 2002). The collected evolutions of the Z value of different materials were utilized to select a consistent high disintegration $Z=0.9$ for their further freezing procedure.

Freezing kinetics of untreated and PEF treated potatoes, apples and carrots are shown in Fig. V. 3. Freezing curves obtained for the continuous vacuum freezing (Protocol P₁) can represent a valuable tool for understanding the freezing behavior of different

raw materials, depending on their specific compositional and structural characteristics. It is shown that the freezing speeds of untreated samples rank as apple>potato>carrot. During vacuum freezing, water evaporates inside the macropores of the sample due to pressure difference between pore center and surface. The generated vapor must diffuse through the pore space and escape to the surroundings. Resulting from this, water evaporation rate is largely affected by the internal porous structure of the sample (Sun & Zheng, 2006). McDonald et al. also concluded that sample porosity has a direct influence on vacuum cooling rates and efficiency in their research on the formation of pores and their effects in a cooked beef product on the efficiency of vacuum cooling (McDonald & Sun, 2001). For apple tissue, the characteristic of many voids in the cellular structure is beneficial to the transmission of water during vacuum processing. For potatoes and carrots with small porosity, their composition and density may be the factors that affect their heat transfer efficiency. Although potatoes freeze relatively faster, it was observed that carrots were able to reach a lower ultimate temperature, probably due to the presence of the vascular structure of the carrot tissues, which allows the continuous evaporation of the internal water even with the presence of the impediment of the ice that was first formed on the surface layer.

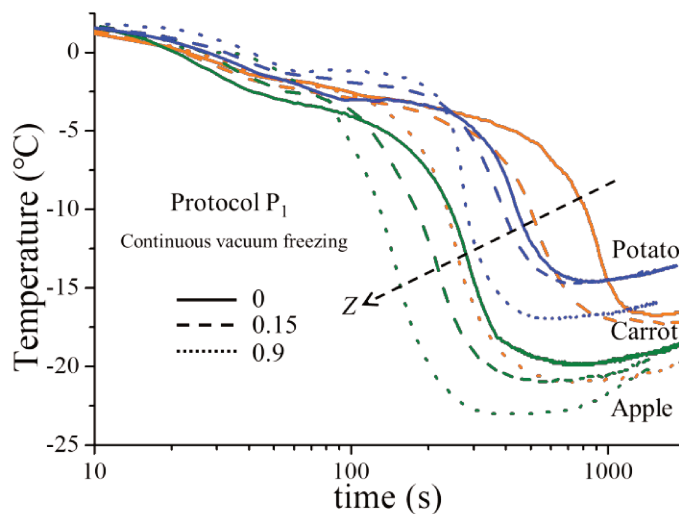


Fig. V. 3: Temperature in the geometry center of the potato, apple, and carrot discs, versus time during continuous vacuum freezing P_1 (continuous vacuum freezing), for the untreated (solid lines) and PEF pre-treated samples (dashed lines and dotted lines represent $Z=0.15$ and $Z=0.9$, respectively).

In general, PEF treatment showed the acceleration of the freezing in all the temperature curves of the materials, which evidently reflected effects of

electroporation. Besides, with higher cell disintegration, the faster freezing can be observed. This result is the same as the temperature changes during the air-blast freezing of potato tissues with PEF pretreatment (Jalté, Lanoisellé, Lebovka, & Vorobiev, 2009). In this kind of conventional freezing relying on heat conduction, they considered that PEF pretreatment induced membrane damage, and the residues of membranes can serve as fresh nucleation sites that accelerate the nucleation rate. Also, cellular matrix destruction improves the conditions of heat transfer as well, leading to increment of thermal conductivity (Dadan, Nowacka, Czyzewski, & Witrowa-Rajchert, 2020).

But in our case, the reduction in temperature during vacuum freezing more depends on partial moisture evaporation from the sample, leading to the removal of heat and crystallization of the rest water inside the sample. The faster freezing kinetics of samples with PEF pretreatment can be explained that electroporation reduced the obstruction of the cell membrane to water evaporation. This also increased the rate of heat removal while enhancing the mass transfer. Similar acceleration in the removal of water was also observed in the PEF pretreated freeze-drying of apple tissue, since sublimation of ice at low pressures was improved by the induced pore formation and therefore the more opened cell structure of the PEF pre-treated samples (Lammerskitten, et al., 2019). Besides, the ultimate temperatures they could reach were also lowered. This may be attributed to the amount of water that can be evaporated to maintain the continuous temperature reduction increased as well, as water is redistributed inside and outside the cells. In the study on the characterization of the food tissue response in terms of water mobility to different levels of electric field strength by the MRI technique, Genovese et al. observed a general decrease of T_2 (transverse relaxation time) in plant tissues that can be ascribed to the loss of compartmentalization and diffusion of intracellular water and ion leakage through the tonoplast and the plasmalemma membranes, leading to a redistribution of water between different compartments and tissue structures (Genovese, et al., 2021). They also demonstrated the use of T_2 mapping technique in the analysis of the effects of PEF on plant tissue structures and visualized the water distribution and redistribution within the electroporated tissues (Genovese, et al., 2023). With a long time of pumping, the water in the sample evaporates, and an ice layer is formed and extends inward subsequently. Therefore, the decreasing amount of liquid water, which is

progressively more difficult to migrate from the interior to the surface for evaporation, is not sufficient to support a continued temperature decrease. Finally, the curves all end in a rise.

Interestingly, their freezing curves were also affected by the PEF treatment to different degrees, although we've controlled the cell disintegration to the same values (0, 0.15, and 0.9). In particular, the difference between the time to reach the ultimate temperature of the untreated sample and the PEF-treated ($Z=0.9$) sample, was significantly larger for carrots. This may be due to the heterogeneous nature of carrot, so that during PEF treatment, inhomogeneous effects are generated in the vascular system and the surrounding parenchyma. Thus, compared to potatoes and apples, which are relatively homogeneous in structure, it exhibited more mobility of water protons during PEF treatment, that is, diffusion from sites of low resistance to water permeation (i.e. vascular bundles) to high ones (i.e. cortex) (Genovese, et al., 2023). This allowed a larger acceleration of evaporation in the subsequent vacuum freezing.

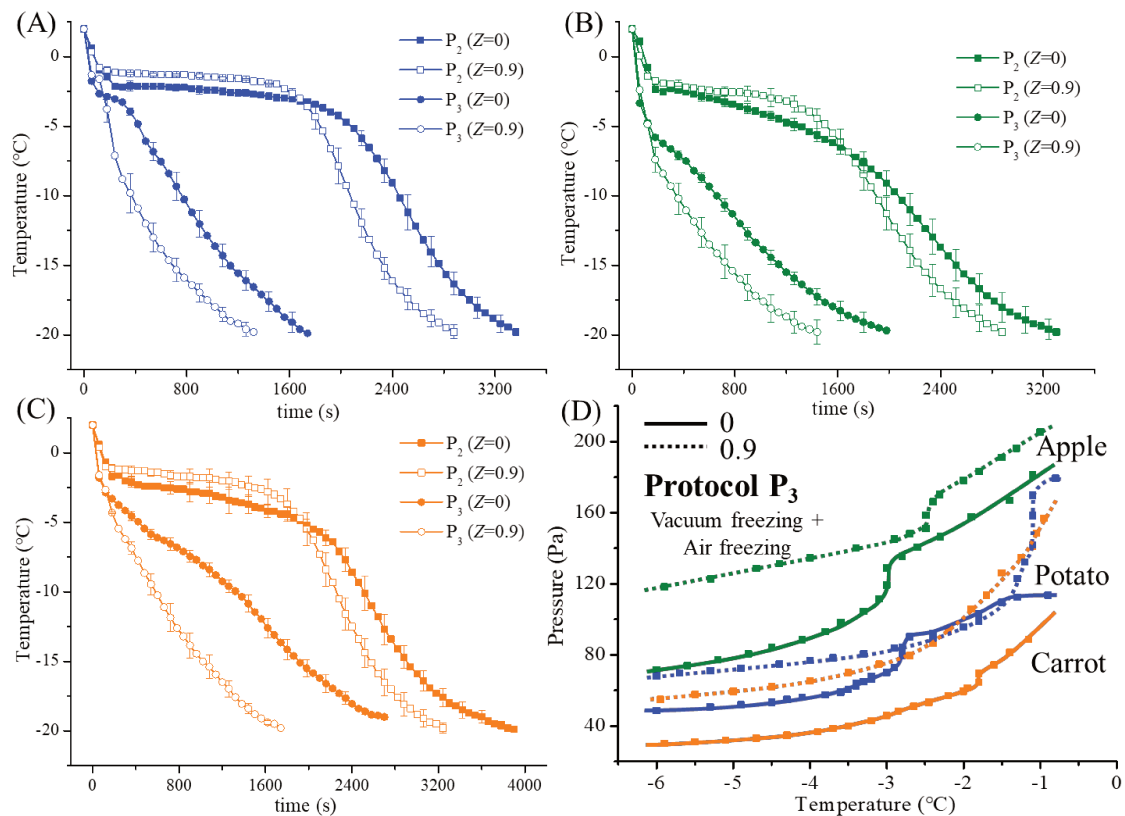


Fig. V. 4: The freezing curves during P₂ (AF) and P₃ (VF+AF) of untreated and PEF treated potato (A), apple (B), and carrot (C) discs, respectively. The pressure inside the vacuum chamber, versus the

temperature in the geometry centre of potato, apple, and carrot discs (D). Here, the solid lines represent the untreated samples, and the dotted lines represent the PEF treated samples ($Z=0.9$).

Fig. V. 4 shows the freezing curves of untreated and PEF treated ($Z=0.9$) potato, apple, and carrot discs during P_2 (air freezing at $-20\text{ }^\circ\text{C}$) and P_3 (vacuum freezing + air freezing at $-20\text{ }^\circ\text{C}$). The detailed freezing times at different stages including 2 to $-6\text{ }^\circ\text{C}$, -6 to $-20\text{ }^\circ\text{C}$, and 2 to $-20\text{ }^\circ\text{C}$ are shown in Table V. 2. The difference between P_2 and P_3 mainly comes from the temperature range from 2 to $-6\text{ }^\circ\text{C}$, which covers the area where most ice crystals are formed. It is obvious that the freezing times were significantly longer for conventional air freezing (P_2) for all samples ($p < 0.05$). This is due to the heat conduction adopted in P_2 is much slower in removing the latent heat released during the crystallization, thus showing a longer plateau period. Whereas the latent heat of water evaporation during P_3 (vacuum freezing from 2 to $-6\text{ }^\circ\text{C}$) is much greater, which allowed a faster freezing rate than that of P_2 . Besides, as observed in P_1 , PEF pretreatment also accelerated freezing process in P_2 and P_3 . The freezing points of the different materials all increased after PEF treatment. This may be because the medium in PEF treatment is pure water, and the mass transfer that occurred in this process slightly increased the water content of the materials. However, the crystallization process is too fast in P_3 , thus no significant change in freezing points was found between untreated and PEF treated samples.

Table V. 2: Freezing time of temperature range of 2 to $-6\text{ }^\circ\text{C}$, -6 to $-20\text{ }^\circ\text{C}$, and 2 to $-20\text{ }^\circ\text{C}$ of untreated and PEF treated potato, apple, and carrot discs in P_2 (AF) and P_3 (VF+AF), respectively. Water loss (%) for thawed potato, apple, and carrot discs after different freezing protocols. Values with different superscripts among the data of freezing time and water loss in the same column respectively indicate that the means are significantly different at $p < 0.05$.

Protocols		Potato	Apple	Carrot
AF P_2 ($Z=0$)	t (2 to $-6\text{ }^\circ\text{C}$), s	2170 \pm 40 ^h	1605 \pm 74 ^{cd}	2143 \pm 80 ^f
	t (-6 to $-20\text{ }^\circ\text{C}$), s	1218 \pm 115 ^{de}	1733 \pm 97 ^{de}	1814 \pm 105 ^{de}
	t (2 to $-20\text{ }^\circ\text{C}$), s	3388 \pm 69 ^j	3338 \pm 138 ^h	3957 \pm 188 ⁱ
	WL, %	12.75 \pm 0.25 ^a	19.38 \pm 0.70 ^b	14.31 \pm 0.49 ^{bc}
PEF+AF P_2 ($Z=0.9$)	t (2 to $-6\text{ }^\circ\text{C}$), s	1887 \pm 89 ^g	1523 \pm 70 ^{bcd}	2022 \pm 92 ^{ef}
	t (-6 to $-20\text{ }^\circ\text{C}$), s	1009 \pm 45 ^c	1449 \pm 126 ^{bc}	1233 \pm 78 ^c

	t (2 to -20°C), s	2896±67 ⁱ	2972±102 ^g	3255±117 ^h
	WL, %	23.04±0.77 ^c	22.36±1.03 ^c	15.34±1.00 ^c
	t (2 to -6°C), s	484±55 ^b	212±28 ^a	567±65 ^b
VF+AF	t (-6 to -20°C), s	1588±86 ^f	2060±96 ^e	2133±79 ^{def}
P ₃ (Z=0)	t (2 to -20°C), s	2072±149 ^h	2272±160 ^f	2700±85 ^g
	WL, %	12.58±0.32 ^a	9.52±1.39 ^a	11.57±0.96 ^a
	t (2 to -6°C), s	260±72 ^a	141±13 ^a	279±46 ^a
PEF+VF+AF	t (-6 to -20°C), s	1082±117 ^{cd}	1353±47 ^b	1461±77 ^c
P ₃ (Z=0.9)	t (2 to -20°C), s	1342±180 ^e	1494±185 ^{bc}	1740±165 ^d
	WL, %	21.58±1.12 ^b	37.02±1.55 ^d	14.85±0.99 ^{bc}

Fig. V. 4 shows the changes of pressure P inside the vacuum chamber with the temperature T inside the geometrical center of samples at the initial vacuum freezing stage of P₃. The solid lines represent the untreated samples, and the dotted lines represent the PEF-treated samples, respectively. For untreated samples, the pressure-temperature curves showed parallel trends for different materials, which all followed the gas-solid phase transition curve at low pressure. The difference in pressure at the same temperatures revealed the difference in the rate of water evaporation in these materials, and here we observed that the pressure values were ranked from high to low as apples > potatoes > carrots. Among the three materials, water evaporated more easily from apples, which may be related to their cellular structure. On the one hand, the apple cells are larger and the tissue is more porous, and the air in the exocellular pores is more likely to spill out under vacuum compared to water or other solvents. On the other hand, the apple cell walls are thinner, which make them less resistant to the stresses generated by the vacuum process. These make the apple cell compartments more susceptible to deformation or even rupture damage, and as a result, the release of large amounts of air and water raises the pressure values in the vacuum chamber. As water was much easier to evaporate from the electroporated samples, the vapor increased the pressure inside the vacuum chamber. Therefore, at the same temperature, higher pressure can be observed during the vacuum freezing of PEF treated samples. In addition, the pressure-temperature curves of the three materials during vacuum freezing also implied the ease of evaporation of water from different materials, which correlated with their freezing rates.

The water loss for P₂ and P₃ of potato, apple, and carrot discs are shown in Table V. 2. For untreated potato discs, there was no significant difference in water loss after P₂ (AF) and P₃ (VF+AF), whereas PEF treatment was the contributing factor. This may be due to the fact that PEF led to the formation of large amounts of extracellular ice crystals. The situation is different in apples. Untreated samples after P₃ showed the smallest water loss, but in both protocols, PEF pretreatment increased the water loss, even resulting the highest water loss after P₃. This might be due to the PEF pretreatment reduced the ability of apple tissue to withstand microstructural stress induced by the removal of moisture. From this point, P₃ without PEF pretreatment is more suitable for the freezing of apple discs. As for carrots, it is obvious that the combined freezing P₃ significantly decreased the water loss.

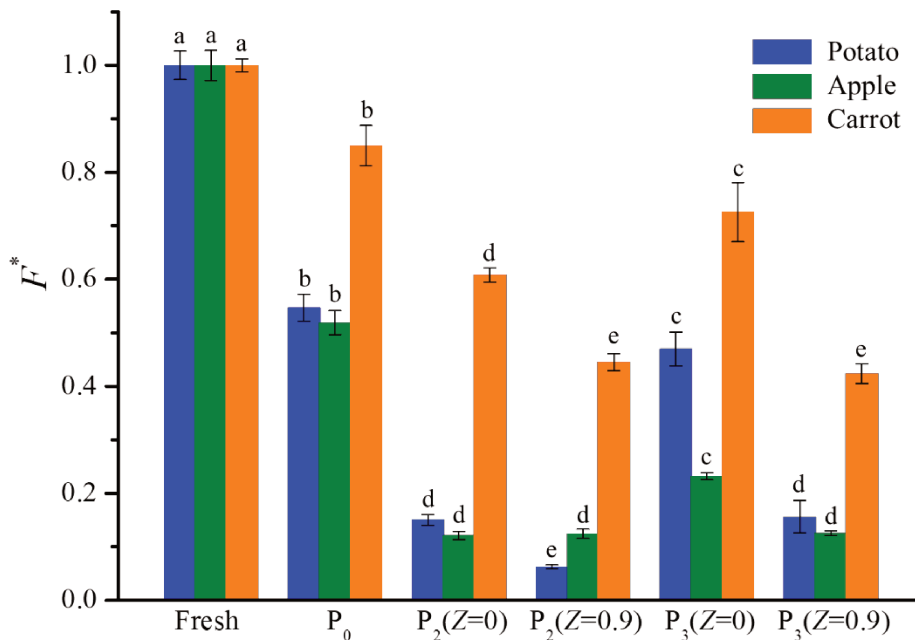


Fig. V. 5: Relative texture index F^* of fresh samples, PEF treated samples, untreated and PEF treated thawed samples after P₂ (AF) and P₃ (VF+AF), respectively. Values with different superscripts among the data for each material indicate that they are significantly different at $p < 0.05$.

Fig. V.5 shows the relative texture index F^* of fresh samples, PEF treated samples, and samples after P₂ (AF) and P₃ (VF+AF), respectively. The PEF treatment causes a non-thermal rupture of cellular membranes and decrease or loss of the turgor component of cells (Nikolai I. Lebovka, Praporscic, & Vorobiev, 2004). Despite of certain loss in the firmness of tissue structure, induced by the PEF, carrot tissue still

exhibited relatively higher F^* after PEF treatment, which may be related to the fact that it was originally the strongest among the three materials.

Freezing caused more severe damage to the texture due to the formation of ice crystals. For untreated samples, the F^* values of samples after P₃ were all higher than those after P₂. This is due to the faster freezing rate during vacuum freezing through the temperature range from 2 to -6 °C. The carrot discs, among others, showed relatively less variation in both freezing procedures compared to the fresh samples, which may be due to their inherent stronger texture. Although PEF pretreated samples after P₃ exhibited faster freezing rate than untreated ones, they showed much lower F^* values in potatoes and carrots. This means PEF pretreatment caused further softening to them. Previous studies on the PEF pretreated apple and potato both indicated that PEF treatment altered mechanical properties of plant tissue after thawing, causing softening of the material (A Wiktor, Schulz, Voigt, Knorr, & Witrowa-Rajchert, 2015; Artur Wiktor, Schulz, Voigt, Witrowa-Rajchert, & Knorr, 2015). On one hand, PEF treatment weakened the cellular resistance to microstructural stress caused by water removal during vacuum freezing. On the other hand, electroporation resulted in an easier movement of cellular water across the cell membranes toward the ice crystals formed first, thus forming bigger ice crystals. For apple tissue, except for untreated samples in P₃, apple discs in other conditions all showed the same level of severity of damage degree. This might be due to its physical structure which is highly susceptible to freezing, causing complete destruction of the tissue even without PEF pretreatment. From this perspective, the application of VF significantly improved the texture of thawed apple discs ($p < 0.05$), although still not well preserved compared to the fresh apple discs. In addition, it should be noted that the firmness is also largely influenced by the cell wall properties. Actually, larger porosities imply thinner cell walls and thinner cell walls give rise to softer matrices (Ozuna, Gómez Álvarez-Arenas, Riera, Cárcel, & Garcia-Perez, 2014). Thus, apple tissues might be considered as a cellular solid with a low mechanical resistance to deformation, especially during vacuum processing.

The scanning electron micrographs (SEM) were used to analyze the microstructure of untreated and PEF pretreated potato, apple, and carrot samples, after different protocols. As can be seen in [Fig. V. 6](#), cell walls of all the fresh samples were intact with a well-organized structure of typical polyhedral shape. The cell size of the

different materials ordering was observed as: apple>potato>carrot. This is consistent with previous literature (Table V. 1). When the PEF treatment was applied, cells size seemed to be somewhat changed (A2, B2, C2 in Fig. V. 6). However, the basic structure was not noticeably modified. After freezing by the different processes, changes in the cell microstructures were observed. Regardless of the disintegration degree, samples treated by P₂ showed much more severe tissue damage and cell disruption, due to the low freezing rate induced big ice crystals growth (Tian, Chen, Zhu, & Sun, 2020). This also corresponds to the previous variation of the texture properties. Besides, the microstructure of frozen samples with PEF pretreatment displayed more extensive destruction. It can be reasoned for different protocols. Based on the fact that PEF-induced electroporation leads to cell membrane damage, the intracellular cytoplasmic solution is transferred to the extracellular environment more freely rather than relying solely on the osmotic pressure to across the intact cell membrane. The long duration in the freezing critical zone of the P₂ resulted in the movement of more water to form large extracellular ice crystals. However, more intensive flash evaporation of inner original free water in PEF treated sample might be the reason that caused the mechanical damage to the cell structure during P₃. In addition, among all freezing protocols, combined vacuum freezing P₃ demonstrated the best retention of the microstructure of potato and carrot tissues (A5, C5 in Fig. V. 6).

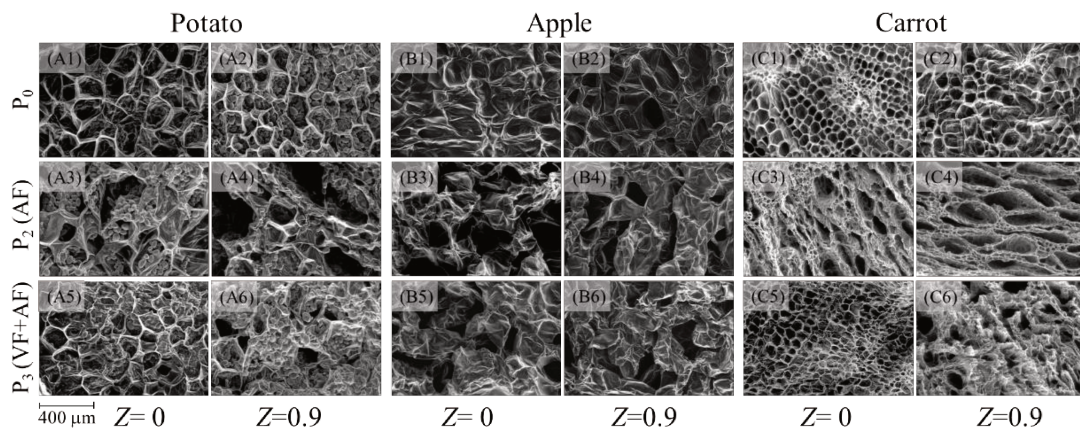


Fig. V. 6: SEM images. Potato (A), apple (B), carrot (C). Numbers 1-7 represent samples of fresh, PEF treated, air freezing, PEF treated air freezing, combined vacuum freezing, and PEF treated vacuum freezing, respectively.

V.3 Chapter conclusion

The PEF pretreatment was applied before different freezing protocols of potato, apple, and carrot discs, including P₁ continuous vacuum freezing, P₂ conventional air freezing at -20 °C, and P₃ vacuum freezing to -6 °C and then transferred to air freezing at -20 °C. The effectiveness of PEF treatment in enhancing the vacuum freeze kinetics, freezing times in different protocols, and quality attributes of frozen products is strongly influenced by the native physical and chemical characteristics of the raw materials. Experiments showed a significant acceleration in continuous vacuum freezing kinetics on all the materials by PEF pre-treatment and increase with the degree of electroporation. However, the degree of the effect of PEF treatment on continuous vacuum freezing varied for different materials. This may be due to differences in the homogeneity of the materials, which correlates with the mobility of the water in the tissue. PEF treatment also shortened the freezing time in both air freezing and combined vacuum freezing. However, it did not demonstrate positive results for the quality attributes of thawed samples. In air freezing, the cell membrane damage induced by PEF treatment made the intracellular cytoplasmic solution transfer to the extracellular environment more freely, which increased the formation of large extracellular ice crystals when passing through the plateau period slowly in P₂. In combined vacuum freezing, due to the fast freezing rate in the temperature range covering the freezing critical zone, the water loss, texture, and the microstructure of samples were all better preserved. But PEF pretreatment somewhat minimized the benefit from rapid freezing, which might associate with the intensified evaporation during the removal of moisture inside the samples. Potato and carrot proved to be more suitable for freezing than apple, since the quality attributes of the apple couldn't be well preserved in all the protocols, even in combined vacuum freezing without PEF pretreatment. This may contribute to its larger porosity and thinner cell walls with a low mechanical resistance to deformation. The low water loss, high textural and microstructural preservation demonstrated in combined vacuum freezing P₃ (VF+AF) all evidenced that this freezing protocol can be applied to fruits and vegetables with low porosity and a rigid initial structure.

- Alinovi, M., Paciulli, M., Rinaldi, M., Falsafi, S. R., & Chiavaro, E. (2024). 9 - Freezing of fruits and vegetables. In S. M. Jafari & H. Rostamabadi (Eds.), *Low-Temperature Processing of Food Products* (pp. 199-224): Woodhead Publishing.
- Bazhal, M., Lebovka, N., & Vorobiev, E. (2003). Optimisation of Pulsed Electric Field Strength for Electroporation of Vegetable Tissues. *Biosystems Engineering*, 86(3), 339-345. [https://doi.org/10.1016/S1537-5110\(03\)00139-9](https://doi.org/10.1016/S1537-5110(03)00139-9)
- Ben Ammar, J., Lanoisellé, J. L., Lebovka, N. I., Van Hecke, E., & Vorobiev, E. (2011). Impact of a Pulsed Electric Field on Damage of Plant Tissues: Effects of Cell Size and Tissue Electrical Conductivity. *Journal of Food Science*, 76(1), E90-E97. <https://doi.org/10.1111/j.1750-3841.2010.01893.x>
- Boonsupthip, W., Heldman, D. R., & Choachamnan, J. (2015). Application of Vacuum Impregnation in Vegetables. In *Handbook of Vegetable Preservation and Processing* (2nd Edition ed., pp. 251-274): CRC Press.
- Dadan, M., Nowacka, M., Czyzewski, J., & Witrowa-Rajchert, D. (2020). 9 - Modification of food structure and improvement of freezing processes by pulsed electric field treatment. In F. J. Barba, O. Parniakov & A. Wiktor (Eds.), *Pulsed Electric Fields to Obtain Healthier and Sustainable Food for Tomorrow* (pp. 203-226): Academic Press.
- Genovese, J., Kranjc, M., Serša, I., Petracci, M., Rocculi, P., Miklavčič, D., & Mahnič-Kalamiza, S. (2021). PEF-treated plant and animal tissues: Insights by approaching with different electroporation assessment methods. *Innovative Food Science & Emerging Technologies*, 74, 102872. <https://doi.org/10.1016/j.ifset.2021.102872>
- Genovese, J., Stručić, M., Serša, I., Novickij, V., Rocculi, P., Miklavčič, D., Mahnič-Kalamiza, S., & Kranjc, M. (2023). PEF treatment effect on plant tissues of heterogeneous structure no longer an enigma: MRI insights beyond the naked eye. *Food Chemistry*, 405, 134892. <https://doi.org/10.1016/j.foodchem.2022.134892>
- Jaeger, H., Schulz, M., Lu, P., & Knorr, D. (2012). Adjustment of milling, mash electroporation and pressing for the development of a PEF assisted juice production in industrial scale. *Innovative Food Science & Emerging Technologies*, 14, 46-60. <https://doi.org/10.1016/j.ifset.2011.11.008>
- Jalté, M., Lanoisellé, J.-L., Lebovka, N. I., & Vorobiev, E. (2009). Freezing of potato tissue pre-treated by pulsed electric fields. *LWT - Food Science and Technology*, 42(2), 576-580. <https://doi.org/10.1016/j.lwt.2008.09.007>
- Lammerskitten, A., Wiktor, A., Siemer, C., Toepfl, S., Mykhailyk, V., Gondek, E., Rybak, K., Witrowa-Rajchert, D., & Parniakov, O. (2019). The effects of pulsed electric fields on the quality parameters of freeze-dried apples. *Journal of Food Engineering*, 252, 36-43. <https://doi.org/10.1016/j.jfoodeng.2019.02.006>
- Lebovka, N. I., Bazhal, M. I., & Vorobiev, E. (2002). Estimation of characteristic damage time of food materials in pulsed-electric fields. *Journal of Food Engineering*, 54(4), 337-346. [https://doi.org/10.1016/S0260-8774\(01\)00220-5](https://doi.org/10.1016/S0260-8774(01)00220-5)
- Lebovka, N. I., Praporscic, I., & Vorobiev, E. (2004). Effect of moderate thermal and pulsed electric field treatments on textural properties of carrots, potatoes and apples. *Innovative Food Science & Emerging Technologies*, 5(1), 9-16. <https://doi.org/10.1016/j.ifset.2003.12.001>

- Liu, C., Grimi, N., Bals, O., Lebovka, N., & Vorobiev, E. (2021). Effects of pulsed electric fields and preliminary vacuum drying on freezing assisted processes in potato tissue. *Food and Bioprocess Processing*, 125, 126-133. <https://doi.org/10.1016/j.fbp.2020.11.002>
- McDonald, K., & Sun, D.-W. (2001). The formation of pores and their effects in a cooked beef product on the efficiency of vacuum cooling. *Journal of Food Engineering*, 47(3), 175-183. [https://doi.org/10.1016/S0260-8774\(00\)00111-4](https://doi.org/10.1016/S0260-8774(00)00111-4)
- Ozuna, C., Gómez Álvarez-Arenas, T., Riera, E., Cárcel, J. A., & Garcia-Perez, J. V. (2014). Influence of material structure on air-borne ultrasonic application in drying. *Ultrasonics Sonochemistry*, 21(3), 1235-1243. <https://doi.org/10.1016/j.ultsonch.2013.12.015>
- Parniakov, O., Bals, O., Lebovka, N., & Vorobiev, E. (2016). Effects of pulsed electric fields assisted osmotic dehydration on freezing-thawing and texture of apple tissue. *Journal of Food Engineering*, 183, 32-38. <https://doi.org/10.1016/j.jfoodeng.2016.03.013>
- Shynkaryk, M. V., Lebovka, N. I., & Vorobiev, E. (2008). Pulsed Electric Fields and Temperature Effects on Drying and Rehydration of Red Beetroots. *Drying Technology*, 26(6), 695-704. <https://doi.org/10.1080/07373930802046260>
- Sun, D.-W., & Zheng, L. (2006). Vacuum cooling technology for the agri-food industry: Past, present and future. *Journal of Food Engineering*, 77(2), 203-214. <https://doi.org/10.1016/j.jfoodeng.2005.06.023>
- Tian, Y., Chen, Z., Zhu, Z., & Sun, D.-W. (2020). Effects of tissue pre-degassing followed by ultrasound-assisted freezing on freezing efficiency and quality attributes of radishes. *Ultrasonics Sonochemistry*, 67, 105162. <https://doi.org/10.1016/j.ultsonch.2020.105162>
- Toepfl, S., Siemer, C., Saldaña-Navarro, G., & Heinz, V. (2014). Chapter 6 - Overview of Pulsed Electric Fields Processing for Food. In D.-W. Sun (Ed.), *Emerging Technologies for Food Processing (Second Edition)* (pp. 93-114). San Diego: Academic Press.
- Trusinska, M., Drudi, F., Rybak, K., Tylewicz, U., & Nowacka, M. (2023). Effect of the Pulsed Electric Field Treatment on Physical, Chemical and Structural Changes of Vacuum Impregnated Apple Tissue in Aloe Vera Juices. In *Foods* (Vol. 12).
- Wiktor, A., Schulz, M., Voigt, E., Knorr, D., & Witrowa-Rajchert, D. (2015). Impact of pulsed electric field on kinetics of immersion freezing, thawing, and on mechanical properties of carrot. *J Food Science Technology. Quality*, 22(2), 124-137
- Wiktor, A., Schulz, M., Voigt, E., Witrowa-Rajchert, D., & Knorr, D. (2015). The effect of pulsed electric field treatment on immersion freezing, thawing and selected properties of apple tissue. *Journal of Food Engineering*, 146, 8-16. <https://doi.org/10.1016/j.jfoodeng.2014.08.013>

General conclusion and prospects

Nowadays food freezing has become one of the most important unit operations in food processing and preservation. Almost all food products—raw, partially processed, and prepared foods—can be preserved by freezing. Numerous innovative freezing approaches aimed at minimizing structural damages and better preservation of food quality have been studied.

This thesis focuses on the application of vacuum for the intensification of fruits and vegetables freezing. Vacuum freezing is a rapid freezing technique based on the phase change of water at low pressure. It removes heat from samples by the internal water evaporation in order to achieve fast temperature reduction and even freezing without any cryogenic medium. To minimize the negative effect of excessive water loss, the application of vacuum freezing in a fixed small temperature range followed by the conventional slow freezing protocol has been proposed. In addition, as one of the effective pre-treatments to enhance mass transfer in food processing, the PEF pretreatment may also be a promising approach to improve vacuum freezing. However, the effect of vacuum freezing of fruits and vegetables in practice remains to be explored. Its application temperature range, applicability to different sample sizes and different varieties of materials all need to be further determined. The impact of PEF treatment on the vacuum freezing and the quality attributes of thawed products is also the scope of this study. We addressed these problems through the following three sections, as follows:

- (1) A laboratory vacuum freezing system was firstly constructed, instead of the existing lyophilizer in the laboratory, for reducing the delay of the reduction in pressure due to the big volume of vacuum chamber, as well as the inflexibility in controlling the start and the end of the vacuum freezing. The four combinations of two freezing rates (vacuum freezing represents fast freezing, conventional air freezing at $-20\text{ }^{\circ}\text{C}$ represents slow freezing) in two temperature ranges (2 to -6 and -6 to $-20\text{ }^{\circ}\text{C}$) verified that the temperature range of 2 to $-6\text{ }^{\circ}\text{C}$ contains the freezing critical zone, and the textural property is more affected by the freezing rate in the freezing critical zone. Thus, the application temperature range of vacuum freezing of carrot discs was determined to be 2 to $-6\text{ }^{\circ}\text{C}$, and the remaining freezing was

completed by air freezing at $-20\text{ }^{\circ}\text{C}$. The result in the chapter III also indicated that thawed carrot discs after the freezing protocol of VF + AF-20 could obtain texture as good as fast freezing with less water loss and a more homogeneous microstructure. This can be attribute to the rapid freezing rate of vacuum freezing during the freezing critical zone. And the investigation on lager size of carrot discs also showed its broad applicability than conventional air freezing. The use of predictive modelling of freezing times also enables an easier comparison between conventional air freezing and vacuum freezing or other innovative freezing technologies.

- (2) Since the application of vacuum freezing improved the quality of thawed carrot discs, we introduced PEF pretreatment with different cell disintegration index to explore its possible effect for further intensification. In this section, PEF treatment with different cell disintegration indexes of 0, 0.15, and 0.9 was applied before continuous VF, conventional AF-20, and the previously mentioned combined VF+AF-20 protocols, respectively. PEF pretreatment could significantly shorten the freezing time with the increase of Z in all the three freezing protocols. Although the application of PEF pretreatment on both AF-20 and VF+AF-20 protocols resulted in significant tissue softening with the increase of Z . The water losses for AF-20 protocol were significantly higher than those for the combined VF+AF-20 protocol, which reflected different water distribution in two freezing protocols. Combined with SEM image analysis, it can be implied that PEF treatment affected the formation of ice crystals inside the carrot discs.
- (3) Subsequently, we conducted further comparisons on different species of fruits and vegetables to investigate the effects of the mentioned freezing protocols on materials of different compositions and structures. In addition to carrots, the effectiveness of PEF treatment in enhancing the vacuum freeze kinetics was also proven in potato and apple discs. However, the degree of the effect of PEF treatment on continuous vacuum freezing varied for different materials. This may be due to differences in the homogeneity of the materials, which correlates with the mobility of the water in the tissue. At the same time, we speculated differently about the softening caused by PEF treatment in the freezing protocols of AF-20 and combined VF+AF-20. For AF-20, electroporation induced by PEF treatment accelerated the water transfer across the cell membrane, thus long duration in the

plateau stage increased water movement toward the formed ice crystals, resulting in the formation of large ice crystals. However, the deformation caused by more intensive water evaporation was the main reason for greater damage in combined VF+AF-20. Therefore, the combined freezing protocol VF+AF-20 is more suitable for fruits and vegetables with low porosity and a rigid initial structure.

Nevertheless, there are still some aspects that haven't been fully explored in this thesis. More investigations should be done to know more about this innovative freezing technique, vacuum freezing. The prospects are as follows:

- (1) Modeling of heat and mass transfer during vacuum freezing for better prediction and controlling of the freezing time and freezing curves.
- (2) Deeper measurement to understand the mechanism of the vacuum freezing (e.g. cryogenic microtome to understand a more comprehensive evolution rather than a specific point or aspect).
- (3) Study on the mechanism of PEF pretreatment affecting vacuum freezing.
- (4) Determine other quality parameters of thawed products, for instance nutritional or sensory value.
- (5) Optimization of vacuum freezing conditions (e.g. pressure drop rate) and operation parameters for PEF treatment (e.g. slight electroporation) to get a better quality of thawed products.
- (6) The effect of addition of the external water on the quality attributes of thawed samples including the internal water loss during vacuum freezing.
- (7) The exploration of the combination of vacuum freezing with other innovative techniques, e.g. ultrasound (intensification of the mass transfer), microwave (size of ice crystals).



Application of Vacuum Freezing to Improve the Quality of Thawed Carrot Discs

Yuqi Huang¹ · Olivier Bals¹

Received: 11 April 2024 / Accepted: 29 May 2024

© The Author(s), under exclusive licence to Springer Science+Business Media, LLC, part of Springer Nature 2024

Abstract

Freezing is a good way for food preservation. In addition to the process effectiveness, modern food freezing techniques should guarantee the high quality of the products after freezing. This study concerns the application of low pressure for food freezing covering a specific temperature range named *freezing critical zone*. Vacuum freezing (VF) allows a fast freezing rate without the use of a cryogenic medium. The application of VF allowed a comparable freezing rate as air freezing at $-80\text{ }^{\circ}\text{C}$ in the temperature range of about 2 to $-6\text{ }^{\circ}\text{C}$, which constitutes an advanced technology. Carrot discs with VF (from 2 to $-6\text{ }^{\circ}\text{C}$) were still of good quality by controlling the duration of the freezing critical zone, even with subsequent slow freezing (SF) (from -6 to $-20\text{ }^{\circ}\text{C}$). Carrot samples frozen under different conditions were extensively compared by the results in mass loss, textural property, and microstructural changes of SEM, quantifying the freezing damage. The results showed that carrot discs subjected to the freezing procedure of VF + SF contributed to a comparable texture to that of fast freezing, minimal mass loss, as well as reduced microstructure destruction. Even in the case of increased sample size, which requires more intense freezing conditions, the carrot discs maintained their good quality attributes after VF + SF. In conclusion, the application of VF in the temperature range covering the freezing critical zone can be a promising approach for improving the quality of frozen food products.

Keywords Vacuum freezing · Temperature critical zone · Quality characteristics · Applicability

Introduction

Carrot (*Daucus carota* L.) is one of the most consumed root vegetables and major food crops worldwide. Importantly, it is highly sought-after by consumers due to the rich content of nutrients and functional components, especially carotenoids which impart distinctive orange colors, with ample

health-promoting properties (Vicent et al., 2019). High water content makes carrots as perishable as most vegetables and fruits thus leading to a short shelf life. As the most common post-harvest processing method in food industry, freezing plays an invaluable role in the preservation and waste limitation of carrots which inhibits microbial activity and reduces biochemical reactions through the lowered temperature, thereby expanding the selection of carrots, independent of seasonal conditions or geography (Behnsilian & Mayer-Miebach, 2017; Stebel et al., 2021). However, the conventional freezing methods can cause undesired frozen damages due to possible low freezing rates and unevenly distributed big ice crystals, leading to quality loss, especially texture loss, of frozen fruit and vegetables (Tian et al., 2020; Schudel et al., 2021). Thus, it is critical to search for optimal freezing techniques, which help reduce the harmful damages caused by freezing, to satisfy the consumers' demand of fresh-like in organoleptic properties while well preserved.

Apart from internal factors such as sample size and composition, the quality preservation mainly depends on controlling the size, number, and location of ice crystals during the

Highlights

- Vacuum freezing (VF) is promising for freezing vegetables.
- VF was compared with conventional freezing for different size carrot discs.
- The textural property, mass loss, and microstructure of the carrot disc were better maintained with the application of VF.
- Vacuum freezing is also applicable to relatively large size carrot discs.

✉ Yuqi Huang
yuqi.huang725@gmail.com

¹ ESCOM, TIMR (Integrated Transformations of Renewable Matter), Centre de Recherche Royallieu, Université de Technologie de Compiègne, Compiègne CEDEX CS 60319, 60203, France

freezing process. Thus, the *freezing critical zone*, the temperature range in which the majority of ice crystals formed since the initial freezing point temperature, is recognized to be an important stage in the freezing process (Dalvi-Isfahan et al., 2019). Generally, the faster the freezing rate, the less time it takes to pass through the critical zone. In this condition, rapid and homogeneous nucleation with very little water migration leads to a greater number of ice crystals, smaller sizes and a more even distribution (Li et al., 2018). Numerous approaches have been adopted to accelerate the freezing rate. Based on conventional freezing methods, lowering the temperature of the cryogenic medium and increasing the velocity of the cryogenic medium can increase the freezing rate by accelerating the removal of latent and sensible heat (Muthukumarappan et al., 2019). But the energy consumption during the process is the main limitation. Some emerging techniques are investigated to affect the freezing process including ultrasound, high pressure, magnetic field, and pulsed electric field (Chen et al., 2022; Muthukumarappan et al., 2019; Ben Ammar et al., 2010; Gan et al., 2024). However, these approaches are attractive, but can be challenging. Their utilization is usually coupled with high energy consumption, potential environmental impact, and additional infrastructure investment.

Vacuum freezing is a rapid freezing technology that involves the water evaporation under low pressure, removing latent heat so that the temperature of the food product can be quickly reduced. Indeed, the heat transfer rate associated to evaporation (in vacuum freezing) is much higher than that of conduction (in conventional freezing methods) (Wang & Sun, 2001). Also, as water is evaporated, with the effect of prior dehydration, the amount of ice crystals formed during the freezing process can be reduced, which has been reported to decrease the initial moisture and accelerate the freeze-drying process of fruits and vegetables (Silva & Schmidt, 2022; Wang et al., 2018). Vacuum freezing also has the advantage of low energy consumption compared to conventional freezing because it does not require movement of the cooling medium in the system and vacuum can minimize heat loss from the environment. For the principle of water evaporation, the available studies in food industry have mainly focused on its application in the pre-cooling process of fruits and vegetables with high moisture content, porous structure and adequate specific surface area (Zhu et al., 2021). Pure water, simulated puree droplets, and nanodroplets were used in the initial exploration of the vacuum freezing process, including the mathematical simulation and visualization (Cheng & Lin, 2007; Cogné et al., 2013; Zhang et al., 2016; Ando et al., 2018). Recently, studies have shown that process conditions of vacuum freezing including pressure reduction modes, addition of external water, and different pretreatment (freeze-thaw, blanching, and ultrasound) can affect the vacuum-freezing characterizes in various

extent (Zhu et al., 2021; Wang et al., 2016, 2022). However, few studies have focused on the quality of the final product (fruits and vegetables) after vacuum freezing and thawing.

In the current study, a laboratory vacuum freezing system was designed for the freezing process of carrot discs in the temperature range covering the freezing critical zone. Preliminary calculations were applied to predict the variation of the potential loss of moisture with temperature range during vacuum freezing. Due to the high enthalpy of evaporation of water, vacuum freezing can achieve a very fast freezing rate. The application temperature range of vacuum freezing was determined under comprehensive consideration of a small water loss (reducing the application temperature range) and fast passing through the freezing critical zone (covering the freezing critical zone). The texture, mass loss, and microstructure of thawed samples after conventional freezing with different freezing rate and freezing procedure with application of vacuum freezing were detected respectively to evaluate of the quality promotion of vacuum freezing. Besides, the applicability of vacuum freezing from the variation of size was also investigated. This study would provide theoretical support for the application of vacuum freezing in the freezing storage of carrots, which is hoped to serve as a guidance for industrial applications.

Materials and Methods

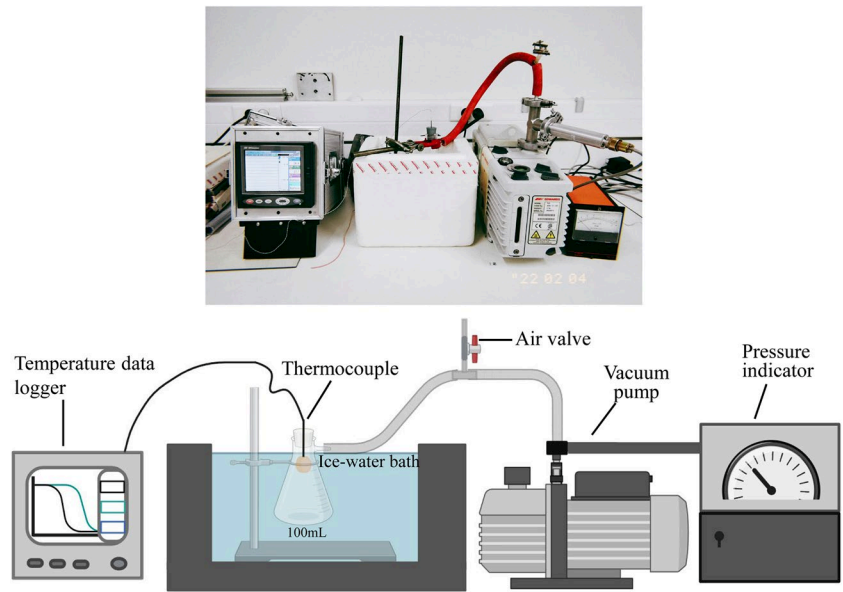
Sample Preparation

Carrot roots (*Daucus carota* L.) were obtained from a local market (Compiègne, France) and stored in a darkness at 6 °C until analysis maximally for 1 week. The wet-base moisture content of carrot samples was 88–91% that was detected by MA160 Infrared Moisture Analyzer (Sartorius, Germany). The carrot disc-shaped samples ($d=18$ mm in diameter and $h=10$ mm/20 mm in thickness) were manually prepared by using the special cylindrical knife. Samples were taken from the medium part of the carrots with 3 cm removed from the head and tail. And the carrot discs of 10 mm in thickness were with an approximate mass of 2.60 ± 0.10 g.

Setup and Temperature Range for the Application of Vacuum Freezing

Tests were performed by using a self-constructed vacuum freezing system (Fig. 1), which consisted of a vacuum pump RV8 (Edwards, Sweden), a PB 101 vacuum manometer (Alcatel, France), a switching valve, and a vacuum chamber that was performed by a buchner flask with a capacity of 100 mL, whose stopper hermetically connected with a T-type thermocouple of 0.5 mm of diameter (TC, Ltd., Dardilly, France) with an accuracy of ± 0.1 °C. The vacuum chamber was placed in

Fig. 1 Schematic diagram of the VF system. As soon as the vacuum pump started, the pressure inside the small vacuum chamber was reduced immediately



the ice-water bath (0 ± 0.1 °C) to maintain a stable environmental temperature. And the pressure during vacuum freezing and temperature of sample was recorded by the data acquisition module during the process.

According to the conversion of energy, the decrease in sample temperature and formation of internal ice crystals during vacuum freezing is achieved by the evaporation of water within the sample induced by low pressure. If it is assumed that the loss of mass is quite small and the heat transfer between the system and the external environment is negligible, the sample mass can be considered constant. Thus, the mass of evaporated water during vacuum freezing can be calculated by Eq. 1.

$$\frac{dm_{vap}}{dt} L_{vap} = mC_p \frac{dT}{dt} + \frac{dm_f}{dt} L_f \tag{1}$$

where m_{vap} is the mass of vaporized water during vacuum freezing (kg); L_{vap} is the latent heat of vaporization of water at 273.16 K, 611.73 Pa, about 2500 kJ/kg; m is the mass of the sample (kg); C_p is the specific heat capacity of the sample, $\text{kJ}\cdot\text{kg}^{-1}\cdot\text{K}^{-1}$; T is the sample temperature (K); m_f is the mass of frozen water in the sample (kg); and L_f is the latent heat of fusion of water, 334 kJ/kg.

For the aim of freezing rather than drying, the start temperature of vacuum freezing was set at 2 °C in consideration of reducing the loss of moisture and covering the critical zone. Besides, from the evolution of unfrozen water content

of carrot with temperature (Table 1) (Heldman et al., 2018), most of water (80%) turns into ice when temperature drops to -6 °C, and with little change subsequently. Based on the proposal of the International Institute of refrigeration, food can be considered frozen if the temperature is reduced to -10 °C or to a temperature for which 80% of the freezable water has been frozen (Dalvi-Isfahan et al., 2019). Therefore, vacuum freezing can be applied in a small temperature range from 2 to -6 °C.

According to the Eq. 1, the simplified calculation of the evaporated water during 2 to -6 °C is as follows:

$$m_{vap} = (mC_{pu}(T_i - T_{fp}) + mC_{pf}(T_{fp} - T_f) + m_f L_f) / L_{vap} \tag{2}$$

where m is the mass of the carrot disc in this study with a thickness of 10 mm, around 2.60 ± 0.10 g, which is assumed to be constant. C_{pu} is the specific heat capacity of the unfrozen carrot disc, which is assumed to be 3.87×10^3 J/(kg·K). T_i is the initial temperature in the geometry center of the carrot disc, 2 °C. T_{fp} is the freezing point of the carrot, which is assumed to be -1.6 °C. C_{pf} is the specific heat capacity of the frozen carrot disc, which is assumed to be 2.34×10^3 J/(kg·K). T_f is the final temperature in the geometry center of the carrot disc, -6 °C. m_f is the mass of frozen water in the carrot disc, calculated as $m \times$ water content of carrot \times frozen water content at -6 °C, which is assumed to be 1.84 g. Based on these parameters, the m_{vap} can be

Table 1 Evolution of unfrozen water content of carrot with temperature (Heldman et al., 2018)

T	0	-1	-2	-3	-4	-5	-6	-7	-8	-9	-10	-12	-14	-16	-18	-20
%	-	100	53	37	29	24	20	18	17	15	14	11	9	8	7	-

calculated as 0.27 g. The experimental value of water loss during vacuum freezing was detected by three replicates of the difference between the initial mass of the carrot disc (2.60 ± 0.10 g) and the mass after vacuum freezing from 2 to -6 °C (2.34 ± 0.08 g), which is approximately 0.26 g, close to the calculated value. Moreover, this water loss is very small compared to the mass of the carrot disc, only about 10%, and we can regard it as negligible.

Verification of the temperature range of the application of vacuum freezing was accomplished by the combinations of different freezing rates at temperature range of 2 to -6 °C and -6 to -20 °C. For a carrot disc with a thickness of 10 mm and a diameter of 18 mm, freezing at -20 °C was recognized as slow freezing, while at -45 °C was fast in preliminary tests. Besides, vacuum freezing could achieve a faster freezing rate than freezing at -45 °C during 2 to -6 °C. However, it is difficult to rapidly change freezing conditions from slow to fast within one freezer. A self-made box containing the sample was placed at -45 °C to achieve similar slow freezing condition as freezing at -20 °C. When it is time to switch, the sample was taken out from the box and directly exposed to -45 °C to complete the slow-to-fast transition. Thus, four sets of freezing procedures were carried out in two parts (2 to -6 °C and -6 to -20 °C) as follows ① fast + fast (vacuum freezing + freezing at -45 °C), ② fast + slow (vacuum freezing + freezing at -20 °C), ③ low + fast (freezing at -45 °C in the self-made box + freezing at -45 °C), and ④ slow + slow (freezing at -20 °C + freezing at -20 °C).

Freezing Experiments (Table 2)

On the one hand, to maintain the same freezing condition as vacuum freezing, the starting temperature of conventional freezing for comparison was also set at 2 °C. On the other hand, Schudel et al. showed that pre-cooling prior to conventional freezing significantly reduced drop loss of carrots by 13% and doubled the firmness, which implied that pre-cooling also reduced damage to cell walls and cell membranes by ice crystals in conventional freezing

(Schudel et al., 2021). Therefore, carrot discs were pre-cooled to 2 °C in an ice-water bath mentioned in “[Setup and Temperature Range for the Application of Vacuum Freezing](#)” across a plastic bag. Freezing process were all carried out from 2 to -20 °C. The thawing experiments were started immediately after freezing by placement of the sample in the room maintained at 20 °C (Parniakov et al., 2016). All freezing experiments were performed in 3 replicates.

Conventional Freezing

Conventional freezing with three different freezing rates were performed in a ventilated ultra-low-temperature freezer MDF-U2086S (Sanyo, Gunma, Japan) from 2 to -20 °C. With a modular-type temperature controller SR Mini System (TC Ltd., Dardilly, France) and the software Spec-View Plus (SpecView Corporation, Gig Harbor, USA) supplied, the samples were placed inside the freezer with an air flow rate of 1 m/s controlled by an electronic device VEAT 2.5 A (Air-technic, Firminy, France), at temperatures of -20 °C (SF (slow freezing)), -45 °C (MF (medium speed freezing)), and -80 °C (QF (quick freezing)), respectively. T-type thermocouple mentioned in “[Setup and Temperature Range for the Application of Vacuum Freezing](#)” was inserted in the geometrical center of the sample to measure and record the temperature evolution during the whole freezing process, and the freezing ended when the temperature of the geometrical center of the carrot discs reached -20 °C.

Vacuum Freezing

Vacuum freezing was performed in the setup of Fig. 1 in the temperature range of 2 to -6 °C. Then the samples were quickly transferred to the freezer mentioned in “[Conventional Freezing](#)” to complete the freezing process of

Table 2 Experiment procedures for SF, MF, QF, and VF+SF

Experiments	Precooling	Freezing conditions	Thawing
SF	Ice-water bath at 0 ± 0.1 °C from room temperature to 2 °C	Conventional freezing at -20 °C from 2 to -20 °C	Room temperature (20 ± 1 °C) in the air (free convection).
MF		Conventional freezing at -45 °C from 2 to -20 °C	
QF		Conventional freezing at -80 °C from 2 to -20 °C	
VF+SF		Vacuum freezing from 2 to -6 °C, and then immediately transferred to conventional freezing at -20 °C until -20 °C	

– 6 to – 20 °C by conventional freezing at temperature of – 20 °C (SF).

Analysis of the Samples

Force Relaxation Test

Texture properties were measured using a texture analyzer TA-XT plus (Rhéo, Champlan, France), to perform force relaxation test. The force was set at the level of 5 N, with the speed of piston displacement of 1.0 mm/s. The deformation curves (plot of force vs. time) were recorded with 0.1 s resolution during 60 s (Parniakov et al., 2016). The F ($t=50$ s) for untreated and thawed samples after different freezing procedures were selected for subsequent comparison. All force relaxation tests were performed in 3 replicates.

Mass Loss (ML) Measurement by Gravimetric Method

The ML of the samples, which represents the amount of water loss, was calculated using the mass of carrot discs before freezing (m_0) and after thawing (m_1) as follows (Ajani et al., 2023):

$$ML(\%) = (m_0 - m_1)/m_0 \times 100 \quad (3)$$

Scanning Electron Microscopy (SEM) Observation

The surface and cross-section of carrot discs were observed with Quanta 250 FEG SEM equipment (FEI, Oregon, USA). 15 images from three different samples were analyzed. Distribution of the cell size was obtained from the images by Nano Measurer 1.2, with statistical measurements of the mean isometric diameter of 120 randomly selected cells.

Applicability Analysis of Vacuum Freezing on Carrots

Two sizes of carrot discs were prepared ($d=18$ mm in diameter, $h=10$ mm, and $h=20$ mm in thickness), and then frozen by the same procedures, followed by texture and mass loss analysis.

Statistical Analysis

All experiments and measurements of characteristics were repeated at least, three times. Significant differences at 95% confidence were evaluated by one-way analysis of variance (ANOVA), using SPSS 25.0. The figures were drawn with Origin Pro 8.5, and the error bars inside correspond to the standard deviations (SD).

Results and Discussion

Identification and Verification of the Freezing Critical Zone of Carrots

The final freezing temperature-force plots recorded from 2 to – 20 °C during SF, MF, and QF are depicted in Fig. 2, with the data in Table 1 shown on the right ordinate. It is shown that at the three different temperatures, the compression stress values become lower as the final temperature of freezing decreases, which means a worse texture for the carrot discs. Meanwhile, this same trend is displayed consistent with the unfrozen water content in carrots. This result is due to the destruction of the cellular structure of food cells during the freezing process, mainly due to mechanical damage caused by ice crystal formation and osmotic dehydration caused by intracellular water migration (Li et al., 2018). In other words, the evolution of the texture of the food is related to its unfrozen water content.

However, in this study, the situation is observed to be not exactly the same for the different freezing rates provided by changing the freezing temperatures, especially in the temperature range of – 6 to – 20 °C. In Fig. 2, the decrease in texture tends to plateau for faster freezing (freezing at – 45, – 80 °C), while slow freezing (freezing at – 20 °C) continues to decrease substantially in the temperature range of – 6 to – 20 °C. This may be due to the fact that slow freezing starts with the crystallization of extracellular water (Schudel et al., 2021). The formation of extracellular ice crystals immediately alters the balance of intracellular and extracellular osmotic pressure. During slow freezing, the long duration in freezing critical zone provides more time for water movement to transfer across the cell membrane, leading to dehydration of the cells and further mechanical injury from

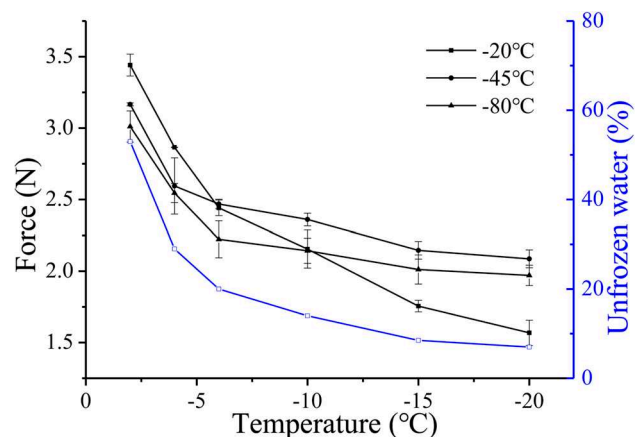


Fig. 2 Evolution of texture of carrot discs (thickness of 10 mm) with temperature during freezing (SF, MF, and QF). Evolution of unfrozen water content of carrot with temperature (data from Table 1)

the growth of ice crystals (Dalvi-Isfahan et al., 2019). On the contrary, for fast freezing conditions, the time required to pass through the freezing critical zone is smaller. Ice crystals are then more evenly distributed inside and outside the cells (Schudel et al., 2021). Simply defined, it's as if the internal water was instantly immobilized (-1 to -6 °C), causing little further deterioration during the subsequent freezing process (-6 to -20 °C). At the end of the freezing critical zone (-6 °C), a similar degree of damage occurs to them, while because of their different durations from -1 to -6 °C (as shown in Fig. 4C), the migration of water and ice crystals distribution inside of carrot tissue at this point are already very different, as well as the differences in ice crystals size and numbers (Muthukumarappan et al., 2019), thus affecting the results of subsequent freezing.

Comparisons of the freezing curves and their texture after thawing among combinations of different freezing rates in temperature ranges from 2 to -6 °C and -6 to -20 °C are shown in Fig. 3. For procedure ① and ②, their freezing time in temperature range covering freezing critical zone is much shorter than ③ and ④, which corresponds to their better textural results. And from the comparison between procedure ① and ②, it is found that if frozen rapidly in the temperature range covering the freezing critical zone, the subsequent freezing speed has no obvious effect on the final texture. That's also the reason why the texture of carrot disc plateaued after -6 °C when freezing at -45 °C and -80 °C (Fig. 2). But if frozen slowly first, as in procedure ③ and ④, degradation of the texture is inevitable, regardless of whether the following freezing is fast or slow. Moreover, comparisons of ① and ③, as well as ② and ④ further demonstrate that although they have the same freezing process from -6 to -20 °C, respectively, the textural results are significantly altered by the different freezing rates from 2 to -6 °C. All these results confirmed that the final texture of

carrot discs can be changed by controlling the time staying in the temperature range covering the freezing critical zone.

Pressure and Temperature Monitoring of the Freezing Process

Temperature-time and pressure-time curves as well as the temperature-pressure curve presented in the phase diagram of water during vacuum freezing are shown in Fig. 4A. Due to the small volume (100 mL) of the vacuum chamber, it is possible to reduce the pressure rapidly from atmospheric pressure (101,325 Pa) to 240 Pa in about 8 s. Since the pressure fall sharply and reached the flash point of water evaporation, the evaporation of the inner water of the carrot disc start, removing most of the sensible heat from the sample, which resulted in a rapid reduction of the temperature. Similar phenomena were found in the initial stage of vacuum freezing (0–2 min) of apple slices (Wang et al., 2022). Subsequently, with the formation of ice crystals in the carrot disc, a large amount of latent heat was released and the sample temperature would stay briefly near the freezing point (around -1.6 °C). The solute concentration inside the sample also continuously increased, which can be attributed to the formation of ice crystals and to the water loss from the evaporation. Due to this concentration increase, the freezing point is lowered. Besides, due to the presence of the solute components of carrot, the temperature-pressure curve shifted to lower pressure and lower temperature compared to pure water. The triple point of carrot occurred around 80 Pa, -1.6 °C (Fig. 4B).

Typical time-temperature plots recorded during SF, MF, QF, and VF + SF experiments are shown in Fig. 4C, and detailed freezing time during 2 to -6 °C, -6 to -20 °C, and 2 to -20 °C can be seen in Table 3. For the temperature range from 2 to -6 °C, there was no significant

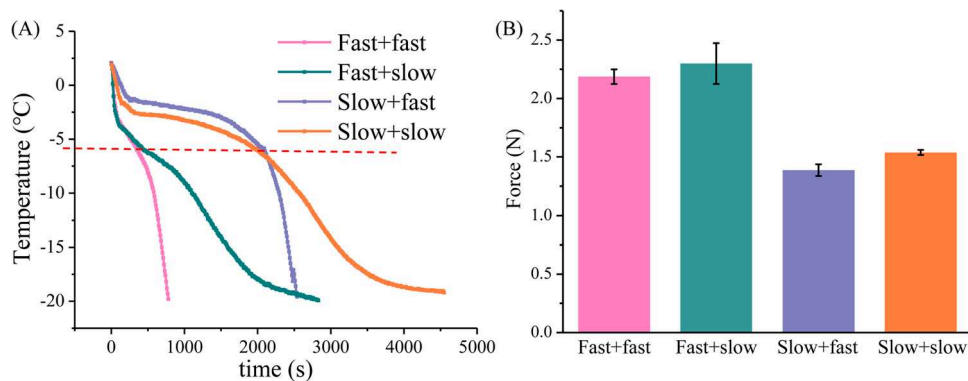


Fig. 3 **A** Evolution of the temperature of the carrot discs (thickness of 10 mm), during ① fast + fast (vacuum freezing + freezing at -45 °C), ② fast + slow (vacuum freezing + freezing at -20 °C), ③ slow + fast (freezing at -45 °C in the self-made box + freezing at -45 °C), and

④ slow + slow (freezing at -20 °C + freezing at -20 °C), as well as **B** their texture after thawing, respectively. The red dotted line in the temperature curves represents the temperature of -6 °C, which is also the transition point of the freezing procedures

Fig. 4 **A** Temperature-time and pressure-time curves of carrot discs (thickness of 10 mm) during VF. **B** Temperature-pressure curve of carrot discs (thickness of 10 mm) presented in the phase diagram of water during VF. **C** Evolution of the temperature of the carrot discs (thickness of 10 mm), during SF, MF, QF, and VF+SF, respectively

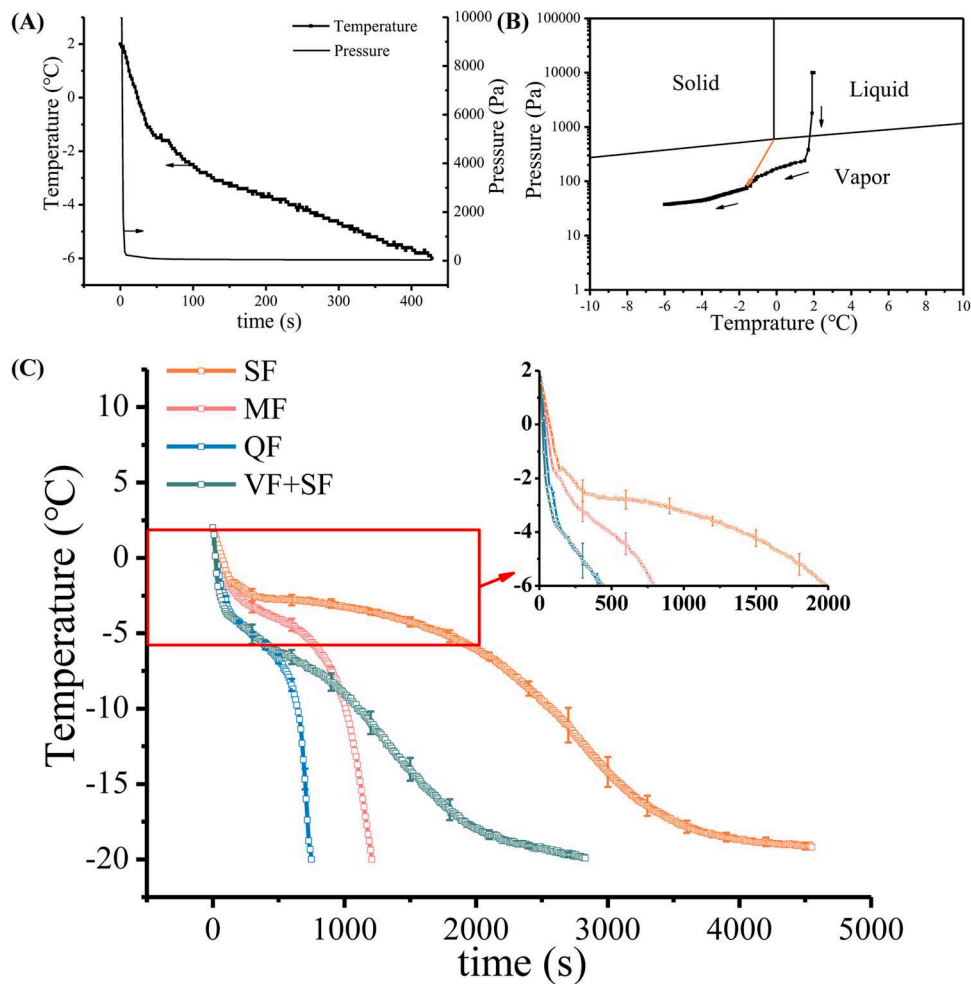


Table 3 Freezing time of temperature range of 2 to - 6 °C, - 6 to - 20 °C, and 2 to - 20 °C for carrot discs (thickness of 10 mm) during SF, MF, QF, and VF+SF, respectively. Mass loss (%), and texture (N) for thawed carrot discs (thickness of 10 mm) after SF, MF, QF,

and VF+SF, respectively. Values with different superscripts among the data in the same column indicate that the means are significantly different at ($p < 0.05$)

Freezing conditions	Freezing time (s)			Mass loss (%)	Texture (N)
	2 to - 6 °C	- 6 to - 20 °C	2 to - 20 °C		
SF	1977 ± 81 ^c	2557 ± 105 ^a	4533 ± 29 ^a	17.46 ± 0.49 ^c	1.54 ± 0.02 ^c
MF	797 ± 12 ^b	413 ± 32 ^b	1210 ± 30 ^c	10.97 ± 0.02 ^a	2.37 ± 0.02 ^a
QF	423 ± 29 ^a	320 ± 36 ^c	743 ± 12 ^d	13.78 ± 0.44 ^b	2.10 ± 0.10 ^b
VF+SF	427 ± 75 ^a	2483 ± 56 ^a	2910 ± 69 ^b	11.57 ± 0.27 ^a	2.30 ± 0.18 ^a

difference in the freezing time of VF+SF (427 s) and QF (423 s), but they were significantly smaller than MF (797 s) and SF (1977 s) ($p < 0.05$). This result showed that VF achieved the same fast freezing speed as conventional freezing at - 80 °C. Because of the higher efficiency of heat transfer compared with SF and MF, the freezing critical zone is rapidly covered without the use of a cryogenic

medium. As for the temperature range from - 6 to -20 °C, VF+SF (2483 s) and SF (2557 s) show similar variation because of the same freezing process. Compared to MF and QF, the temperature difference between the freezer and sample is much smaller for SF. This would directly lead to a smaller convective heat transfer, thus resulting in a longer freezing time to reach the same final temperature.

Main Quality Characteristics of Thawed Carrot Discs

Carrot discs quality frozen under SF, MF, QF, and VF + SF was assessed by mass loss, texture, and SEM. Mass loss for conventional freezing was mainly associated to the drip loss during thawing, while for VF + SF it was due to the drip loss and also water evaporated during vacuum freezing. As shown in Table 3, the mass loss in the SF was significantly higher than that in other freezing processes ($p < 0.05$). Usually, the number and the size of the formed ice crystals can be determined by the freezing rate, equivalent to the velocity of operation to pass through the critical zone (Dalvi-Isfahan et al., 2019). The freezing time during 2 to -6 °C of MF (797 s), QF (423 s), and VF + SF (427 s) were all significantly shorter than that of SF (1977 s), resulting in fewer internal changes, including tissue rupture from big ice crystals and volumetric changes from expansion stress in the cellular structure (Panayampadan et al., 2022), reducing the drip loss during thawing. Intriguingly, the moisture loss during VF did not result in an increase in overall mass loss, a small mass loss (11.57%) was observed after VF + SF in contrast. Moreover, as we calculated and experimentally verified that the amount of evaporated water of carrot disc with a thickness of 10 mm during vacuum freezing from 2 to -6 °C was around 10%, this means that the drip loss during thawing after VF + SF was about 1.57%, which is quite smaller compared to conventional freezing. In addition to the rapid freezing rate, this may also be contributed to moisture loss at the beginning of the freezing process limiting the damage to the cell wall structure. Previous studies on dehydrofreezing indicated that pre-drying increased the protecting potential of tissue during freezing, with lower drip loss observed in carrots and strawberries (Schudel et al., 2021; Hajji et al., 2022).

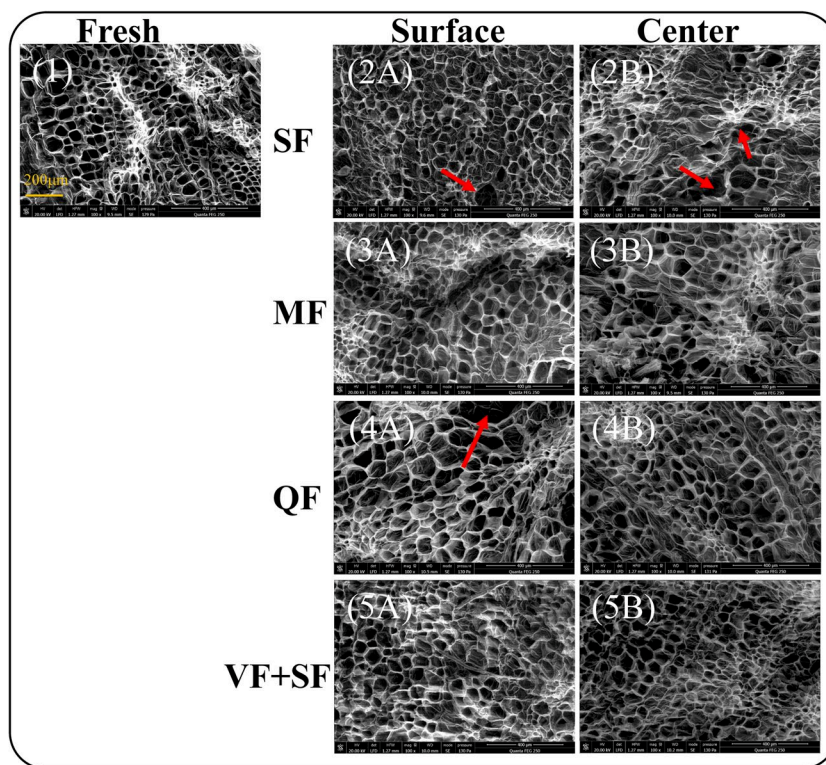
The textural property is also an important quality indicator for potential damage in the collection, handling, processing, and storage of fruits and vegetables, which can be evaluated by force relaxation test (Wu et al., 2020). Compared with SF (1.54 N), the stress values of the carrot disc after MF (2.37 N) and QF (2.10 N) was significantly higher by a rapid freezing rate induced by a lower temperature of the air in conventional freezing ($p < 0.05$). The same results were reported by Van Buggenhout et al. (Van Buggenhout et al., 2006), where applying rapid conventional and cryogenic freezing conditions minimized the texture loss of frozen carrots, revealing that reduced texture loss of carrots was associated with the reduction in cell wall damage in carrot tissue. It can be noted that the compression stress value of the carrot disc after VF + SF was as good as that of fast freezing, although the freezing time in the temperature range of -6 to -20 °C was much longer. This also proved that the quality of the final product could be modified by controlling the freezing process in the critical zone, VF applied in this

study. In this way, the loss of cell turgidity and breakdown of cell wall structure was reduced, leading to less cell rupture and tissue collapse (Tian et al., 2020). The decrease in water during vacuum freezing may also perform a role. Although the removal of water varied, a previous study has shown that reducing the water content in carrot tissue induced a protective effect by the alleviation of fracture stress relating to cell wall strength after freeze-thawing (Ando et al., 2012).

As both texture and drip loss are expected to rely on tissue integrity (Sun, 2011), micrographs were acquired to shed light on the effect of the different freezing processes on carrot discs, further verifying the improvement of quality attributes by VF. Microstructural changes of the surface and central section of carrot discs from SEM produced by the different treatments are shown in Fig. 5.

Fresh carrot tissue displayed a regular and complete cell structure with an isodiametric diameter of about 47 μm , which was in accordance with the findings of Van Buggenhout et al. (Van Buggenhout et al., 2006) who described carrot parenchyma cells as small cells with an isodiametric diameter of about 50 μm . Upon SF, large ice crystals were formed especially in the center of the carrot disc (Fig. 5), contributing to more cell disruption and morphological changes, which gave reason for the considerable mass loss and decrease in texture observed after thawing (Table 3). Generally, faster freezing rate results in a greater number of ice crystals with a smaller median size and more uniform size distribution, with fewer adverse effects on the thawed cell structure. However, it can be seen that the surface of the QF sample also exhibited ruptures and contortions in the microstructure. These freeze cracking were possibly caused by the rapid water expansion induced by very fast freezing at ultra-low temperatures on the surface of the carrot disc at the beginning, leading to uniform tensile stresses in the unfrozen core and tensile radial stresses and compressive tangential stresses in the outer surface of frozen food (shell) (Schudel et al., 2021). After solidification and expansion, solid ice contracts, and the shell frozen body is then exposed to tangential tensile stress instead of compression at the beginning of freezing (Dalvi-Isfahan et al., 2019). A relatively large isometric diameter was also obtained by about 76 μm on the surface of the carrot disc after QF. VF was carried out with a much faster freezing rate than SF during the critical zone, resulting in smaller and more uniform ice crystals in the extracellular and intracellular regions, which is consistent with the favorable results in mass loss and texture. The same result was found in the photomicrograph of apple tissues after VF (Wang et al., 2022). Although they considered that the intensive flash evaporation of the inner original free water inside the apple tissue during VF could destroy the integrity of the cell structure. This phenomenon was not observed for carrots in our study. One possibility is that the large vacuum chamber resulted in a slower pressure

Fig. 5 SEM images of carrot discs (thickness of 10 mm) after different freezing treatments. (1) fresh carrot, (2A) the surface of carrot disc after SF, (2B) the center of carrot disc after SF, (3A) the surface of carrot disc after MF, (3B) the center of carrot disc after MF, (4A) the surface of carrot disc after QF, (4B) the center of carrot disc after QF, (5A) the surface of carrot disc after VF + SF, and (5B) the center of carrot disc after VF + SF



drop (2 min to flash point of water evaporation), instead of 8 s in our device. Also, it may be due to the differences in the species of food. It was found by Nikolai I Lebovka et al. that carrots were stronger than apples based on the stress-deformation curves for their tissues after freeze-thawed (Lebovka et al., 2004). Furthermore, vacuum-induced nucleation of VF + SF may also be one of the factors for its uniform microstructure. Applied before freeze-drying, samples produced using the controlled freezing (VF) were more homogeneous than those produced by the uncontrolled freezing (Oddone et al., 2017; Silva & Schmidt, 2019, 2022).

As shown in Fig. 5, the difference in microstructure corresponds to the results of mass loss and texture (Table 3), confirming the interpretation of their relationship as previously inferred in the analysis of Table 3. For freezing preservation, the least microstructure disruption after VF + SF was desirable to achieve good-quality frozen products.

Verification of the Applicability of Vacuum Freezing

As it was discussed in “Main Quality Characteristics of Thawed Carrot Discs,” the application of VF during the critical zone could be a promising approach to improve the quality of frozen carrots, which was based on the results from small carrot discs with a diameter of 18 mm and thickness of 10 mm. Carrot discs with double thickness (18 mm diameter and 20 mm thickness) were tested in the same four freezing procedures. Their freezing times in the temperature

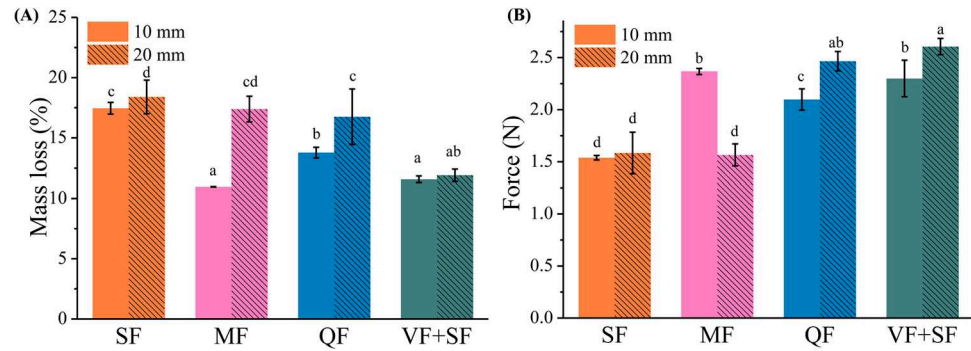
range of 2 to – 6 °C, covering the critical zone, are shown in Table 4, as expected to be relatively longer than those of the smaller size. Figure 6 presents the comparison of the mass loss and texture between the two sizes of carrot discs after thawing.

For conventional freezing, the freezing time increased as the sample size increased (Table 4). Similar results were obtained in a study on spherical potatoes freezing, which mentioned that the freezing time should be proportional to the square of the sample diameter based on numerical prediction models for the freezing time (Stebel et al., 2021). This is because the heat transfer inside the sample is due to conduction. The conduction resistance depends on the sample size. The larger the sample size, the greater the conductive resistance and the greater the amount of heat to be removed. Thus by increasing the size of the sample, the freezing time is increased (Muthukumarappan

Table 4 Freezing time for carrot discs with thicknesses of 10 mm and 20 mm in the temperature range of 2 to – 6 °C during SF, MF, QF, and VF + SF, respectively. Values with different superscripts for each data indicate that the means are significantly different at ($p < 0.05$)

Thick-ness (mm)	SF (s)	MF (s)	QF (s)	VF + SF (s)
10	1977 ± 81 ^f	797 ± 12 ^c	423.33 ± 29 ^a	427 ± 75 ^a
20	3193 ± 99 ^g	1603 ± 47 ^e	1073.33 ± 21 ^d	653 ± 21 ^b

Fig. 6 **A** Mass loss (%) and **B** texture (N) for thawed carrot discs with thicknesses of 10 mm and 20 mm after SF, MF, QF, and VF+SF, respectively. Columns with different letters above indicate that the means are significantly different at ($p < 0.05$)



et al., 2019). In this case, conventional freezing that only relies on heat conduction may not be able to achieve a fast freezing rate even with a large temperature difference as the driving force. It is worth mentioning that both sizes of carrot discs have the shortest freezing time across the temperature range of 2 to -6 °C for vacuum freezing, which can be explained by the fast evaporation of internal water according to the principle of energy conservation (Wang et al., 2022), as the latent heat of evaporation (2500 kJ/kg) removed is much greater than the latent heat of crystallization of water (334 kJ/kg). The fast rate of vacuum freezing of carrot discs may be also attributed to their special vascular system, which has a conductive effect through xylem and phloem (Perrin et al., 2017). The xylem is a water-filled structure with lignified cell walls, mainly responsible for the transport of water and minerals, while the phloem consists mainly of densely packed, thin-walled cells and is responsible for the transport of nutrients (Genovese et al., 2023). In this way, deeper water can be evaporated more easily, thereby removing the latent heat and achieving rapid freezing.

Closely related to the freezing rate, carrot discs consistently performed worst in texture and mass loss under SF, either in small or large sizes. However, for MF, the change in size had a different result. Although the small carrot discs had good texture and low mass loss after MF, these quality characteristics deteriorated with size. When the latent and sensible heat to be transferred is increased (product in larger size), the time for the carrot discs under MF to pass through the freezing critical zone is prolonged from 797 to 1603 s on the basis of the same thermal conductivity. Freezing at -45 °C can't provide enough driving force for large size of carrot discs to achieve a high freezing efficiency. For this case, more intense freezing conditions are required to ensure a fast freezing rate and good final quality of food product, as performed under QF (the greater temperature difference between the cooling medium and the product, the greater the driving force). With the fastest freezing rate during the temperature range of 2 to -6 °C, two sizes of carrot discs after VF+SF both obtained relatively optimal values in texture and mass loss,

which implied that VF could be applied to the relatively large size of carrot discs to improve the final quality.

Conclusion

The results presented in this study show that the application of VF in the temperature range covering the freezing critical zone can improve the quality attributes of thawed carrot discs, due to the reduced freezing damage during VF. The present study suggests that VF can achieve the same fast freezing speed as conventional freezing at -80 °C in the temperature range of 2 to -6 °C. Although followed by SF from -6 to -20 °C, the texture of thawed carrot disc can be as good as fast freezing. The minimal mass loss and the homogenous microstructure verified that VF helped the formation of small and uniform ice crystals. More intense freezing conditions were proven to be required to maintain quality characteristics with increased sample size. Vacuum freezing has broad applicability, and its application can also obtain good texture and small mass loss in relatively large carrot discs, although this may also benefit from the special vascular system of carrot root. These results will provide evidence for the application of VF in reducing freezing damage and maintaining the quality of vegetable products in the food industry. Future research could include optimization of vacuum freezing conditions, such as the addition of external water, pressure reduction rate, and the application of pretreatment to enhance water evaporation. Its application in different species of vegetables is supposed to be further studied.

Author Contribution Yuqi Huang: conceptualization, data curation, formal analysis, investigation, methodology, and writing—review and editing. Olivier Bals: supervision, conceptualization, data curation, formal analysis, methodology, investigation, project administration, and writing—review and editing.

Funding Yuqi Huang thanks the China CSC Scholarship for the financial support (202008420201).

Data Availability No datasets were generated or analyzed during the current study.

Declarations

Competing Interests The authors declare no competing interests.

References

- Ajani, C. K., Zhu, Z., & Sun, D. W. (2023). Shrinkage during vacuum cooling of porous foods: Conjugate mechanistic modelling and experimental validation. *Journal of Food Engineering*, *337*, 111220.
- Ando, H., Kajiwara, K., Oshita, S., & Suzuki, T. (2012). The effect of osmotic dehydrofreezing on the role of the cell membrane in carrot texture softening after freeze-thawing. *Journal of Food Engineering*, *108*(3), 473–479.
- Ando, K., Arakawa, M., & Terasaki, A. (2018). Freezing of micrometer-sized liquid droplets of pure water evaporatively cooled in a vacuum. *Physical Chemistry Chemical Physics*, *20*(45), 28435–28444.
- Behsnilian, D., & Mayer-Miebach, E. (2017). Impact of blanching, freezing and frozen storage on the carotenoid profile of carrot slices (*Daucus carota* L. Cv. Nutri Red). *Food Control*, *73*, 761–767.
- Ben Ammar, J., Lanoisellé, J.-L., Lebovka, N. I., Van Hecke, E., & Vorobiev, E. (2010). Effect of a pulsed electric field and osmotic treatment on freezing of potato tissue. *Food Biophysics*, *5*, 247–254.
- Chen, X., Liu, H., Li, X., Wei, Y., & Li, J. (2022). Effect of ultrasonic-assisted immersion freezing and quick-freezing on quality of sea bass during frozen storage. *LWT*, *154*, 112737.
- Cheng, H. P., & Lin, C. T. (2007). The morphological visualization of the water in vacuum cooling and freezing process. *Journal of Food Engineering*, *78*(2), 569–576.
- Cogné, C., Nguyen, P. U., Lanoisellé, J. L., Van Hecke, E., & Clause, D. (2013). Modeling heat and mass transfer during vacuum freezing of puree droplet. *International Journal of Refrigeration*, *36*(4), 1319–1326.
- Dalvi-Isfahan, M., Jha, P. K., Tavakoli, J., Daraei-Garmakhany, A., Xanthakis, E., & Le-Bail, A. (2019). Review on identification, underlying mechanisms and evaluation of freezing damage. *Journal of Food Engineering*, *255*, 50–60.
- Gan, S., Zhang, M., & Jiang, Q. (2024). Pork freezing and quality improvement: The effect of immersion freezing assisted by Magnetic Field. *Food and Bioprocess Technology*, *17*(1), 73–82.
- Genovese, J., Stručić, M., Serša, I., Novickij, V., Rocculi, P., Miklavčič, D., Mahnič-Kalamiza, S., & Kranjc, M. (2023). PEF treatment effect on plant tissues of heterogeneous structure no longer an enigma: MRI insights beyond the naked eye. *Food Chemistry*, *405*, 134892.
- Hajji, W., Gliguem, H., Bellagha, S., & Allaf, K. (2022). Structural and textural improvements of strawberry fruits by partial water removal prior to conventional freezing process. *Journal of Food Measurement and Characterization*, *16*(5), 3344–3353.
- Heldman, D. R., Lund, D. B., & Sabliov, C. (2018). *Handbook of food engineering*. CRC press.
- Lebovka, N. I., Praporscic, I., & Vorobiev, E. (2004). Effect of moderate thermal and pulsed electric field treatments on textural properties of carrots, potatoes and apples. *Innovative Food Science & Emerging Technologies*, *5*(1), 9–16.
- Li, D., Zhu, Z., & Sun, D.-W. (2018). Effects of freezing on cell structure of fresh cellular food materials: A review. *Trends in Food Science & Technology*, *75*, 46–55.
- Muthukumarappan, K., Marella, C., & Sunkesula, V. (2019). Chap. 15 - food freezing technology. In: Kutz M (Ed.) *Handbook of farm, dairy and food machinery engineering* (third edition). pp 389–415. Academic Press.
- Oddone, I., Barresi, A. A., & Pisano, R. (2017). Influence of controlled ice nucleation on the freeze-drying of pharmaceutical products: The secondary drying step. *International Journal of Pharmaceutics*, *524*(1), 134–140.
- Panayampadan, A. S., Shafiq Alam, M., Aslam, R., Kumar Gupta, S., & Kaur Sidhu, G. (2022). Effects of alternating magnetic field on freezing of minimally processed guava. *LWT*, *163*, 113544.
- Parniakov, O., Bals, O., Lebovka, N., & Vorobiev, E. (2016). Effects of pulsed electric fields assisted osmotic dehydration on freezing-thawing and texture of apple tissue. *Journal of Food Engineering*, *183*, 32–38.
- Perrin, F., Hartmann, L., Dubois-Laurent, C., Welsch, R., Huet, S., Hamama, L., Briard, M., Peltier, D., Gagné, S., & Geoffriau, E. (2017). Carotenoid gene expression explains the difference of carotenoid accumulation in carrot root tissues. *Planta*, *245*(4), 737–747.
- Schudel, S., Prawiranto, K., & Defraeye, T. (2021). Comparison of freezing and convective dehydrofreezing of vegetables for reducing cell damage. *Journal of Food Engineering*, *293*, 110376.
- Silva, A. C. C., & Schmidt, F. C. (2019). Vacuum freezing of coffee extract under different process conditions. *Food and Bioprocess Technology*, *12*(10), 1683–1695.
- Silva, A. C. C., & Schmidt, F. C. (2022). Intensification of freeze-drying rate of coffee extract by vacuum freezing. *Innovative Food Science & Emerging Technologies*, *78*, 103022.
- Stebel, M., Smolka, J., Palacz, M., Piechnik, E., Halski, M., Knap, M., Felis, E., Eikevik, T. M., Tolstorebrov, I., Peralta, J. M., & Zorrilla, S. E. (2021). *Numerical modelling of the food freezing process in a quasi-hydrofluidisation system* (Vol. 74, p. 102834). Innovative Food Science & Emerging Technologies.
- Sun, D. (2011). Quality and safety of frozen foods. *Handbook of frozen food processing and packaging* (pp. 303–456). CRC press.
- Tian, Y., Chen, Z., Zhu, Z., & Sun, D.-W. (2020). Effects of tissue predegassing followed by ultrasound-assisted freezing on freezing efficiency and quality attributes of radishes. *Ultrasonics Sonochemistry*, *67*, 105162.
- Van Buggenhout, S., Lille, M., Messagie, I., Loey, A. V., Autio, K., & Hendrickx, M. (2006). Impact of pretreatment and freezing conditions on the microstructure of frozen carrots: Quantification and relation to texture loss. *European Food Research and Technology*, *222*(5), 543–553.
- Vicent, V., Ndoye, F.-T., Verboven, P., Nicolai, B., & Alvarez, G. (2019). Effect of dynamic storage temperatures on the microstructure of frozen carrot imaged using X-ray micro-CT. *Journal of Food Engineering*, *246*, 232–241.
- Wang, L., & Sun, D.-W. (2001). Rapid cooling of porous and moisture foods by using vacuum cooling technology. *Trends in Food Science & Technology*, *12*(5), 174–184.
- Wang, H., Chen, S., Fu, Q., Wang, R., Zhang, W., Chen, L., & Wu, J. (2016). Effect of different pretreatments on the vacuum-freezing characteristics. *Modern Food Science and Technology*, *32*(11), 241–247.
- Wang, H., Fu, Q., Chen, S., Hu, Z., & Xie, H. (2018). Effect of hot-water blanching pretreatment on drying characteristics and product qualities for the novel integrated freeze-drying of apple slices. *J Journal of Food Quality*. 2018, 1–12.
- Wang, H., Xue, Y., Hu, Z., Ba, L., Shamim, S., Xie, H., Xia, T., & Zhao, R. (2022). *Addition of external water improves the quality*

attributes of vacuum-frozen and thawed apple slices. International Journal of Refrigeration.

- Wu, X., Wang, C., & Guo, Y. (2020). Effects of the high-pulsed electric field pretreatment on the mechanical properties of fruits and vegetables. *Journal of Food Engineering*, 274, 109837.
- Zhang, Z., Zhang, S., & Zhang, Y. (2016). Vacuum spray evaporate-freezing of nano-droplet. *Nanomedicine: Nanotechnology Biology and Medicine*, 12(2), 572.
- Zhu, Z., Geng, Y., & Sun, D.-W. (2021). Effects of pressure reduction modes on vacuum cooling efficiency and quality related attributes of different parts of Pakchoi (*Brassica Chinensis* L). *Postharvest Biology and Technology*, 173, 111409.

Publisher's Note Springer Nature remains neutral with regard to jurisdictional claims in published maps and institutional affiliations.

Springer Nature or its licensor (e.g. a society or other partner) holds exclusive rights to this article under a publishing agreement with the author(s) or other rightsholder(s); author self-archiving of the accepted manuscript version of this article is solely governed by the terms of such publishing agreement and applicable law.